STUDIES ON THE PATHOLOGY OF BOVINE THEILERIOSES

LYNN MARGARET GRACE FORSYTH

DOCTOR OF PHILOSOPHY

UNIVERSITY OF EDINBURGH

1997

CONTENTS

LIST OF TABLES

LIST OF FIGURES

ABBREVIATIONS

%	percentage
&	and
µg	microgram
µl	microlitre
µM	micromole
µm	micron
<	less than
=	equal to
>	greater than
^{0}C	degree centigrade
^{3}H	tritium
ABC	avidin/biotin complex
AIDS	acquired immune deficiency syndrome
Anon	anonymous
AP	alkaline phosphatase
bio-dUTP	biotinylated deoxyuridine
BL	bovine lymphosarcoma
Bo	bovine
Bq	becquerel
BSA	bovine serum albumin
CC	Institute for Animal Health
CD	cluster of differentiation
cl	clone
cm^2	centimetre squared
CR	complement receptor
CTVM	Centre for Tropical and Veterinary Medicine
DAB	diaminobenzidine tetrahydrochloride
DNA	deoxyribonucleic acid
dpm	disintegrations per minute
DWBC	differential white blood cells
e.u.	enzyme unit
ECACC	European Cell and American Culture Collection
EDTA	ethylenediamine tetra-acetic acid
EU	Edinburgh University
FACS	fluorescent activated cell sorter
FCS	foetal calf serum
FITC	fluorescein isothiocyanate
g	gram
g.	relative centrifugal force
gp	glycoprotein
GUTS	ground up tick supernatant
h	hour
H_2O_2	hydrogen peroxide
HCl	hydrochloric acid
HIV	human immunodeficiency virus
HRP	horseradish peroxidase
Hu	human
i.u.	international units

IFN	interferon
IFN-α	interferon alpha
IFN-γ	interferon gamma
Ig	immunoglobulin
IL	interleukin
ILRAD	International Laboratory for Research in Animal Diseases
IMDM	Iscove's modified Dulbecco's medium
l	litre
L-NMMA	N^G-monomethyl-l-arginine
LN	lymph node
M	Molar
MAb	monoclonal antibody
$MgCl_2$	magnesium chloride
MHC	major histocompatibility complex
ml	millilitre
mM	millimole
NaCl	sodium chloride
NaN_3	sodium azide
$NaNO_2^-$	sodium nitrite
NaOH	sodium hydroxide
NK	natural killer
NO	nitric oxide
NO_2^-	nitrite
OD	optimal density
PBM	peripheral blood mononuclear cells
PBS	phosphate buffered saline
PCV	packed cell volume
r	recombinant
RBC	red blood cell
SAPU	Scottish Antibody Production Unit
SNAP	S-nitroso-N-acetyl-DL-penicillamine
T. a	*T. annulata*
T. p	*T. parva*
t.e.	tick equivalent
TaAnk	*T. annulata* (Ankara)
TaH	*T. annulata* (Hisar)
TBS	tris buffered saline
TCC	total cell count
TcR	T cell receptor
TdT	terminal deoxynucleotidyl transferase
TNF	tumour necrosis factor
TNF-α	tumour necrosis factor alpha
TUNEL	TdT-mediated-dUTP-biotin nick end labelling
TWBC	total white blood cell counts
WSU	Washington State University, USA
WUMP	Welcome Unit of Molecular Parasitology, University of Glasgow
x	multiplied by

ACKNOWLEDGEMENTS

I would like to express my gratitude to my supervisors Dr. Patricia M. Preston and Prof. C. G. D. Brown for their guidance and support over the past few years. I would also like to thank Dr. Steve McOrist for his assistance in the interpretation of pathological findings. I would especially like to thank the staff at the CTVM, in particular Dr. Erol Kirvar, Mrs. Gwen Wilkie and Mrs. Mary Thomas for their assistance and the supply of material.

I am most grateful to Mr. David Elliot and the staff at the Pathology Department, University of Edinburgh Medical School for the use of equipment and technical assistance. I would especially like to thank Mr. John Lauder for his help and encouragement with the practical aspects of pathology.

I would also like to thank Dr. Carol Ross and Mr. Bob Munro for their assistance with the practical aspects of photography.

I am grateful to the European Commission for their financial support of this work.

ABSTRACT

The lesions of bovine theilerioses were investigated in calves inoculated with potentially lethal doses of sporozoites of two different stocks of *T. annulata* or of the Muguga stock of *T. parva*. The clinical, haematological and parasitological responses monitored during the course of infection indicated that all the calves had undergone 'acute' (lethal) infections. In all the calves a severe pyrexia and leucopenia was accompanied by a severe macroschizont parasitosis. Those infected with *T. annulata* (Hisar) also exhibited a severe piroplasm parasitaemia which was associated with anaemia. The peripheral blood mononuclear cells (PBM) harvested from the calves infected with *T. annulata* (Hisar) at intervals during the course of infection produced nitric oxide (NO) *in vitro*.

Macroscopic examination revealed extensive oedema and haemorrhage of the lymphoid and non-lymphoid organs of calves infected with *T. annulata*, i.e. the prescapular lymph nodes, precrural lymph nodes, mesenteric and hepatic lymph nodes, spleen, thymus, kidney, liver, abomasum, lung and adrenal gland. Examination of the lymphoid and non-lymphoid organs of the calf infected with *T. parva* (Muguga) showed extensive oedema and haemorrhage of the lymphoid organs alone. In all calves the most adversely affected organ was the prescapular lymph node which drained the site of inoculation.

Microscopic examination of tissue sections of the prescapular lymph nodes, precrural lymph nodes and mesenteric and hepatic lymph nodes from the calf infected with *T. annulata* (Hisar) during the early stages of disease revealed extensive paracortical lymphoid cellular depletion, focal haemorrhaging and mass infiltration of medullary sinuses with macrophages. As infection progressed extensive numbers of macrophages, often accompanied by granulomatous formations, were now observed in the paracortical and medullary regions of all the lymph nodes. By the nadir of disease extensive areas of diffuse necrosis and haemorrhage occurred throughout the cortical, paracortical and medullary regions of all the lymph nodes. The lymphoid follicles, in most cases, had been destroyed. Lymphoid cellular depletion was also observed in the spleen and thymus. A disruptive cellular infiltrate was seen in the

kidney, liver, abomasum, lung and adrenal gland. A diffuse paracortical lymphocytic hyperplasia was detected in the prescapular lymph node draining the site of inoculation in the calf infected with *T. parva* (Muguga) whereas, extensive paracortical lymphoid cellular depletion occurred in the remaining lymph nodes. Lymphoid cellular depletion was also seen in the spleen and thymus. A disruptive cellular infiltrate was observed in the kidney and lung.

Examination of impression smears stained with Giemsa's stain detected macroschizonts, microschizonts and piroplasms in all or most of the lymphoid and non-lymphoid organs of the calves infected with *T. annulata* or *T. parva* (Muguga) by the terminal stages of disease. Analysis of tissue sections immunocytochemically labelled with monoclonal antibodies, which recognised schizont-infected cells, and counterstained with Harris's haematoxylin detected both macroschizont- and microschizont-infected cells in the lesions of all the infected calves.

Phenotypic analysis of both macroschizont- and microschizont-infected cells in tissue sections, immunocytochemically labelled with antibodies to parasite and bovine leucocyte surface markers, indicated *T. annulata* resided within myeloid cells which expressed CD11b, the C3bi complement receptor. In contrast, *T. parva* (Muguga) resided within cells which expressed CD3, the marker for T cells; this parasite also inhabited cells which expressed CD11b, which may have been B and/or natural killer (NK) cells.

Uninfected cells in the parasitised lymphoid organs of *T. annulata* or *T. parva* (Muguga) infected calves were phenotyped using monoclonal antibody IL-A15, a marker for macrophages, B and NK cells ($CD11b^+$), and polyclonal antibody A452, a marker for T cells ($CD3^+$). Results showed uninfected $CD11b^+$ cells, which may have been B and/or NK cells, were markedly increased in the medullary cords of the lymph nodes of both the *T. annulata* and *T. parva* (Muguga) infected animals. In contrast, there were markedly fewer uninfected $CD3^+$ cells in the paracortical regions of the lymph nodes, the spleen and thymus of these animals than in the lymphoid organs of normal cattle. Examination of the parasitised non-lymphoid organs of *T.*

annulata or *T. parva* (Muguga) infected calves detected infiltrates of both uninfected $CD11b^+$ and $CD3^+$ cells.

Assessment of apoptosis in the prescapular lymph node draining the site of inoculation of a calf undergoing the latter stages of infection with *T. annulata* (Hisar) using the TdT-mediated-dUTP-biotin nick end labelling (TUNEL) technique detected more apoptotic cells in this lymph node than in the prescapular lymph node of a normal calf.

The *in vitro* effect of NO on uninfected bovine cells and *T. annulata* macroschizont-infected cell lines was examined for the following reasons. PBM harvested from calves infected with *T. annulata* (Hisar) had produced NO *in vitro*, NO had been reported to induce apoptosis under other circumstances and damaged tissues in calves infected with *T. annulata* had been infiltrated with macrophages, a potential source of NO. Incubation of uninfected and parasitised bovine macroschizont cell lines with S-nitroso-N-acetyl-DL-penicillamine (SNAP), a NO donor, resulted in increased apoptosis in uninfected and parasitised bovine macroschizont cell lines as compared to uninfected and parasitised bovine macroschizont cell lines incubated in medium alone and caused malformation and elimination of schizonts. It was postulated that macrophage derived NO could be both detrimental to the host by inducing tissue damage and beneficial to the host by controlling the parasite.

CHAPTER ONE

INTRODUCTION

Tropical theileriosis (Dschunkowsky & Luhs 1904) and East Coast fever (Theiler 1904) are diseases of cattle caused by the tick-borne protozoan parasites *Theileria annulata* and *Theileria parva* respectively. These economically important diseases are endemic in tropical and sub-tropical regions, where an estimated 250 million cattle may be at risk from disease (Purnell 1978). Indigenous cattle breeds may be resistant to infection with *T. annulata* or *T. parva*, but imported high yielding European breeds of cattle and cross-bred progeny tend to be highly susceptible. A mortality rate up to 25% and 80% has been reported for indigenous and European breeds of cattle respectively (Delpy 1937). Although cattle may survive infection recovery is prolonged and often incomplete resulting in permanent debilitation, loss of productivity and a prolonged carrier state (Uilenberg 1981a; Irvin & Morrison 1987). Bovine tropical theileriosis and East Coast fever therefore impose serious constraints upon breed improvement programmes and livestock production.

When this project began, the clinical manifestations, macroscopic and microscopic lesions of *T. annulata* (Dschunkowsky & Luhs 1904; Sergent, Donatien, Parrot, Lestoquard, Plantureux & Rougebief 1924; Sergent, Donatien, Parrot & Lestoquard 1945; Neitz 1957; Gill, Bhattacharyulu & Kaur 1977; Baharsefat, Amjadi, Hashemi-Fesharki, Ahourai & Arbabi 1977; Srivastava & Sharma 1981; Eisler 1988) and *T. parva* (Steck 1928; Neitz 1957; De Kock 1957; Barnett 1960; Wilde 1966; DeMartini & Moulton 1973; Barnett 1977; Irvin & Morrison 1987) had already been documented. Although both *T. annulata* and *T. parva* were generally recorded as lymphoproliferative diseases (Irvin & Morrison 1987) the mechanisms underlying tissue damage were little understood and the *in vivo* identity of the schizont-infected cell was unclear. Both *T. annulata* (Sergent *et al.* 1945; Neitz 1957; Gill *et al.* 1977; Srivastava & Sharma 1981; Eisler 1988) and *T. parva* (Steck 1928, Cowdry & Danks 1933; Neitz 1957; De Kock 1957; DeMartini & Moulton 1973; Barnett 1977; Morrison, Buscher, Murray, Emery, Masake, Cook & Wells 1981a) have been reported to reside within the cytoplasm of lymphocytes. However *T. annulata* has

been reported to infect and transform not only lymphocytes but also cells of the reticulo-endothelial system (Sergent *et al.* 1945).

The primary objective of this study was to investigate the lesions of tropical theileriosis (*T. annulata* infection) in particular the identity of the schizont-infected cell and the contribution of macrophages to tissue damage. During the course of the study, tissues from a *T. parva* infected animal became available and were included for comparison. Macrophages were of interest because they had previously been shown in both infections with *T. annulata* and infections with *T. parva* to produce factors, in particular nitric oxide, known to be both detrimental and beneficial to the host.

It has been suggested that immune responses may be involved in tissue damage in *Theileria* infections. Therefore the investigation of the lesions of tropical theileriosis and the subsequent identification of potentially detrimental immune responses will be essential if potentially damaging antigens are not to be included in subunit vaccines. The importance of such investigations was highlighted by Cowdry & Danks (1933) who stated that "it is only by learning how the host responds to the parasite, and in some cases survives the attack, that we can hope rationally to plan therapeutic measures designed to increase its resistance and others to kill the parasites without at the same time seriously injuring the host".

CHAPTER TWO

LITERATURE REVIEW

2.1 IDENTIFICATION & CLASSIFICATION OF THE GENUS *THEILERIA*

The genus *Theileria* (Bettencourt, Franca & Borges 1907) comprises tick-transmitted parasitic protozoa belonging to the family Theileriidae, order Piroplasmida, subclass Piroplasmia, class Sporozoea and phylum Apicomplexa (Levine, Corliss, Cox, Deroux, Grain, Honigberg, Leedale, Loeblich, Lom, Lynn, Nerinfield, Page, Poljansky, Sprague, Vaura, & Wallace 1980). The taxonomy of the genus at the species level has been controversial and is still not satisfactorily resolved (Uilenberg 1976). Of the species of *Theileria* that infect cattle, *T. annulata* (Dschunkowsky & Luhs 1904) and *T. parva* (Theiler 1904) are among the most important.

Several criteria are used for the differentiation of *Theileria* species including serological characterisation by immunofluorescent antibody tests (Schindler & Wokatsch 1965), cross immunity tests, host specificity for the tick vector as well as for the mammalian host and biological differences detected by isoenzyme electrophoresis (Melrose, Brown & Sharma 1980a; Musisi, Kilgour, Brown & Morzaria 1981). In order to reach a definite conclusion as to the species of *Theileria* detected, a combination of criteria should be used (Uilenberg 1981a).

2.2 HOST RANGE, VECTORS & TRANSMISSION OF *T. ANNULATA* & *T. PARVA*

Members of the genus *Bos* (cattle), water buffaloes and American bison are susceptible to *T. annulata* infection in the field. The Asiatic water buffalo (*Bubalus bubalis*) is considered to be its natural host and the one in which it evolved (Uilenberg 1981b). The parasite causes mild infection in buffaloes and bison but can be highly pathogenic to cattle, especially taurine breeds. Cattle, Asiatic water buffalo and African buffalo are susceptible to *T. parva* infection in the field. The parasite causes mild infection in the African buffalo but can be highly pathogenic to cattle and Indian buffalo (Barnett 1968).

T. annulata is transmitted transstadially by two and three host ticks of the genus *Hyalomma*, but infected male ticks that accidentally become detached from one host

may reattach to another and transmit the disease to more than one animal (Sergent *et al.* 1945). *Hyalomma detritum, H. anatolicum* and *H. excavatum* are the principal vectors in the field (Uilenberg 1981b). *Hyalommid* ticks are restricted to areas with a warm climate and are prone to hide in crevices and the stone walls of stables where they remain dormant in the winter. The engorged adult tick can produce large numbers of infective sporozoites and 50, 000 sporozoites have been estimated to be present in a single type III alveoli cell of the tick salivary gland (Melrose, Walker & Brown 1980b). Since many such cells are generally infected, a bovine host may receive an enormous inoculum from a single tick feeding to repletion (Melrose *et al.* 1980b) and a single tick is capable of transmitting a fatal infection (Pipano, Samish & Krigel 1982). Only a few infected ticks may cause extensive disease out-breaks in herds of cattle.

The main tick vector of *T. parva* is the three host tick *Rhipicephalus appendiculatus.* The transmission of *T. parva* is achieved only by nymphs infected during the preceding larval stage or by adults infected during the preceding nymphal stage. Transovarial transmission does not occur, nor is there transmission between larva and adult if the intervening nymph feeds on a non-susceptible host. Although other *Rhipicephalus* species are less important vectors, they assist in maintaining the infection in the field. *Rhipicephalus* species are restricted to countries with a warm climate and an average annual rainfall of more than 10 inches (Theiler 1904). Adult cattle may contract fatal *T. parva* infection from the bite of a single tick (Lounsbury 1904).

2.3 DISTRIBUTION & IMPORTANCE OF *T. ANNULATA & T. PARVA*

The distribution of *T. annulata* and *T. parva* in the world are distinct and follow that of their main tick vectors. *T. annulata* occurs in northern Africa, Sudan, Eritrea, southern Europe, the Near and Middle East, southern parts of the former USSR, India, central Asia and southern China (Neitz 1957). *T. parva* occurs in eastern, central and southern Africa (Neitz 1957).

T. annulata and *T. parva* are among the most important tick borne parasites of cattle. These diseases cause extensive economic losses to individual farmers and

governments by lowering livestock production and through costs brought about for their control and research (Dolan & Young 1981). Economic losses vary widely within and among countries due to the differences in livestock production systems, cattle types, level of disease risk and disease control policies and programmes. It is estimated that some 250 million cattle may be at risk from the diseases they cause in endemic regions.

The diseases caused by *T. annulata* and *T. parva* are particularly important in breeding programmes aimed at improving the productivity of indigenous cattle (Rak 1978; Morzaria, Irvin, Wathanga, D'Souza, Katende, Young, Scott & Gettinby 1988) and in intensive dairy and beef units based upon imported European cattle (Robinson 1982). Indigenous Zebu cattle are more resistant than European breeds and cross-bred animals (Cordier, Menager & Delorme 1936). Most indigenous cattle have some natural resistance to *T. annulata* and *T. parva* due to a long evolutionary association with the parasite, which has helped to produce a state of endemic stability (Anon 1991).

Factors favourable for the occurrence and distribution of *T. annulata* and *T. parva* include: a dense population of either cattle or buffaloes; the availability of vertebrate reservoirs; partial or complete absence of fences; uncontrolled movement within an endemic area or into potential endemic regions; negligence of owners in reporting mortality; high incidence of vectors; no dipping tanks and shortage of acaricides; uncontrolled movement of hay and skins from infected farms into potential endemic areas of *T. annulata* and *T. parva* (Neitz 1957).

The disease caused by *T. annulata* is highly pathogenic to susceptible, European or improved breeds of cattle causing 40-60% mortality (Brown 1990). It has been estimated that mortality varies from 35-40% in Palestine (Adler & Ellenbogen 1934), 20-40% in Algiers (Donatien & Lestoquard 1938), up to 76% in India (Sen & Srinivasan 1937), approximately 75% in Bulgaria (Pavlov 1942) and up to 90% in the endemic regions in Russia (Yakimoff & Goussef 1936). Experience in southern Africa has shown that the mortality rate in susceptible calves and adult stock infected with *T. parva* varies from 78% to more than 95% (Dolan & Young 1981).

Animals which have recovered from both *T. annulata* and *T. parva* infections may still suffer from weight loss, produce low milk yields and experience reduced fertility and delays in reaching maturity (Neitz 1957). For example, the estimated total direct cost of *T. parva* in terms of beef, milk, treatment and research of the disease, in eleven countries in eastern, central and southern Africa, has been estimated at $168 million per year, including an estimated mortality of 1.1 million cattle (Mukhebi, Perry & Kruska in press). The value of beef and milk loss from cattle morbidity was estimated to be three times as high as the loss from mortality.

2.4 LIFE CYCLE OF *T. ANNULATA* & *T. PARVA*

The life cycle of *T. annulata* (Fig. 2.1) is similar to that of *T. parva* (Mehlhorn & Schein 1984). Piroplasms in the erythrocytes of the host are ingested with the blood meal of the tick and develop into microgametes and macrogametes. The gametes fuse to form zygotes which invade the epithelial cells of the tick gut. The sexual stages occur in the tick gut (Dschunkowsky & Luhs 1904; Cowdry & Ham 1932; Mehlhorn & Schein 1984). A motile kinete forms within the zygote which is liberated into the tick body cavity prior to migration to the salivary glands via the haemolymph. Kinetes invade epithelial cells of the tick salivary glands and develop into large sporoblasts within which many thousands of sporozoites develop.

The infective sporozoites are liberated into the saliva and inoculated through the skin of the host as the tick feeds for 48-72 hours (Singh, Jagdish, Gautam & Dhar 1979). Mature sporozoites are oval-shaped measuring about 1μm in length. They rapidly enter host cells in a receptor-dependent manner and develop within the cells becoming multinucleate schizonts (Jura, Brown & Kelly 1983). The schizonts vary in diameter from 1-15μm, with an average of about 8μm (Neitz 1957; Mehlhorn & Schein 1984) and harbour chromatin granules varying from 0.4-2.0 μm in diameter. The macroschizont stimulates the host cell to divide and transform into a blasting cell and thereafter the parasite divides synchronously with the host cell as it undergoes mitosis (Hulliger 1965; Bloom 1979; Stagg, Chasey, Young, Morzaria & Dolan 1980). Initially macroschizonts have large chromatin granules and are detectable in smears made from superficial lymph nodes and the liver 7 to 28 days after infection (Sergent *et al.* 1945). The division of the macroschizont-infected

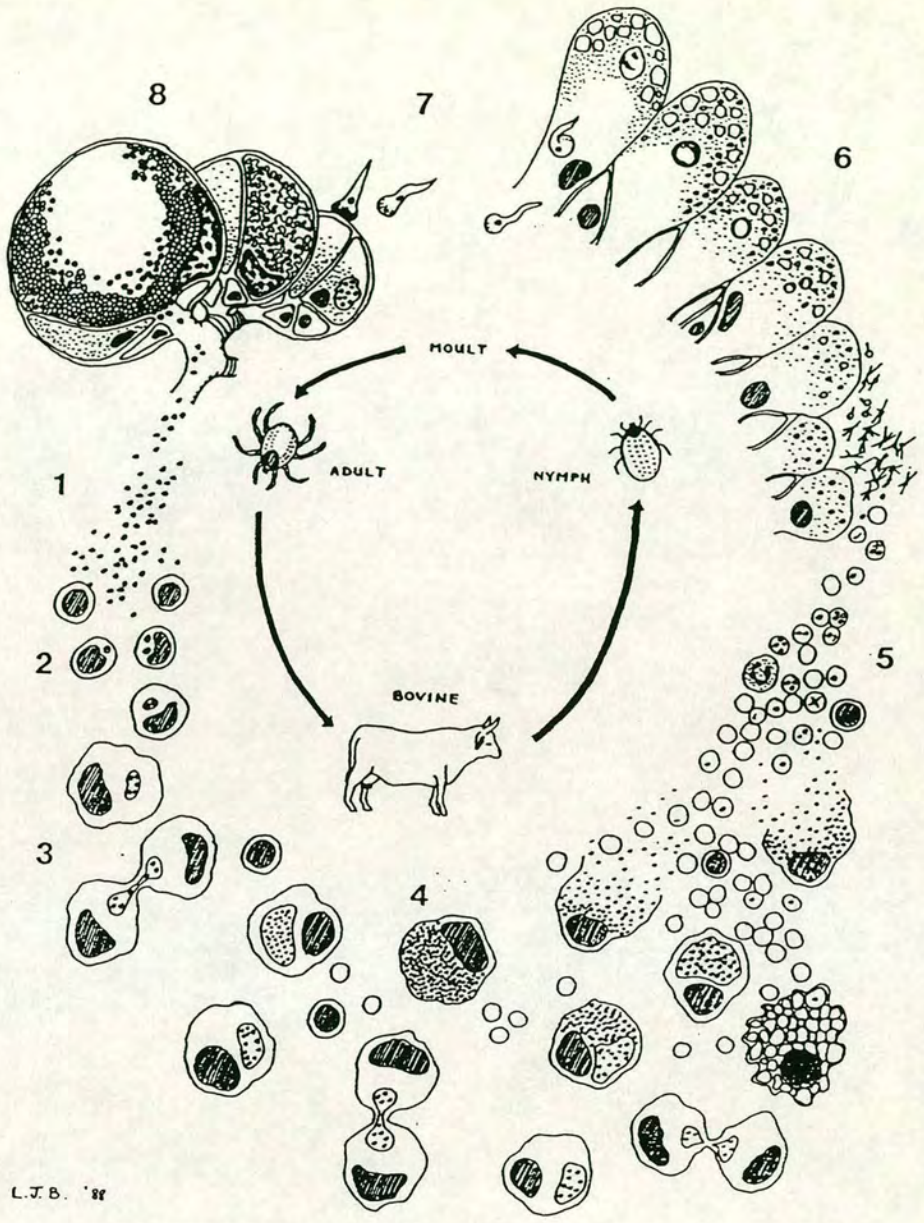

Figure 2.1 Life cycle of *T. annulata.*

1 sporozoites entering bovine host in tick saliva; **2** trophozoites within host cells; **3** macroschizonts within transformed host cells; **4** microschizonts within a host cell; **5** liberated micromerozoites invading erythrocytes to become piroplasms; **6** gamogony cycle in tick gut cells; **7** kinetes in haemolymph; **8** sporogony cycle in tick salivary glands (Figure prepared by Leslie Bell-Sakyi).

cells has been implicated as the main cause of tissue damage (Wilde 1963; Jarrett, Crighton & Pirie 1969; Emery 1981; Irvin & Morrison 1987), but the importance of extracellular parasite division and/or parasite reinvasion remains to be determined. Reinvasion has been suggested to be a common occurrence (Barnett 1968). Later, a generation of schizonts called microschizonts develops with small chromatin granules (Jarrett & Brocklesby 1966). Microschizonts contain chromatin granules varying from 0.3-0.8 μm in size and the mature microschizonts subsequently liberate micromerozoites 0.7-1.0 μm in diameter. Merozoites liberated from microschizonts invade the erythrocytes (Mehlhorn & Schein 1984) to become piroplasms, thus completing the life cycle. Merozoites are detected in erythrocytes one to three days after the first appearance of schizonts and may persist for years in infected cattle.

The schizonts of *T. annulata* are indistinguishable from those of *T. parva* (Sergent *et al.* 1945; Neitz 1957). The intra-erythrocytic piroplasms of *T. annulata* are generally spherical and vary in diameter from 0.5-1.5μm (Neitz 1957). Whereas, the intra-erythrocytic piroplasms of *T. parva* are generally rod-shaped measuring 1-2μm (Koch 1898). The merozoites of *T. annulata* divide within the erythrocytes to produce four daughter merozoites which in turn are liberated to invade other erythrocytes (Conrad, Kelly & Brown 1985; Conrad, Denham & Brown 1986). However, intra-erythrocytic division is uncommon in *T. parva* and most merozoites are derived directly from microschizonts.

2.5 PARASITISED HOST CELL PHENOTYPE OF *T. ANNULATA* & *T. PARVA*

2.5.1 HOST CELL PHENOTYPE OF *T. ANNULATA*

Although the schizonts (macroschizonts and microschizonts) of *T. annulata* were initially reported to reside within both the lymphocytes and reticulo-endothelial cells of the tissues of infected cattle (Sergent *et al.* 1945), it was subsequently generally accepted that schizonts resided only within lymphocytes (Neitz 1957; Gill *et al.* 1977; Srivastava & Sharma 1981; Eisler 1988). Recent work on the identification of the host cells that support growth of *T. annulata* macroschizonts has concentrated on the phenotypic analysis of macroschizont-infected and transformed cell lines using flow cytometry and monoclonal antibodies (MAbs) to bovine leucocyte antigens.

The majority of *in vitro* derived *T. annulata* cell lines all express major histocompatibility complex (MHC) class II antigens, lack the T cell markers CD4 and CD8 and rapidly lose B cell and monocyte markers (Spooner, Innes, Glass, Millar & Brown 1988; Spooner, Innes, Glass & Brown 1989; Glass, Innes, Spooner & Brown 1989). The MHC class II positive cells are either infected initially or class II expression is switched on by the infection. *In vitro* the sporozoites of *T. annulata* infect and transform B cells and monocytes/macrophages with a much greater efficiency than T cells (Glass *et al.* 1989; Innes, Miller, Glass, Brown & Spooner 1989a; Spooner *et al.* 1989). The sporozoites infect both immature and mature monocytes, but more readily infect mature populations. All monocytes lose the expression of CD14 (the lipopolysaccharide receptor) upon infection by the sporozoites (Campbell, Brown, Glass, Hall & Spooner 1994).

In addition, *in vitro* derived *T. annulata* cell lines express the T cell markers bovine (Bo) CD3 and J5 (Ahmed, Rehbein & Schein 1984; Naessens, Newson, Bensaid, Teale, Magondu & Black 1985; Spooner *et al.* 1988; Glass *et al.* 1989). However, these markers indicate cell activation rather than cell lineage. The production of type 1 interferon (IFN) by *T. annulata* schizont-infected cells (Entrican, McInnes, Logan, Preston, Martinod & Brown 1991; Preston, Brown, Entrican, Richardson & Boid 1993) is consistent with the previous indications that bovine cells infected with this parasite are predominantly macrophage-like (Spooner *et al.* 1989).

In vivo derived *T. annulata* cell lines express CD3, gamma-delta TCR and CD2 (Howard, Sopp, Preston, Jackson & Brown 1993). In addition they have been shown to express MHC class II antigens, CD11b, IL-A24, IL-A96, J5 , CD4, CD8 and IL-A109 (Forsyth, Jackson, Wilkie, Sanderson, Brown & Preston in press). The finding of this pattern of expression of leucocyte antigens on *in vivo* derived cell lines suggests sporozoites may well invade different cells *in vivo* and *in vitro* and/or that macroschizont-infected cells *in vivo* may express an unusual pattern of surface molecules. If this is the case, such events may have a profound influence on the pathogenesis of the disease (Howard *et al.* 1993; Forsyth *et al.* in press).

2.5.2 HOST CELL PHENOTYPE OF *T. PARVA*

T. parva has been reported to reside within the lymphocytes of the tissues of infected cattle (Steck 1928, Cowdry & Danks 1933; Neitz 1957; De Kock 1957; DeMartini & Moulton 1973; Barnett 1977; Morrison *et al.* 1981a). Recent work on the identification of the host cells that support growth of *T. parva* macroschizonts has concentrated on the phenotypic analysis of macroschizont-infected and transformed cell lines using flow cytometry and MAbs to bovine leucocyte antigens. The majority of *in vitro* derived *T. parva* cell lines are subsets of T lymphocytes, B lymphocytes and null cells (Duffus, Wagner & Preston 1978; Emery 1981; Pinder, Withey & Roelants 1981; Baldwin, Black, Brown, Conrad, Goddeeris, Kinuthia, Lalor, McHugh, Morrisson, Morzaria, Naessens & Newson 1988; Morrison, Goddeerris, Brown, Baldwin & Teale 1989) and not monocytes (Lalor, Morrison & Black 1986). It has been suggested that *T. parva* may infect and transform not only lymphocytes but also cells of the monocyte/macrophage lineage (Moulton, Krauss & Malmquist 1971). Interestingly, a large proportion of $CD4^+/CD8^+$ infected lymphocytes appear in peripheral blood mononuclear cells (PBM) and efferent lymphatic lymphocytes and persist until death of the host (Emery, MacHugh & Morrison 1988). Lymphocytes which coexpress these markers can not be detected in populations of cells obtained from PBM or lymph nodes of healthy cattle. Coexpression of CD4 and CD8 molecules have been demonstrated on > 30% of human T cells activated by mitogens (Blue, Daley, Levine & Schlossman 1985) and on a similar proportion of rat T cells activated by mitogen or alloantigens (Bevan & Chisholm 1986).

Although *T. parva* schizont-infected cell lines express markers for MHC class II determinants (Baldwin, Goddeeris & Morrison 1987; Conrad, Baldwin & Brown 1989), these markers indicate cell activation rather than cell lineage. In addition, *T. parva* macroschizont-infected cells produce interferon gamma (IFN-γ) (Entrican *et al.* 1991; DeMartini & Baldwin 1991) which is in accordance with the parasite's apparent preference for T and B cells (Dobbelaere, Prospero & Roditi 1990). Analysis of *in vitro* derived *T. parva* cell lines with a panel of MAbs to lymphocyte cell surface antigens show considerable heterogeneity in the phenotype of different clones of infected T cells (Lalor *et al.* 1986).

In summary, there are both similarities and differences between cell lines infected with *T. annulata* and *T. parva*. Cells infected with both parasites express class I antigens to a similar degree (Spooner & Brown 1980). Whereas, the most striking difference is that *T. annulata* cell lines seldom express CD4 or CD8 markers unlike *T. parva* cell lines. Such observations have important implications in the pathogenesis of the disease since schizont-infected cells of different phenotype may behave differently and so cause different disease patterns. When this work began there were no reports of any attempts to characterise schizont-infected cells in tissues from cattle infected with either *T. annulata* or *T. parva* using phenotypic markers.

2.6 CLINICAL RESPONSES OF *T. ANNULATA* & *T. PARVA*

2.6.1 CLINICAL RESPONSES OF *T. ANNULATA*

The clinical responses of animals infected with Russian (Dschunkowsky & Luhs 1904) and North African (Sergent *et al.* 1945) stocks of *T. annulata* have been investigated. Depending on the virulence of the strain and the resistance of the animal, the disease caused by *T. annulata* may be classified according to its symptoms into mild, peracute, acute, subacute and chronic forms (Neitz 1957).

The mild form is usually observed in cattle, particularly young calves, infected with a relatively mild *T. annulata* strain. Frequently animals pass through the reaction without exhibiting any symptoms and the presence of the infection may be entirely overlooked.

The peracute form is of fairly common occurrence with sudden onset. The affected animal has a high temperature and shows listlessness, drooping ears, lowered head, lachrymation, serous nasal discharge, salivation, swelling of superficial lymph nodes, muscular tremours, sluggish gait, marked drop in milk production, accelerated pulse, dyspnoea, anorexia, constipation and also anaemia and icterus. Death occurs fairly rapidly and is preceded by hypothermia (Neitz 1957).

In the acute form of the disease the affected animal usually exhibits pronounced symptoms often terminating fatally. There is an elevation of body temperature which persists for 5-20 days with clinical symptoms usually appearing a few days after the

initial rise in temperature. The animal shows inappetence, cessation of rumination, drooling from the mouth, serous nasal discharge, swelling of the superficial lymph nodes, swelling of the eyelids, lachrymation, accelerated pulse, general weakness, drop in milk production and on some occasions nervous symptoms (Khanna, Kharole, Dhar & Gautam 1980). Leucopenia is a prompt and normal response which coincides with the onset of the febrile reaction (Laiblin 1978; Preston, Brown, Bell Sakyi, Richardson & Sanderson 1992a). As described by Neitz (1957), in the course of a few days marked anaemia develops with bilirubinaemia and bilirubinuria present. At the beginning of the pyrexial period the faeces are firm but diarrhoea soon sets in, and when the disease runs a prolonged course, the evacuations are frequently mixed with blood and mucus. The animal becomes markedly emaciated and assumes a recumbent position. If regeneration of the erythrocytes does not take place, anaemia becomes so severe and dyspnoea so pronounced that death ensues 8-15 days after onset of disease. The severe anaemia may be a result of the progressive failure of the bone marrow to develop new blood cells (Laiblin 1978). Autoimmune mechanisms have been suggested as playing a role in the pathogenesis of the anaemia (Hooshmand-Rad 1976).

The subacute form as described by Neitz (1957) is often encountered in animals suffering from relatively mild strains of *T. annulata*. The symptoms resemble those of the acute form but are not so marked. Animals usually recover from this form but instances of abortion have been recorded.

The chronic form takes a more protracted course than either the acute or subacute type. The fever is irregularly intermittent. Inappetence, marked emaciation and a variable degree of anaemia and icterus are observed. Animals may recover after about four weeks but it may take two months and longer before the animals regain their former condition. In other instances the disease may suddenly assume an acute form and terminate fatally in one or two days.

Experimental and field observations have shown that there is a wide variation in the virulence between the various strains of *T. annulata*. Not only does this difference exist between strains of different countries but it has also been observed between

strains isolated from the same endemic region (Sergent *et al.* 1945; Rampon 1948; Pipano 1989).

2.6.2 CLINICAL RESPONSES OF *T. PARVA*

T. parva may be classified according to its symptoms into acute, subacute and mild forms (Neitz 1957). The acute form is the usual type observed. The affected animal exhibits pronounced symptoms usually terminating fatally. There is an elevation in the body temperature. A severe leucopenia coincides with the onset of the febrile reaction (Steck 1928; Wilde 1966). A rapid drop in temperature takes place before death. Clinical symptoms usually appear a few days after the initial rise in temperature. The animal shows inappetence, cessation of rumination, serous nasal discharge, lachrymation, sometimes swelling of the eyelids, ears and jowl region, swelling of the superficial lymph nodes, general weakness and a decreased milk production and in some cases icterus. At the beginning of the pyrexia the faeces are firm but diarrhoea usually sets in with evacuations frequently mixed with blood and mucus. The animal becomes markedly emaciated and resumes a recumbent position and often coughs. The respiration becomes accelerated and dyspnoea becomes pronounced shortly before death. A variable amount of froth exudes from the nostrils. Non-regenerative anaemia in which erythrocytes fall to 50% of normal together with a deficiency of platelets and icterus have been reported on occasion as a prominent feature of the disease. Pregnant cows may abort. An atypical cerebral form of *T. parva* has also been described (Flanagan & Le Roux 1957). A small proportion of animals, usually about 5%, may recover but convalescence is prolonged and the animals remain emaciated and unproductive for months.

The subacute form is often encountered in calves and to a lesser extent in adult stock in the endemic regions of east Africa. The symptoms resemble those of the acute form but are not so pronounced. Animals usually recover from this form but it may take several weeks before they regain their former condition. Clinical symptoms in the mild form include a relatively mild fever, listlessness and swelling of the superficial lymph nodes (Neitz 1957).

In summary, in lethal infections with *T. annulata*, death is usually delayed until piroplasm parasitaemia and haemolytic anaemia are well advanced (Barnett 1977; Preston *et al.* 1992a). In contrast, lethal infections with *T. parva* progress rapidly, accompanying proliferation of schizont-infected cells, pyrexia, lymphoid depletion and lymphocytolysis (Morrison *et al.* 1981a). Studies on naturally and artificially infected cattle have established that the severity of *T. annulata* and *T. parva* infection usually depends upon the virulence of the parasite strain (Neitz 1957), the breed and resistance of the animal (Pipano 1989) and the intensity and duration of the parasitic attack (Wilde 1967; Irvin & Mwamachi 1983; Preston *et al.* 1992a). The cause of death in the majority of cases of *T. annulata* and *T. parva* infected animals appears to be respiratory failure due to pulmonary oedema. However, if animals were not to develop respiratory symptoms, they might eventually die due to the widespread destruction of lymphoid and haemopoietic tissues.

2.7 MACROSCOPIC LESIONS OF *T. ANNULATA* & *T. PARVA*

2.7.1 MACROSCOPIC LESIONS OF *T. ANNULATA*

In animals infected with *T. annulata* the carcass is typically emaciated, anaemic and icteric with gelatinous connective tissues (Dschunkowsky & Luhs 1904; Sergent *et al.* 1924; Sergent *et al.* 1945; Neitz 1957). Numerous petechiae or larger haemorrhages are seen in the subcutaneous tissues and on the mucous and serous membranes. The superficial and internal lymph nodes are markedly swollen and often haemorrhagic. The spleen is enlarged mainly as a result of hyperplasia of lymphoid tissue and the Malpighian corpuscles are prominent. The thymus is mildly congested (Srivastava & Sharma 1981).

Petechiae may be present in the cortex of the adrenal glands. The kidneys are congested and show a variable number of "infarcts". The liver is enlarged with parenchymatous degeneration evident. The gall bladder is often markedly distended with dark green viscid bile. The abomasum usually shows characteristic ulcers consisting of a central necrotic area surrounded by a haemorrhagic zone. Similar ulcers may be encountered along the entire length of the small and large intestine. The lungs are frequently oedematous. The mucous membranes of the pharynx, larynx, trachea and bronchi are often spotted with petechiae. The myocardium shows

signs of muscular degeneration and a variable number of petechiae appear on the epicardium and endocardium (Dschunkowsky & Luhs 1904; Sergent *et al.* 1924; Sergent *et al.* 1945; Neitz 1957). Cerebral haemorrhages have been observed in affected animals (Barboni 1942). In some cases, parasitic embolisms result in cutaneous nodules on the skin (Manickam, Dhar, Singh & Kharole 1984).

2.7.2 MACROSCOPIC LESIONS OF *T. PARVA*

In animals infected with *T. parva* the carcass is typically emaciated. The mucous membranes may be unaffected, slightly hyperaemic or even anaemic. Muscles and fat appear normal. Petechial haemorrhages are commonly seen under the tongue. Anaemia and icterus may be seen in protracted cases. (Irvin & Mwamachi 1983). There is a variable degree of enlargement of peripheral and visceral lymph nodes, which results from hyperplasia and necrosis of cells of the lymphocyte series, as well as oedema. The nodes are sometimes discoloured by haemorrhage. Splenomegaly may be present with prominent Malpighian corpuscles. The thymus may be enlarged in young animals (Neitz 1957).

Petechiae may be present in the cortex of the adrenal glands. The kidneys frequently exhibit raised red or white foci of "infarcts" which are aggregations of large lymphoid cells. The liver may be congested and small haemorrhages are detected (De Kock 1957). The gall bladder may be markedly distended with dark green viscid bile. The mucosa of the abomasum is generally thickened due to lymphoid hyperplasia and congested. The abomasum shows characteristic ulcers which consist of a central necrotic area surrounded by a haemorrhagic zone. Peyer's patches are swollen. Severe pulmonary oedema is the most prominent feature at necroscopy (Gray & Robertson 1902). There is a copious amount of froth in the bronchi and trachea and often also in the nasal passages. Emphysema of the lungs may develop. The myocardium is flabby and a variable number of petechiae appear on the epicardium and endocardium. The meninges may be slightly congested and the brain may show lesions (Giles, Davies, Duffus & Heinosten 1978). Nodular skin lesions have been described in a small number of cases; it is conceivable that their development is strain-dependent (Uilenberg & Zwart 1979).

In summary, the macroscopic lesions in *T. annulata* resemble those of *T. parva*, but the greater erythrocyte destruction in *T. annulata* infected animals is evident by the watery blood, pale muscles and yellowish connective tissue (Barnett 1977). The macroscopic lesions in animals infected with *T. annulata* (Neitz 1957) or *T. parva* (Irvin & Mwamachi 1983) vary according to the duration and severity of the disease.

2.8 MICROSCOPIC LESIONS OF *T. ANNULATA* & *T. PARVA*

2.8.1 MICROSCOPIC LESIONS OF *T. ANNULATA*

Past reports have described the microscopic lesions seen in *T. annulata* infected animals as usually involving congestion and haemorrhages in lymphoid and non-lymphoid organs (Sergent *et al.* 1924; Gill *et al.* 1977; Baharsefat *et al.* 1977; Srivastava & Sharma 1981). Lesions may resemble those observed in haemorrhagic septicaemias (Sergent *et al.* 1924; Sergent *et al.* 1945). It has been suggested that haemorrhages are caused by toxins (Neitz 1957), but such substances have not yet been isolated. Microscopically the blood shows degenerative and regenerative changes (Neitz 1957).

In animals infected with Indian stocks of *T. annulata* the lymph nodes show proliferative changes characterised by a diffuse hyperplasia of the lymphoid follicles of the cortex. Occasionally, as a result of the fusion of the follicles, the cortex is replaced by a sheet of lymphocytes which often extends into the medullary zone. Medullary sinuses are inflammed with large numbers of macrophages (Gill *et al.* 1977). Blastogenesis of uninfected cells has been noted to accompany the replication of schizont-infected cells throughout the lymphoid and reticulo-endothelial tissues (Eisler 1988). Capillaries are filled with erythrocytes with some focal haemorrhages. Some lymph nodes show depletive changes characterised by a loss of distinction between the cortex and the medulla. With the progress of the infection the lymphopoietic tendency is exhausted as evident from depletion of the lymphoid cells at the germinal centres leading to their regression and degeneration. (Gill *et al.* 1977; Baharsefat *et al.* 1977). The white pulp of the spleen is surrounded by irregular wide eosinophilic zones, while germinal centres show some degree of necrosis. The red pulp of the spleen is congested and haemorrhagic with large amounts of

haemosiderin scattered throughout. (Gill *et al.* 1977; Baharsefat *et al.* 1977). Degenerative changes are also seen in the thymus (Srivastava & Sharma 1981).

The intertubular vessels of the kidneys are congested and degenerative changes are seen in the lining cells of the tubules. Focal aggregations of lymphocytes were also seen in the perivascular areas of the kidneys. The liver shows diffuse infiltration of the periportal areas by large numbers of lymphocytes and the hepatic cells show moderate fatty changes. Haemorrhagic ulceration is seen in the abomasal mucosa extending to the lamina propria and the muscularis mucosa layers. The intercellular spaces were distended and infiltrated by large numbers of neutrophils, macrophages, lymphocytes and plasma cells (Sergent *et al.* 1924; Gill *et al.* 1977; Baharsefat *et al.* 1977; Srivastava & Sharma 1981). Increases of calcium, chloride and sodium ions and of total protein in the contents of the abomasum during the acute stage of *T. annulata* infection have been reported. It has been suggested that the loss of these ions and proteins from the interstitial fluid into the lumen of the digestive tract may explain the rapid debilitation of diseased cattle (Ouhelli, Dakkak & Ouazzani 1987). The lungs show thickened interalveolar septa with prominent blood vessels and at places haemorrhages in the alveolar spaces. The heart shows degeneration of myocardial fibres and diffuse infiltration of the intermysial area by a large number of lymphocytes and macrophages, which cause atrophy of the surrounding musculature (Gill *et al.* 1977). Changes in the brain include a mild swelling of the vascular endothelial cells and areas of perineuronal and perivascular oedema (Gill *et al.* 1977; Baharsefat *et al.* 1977). Skin lesions include epidermal ulcers, haemorrhage, oedema, necrosis and inflammatory cell infiltration by neutrophils and lymphocytes, many of the latter containing parasites (Manickam *et al.* 1984).

Schizonts can be detected in the lymph nodes, spleen, thymus, kidneys, liver, lamina propria of the gut, interstitial tissues of the lungs, brain (Dschunkowsky & Luhs 1904; Sergent *et al.* 1945; Neitz 1957) and skin (Manickam *et al.* 1984).

2.8.2 MICROSCOPIC LESIONS OF *T. PARVA*

The lymph nodes of the *T. parva* infected animals do not show the normal clear demarcation into cortical and medullary regions and extensive areas of hyperplasia,

haemorrhage and necrosis are often present in the paracortical zone (DeMartini & Moulton 1973; Irvin & Morrison 1987). It has been suggested that haemorrhages are caused by toxins (Neitz 1957; Barnett 1960), but such substances have not yet been isolated. Medullary sinuses show a large number of macrophages with the remains of damaged cells (De Kock 1957; Barnett 1960). With the progress of the infection the lymphopoietic tendency is exhausted as evident from depletion of the lymphoid cells at the germinal centres leading to their regression and degeneration (Barnett 1960; DeMartini & Moulton 1973) and lymphocytolysis is observed in the paracortical zone (Irvin & Morrison 1987).

The rapid growth of schizont-infected and uninfected lymphoid cells with their concomitant destruction appears to be the main cause of tissue damage (Wilde 1963; Jarrett *et al.* 1969; Emery 1981; Irvin & Morrison 1987). This appears to be the result of the activation of specific protective cytotoxic T lymphocytes and natural killer cells (NK) (Emery, Eugui, Nelson & Tenywa 1981a). Lymphocyte destruction causes a fall in serum immunoglobulin levels (Spooner, Penhale, Burridge & Brown 1973). It is possible that the massive destruction of lymphocytes by the schizonts leads to a deficient immune response (Sharpe & Langley 1983) and therefore results in immunosuppression (Wagner, Jessett, Brown & Radley 1975). This may enhance the progress of the disease and facilitate secondary respiratory infections which may eventually prove fatal. The mechanism by which lymphocytolysis occurs remains obscure. While infection with the parasite itself may result in the destruction of some cells, it is unlikely to account for the widespread cell death which occurs. It has been suggested that auto-antibodies may contribute to lymphocytolysis (Wilde 1967), but so far no evidence has been obtained for the presence of anti-lymphocyte antibodies (Wagner & Duffus 1974) or of antibody-mediated lytic reactions (Creemers 1982) in clinical disease. It is probable that material released from dying cells will have a toxic effect exacerbating the process of cellular destruction. Free schizonts are numerous during this latter stage of the disease (DeMartini & Moulton 1973).

The spleen shows changes similar to those observed in the lymph nodes. The periphery of the white pulp assumes an irregular and frayed appearance and eventually it is no longer possible to define the boundaries between the white and red

pulps. There is also an irregular discharge of lymphocytic cells from the white pulp into the red pulp where they are irregularly dispersed amongst the red cells. The red pulp is often congested (De Kock 1957). There is usually atrophy of the thymus, with a marked depletion of lymphocytic cells, which often contains areas of haemorrhage.

The adrenal gland is regularly affected with the occurrence of large numbers of lymphocytic cells which vary in their distribution, frequency, size and shape. Lymphocytic cells are observed as nodular-like formations but more often they are irregularly distributed in streaks between columns of parenchymal cells. In most instances the zona reticularis is implicated. Large aggregates of these cells caused a certain amount of atrophy and degeneration of adjacent adrenal gland parenchyma. Kidneys reveal congestion of intertubular vessels and degenerative changes in the lining of the tubules. Focal areas of infiltration of the interstitial spaces of the cortex mostly and of the medulla occasionally by lymphocytes are also present (De Kock 1957). The liver shows signs of congestion with large numbers of lymphocytic cells in the sinusoids and central veins. There may be a diffuse fatty infiltration or presence of hyaline droplets. The erosions and ulcers in the mucous membranes of the gastrointestinal tract result from localised superficial necrosis associated with extensive proliferation of lymphoblastoid cells in the propria. Lungs show thickened interalveolar septa with prominent blood vessels and at places haemorrhages in the alveolar spaces. The endothelial lining of blood vessels becomes affected resulting in oedema of the lungs. It has been suggested that pulmonary congestion and oedema are related to lymphocytolysis of schizont-infected cells within the lungs (Irvin & Morrison 1987).

The heart shows degeneration of myocardial fibres and diffuse infiltration of intermysial area by a large number of mononuclear cells, lymphocytes and macrophages, which caused atrophy of the surrounding musculature. The brain shows signs of acute congestion, oedema and haemorrhage and the capillaries are filled with parasitised lymphoblastoid cells (Giles *et al.* 1978). Skin lesions included epidermal ulcers, haemorrhage, oedema, necrosis and inflammatory cell infiltration

by polymorphonuclear and mononuclear cells and parasitised lymphocytes (Kimeto 1978).

Schizonts do not appear to be restricted to particular compartments within the lymphoid tissues, although in the lymph node cortices and splenic white pulp they tend to be more numerous in the T dependent areas than in the B dependent areas (Morrison, Buscher, Emery, Nelson & Murray 1981b). The schizonts can be detected in the lymph nodes, spleen, thymus, adrenal glands, kidneys, liver, lamina propria of the gut, interstitial tissues of the lungs, brain (Steck 1928; Neitz 1957; Barnett 1960) and skin (Kimeto 1978).

In summary, as described by Neitz (1957) and Barnett (1960), previous microscopic findings were essentially the same in *T. annulata* (Neitz 1957) and *T. parva* (Barnett 1960) infected animals, except that the erythrocytes of *T. parva* infected animals, unlike those of *T. annulata* infected animals, showed no degenerative or regenerative changes (Neitz 1957). As described above for the clinical responses (2.6) the microscopic lesions in animals infected with *T. annulata* (Neitz 1957; Gill *et al.* 1977) or *T. parva* (Neitz 1957) varied according to the duration and severity of the disease. It should be noted that it is not at all clear which cells are infected, whether macrophages or lymphocytes, or even which lymphoid cells, whether B lymphocytes or T lymphocytes, were being referred to in the literature summarised above.

2.9 IMMUNE RESPONSES OF *T. ANNULATA* & *T. PARVA*

To date, there has been very little work done on the physiological mechanisms underlying damage. Since the only indications of possible processes come from work on protective immune mechanisms, these observations will be discussed before reviewing potential mechanisms of damage.

Antibodies against *T. annulata* (Preston & Brown 1985) and *T. parva* (Musoke, Nantuyla, Buscher, Masake & Otim 1982) sporozoites have been detected. However, it appears that the short time period in which sporozoites are free in the host's tissues after being injected by the tick and before they enter their target cells together with

the continuous intracellular location of the schizonts offer little opportunity for circulating antibody to act upon the parasites.

There is evidence that cell-mediated immune mechanisms are involved in protective immunity to both *T. annulata* and *T. parva* schizont-infected cells. Importantly, the expression of a cell mediated immune response involves inflammation, lymphocyte infiltration, macrophage accumulation and activation, and may therefore cause pathological changes (Zinkernagel 1979).

Immunity against *T. annulata* involves cytostatic macrophages (Preston & Brown 1988) and two kinds of cytotoxic effector cells, specific MHC class I restricted T lymphocytes which destroy the schizont-infected cells and cytotoxic cells (possibly NK cells) that destroy schizont-infected cells in a non-restricted manner (Preston, Brown & Spooner 1983; Innes *et al.* 1989a). Cytotoxic cells have been detected in animals that recover from *T. annulata* infection, but not in those succumbing to infection (Preston *et al.* 1983). T cells are thought to be important components of defence mechanisms against intracellular parasites because of their ability to release cytokines, such as IFN-γ, which activate macrophages to kill intracellular parasites (Scott, Pearce & Cheever 1989). Genetically restricted lysis of *T. annulata* macroschizont-infected cell lines by lymphocytes from cattle immune to *T. annulata* (Preston *et al.* 1983) has provided circumstantial evidence that *T. annulata* macroschizont-infected cells possess infection associated antigens on their surface membranes.

Immunity against *T. parva* involves the class I restricted cytotoxic T lymphocytes (Eugui & Emery 1981; Morrison *et al.* 1989) and non-restricted cytotoxic cells (Pearson, Lundin, Dolan & Stagg 1979). It is thought that host T cells recognise *Theileria* associated antigens on the surface of the infected lymphocyte (Pearson *et al.* 1979). Recovery from *T. parva* infection can be correlated with the production of the MHC restricted T cells (Emery *et al.* 1981a; Emery, Tenywa & Jack 1981b; Eugui & Emery 1981). It is not known if cytotoxic cells detected in cattle undergoing lethal infections are infected with the parasite.

Nitric oxide (NO) has been implicated in the protective immune mechanisms against both *T. annulata* and *T. parva* (Visser, Abraham, Brown & Preston 1995) and has been suggested as a mediator of the macrophage anti-*Theileria* cytostatic activity described by Preston & Brown (1988).

While bovine recombinant tumour necrosis factor (BorTNF), BorIFN-γ, human interferon alpha (HuIFN-α), human interleukin 1 (HuIL-1) and HuIL-2 have all been shown to inhibit the *in vitro* development of trophozoite-infected cells of *T. annulata* and *T. parva* (Preston, Brown & Richardson 1992b), indicating a fundamental role for cytokines in the rapidly expressed solid resistance observed to sporozoite challenge which follows recovery from infection, none of these cytokines inhibited the proliferation of established *T. annulata* and *T. parva* macroschizont-infected cell lines. Indeed, TNF-α and IL-2 consistently enhanced proliferation of both species and the blastogenesis of uninfected cells in trophozoite-infected cultures. The ways by which cytokines modify development of trophozoite-infected cells (Preston *et al.* 1992b) are as yet unknown, but IFN-α, IFN-γ and TNF-α may act directly on the parasite or host cell to render it uninhabitable for the parasite, as suggested by work with IFN-γ and *Toxoplasma gondii* and *Plasmodium bergei* (Pfefferkorn 1984; Schofield, Ferreira, Altszuler, Nussenzweig & Nussenzweig 1987).

It is generally held that immunity to *T. annulata* and *T. parva* is potentially very effective but may develop too slowly to protect the infected animals from rapidly fulminating infection. If the infection can be modulated or delayed the immune response may bring the infection under control (Emery & Morrison 1980) and this has been the basis of several methods of immunisation.

Naturally recovered animals develop a durable premunity and are thus capable of serving as reservoirs for the infection in ticks. Immunity may however wane within three years after recovery (Sturman 1935), but natural reinfection in these circumstances is usually followed by a non-fatal disease. Animals which have recovered from a natural or an artificial *T. annulata* infection are fully susceptible to *T. parva* and *vice versa* (Sergent *et al.* 1945; Neitz & Jansen 1956).

2.10 MECHANISMS OF PATHOLOGICAL DAMAGE

2.10.1 CYTOKINES

It has been difficult to envisage how the diverse clinical symptoms of *T. annulata* and *T. parva* relate to the presence of the parasites. However, reports that the administration of macrophage-derived TNF-α has been found to induce anorexia, cachexia (Oliff, Defeo-Jones & Boyer 1987) and pyrexia (Beutler & Cerami 1986) as well as leucopenia (Ulich, Del Castillo, Keys Granger & Ni 1987) in other animals as well as cattle (Bielefeldt Ohmann, Campos & Snider 1989) suggests that cytokines might be the link between parasites and clinical symptoms. The circumstantial evidence for the *in vivo* generation of cytokines during *T. annulata* and *T. parva* infection include the massive blastogenesis of uninfected cells which accompanies replication of schizont-infected cells throughout the lymphoid and reticulo-endothelial tissues (Eisler 1988), possibly due to IL-2 activity (Dobbelaere *et al.* 1990), and the generation of immunoreactive lymphocytes and macrophages as infection progresses (Preston *et al.* 1983; Preston & Brown 1988).

The finding that macroschizont-infected cells produce cytokines (Entrican *et al.* 1991; Ahmed, Wiegers, Steuber, Schein, Williams & Dobbelaere 1993; Preston *et al.* 1993; Brown, Campbell, Russell, Hopkins & Glass 1995), therefore suggests that the proliferation of macroschizont-infected cells could contribute to tissue damage. The immunologically more reactive manifestations of *T. parva* infections may be due to IFN-γ synthesised by parasitised cells (DeMartini & Baldwin 1991), since this IFN upregulates lymphoproliferation, development of T cell mediated cytotoxicity (Siegel 1988) and increased MHC class II antigen expression (De Maeyer & De Maeyer-Guignard 1988). The less severe disease caused by *T. annulata* and the absence of lymphocytolysis (Eisler 1988; Preston *et al.* 1992a) would agree with the ability of type 1 IFN to downregulate lymphocyte proliferation (Balkwill 1989). Many features of *T. annulata* and *T. parva* infections may therefore be due both to secretion of IFNs by the parasitised cells and to cytokines such as IFN-γ and TNF-α produced by the host cells in response to infection (Preston *et al.* 1993).

The production of IFN (Ahmed *et al.* 1993) together with other cytokines may play a role in the immortalisation of *T. annulata* and *T. parva* schizont-infected cells. NK

cells, proposed to be involved in lymphopenia (Eugui & Emery 1981), can also be stimulated by IFN (Diejeu, Heinbaugh, Holden & Herbermann 1978). Importantly, IFN activates macrophages (Mogensen & Vierelizier 1987) to produce high levels of TNF. TNF after reaching the circulation can bind to high affinity receptors on normal tissues and induce a wide variety of biological effects. These changes can include pulmonary oedema, respiratory failure and disseminated haemorrhagic necrosis that closely resembles toxic shock. Cytokines are also extremely important regulators of cellular infiltration, tissue damage, ulceration, secretion/diarrhoea and fibrosis. The cytokine response initiated by *T. annulata* and *T. parva* infected animals may therefore be very dangerous to host tissues as already described in other parasitic infections (Cox 1989).

2.10.2 NITRIC OXIDE

Macrophages harvested from cattle undergoing infection with *T. annulata* or *T. parva* spontaneously produce NO *in vitro*; production may be enhanced by exposure to IFN-γ (Visser *et al.* 1995). The pluripotential nature of NO activity in man and rodents has been well documented (Moncada, Palmer & Higgs 1991). Since NO may be a neurotransmitter and vasodilator (Moncada *et al.* 1991), mediate cell lysis (Kolb & Kolb-Bachofen 1992), mucosal damage and haemorrhage (Lopez-Belmonte, Whittle & Moncada 1993) and inhibit lymphocyte proliferation (Sternberg & McGuigan 1992), its potential production by bovine macrophages is of interest with respect to the clinical symptoms and pathological lesions of *T. annulata* and *T. parva* described above. The observations described by Visser *et al.* (1995) on *T. annulata* and *T. parva* indicate that macrophage derived NO may contribute both to protective immunity and to the pathogenesis of theileriosis.

Since macroschizont-infected cells produce IFN-α (Entrican *et al.* 1991), a recognised stimulator of NK cell activity (Romagnani 1992) and can stimulate macrophages to produce TNF-α (Preston *et al.* 1993), parasite proliferation could induce NK cells and macrophages to produce IFN-γ and TNF-α respectively and so promote NO synthesis during the early stages of primary and challenge infections.

2.10.3 APOPTOSIS

Apoptosis, programmed cell death, is an important basic biological phenomenon which plays a complementary but opposite role to mitosis in the regulation of animal cell populations (Kerr, Wyllie & Currie 1972). It is a normal immune regulatory mechanism that is activated to prevent anti-self responses and also to delete expanded but no longer required cell populations.

Phagocyte recognition of cells undergoing apoptosis is an efficient way of removing unwanted cells from tissues without the release of potentially toxic cell contents which might otherwise damage neighbouring cells and elicit an inflammatory/immune response (Golstein, Ojcius & Young 1991). Apoptosis also has a natural regulatory function that protects against excessive production of toxic cytokines. NO-induced apoptosis has been shown to occur in the very same macrophages that produce NO (Sarih, Souvannavong & Adam 1993; Albina, Cui, Mateo & Reichner 1993) and apoptosis has also been shown to be induced by TNF (Wyllie, Kerr & Currie 1980). It is possible that deficiencies in clearance of apoptotic cells might be a pathway by which tissue injury is initiated or perpetuated in disease and defective regulation of apoptosis may play a part in the aetiology of cancer, AIDS, autoimmune diseases and degenerative diseases of the central nervous system (Carson & Ribeiro 1993).

Activation induced cell death can be triggered in mature peripheral T cells (Kabelitz, Pohl & Pechhold 1993) and can be enhanced by IL-2 (Lenardo 1991) by driving activated T cells to the S phase of the cell cycle where they are susceptible to TCR-induced death (Boehme & Lenardo 1993). The sensitivity of the activated T cells to apoptosis does not appear to correlate with a distinct phenotype. High levels of induced cell proliferation predisposes proliferating T cells to apoptosis and it is suggested that superantigens cause T cell deletion by exploiting a natural regulatory pathway called "propriocidal regulation" that is used to remove activated T cells (Boehme & Lenardo 1993). Superantigens are potent inducers of apoptosis in activated reactive T cells both *in vivo* (Kawabe & Ochi 1991) and *in vitro* (Kabelitz & Wesselborg 1992). In contrast, IFN-γ has been shown to rescue cells from apoptosis (Mangan & Wahl 1991).

Unfortunately immunisation against *T. parva* is not so easily achieved as that against *T. annulata*. The *T. parva* schizont-infected cells are destroyed in genetically unmatched cattle (Teale 1983; Dolan, Teale, Stagg, Kemp, Cowan, Young, Groocock, Leitch, Spooner & Brown 1984a; Morrison, Goddeeris, Teale, Groocock, Kemp & Stagg 1987) thus protection is only possible where the donor and recipient cells are matched. However, it has been shown that immunisation against *T. parva* schizont-infected cell lines is possible in genetically unmatched cattle using high cell doses (over 10^8 cells per animal; Brown 1981). Differences in the ease of immunisation and pathogenesis may arise because of the two parasites infecting and surviving within phenotypically distinct cells.

An alternative approach to immunisation has been the use of sporozoites, based on the assumption that small numbers of sporozoites multiply slowly giving the immune response time to develop and control the infection (Wilde 1967). This approach has been used to develop the infection and treatment method of immunisation for *T. parva* infected animals. The use of chemotherapy to control infection with *T. parva* sufficiently long enough to permit the establishment of a solid protective immune response has been developed as a routine vaccination procedure with considerable success (Radley 1981).

The present live, attenuated vaccines are far from perfect and from a practical viewpoint, preparation is labour intensive, batch control is difficult and costly and the vaccine has to be transported frozen in liquid nitrogen. There is also the danger of pathogenic contamination or the occurrence of low level infections inducing a carrier state in some animals that could serve as a source of infection to ticks. The possibility that the infection and treatment method of immunisation could throw up mutant forms of parasite resistant to the chemotherapy used and capable of evading the immune response generated is also important. Attention has therefore turned to the development of molecular vaccines and the well tried methods of identifying potentially protective antigens (Tait & Hall 1990).

In the search for an improved molecular or genetically engineered vaccine it should be remembered that in order to provide a significant advance over the vaccines

Apoptosis has also been shown to be the mechanism of cell death in the lysis mediated by cytotoxic lymphocytes (Duke, Chervenak & Cohen 1983) and is responsible for the depletion of $CD4^+$ T cells in AIDS (Ameisen & Capron 1991). Apoptosis in $CD8^+$ T cells may not be TCR-mediated but may result from the action of cytotoxic cytokines, such as TNF (Lopes, Veiga, Santos, Fonseca & DosReis 1995). *Trypanosoma cruzi* has been shown to prime $CD4^+$ cells for apoptosis (Lopes *et al.* 1995).

Unfortunately, detrimental pathological processes may be a side effect of the protective immune responses elicited by either *T. annulata* or *T. parva* infections. A greater understanding of these processes is therefore required to develop safe and effective methods of immunisation for the future.

2.11 VACCINES

The potential impact of effective vaccines for the control of *T. annulata* and *T. parva* in cattle has been long recognised (Pipano 1989). Animals that recover from infection with *T. annulata* or *T. parva* are solidly immune to subsequent challenge, at least with homologous strains.

Cattle infected with *T. annulata* have been successfully immunised with *T. annulata* schizont-infected cell lines (Gill, Bhattacharyulu, Kaur & Singh 1976a) and with the discovery that cultured *T. annulata* cell lines lose their virulence (Gill *et al.* 1976a; Brown, Crawford, Kanhai, Njuguna & Stagg 1978; Pipano 1981) this method of immunisation has been pioneered in many countries. When *T. annulata* schizont-infected cells are artificially transferred between hosts, there is clearly transfer of parasite from donor to recipient. This was demonstrated by having donor and recipient of different sexes and karyotyping parasitised cells before and after transfer (Brown *et al.* 1978). The mechanism by which parasites' transfer and the frequency with which transfer occurs are not known. Immunisation against *T. annulata* is possible with cell doses as low as 10^2 cells (Ouhelli, Innes, Brown, Walker & Spooner 1989) and MHC matching of cell line and recipient is not necessary for protection (Pipano 1981; Innes, Millar, Brown & Spooner 1989b).

Unfortunately immunisation against *T. parva* is not so easily achieved as that against *T. annulata*. The *T. parva* schizont-infected cells are destroyed in genetically unmatched cattle (Teale 1983; Dolan, Teale, Stagg, Kemp, Cowan, Young, Groocock, Leitch, Spooner & Brown 1984a; Morrison, Goddeeris, Teale, Groocock, Kemp & Stagg 1987) thus protection is only possible where the donor and recipient cells are matched. However, it has been shown that immunisation against *T. parva* schizont-infected cell lines is possible in genetically unmatched cattle using high cell doses (over 10^8 cells per animal; Brown 1981). Differences in the ease of immunisation and pathogenesis may arise because of the two parasites infecting and surviving within phenotypically distinct cells.

An alternative approach to immunisation has been the use of sporozoites, based on the assumption that small numbers of sporozoites multiply slowly giving the immune response time to develop and control the infection (Wilde 1967). This approach has been used to develop the infection and treatment method of immunisation for *T. parva* infected animals. The use of chemotherapy to control infection with *T. parva* sufficiently long enough to permit the establishment of a solid protective immune response has been developed as a routine vaccination procedure with considerable success (Radley 1981).

The present live, attenuated vaccines are far from perfect and from a practical viewpoint, preparation is labour intensive, batch control is difficult and costly and the vaccine has to be transported frozen in liquid nitrogen. There is also the danger of pathogenic contamination or the occurrence of low level infections inducing a carrier state in some animals that could serve as a source of infection to ticks. The possibility that the infection and treatment method of immunisation could throw up mutant forms of parasite resistant to the chemotherapy used and capable of evading the immune response generated is also important. Attention has therefore turned to the development of molecular vaccines and the well tried methods of identifying potentially protective antigens (Tait & Hall 1990).

In the search for an improved molecular or genetically engineered vaccine it should be remembered that in order to provide a significant advance over the vaccines

currently available a new vaccine will have to meet the following criteria. It will have to be effective in preventing death and reducing illness, stable with a long shelf life, cheap and require only one dose (Tait & Hall 1990).

At the present time it is not known which molecules are responsible for protection. The identification of potentially detrimental immune responses will provide essential information with regard to the selection of antigens for inclusion in subunit vaccines. In addition recent studies indicate that parasite variation will also be an important consideration in the development of any subunit vaccine as well as in the production of vaccine strains for use in specific geographical regions. It is difficult to predict how cross-protective a given vaccine strain is likely to be except by direct experimentation. Variation both within strains and between strains of *T. annulata* has been shown for a number of phenotypes and genotypes by studies on merozoite production *in vitro* (Shiels, Kinnaird, McKellar, Dickson, Ben Miled, Melrose, Brown & Tait 1992), MAb profiles (Shiels, McDougall, Tait & Brown 1986), isoenzyme profiles (Melrose, Brown, Morzaria, Ocama & Irvin 1984), genomic profiles (Ben Miled, Darghouth, Bell Sakyi, Melrose, Brown & Dellagi 1994), a sporozoite surface gene (Williamson, Tait, Brown, Walker, Beck, Shiels, Fletcher & Hall 1989) and merozoite/piroplasm antigens (Dickson & Shiels 1993). *T. annulata* appears to have less antigenic diversity than *T. parva* (Gill, Bonsal, Bhattacharyulu, Kaur & Singh 1980; Preston *et al.* 1992a) and although *T. annulata* is antigenically related to *T. parva* (Burridge, Brown & Kimber 1974), there is no cross immunity between the two species.

2.12 AIMS OF THIS STUDY

The primary objective of this study was to investigate the lesions of tropical theileriosis (*T. annulata* infection) in particular the contribution of macrophages to damage and the identity of the schizont-infected cell. During the course of the study, tissues from a *T. parva* infected animal became available and were included for comparison.

The work was carried out in the following stages:

(1) Examination of clinical responses and parasite development in cattle to ascertain that tissues were being obtained during 'acute' (lethal) infections, i.e. would represent the progression of disease as described previously (Sergent *et al.* 1924; Gill *et al.* 1977; Baharsefat *et al.* 1977; Srivastava & Sharma 1981).

(2) Examination of the macroscopic pathology of the organs to ascertain that lesions represented those described previously at post-mortem examination of lethal infections (Sergent *et al.* 1924; Gill *et al.* 1977; Baharsefat *et al.* 1977; Srivastava & Sharma 1981).

(3) Histological investigation of microscopic lesions in tissues prepared at the initial stages of pyrexia, peak pyrexia and nadir of disease to monitor the progression of lesions over time: particular attention being given to the presence of macrophages and lymphocytes in tissues.

(4) Assessment of parasite distribution throughout organs showing macroscopic lesions (as shown in stage 2) using tissue smears stained with Giemsa's stain.

(5) Assessment of the location of macroschizont- and microschizont-infected cells in relation to microscopic lesions (as shown in stage 3) using MAbs which recognise parasite antigens and immunocytochemical techniques with Harris's haematoxylin counterstain.

(6) Assessment of antibodies to identify reagents for phenotypic analyses.

(7) Use of antibodies A452 (a T (CD3) cell marker) and IL-A15 (a C3bi complement receptor marker), identified in stage 6, to identify schizont-infected cells and to confirm the identity of cells.

(8) Use of A452 and IL-A15 to identify the uninfected cells which accompanied schizont-infected cells.

(9) Assessment of NO production by PBM and the ability of NO to induce apoptosis.

CHAPTER THREE

CLINICAL & HAEMATOLOGICAL RESPONSES, PARASITE DEVELOPMENT & NITRIC OXIDE PRODUCTION IN BOVINE THEILERIOSES

3.1 INTRODUCTION

Calves were infected with potentially lethal doses of sporozoites of two different stocks of *T. annulata* and of one stock of *T. parva* (Muguga) to provide tissues for subsequent pathological studies. Their clinical and haematological responses as well as the development of parasites were monitored to confirm that these responses resembled those reported previously during the course of lethal sporozoite infections (Dschunkowsky & Luhs 1904; Sergent *et al.* 1924; Sergent *et al.* 1945; Neitz 1957; Dolan, Young, Losos, McMillan, Minder & Soulsby 1984b; Preston *et al.* 1992a).

Nitric oxide (NO) has been implicated as a mediator of mucosal damage and haemorrhage (Lopez-Belmonte *et al.* 1993), vasodilation and neurotransmission (Moncada *et al.* 1991), cell lysis (Kolb & Kolb-Bachofen 1992) and as an inhibitor of lymphocyte proliferation (Sternberg & McGuigan 1992). The production of NO by PBM from calves infected with *T. annulata* or *T. parva* has already been described (Visser *et al.* 1995). Its production by the peripheral blood mononuclear cells (PBM) of the calves in this study which were infected with *T. annulata* was examined with respect to their clinical symptoms and subsequent pathological studies on their tissues.

T. annulata has been classified according to its symptoms into five types (Neitz 1957): (i) mild; (ii) peracute; (iii) acute; (iv) subacute; (v) chronic. The mild form of infection is indicated by pyrexia lasting a few days and a moderate anaemia. The peracute form of infection is indicated by the sudden onset of pyrexia persisting until death occurs and the parasitisation of up to 50% of erythrocytes. The acute form of infection is indicated by pyrexia lasting 5 to 20 days and a marked anaemia. The subacute form of infection is indicated by an irregular pyrexia lasting 10 to 15 days followed by the recovery of the animal. The chronic form of infection is indicated by

an irregular pyrexia and a variable degree of anaemia followed by the prolonged recovery of the animal.

T. parva has also been classified according to its symptoms into three types (Neitz 1957): (i) mild; (ii) acute; (iii) subacute. The mild form of infection is indicated by pyrexia lasting 3 to 7 days. The acute form of infection is indicated by pyrexia lasting 8 to 25 days. The subacute form of infection is indicated by an irregular pyrexia lasting 5 to 10 days followed by the recovery of the animal.

More recently the following guidelines were recommended for assessing the severity of response to infection with *T. parva* (Anon 1989). A mild response to infection was indicated by a temperature above 39.4 ^{0}C for less than 4 days, macroschizont parasitosis and piroplasm parasitaemia below 1% and 5% respectively and no significant reduction in haematocrit, i.e. packed cell volume (PCV). A severe response to infection was indicated by a temperature above 39.4 ^{0}C for 8 days or more, macroschizont and piroplasm parasitaemia above 5% and 10% respectively and a PCV below 20%. Responses between these limits were taken as signs of a moderate response to infection. As these descriptions of each type of disease are more detailed than those of Neitz (1957), they have been used here in conjunction with his classification to assess the severity of response to infection with *T. annulata* as well as *T. parva*. The other parameters measured were lymph node enlargement at the site of inoculation, the number of white blood cells, red blood cells and platelets (Preston *et al.* 1992a).

3.2 EXPERIMENTAL DESIGN

Pilot studies were conducted on a calf which had been inoculated with sporozoites of *T. annulata* (Hisar). This calf provided tissues for sampling on day 12 post-infection to assess the lesions during the nadir of disease. Three calves were then inoculated with sporozoites of *T. annulata* (Hisar) to provide: tissues for sampling on days 7, 12 and 14 post-infection to assess the lesions during the initial stages of pyrexia, peak pyrexia and nadir of disease respectively; PBM to assess the production of NO on days 1, 5, 8 and 13 post-infection.

A calf inoculated with sporozoites of *T. annulata* (Doukkalla) from another study provided tissues for sampling on day 24 post-infection to assess the lesions of a different stock of *T. annulata* during the nadir of disease.

During the course of the work a calf which had been inoculated with sporozoites of *T. parva* (Muguga) from another study became available. This calf provided tissues for sampling on day 21 post-infection and was used to assess the lesions of a different species of *Theileria* during the nadir of disease.

The clinical and haematological responses of all these calves and parasite development were monitored at intervals throughout the course of infection.

3.3 MATERIALS & METHODS

3.3.1 PARASITE MATERIAL

The ground up tick supernatant (GUTS) stabilates were prepared and resuscitated by previously described methods (Brown 1983). All stabilates were prepared and maintained by staff at the Centre for Tropical and Veterinary Medicine (CTVM).

3.3.1.1 T. ANNULATA & T. PARVA SPOROZOITE STABILATES

The following stabilates were used: pooled stabilates 43, 46 and 49 of *T. annulata* (Hisar) from India (Gill, Bhattacharyulu & Kaur 1976b) at a dose of 2 tick equivalents (t.e)/ml, i.e. a 1ml solution containing material originally derived from 2 ground up ticks; *T. annulata* (Hisar) stabilate 52 at a dose of 1t.e/0.5ml, i.e. a 0.5ml solution containing material originally derived from 1 ground up tick; *T. annulata* (Doukkalla) from Morocco (Kachani 1990) stabilate 42 at a dose of 2t.e/ml; pooled stabilates 12 and 31 of *T. parva* (Muguga) from Kenya (Brocklesby, Barnett & Scott 1961) at a dose of 1t.e/0.5ml.

3.3.2 CALVES

3.3.2.1 CALVES & MAINTENANCE

All calves were *Bos taurus*, their age, breed, sex and origin are described in Table 3.1. The calves were kept in unheated barns and fed on a diet of hay, calf rearing nuts and *ad libitum* water.

Calf No.	Age	Breed	Sex	Origin	Infection	Euthanased
41B	1 month	Friesian	male	Easter Bush farm	*T. a* Hisar sporozoite stabilate 52 1 t.e.	Day 12
55C	4 months	Friesian	male	Easter Bush farm	*T. a* Hisar sporozoite stabilates 43, 46, 49 2 t.e.	Day 7
19	3 months	Friesian	male	auction		Day 12
20	3 months	Friesian	male	auction		Day 14
861	4 months	Ayrshire	male	Blythbank farm	*T. a* Doukkala sporozoite stabilate 42 2 t.e.	Day 24
8	4 months	Friesian	male	auction	*T. p* Muguga sporozoite stabilates 12, 31 1 t.e.	Day 21

T. a *Theileria annulata* t.e tick equivalent
T. p *Theileria parva*

Table 3.1 ***Bos taurus*** **calves: age, breed, sex, origin, infection and day of euthanasia**

3.3.2.2 INOCULATION OF CALVES

The sporozoite stabilates from different stocks of *T. annulata* and from *T. parva* (Muguga) used to infect the calves are described in Table 3.1. Calves were inoculated subcutaneously using a sterile 1 inch 19 gauge needle above the prescapular lymph node of the right shoulder. The calves were infected by staff at the CTVM.

3.3.3 MONITORING OF INFECTION

3.3.3.1 CLINICAL RESPONSES

The clinical signs of disease including pyrexia and lymph node enlargement at the site of inoculation were assessed by staff at the CTVM. Pyrexia was recorded daily as a rectal temperature above 39.4^{0}C (Anon 1989). Lymph node enlargement was recorded on a subjective scale of mild, moderate and gross enlargement by hand palpation every 2-3 days during the course of infection.

3.3.3.2 HAEMATOLOGICAL RESPONSES

Jugular blood was taken into vacutainer tubes (Becton Dickinson) containing disodium salt of ethylenediaminetetra-acetic acid (EDTA) and used for haematological examinations every 2-3 days.

The total white blood cell (TWBC) counts (x10^6/ml) and red blood cell (RBC) counts (x10^9/ml) were measured by staff at the CTVM using a Coulter Counter (ZM, Coulter Electronics Ltd). The percentage PCV was determined by staff at the CTVM using a haematocrit centrifuge (Heraeus).

The percentage reduction in %PCV was calculated from the following formula: 100 - ((%PCV at a given time / %PCV at day 0) x 100). The percentage reduction in RBC was calculated from the following formula: 100 - ((Number of RBC at a given time / Number of RBC at day 0) x 100).

The percentage reduction in each cell type was calculated from the following formula: 100 - ((Number of cells at a given time / Number of cells at day 0) x 100).

Differential white blood cell (DWBC) counts were evaluated for examining more than 100 WBCs (Figures 3.1 - 3.5) by microscopy at a magnification of 1000x on thin blood smears stained with Giemsa's stain [Appendix I]. Platelet numbers were recorded in 10 microscopic fields (Figures 3.1-3.5) using a magnification of 1000x on thin blood smears stained with Giemsa's stain [Appendix I]. The maximum reduction in platelet numbers was evaluated by comparing the number of platelets at a given time to the number of platelets at day 0 and recorded as a small reduction (+), moderate reduction (++) and large reduction (+++) in platelet numbers. Photographs were taken using a Leitz microscope (Ortholux II: Leitz Wetzlar) and a Leica camera (Wild Leitz Photoautomat MPS 46/52).

3.3.3.3 PARASITE DEVELOPMENT

3.3.3.3.1 SCHIZONTS IN LYMPH NODES

Macroschizonts and hyperplasia were monitored in the lymph node draining the site of inoculation every 2-3 days in biopsy smears stained with Giemsa's stain [Appendix I] by microscopy at 1000x magnification by staff at the CTVM. Macroschizont parasitosis was evaluated as less than 1%, 1-5% and more than 5% of cells containing schizonts (Macroschizont Index 1, 2 & 3 respectively). Hyperplasia was evaluated as the number of hyperplastic cells recorded as less than 5% (+), 50% (++) and 100% (+++) of total cells.

3.3.3.3.2 PIROPLASMS IN BLOOD SMEARS

Piroplasm parasitaemia was monitored every 2-3 days in thin blood smears stained with Giemsa's stain [Appendix I] by microscopy at a 1000x magnification by staff at the CTVM. Piroplasm parasitaemia was evaluated in 1000 RBC and recorded as a percentage. For a parasitaemia less than 0.1% the number of piroplasms per 100 fields at 1000x magnification was assessed. Negative results were recorded if 200 fields (approximately 100,000 RBC) were examined and no piroplasms were observed.

3.3.4 NITRIC OXIDE PRODUCTION BY PERIPHERAL BLOOD MONONUCLEAR CELLS (PBM)

3.3.4.1 CULTURE OF PBM FOR NITRIC OXIDE PRODUCTION

Jugular blood was taken into vacutainer tubes containing lithium heparin 14i.u./ml (Becton Dickinson) for isolation of PBM for culturing by previously described methods (Preston *et al.* 1983) [Appendix II].

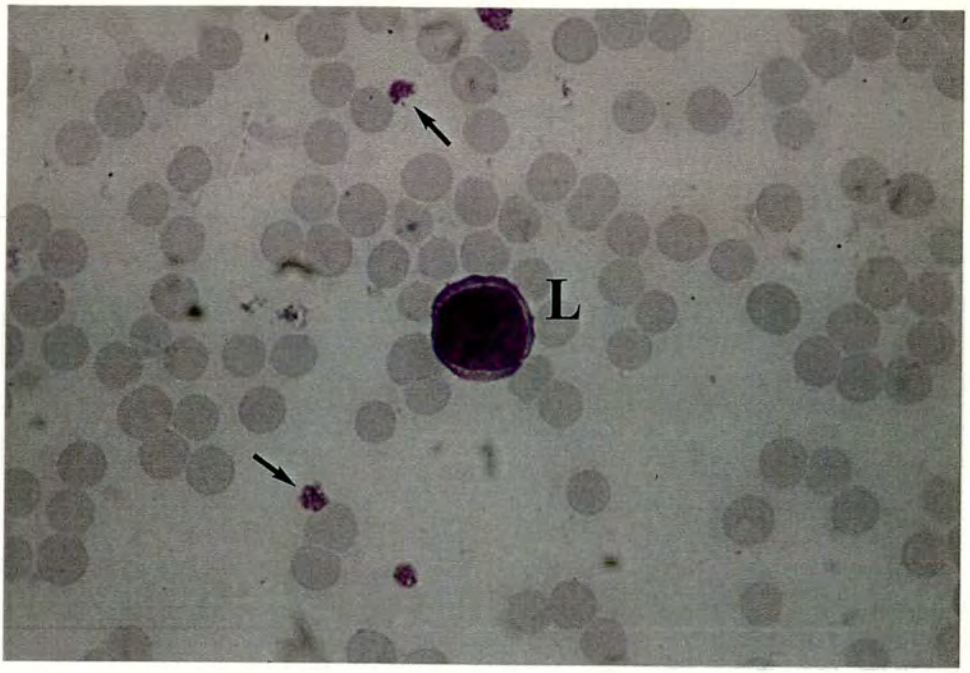

Figure 3.1 Lymphocyte (L) and platelets (arrows) in the blood smear of the calf infected with *T. annulata* (Hisar) on day 7 post-infection during the initial stages of pyrexia, (x1000: Giemsa's stain).

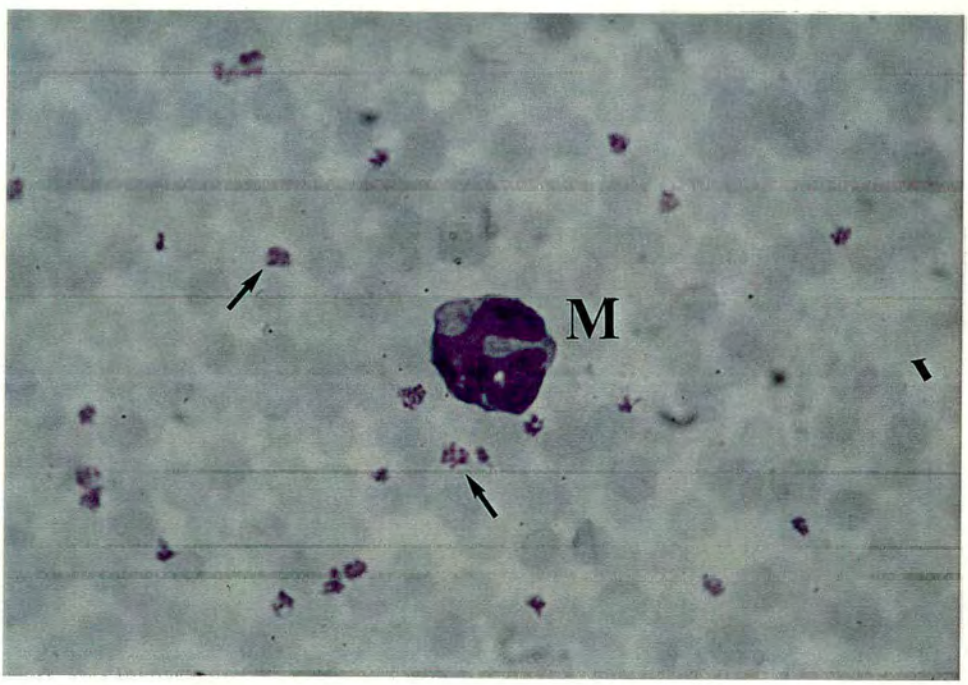

Figure 3.2 Monocyte (M) and platelets (arrows) in the blood smear of the calf infected with *T. annulata* (Hisar) on day 7 post-infection during the initial stages of pyrexia, (x1000: Giemsa's stain).

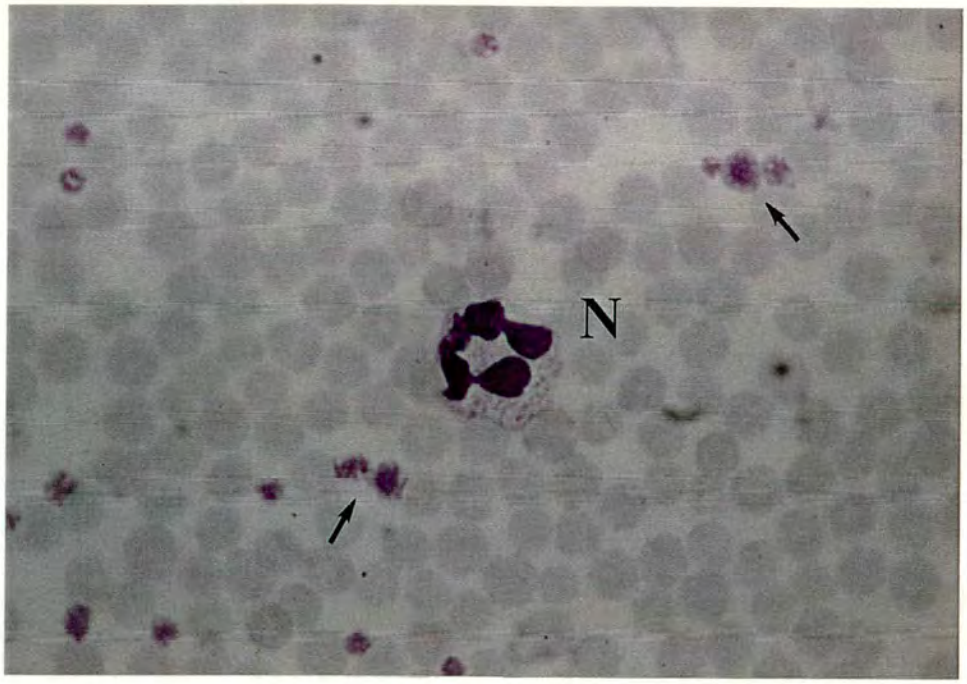

Figure 3.3 Neutrophil (N) and platelets (arrows) in the blood smear of the calf infected with *T. annulata* (Hisar) on day 7 post-infection during the initial stages of pyrexia, (x1000: Giemsa's stain).

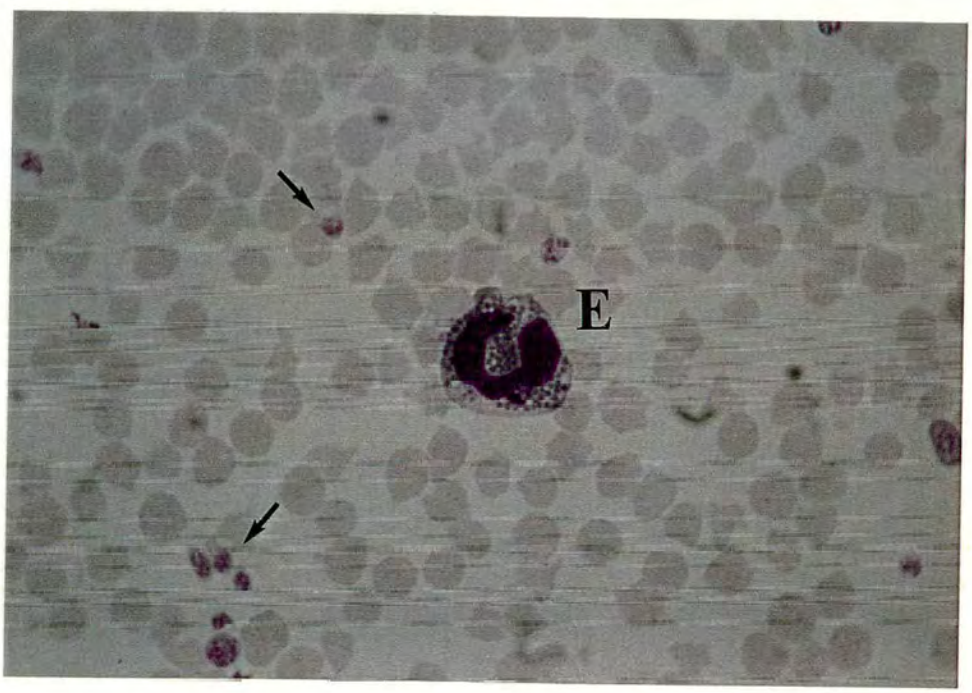

Figure 3.4 Eosinophil (E) and platelets (arrows) in the blood smear of the calf infected with *T. annulata* (Hisar) on day 7 post-infection during the initial stages of pyrexia, (x1000: Giemsa's stain).

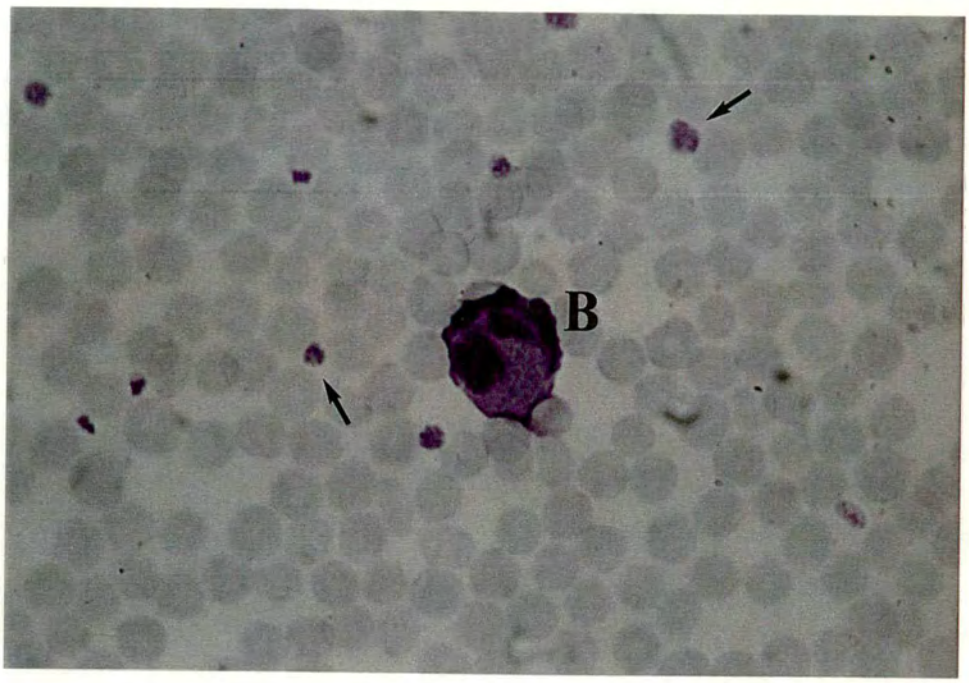

Figure 3.5 Basophil (B) and platelets (arrows) in the blood smear of the calf infected with *T. annulata* (Hisar) on day 7 post-infection during the initial stages of pyrexia, (x1000: Giemsa's stain).

Whole cultures of PBM were initiated by culturing 4 x 10^6 PBM/2ml in $2cm^2$ flat bottomed wells of 24-well plates (Flow Laboratories) in Iscove's modified Dulbecco's medium (IMDM) [Appendix III]. Aseptic techniques were used to avoid contamination. PBM were cultured with the following: (i) medium alone; (ii) medium with Bo rIFN-γ (Ciba-Geigy Ltd) at a final concentration of 100i.u./ml, a known inducer of NO; (iii) medium with N^G-monomethyl-L-arginine (L-NMMA, Calbiochem) at a final concentration of 0.5mM, a competitive inhibitor of the L-arginine: NO synthase pathway; (iv) Bo rIFN-γ with L-NMMA. All cultures were maintained in a humidified atmosphere of 5% CO_2 in air at 37^0C. Supernatants were harvested 24h after initiation and stored at -20^0C until assessed.

3.3.4.2 DETECTION OF NITRIC OXIDE PRODUCTION BY THE GRIESS ASSAY

NO reacts rapidly with water and oxygen in culture medium to produce nitrite (NO_2^-). Since this substance is both stable and quantifiable, its concentration in culture medium was taken as a measure of NO production by cultured PBM. NO_2^- was measured by previously described methods (Migliorini, Corradin & Betz Corradin 1991).

The supernatants stored at -20^0C were allowed to thaw at room temperature. For the assay described in previous studies (Visser *et al.* 1995), 100μl volumes of the test sample were mixed with equal volumes of the Griess reagent (0.1% naphthylethylene diamine 2HCl and 1% sulphanilamide (Sigma)) in 5% phosphoric acid (Aldrich Chemical Co. Inc.) in a 96-well flat-bottomed, microtitre plate. After 10 minutes of incubation at 4^0C, the optical density (OD) of the samples was read at 540nM on a microplate reader. Doubling dilutions of sodium nitrite (Sigma), 0 to 100μM in culture medium were used to generate the standard curve [Appendix IV]. The samples and standards were tested in quadruplicate. Baseline data were taken on day 1 post-infection due to the loss of PBM collected on day 0.

3.4 RESULTS

3.4.1 CLINICAL RESPONSES TO INFECTION

3.4.1.1 RESPONSE OF A CALF (41B) INFECTED WITH T. ANNULATA (HISAR) AS A PILOT STUDY

Calf 41B, infected as a pilot study, responded severely to infection (Figure 3.6) with pyrexia first recorded on day 5 post-infection. Pyrexia was sustained for 8 days reaching a peak of 41.2^{0}C on day 12 post-infection, the day the animal was euthanased. The lymph node at the site of inoculation showed signs of moderate enlargement (Table 3.2).

3.4.1.2 RESPONSE OF CALVES (55C, 19 & 20) EXAMINED AT INTERVALS AFTER INFECTION WITH T. ANNULATA (HISAR)

A severe clinical response was observed in calf 20 (Figure 3.7) euthanased during the nadir of disease. Pyrexia was first recorded on day 5 post-infection and was sustained for 10 days with a peak of 41.3^{0}C on day 14 post-infection, the day the animal was euthanased. The lymph node at the site of inoculation showed signs of moderate enlargement (Table 3.2).

A severe clinical response was observed in calf 19 (Figure 3.7) euthanased during the peak of pyrexia. Pyrexia was recorded first on day 4 post-infection and was sustained for 9 days with a peak pyrexia of 41.3^{0}C on day 11 post-infection, the day before the animal was euthanased. The lymph node at the site of inoculation showed signs of moderate enlargement (Table 3.2).

The response to infection of calf 55C resembled those observed in calves 19 and 20 (Figure 3.7). Pyrexia was first recorded on day 4 post-infection and was sustained for the 4 days before the calf was euthanased. A peak of 40.3^{0}C was recorded on day 7 post-infection, the day the animal was euthanased. The lymph node at the site of inoculation showed signs of mild enlargement (Table 3.2).

3.4.1.3 RESPONSE OF A CALF (861) DURING THE TERMINAL STAGES OF INFECTION WITH T. ANNULATA (DOUKKALLA)

A severe clinical response was observed in calf 861 to infection (Figure 3.8). Pyrexia was first recorded on day 9 post-infection and was sustained for 16 days reaching a

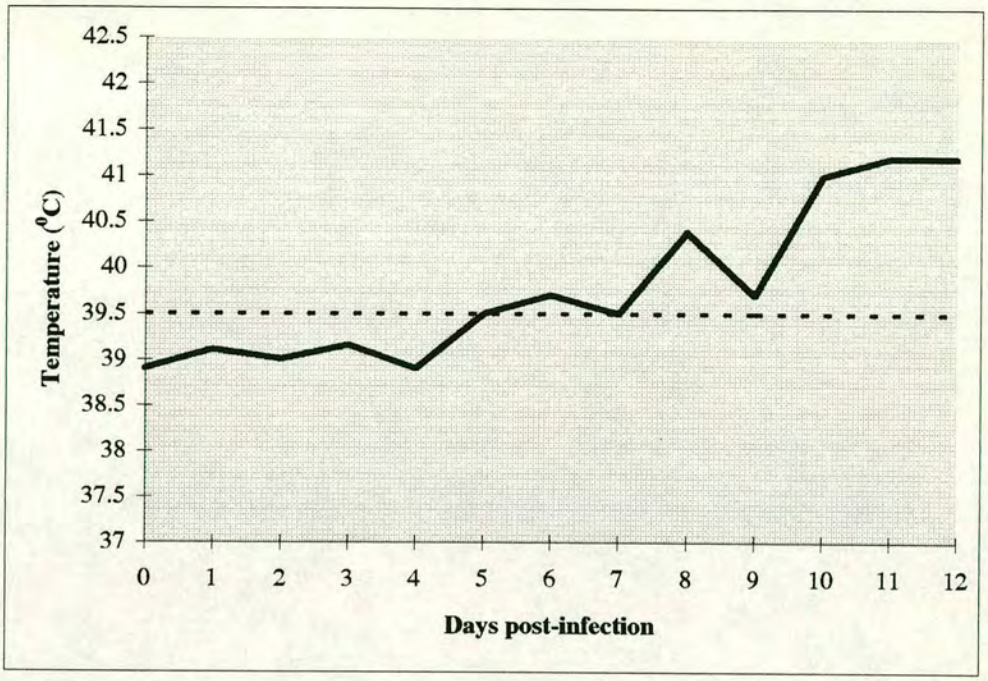

----- Pyrexia

Figure 3.6 Rectal temperature of a calf (41B) infected with *T. annulata* (Hisar) as a pilot study

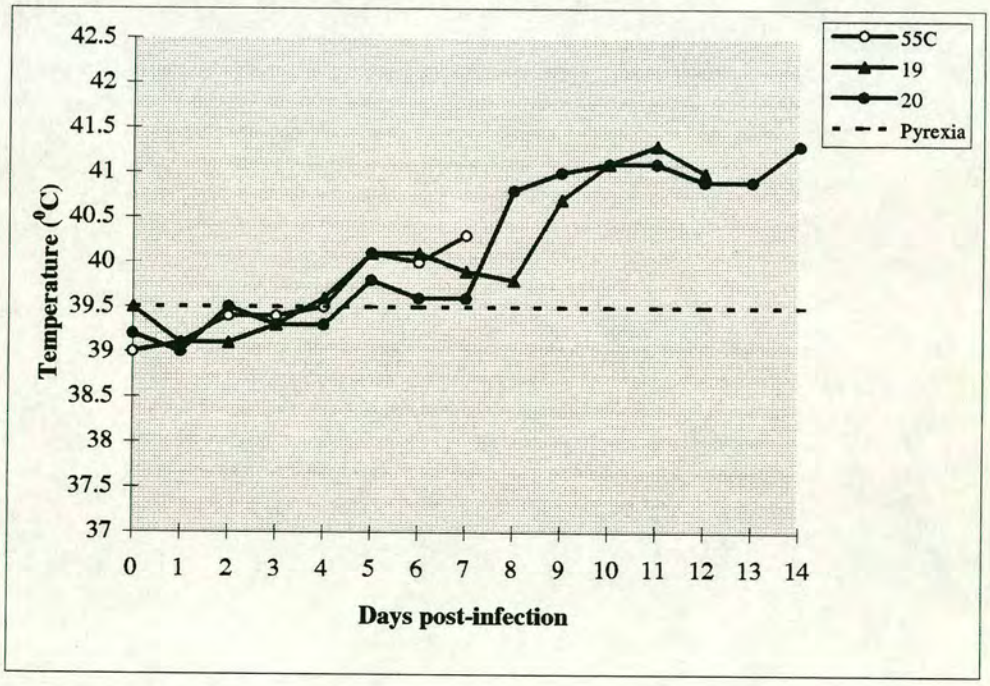

Figure 3.7 Rectal temperature of calves (55C, 19 & 20) infected with *T. annulata* (Hisar)

Calf number	Day of euthanasia	Days to T> 39.5°C	Duration (days) T> 39.5°C	Peak			Duration (days) PCV <20%	Max% redn. PCV	Max redn. platelets	Days to		Duration (days) Ma	Peak	
				T (°C)	LN size	Hyperplasia				1st Ma	1st Piro		Ma	% Piro
41B	12	6	8	41.2	**	+++	-	38	+++	5	11	9	+++	67.4
55C	7	5	4	40.3	*	+++	-	3	+++	6	-	3	+	0
19	12	5	9	41.3	**	+++	-	34	+++	6	10	8	+++	30.2
20	14	6	10	41.3	**	+++	3	53	+++	8	10	8	+++	44.7
861	24	10	16	41.8	***	+++	-	18	+	9	11	17	+++	9
8	21	10	13	42.3	***	+++	-	34	+++	10	15	13	+++	12.8

Ma Macroschizont
T Temperature (°C)
Piro Piroplasm
PCV Packed cell volume

LN Lymph node
Max % redn. Maximum % reduction
Max redn. Maximum reduction

- Not evident
+ Small number
++ Moderate number
+++ Large number

* Mild enlargement
** Moderate enlargement
*** Gross enlargement

Table 3.2 Response of calves (41B, 55C, 19 & 20) infected with *T. annulata* (Hisar), a calf (861) infected with *T. annulata* (Doukkalla) and a calf (8) infected with *T. parva* (Muguga)

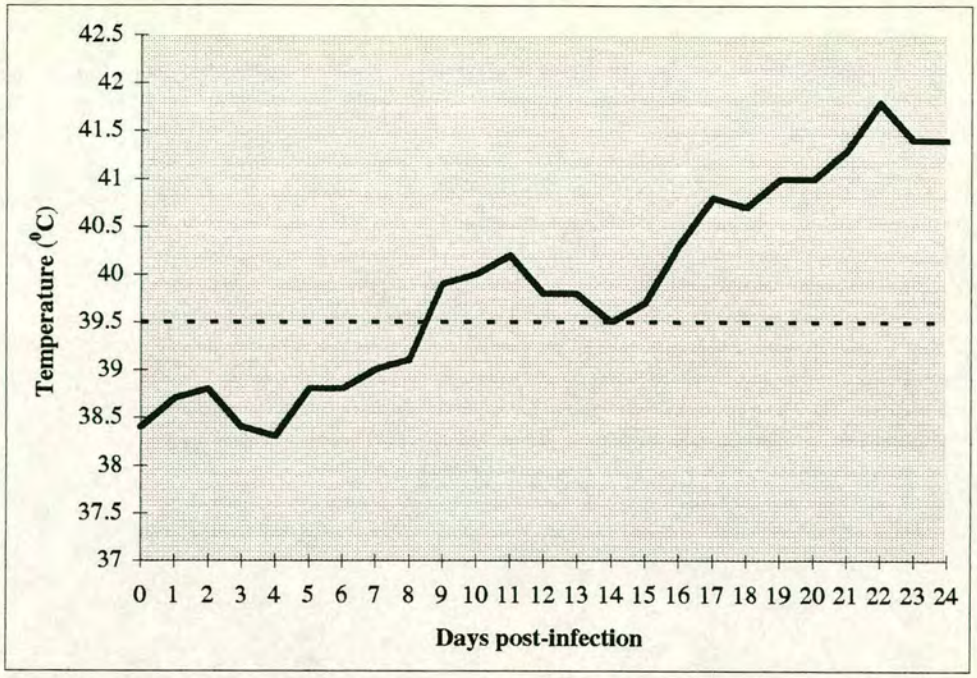

----- Pyrexia

Figure 3.8 Rectal temperature of a calf (861) infected with *T. annulata* (Doukkalla)

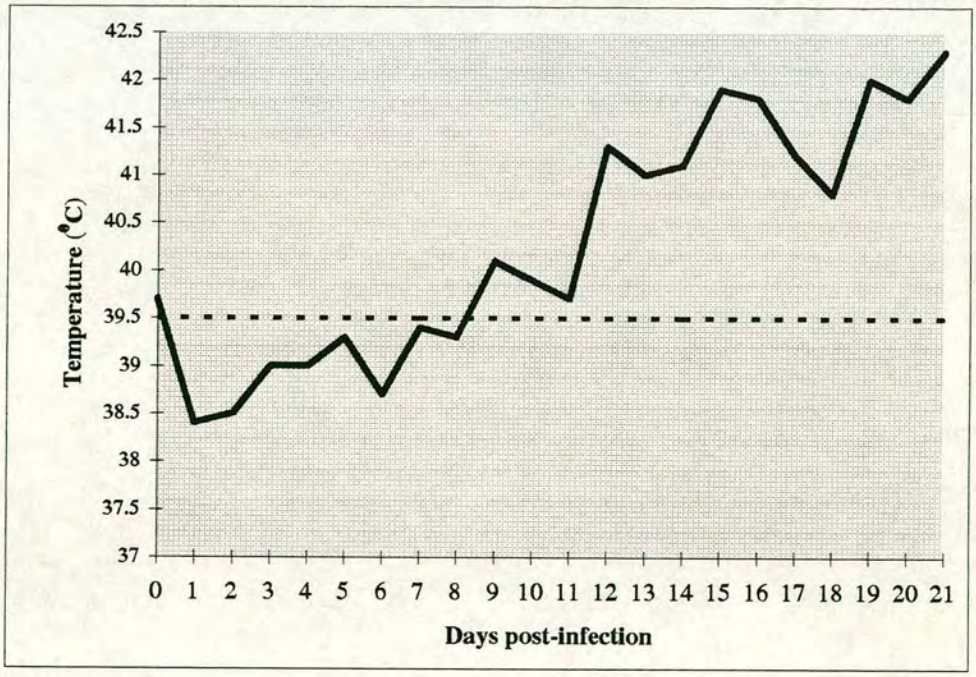

----- Pyrexia

Figure 3.9 Rectal temperature of a calf (8) infected with *T. parva* (Muguga)

peak of 41.8^{0}C on day 22 post-infection, 2 days before the animal was euthanased. The lymph node at the site of inoculation showed signs of gross enlargement (Table 3.2).

3.4.1.4 RESPONSE OF A CALF (8) DURING THE TERMINAL STAGES OF INFECTION WITH T. PARVA (MUGUGA)

A severe clinical response was observed in calf 8 to infection (Figure 3.9). Pyrexia was first recorded on day 9 post-infection and was sustained for 13 days reaching a peak of 42.3^{0}C on day 21 post-infection, the day the animal was euthanased. The lymph node at the site of inoculation showed signs of gross enlargement (Table 3.2).

3.4.2 HAEMATOLOGICAL RESPONSES TO INFECTION

3.4.2.1 RESPONSE OF A CALF (41B) INFECTED WITH T. ANNULATA (HISAR) AS A PILOT STUDY

The TWBC counts (Figure 3.10A) and DWBC counts (Figure 3.11) were characteristic of a severe leucopenic response to infection. The DWBC counts (Figure 3.11) showed a reduction of 62% in the total number of cells with a reduction of 66%, 64% and 50% in lymphocytes, monocytes and neutrophils respectively. The PCV (Figure 3.10B) was reduced by 38% and the RBC counts were reduced by 18% which represented a moderate/severe anaemia. A marked reduction in the numbers of platelets was recorded on day 11 post-infection, the day before the animal was euthanased (Table 3.2).

3.4.2.2 RESPONSE OF CALVES (55C, 19 & 20) EXAMINED AT INTERVALS AFTER INFECTION WITH T. ANNULATA (HISAR)

The TWBC counts (Figure 3.12A) and DWBC counts (Figure 3.13A) of calf 20, in which the infection ran its course, were characteristic of a moderate/severe leucopenic response to infection. The DWBC counts (Figure 3.13A) showed a reduction of 33% in the total number of cells with a reduction of 28% and 57% in lymphocytes and neutrophils respectively. Monocyte numbers doubled from preinfection levels. The PCV (Figure 3.12B) was reduced by 53% and the RBC counts were reduced by 47% which represented a severe anaemia. A marked reduction in the number of platelets was recorded on day 12 post-infection, 2 days before the animal was euthanased (Table 3.2).

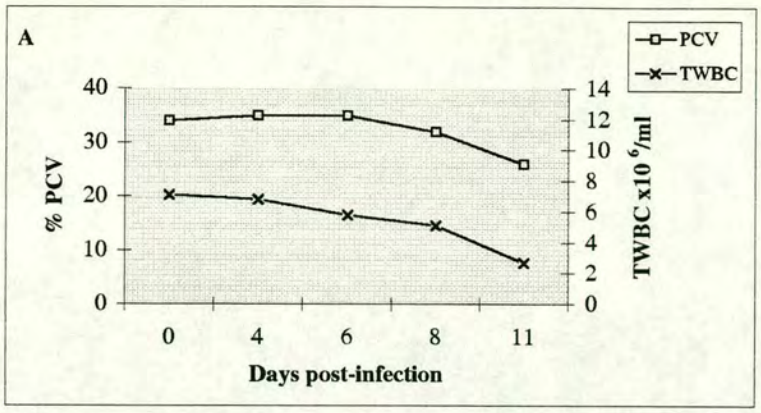

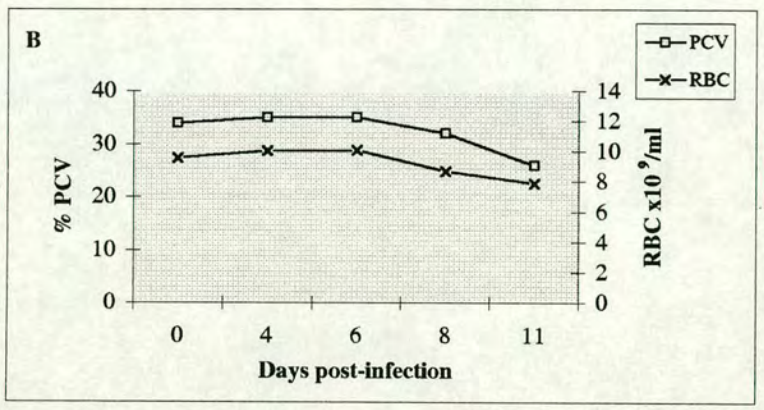

TWBC Total white blood cells
RBC Red blood cells
PCV Packed cell volume

Figure 3.10 Total white blood cell (TWBC) counts assessed by Coulter Counter (A), RBC counts (B) and % PCV (A & B) of a calf (41B) infected with *T. annulata* (Hisar) as a pilot study

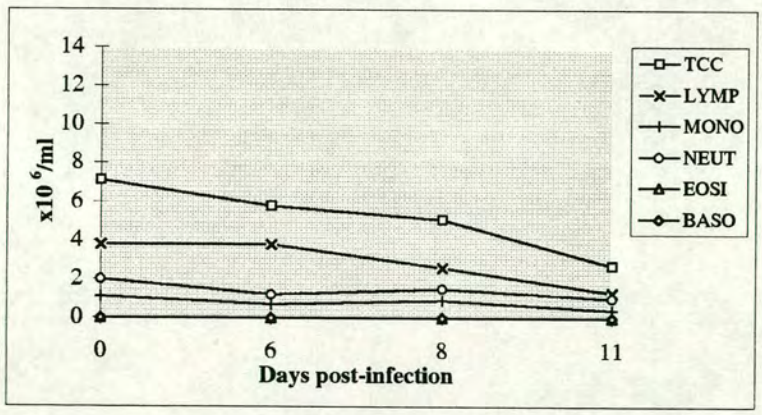

TCC Total cell counts
LYMP Lymphocytes
MONO Monocytes
NEUT Neutrophils
EOSI Eosinophils
BASO Basophils

Figure 3.11 Differential white blood cell (DWBC) counts assessed on blood smears of a calf (41B) infected with *T. annulata* (Hisar) as a pilot study

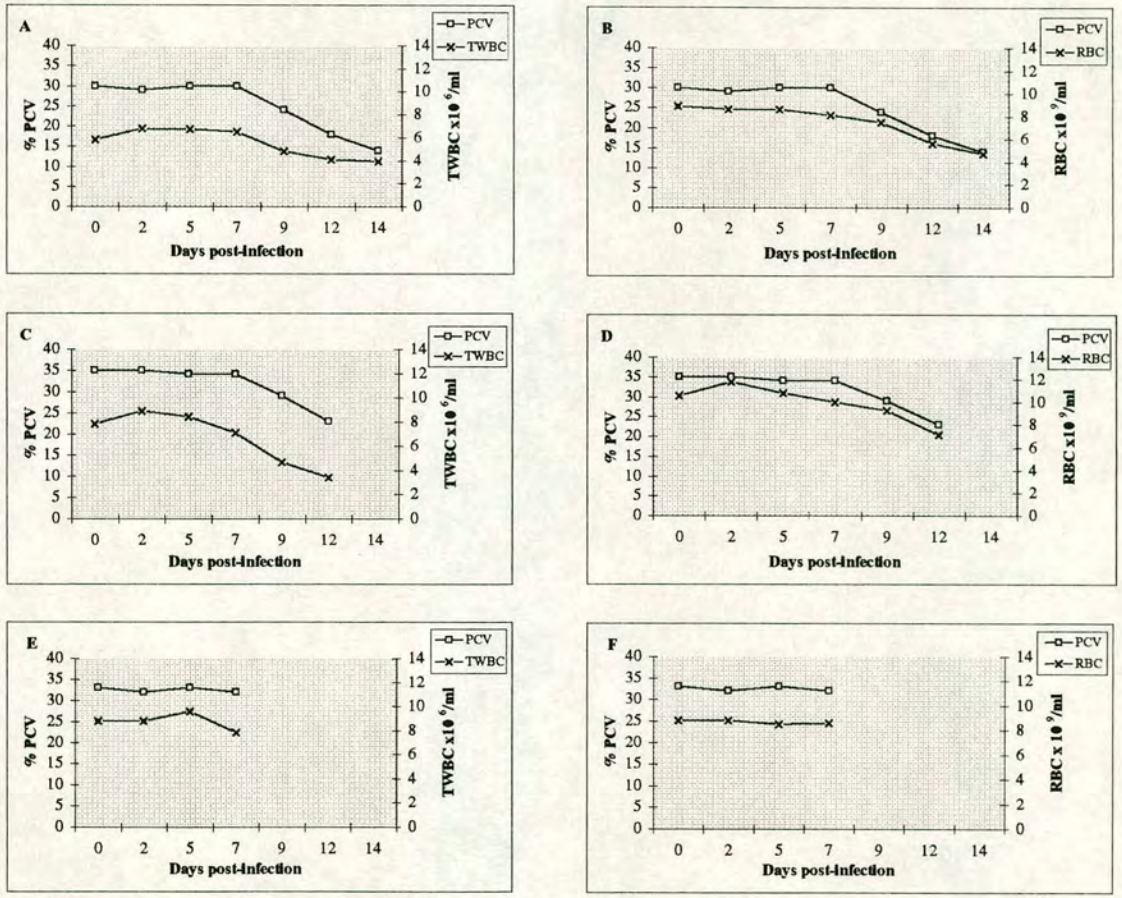

TWBC Total white blood cells
RBC Red blood cells
PCV Packed cell volume

Figure 3.12 Total white blood cell (TWBC) counts assessed by Coulter Counter (A, C & E), RBC counts (B, D & F) and % PCV (A-F) of calves (20 (A, B), 19 (C, D) & 55C (E, F)) infected with *T. annulata* (Hisar)

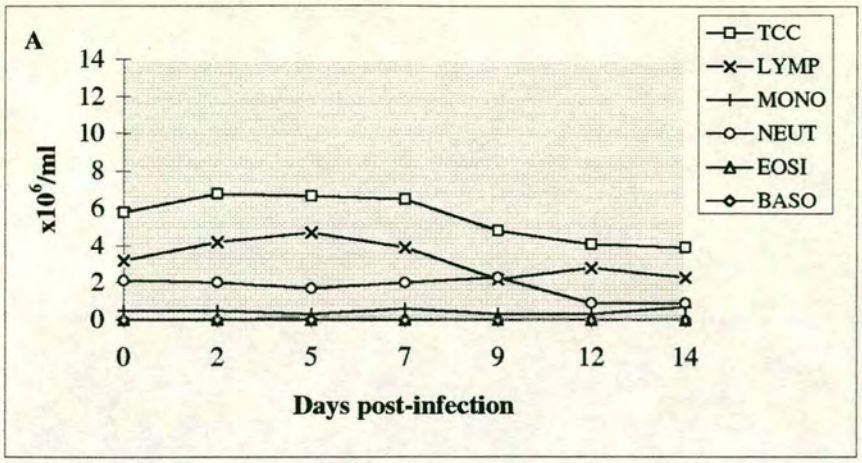

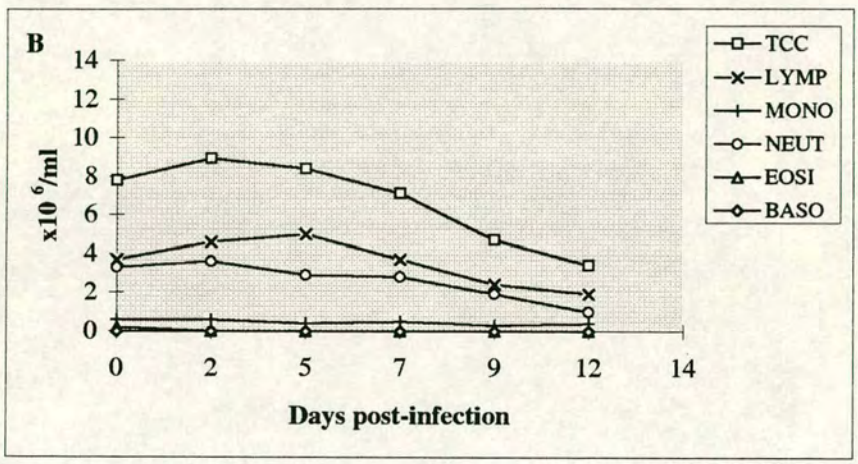

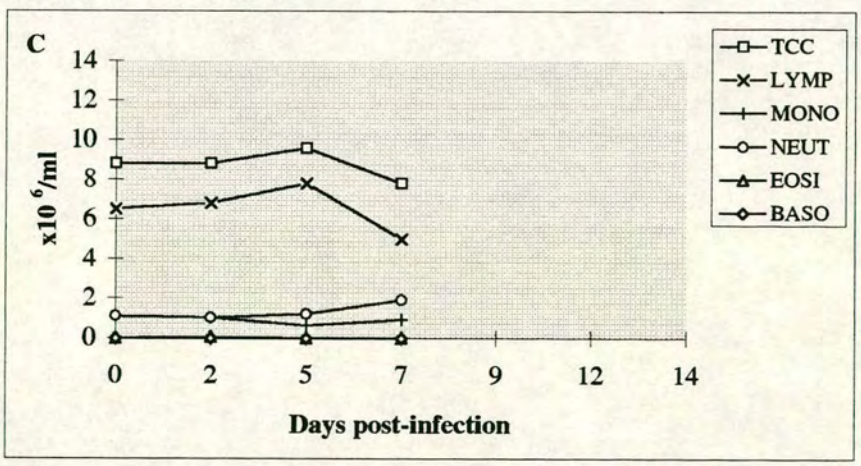

TCC Total cell counts
LYMP Lymphocytes
MONO Monocytes
NEUT Neutrophils
EOSI Eosinophils
BASO Basophils

Figure 3.13 Differential white blood cell (DWBC) counts assessed on blood smears (A, B & C) of calves (20 (A), 19 (B) & 55C (C)) infected with *T. annulata* (Hisar)

The TWBC counts (Figure 3.12C) and DWBC counts (Figure 3.13B) during peak pyrexia of calf 19 which was euthanased on day 12 post-infection were characteristic of a severe leucopenic response to infection. The DWBC counts (Figure 3.13B) showed a reduction of 56% in the total number of cells with a reduction of 49%, 39% and 70% in lymphocytes, monocytes and neutrophils respectively. The PCV (Figure 3.12D) was reduced by 34% and the RBC counts were reduced by 33% which represented a moderate/severe anaemia. A marked reduction in the number of platelets was recorded on day 12 post-infection, the day the animal was euthanased (Table 3.2).

The TWBC counts (Figure 3.12E) and DWBC counts (Figure 3.13C) during the initial stages of pyrexia of calf 55C which was euthanased on day 7 post-infection ran parallel to the counts of calves 19 and 20. The DWBC counts (Figure 3.13C) showed a reduction of 11% in the total number of cells with a reduction of 23% and 54% in lymphocytes and monocytes respectively. Neutrophil numbers showed a two-fold increase from preinfection levels. The PCV (Figure 3.12F) was reduced by 3% and the RBC counts were reduced by 3%. These values ran parallel to those of calves 19 and 20. A marked reduction in the number of platelets was recorded on day 5 post-infection, 2 days before the animal was euthanased (Table 3.2).

3.4.2.3 RESPONSE OF A CALF (861) DURING THE TERMINAL STAGES OF INFECTION WITH T. ANNULATA (DOUKKALLA)

The TWBC (Figure 3.14A) and DWBC counts (Figure 3.15) of calf 861, in which the infection ran its course, were characteristic of a moderate leucopenic response to infection. The DWBC counts (Figure 3.15) showed a reduction of 21% in the total number of cells with a reduction of 17% and 73% in lymphocytes and neutrophils respectively. Monocyte numbers showed a five-fold increase from preinfection levels. The PCV (Figure 3.14B) was reduced by 18% and the RBC counts were reduced by 22% which represented a mild/moderate anaemia. A marked reduction in the number of platelets was recorded on day 23 post-infection, the day before the animal was euthanased (Table 3.2).

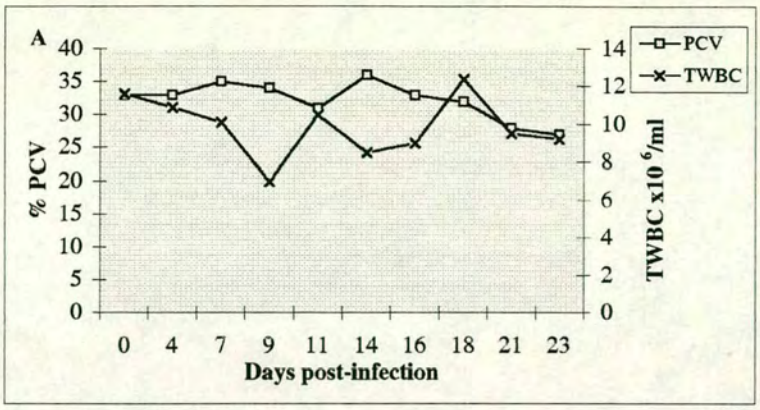

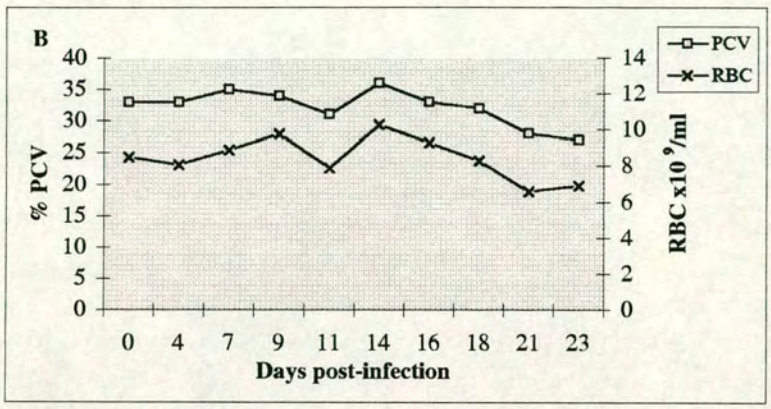

TWBC Total white blood cells
RBC Red blood cells
PCV Packed cell volume

Figure 3.14 Total white blood cell (TWBC) counts assessed by Coulter Counter (A), RBC counts (B) and % PCV (A & B) of a calf (861) infected with *T. annulata* (Doukkalla)

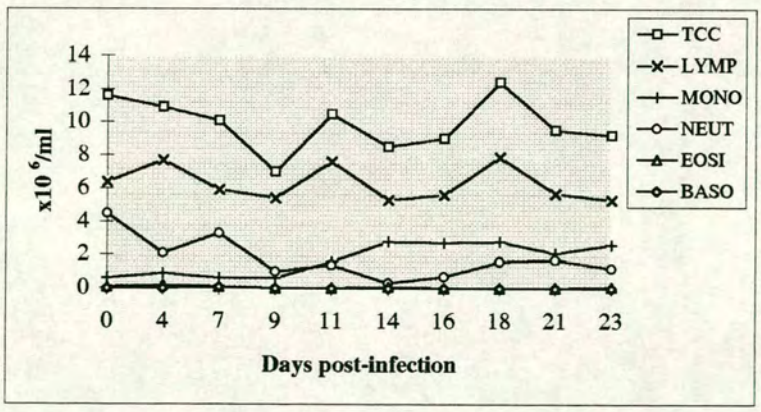

TCC Total cell counts
LYMP Lymphocytes
MONO Monocytes
NEUT Neutrophils
EOSI Eosinophils
BASO Basophils

Figure 3.15 Differential white blood cell (DWBC) counts assessed on blood smears of a calf (861) infected with *T. annulata* (Doukkalla)

3.4.2.4 RESPONSE OF A CALF (8) DURING THE TERMINAL STAGES OF INFECTION WITH T. PARVA (MUGUGA)

The TWBC counts (Figure 3.16A) and DWBC counts (Figure 3.17) of calf 8, in which the infection ran its course, were characteristic of a severe leucopenic response to infection. The DWBC counts (Figure 3.17) showed a reduction of 95% in the total number of cells with a reduction of 83%, 95% and 99% in lymphocytes, monocytes and neutrophils respectively. The PCV (Figure 3.16B) was reduced by 34% and the RBC counts were reduced by 28% which represented a mild/moderate anaemia. A marked reduction in the number of platelets was recorded on day 18 post-infection, 3 days before the animal was euthanased (Table 3.2).

3.4.3 PARASITE DEVELOPMENT DURING INFECTION

3.4.3.1 PARASITE DEVELOPMENT IN A CALF (41B) INFECTED WITH T. ANNULATA (HISAR) AS A PILOT STUDY

The first macroschizonts (Figure 5.1) in the lymph node biopsy smears and piroplasms (Figure 5.3) in the thin blood smears of calf 41B (euthanased on day 12 post-infection) were observed on days 4 and 10 post-infection respectively (Figure 3.18). By day 11 post-infection macroschizont parasitosis was more than 5% and a peak piroplasm parasitaemia of 67% was recorded when the animal was euthanased. Moderate numbers of hyperplastic cells (Figure 4.36) were recorded on day 8 post-infection, 4 days before the animal was euthanased (Table 3.2).

3.4.3.2 PARASITE DEVELOPMENT IN CALVES (55C, 19 & 20) EXAMINED AT INTERVALS AFTER INFECTION WITH T. ANNULATA (HISAR)

The first macroschizonts and piroplasms were observed in calf 20 (euthanased on day 14 post-infection) on days 7 and 9 post-infection respectively (Figure 3.19A). By day 9 post-infection macroschizont parasitosis was more than 5% and a peak piroplasm parasitaemia of 45% was recorded when the animal was euthanased. Large numbers of hyperplastic cells were recorded on day 9 post-infection, 5 days before the animal was euthanased (Table 3.2).

The first macroschizonts and piroplasms were observed in calf 19 (euthanased on day 12 post-infection) on days 5 and 9 post-infection respectively (Figure 3.19B). By day 12 post-infection macroschizont parasitosis was more than 5% and a peak

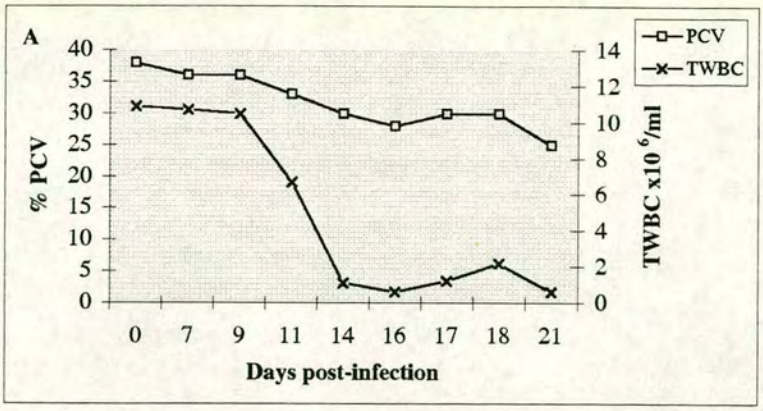

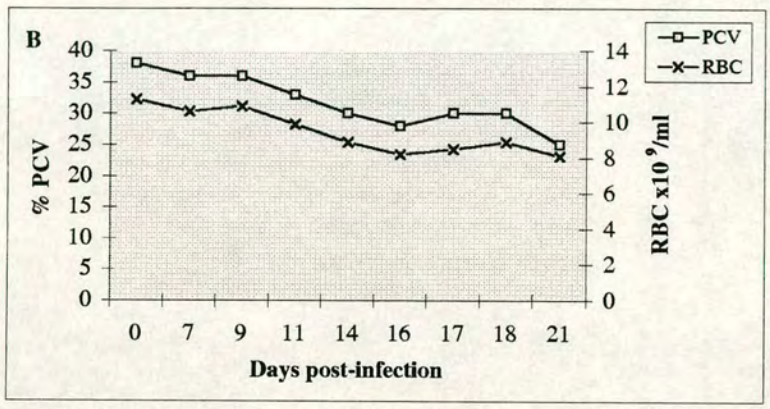

TWBC Total white blood cells
RBC Red blood cells
PCV Packed cell volume

Figure 3.16 Total white blood cell (TWBC) counts assessed by Coulter Counter (A), RBC counts (B) and % PCV (A & B) of a calf (8) infected with *T. parva* (Muguga)

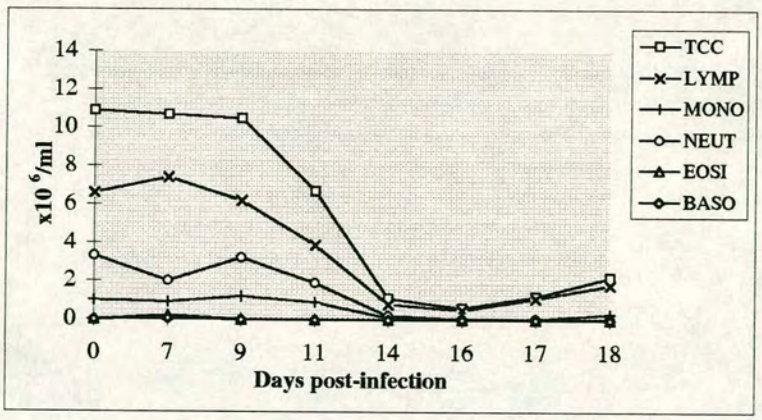

TCC Total cell counts
LYMP Lymphocytes
MONO Monocytes
NEUT Neutrophils
EOSI Eosinophils
BASO Basophils

Figure 3.17 Differential white blood cell (DWBC) counts assessed on blood smears of a calf (8) infected with *T. parva* (Muguga)

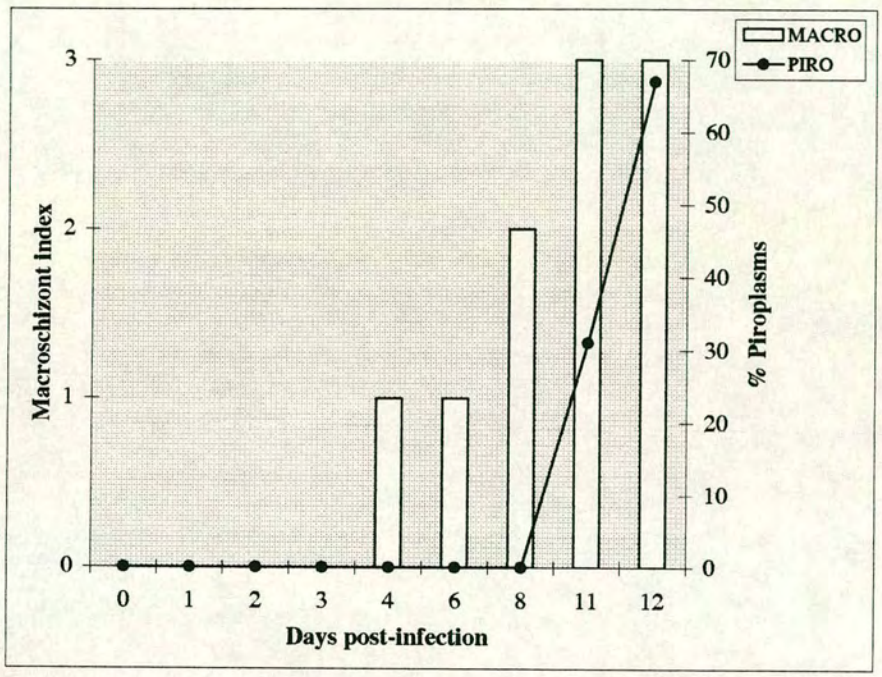

MACRO Macroschizonts
PIRO Piroplasms

Figure 3.18 Parasite development in a calf (41B) infected with *T. annulata* (Hisar) as a pilot study

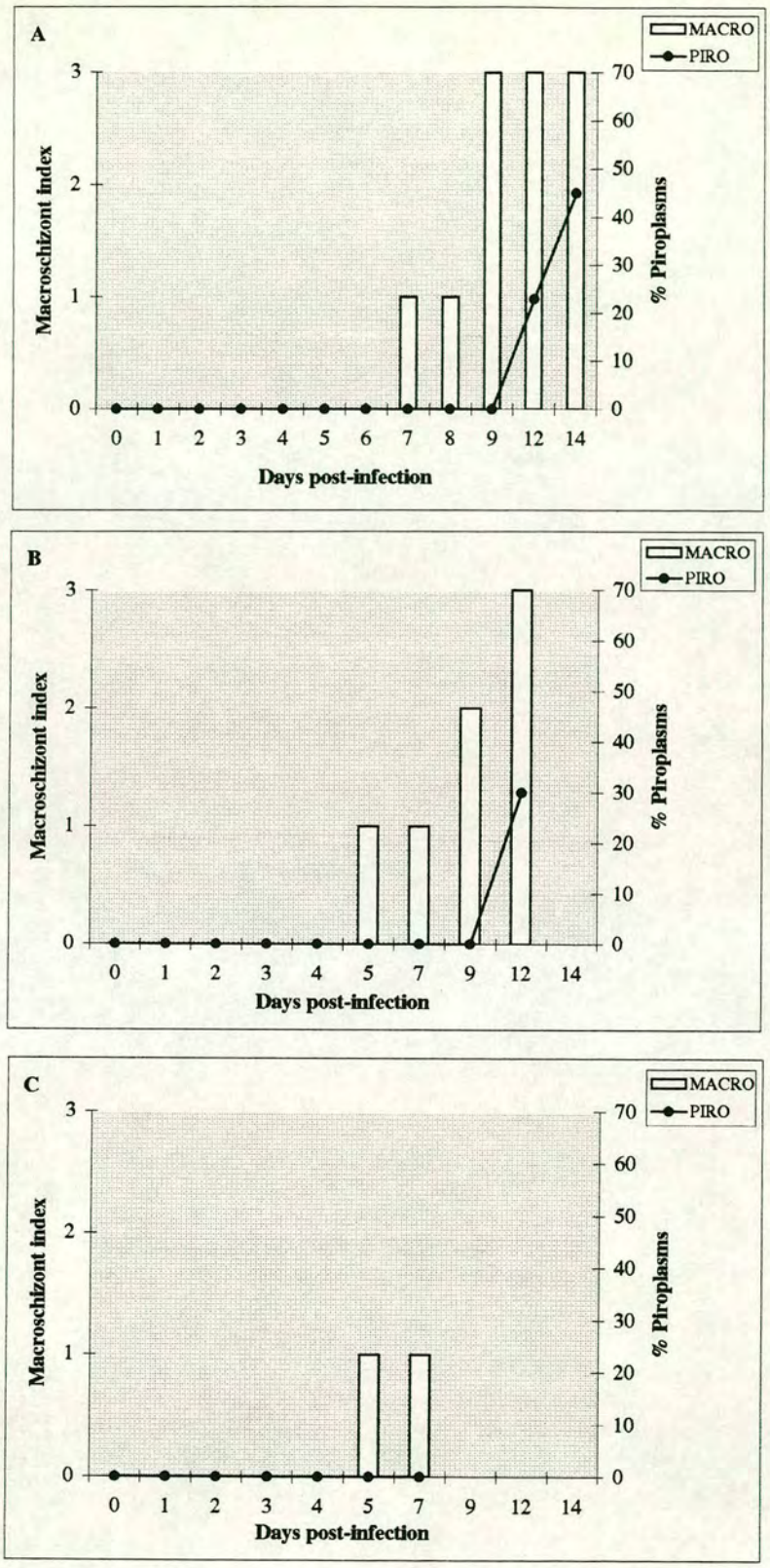

MACRO Macroschizonts
PIRO Piroplasms

Figure 3.19 Parasite development in calves (20 (A), 19 (B) & 55C (C)) infected with *T. annulata* (Hisar)

piroplasm parasitaemia of 30% was recorded when the animal was euthanased. Large numbers of hyperplastic cells were recorded on day 5 post-infection, 7 days before the animal was euthanased (Table 3.2).

The first macroschizonts were observed in calf 55C (euthanased on day 7 post-infection) on day 5 post-infection (Figure 3.19C). No piroplasms had been detected by day 7 post-infection. The macroschizont parasitosis was less than 1% on day 7 post-infection which was similar to the percentage recorded on day 7 post-infection in calves 19 and 20. Large numbers of hyperplastic cells were recorded on day 7 post-infection, the day the animal was euthanased (Table 3.2).

3.4.3.3 PARASITE DEVELOPMENT IN A CALF (861) DURING THE TERMINAL STAGES OF INFECTION WITH T. ANNULATA (DOUKKALLA)

The first macroschizonts and piroplasms were observed in calf 861 (euthanased on day 24 post-infection) on days 8 and 10 post-infection respectively (Figure 3.20). By day 10 post-infection macroschizont parasitosis was more than 5% and a peak piroplasm parasitaemia of 9% was recorded on day 17 post-infection, 7 days before the animal was euthanased. Large numbers of hyperplastic cells were recorded on day 10 post-infection, 14 days before the animal was euthanased (Table 3.2).

3.4.3.4 PARASITE DEVELOPMENT IN A CALF (8) DURING THE TERMINAL STAGES OF INFECTION WITH T. PARVA (MUGUGA)

The first macroschizonts and piroplasms were observed in calf 8 (euthanased on day 21 post-infection) on days 9 and 14 post-infection respectively (Figure 3.21). By day 14 post-infection macroschizont parasitosis was more than 5% and a peak piroplasm parasitaemia of 13% was recorded when the animal was euthanased. Large numbers of hyperplastic cells were recorded on day 9 post-infection, 12 days before the animal was euthanased (Table 3.2).

3.4.4 NITRIC OXIDE PRODUCTION DURING INFECTION

3.4.4.1 PRODUCTION OF NITRIC OXIDE IN CALVES (55C, 19 & 20) EXAMINED DURING INFECTION WITH T. ANNULATA (HISAR)

The NO_2^- produced *in vitro* by the PBM of calf 20 on day 5 post-infection was 3.9μM which was the same as the baseline value. After an initial marked rise in

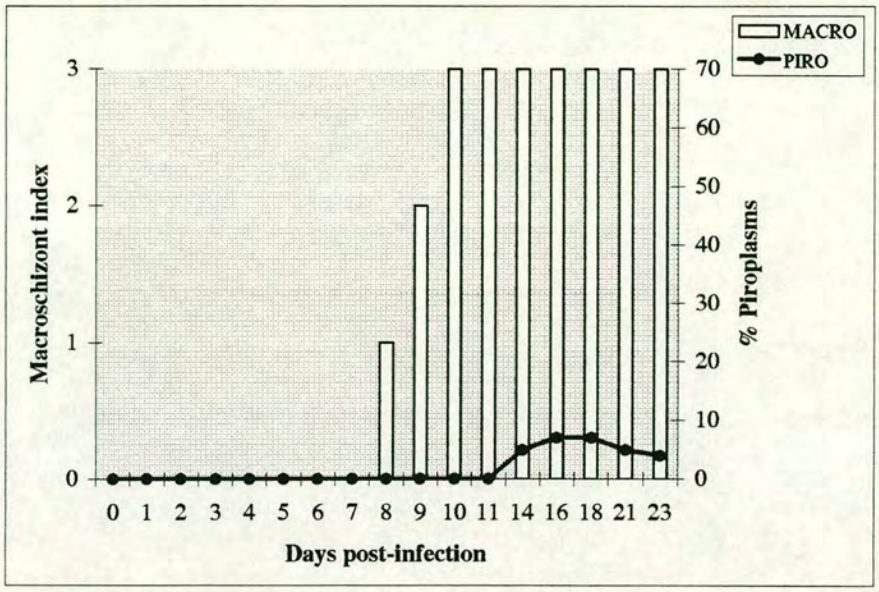

MACRO Macroschizonts
PIRO Piroplasms

Figure 3.20 Parasite development in a calf (861) infected with *T. annulata* (Doukkalla)

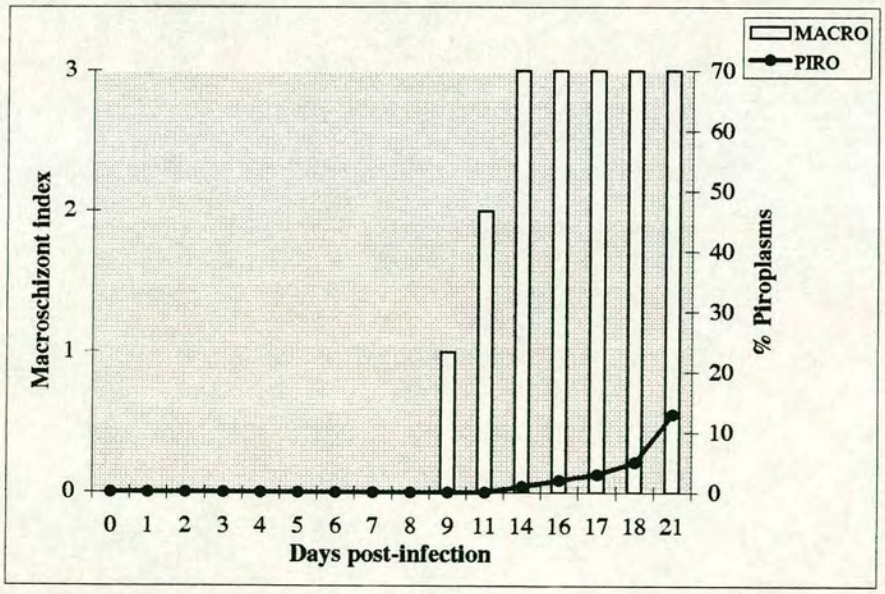

MACRO Macroschizonts
PIRO Piroplasms

Figure 3.21 Parasite development in a calf (8) infected with *T. parva* (Muguga)

pyrexia on day 8 post-infection the NO_2^- levels had fallen markedly to 0.2μM. At the height of disease on day 13 post-infection (the day before the animal was euthanased) NO_2^- levels increased to 4.7μM (Figure 3.22A). A rise in the production of NO_2^- by the PBM was accompanied by the following: several days of pyrexia; large numbers of macroschizonts, piroplasms and hyperplastic cells. No obvious parameters could be associated with the decrease in NO_2^- production by the PBM of calf 20 on day 8 post-infection.

The NO_2^- produced by the PBM of calf 19 on day 5 post-infection increased to 9.6μM. The baseline value was 0μM. The NO_2^- levels fell markedly to 1.1μM on day 8 post-infection (Figure 3.22B) (4 days before the animal was euthanased) prior to the initial marked rise in temperature. A rise in the production of NO_2^- by the PBM was associated with the following: the second day of pyrexia; the first signs of lymph node enlargement and hyperplastic cells; the initial appearance of macroschizonts. No obvious parameters could be associated with the decrease in NO_2^- production by the PBM of calf 19 on day 8 post-infection.

The NO_2^- produced by the PBM of calf 55C on day 5 post-infection (2 days before the animal was euthanased) increased to 2.5μM. The baseline value was 0.8μM (Figure 3.22C). A rise in the production of NO_2^- by the PBM of calf 55C was associated with the same parameters described for calf 19.

Bo rIFN-γ slightly enhanced NO_2^- production by the PBM of the calves (Figure 3.22). L-NMMA completely inhibited NO_2^- production by the PBM of the calves, showing NO_2^- was derived from the degradation of NO.

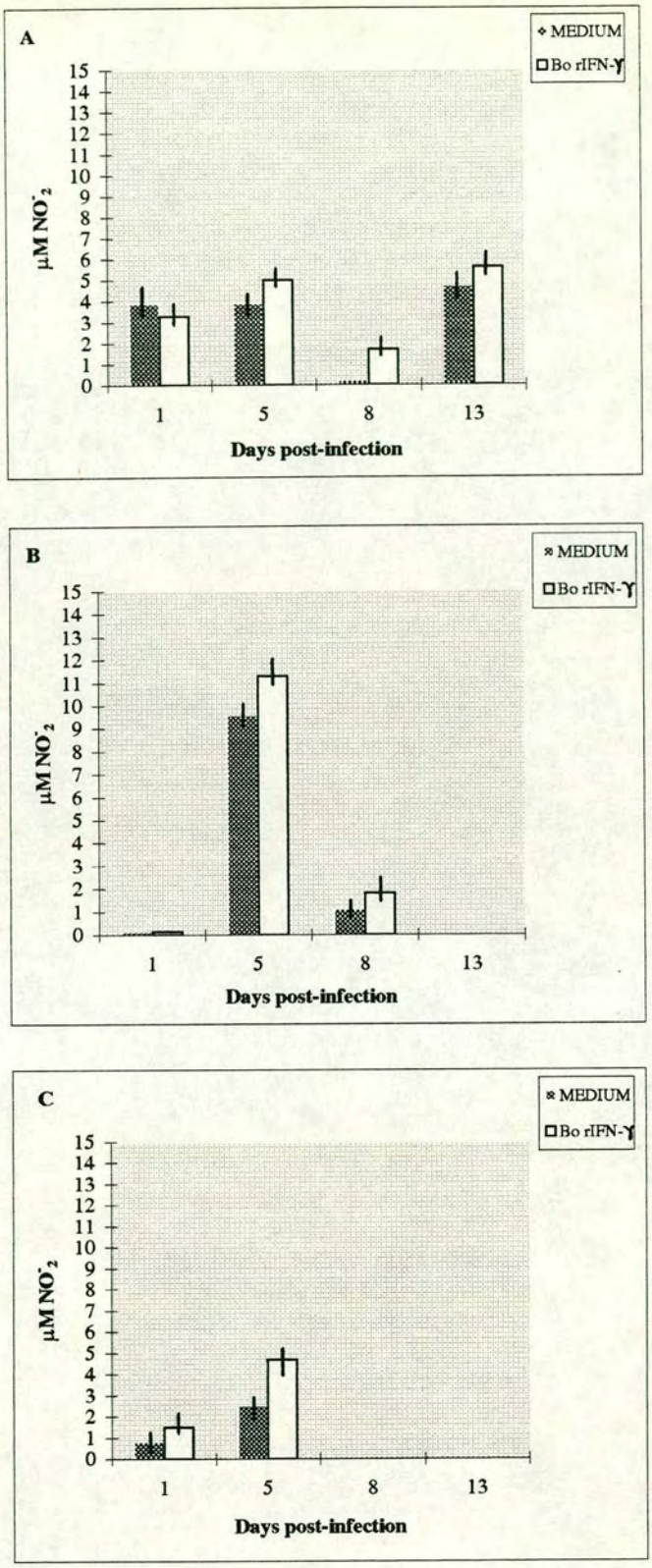

Bo rIFN-γ Bovine recombinant interferon gamma
NO_2^- Nitrite

Figure 3.22 Nitrite production by PBM harvested from calves (20 (A), 19 (B) & 55C (C)) infected with *T. annulata* (Hisar)

3.5 DISCUSSION

The clinical and haematological responses and parasite development monitored over the course of infection showed that all calves, with the exception of the calf euthanased on day 7 post-infection, exhibited a severe response (Anon 1989) to the administered doses of sporozoites of different stocks of *T. annulata* and of *T. parva* (Muguga). All the calves, with the exception of calf 55C (euthanased on day 7 post-infection), exhibited symptoms associated with an 'acute' form of infection (Neitz 1957).

Pyrexia was severe in all the calves inoculated with sporozoites of *T. annulata* (Hisar) with the exception of calf 55C (euthanased on day 7 post-infection) as demonstrated by a temperature above 39.4^{0}C for 8 days or more. Leucopenia was prompt with a substantial reduction in the numbers of lymphocytes, neutrophils and monocytes. The numbers of eosinophils and basophils remained unchanged. The leucopenic response coincided with the onset of pyrexia and enlargement of the lymph node at the site of inoculation. Severe anaemia was recorded and was demonstrated by a substantial decline in the numbers of RBC and PCV. This response coincided with a piroplasm parasitaemia equal to or more than 30%. The number of platelets (Table 3.2) was markedly reduced. A macroschizont parasitosis in the draining lymph node greater than 5% was recorded which coincided with a marked increase in the number of hyperplastic cells. These findings were similar to previous studies where calves underwent lethal infections (Prasad 1946; Laiblin 1978; Preston *et al.* 1992a).

The clinical and haematological responses and parasite development monitored over the course of infection for the calf (55C) euthanased on day 7 post-infection, inoculated with sporozoites of *T. annulata* (Hisar), were similar to and often ran parallel to the other *T. annulata* (Hisar) infected calves whose infections ran to completion. It was therefore concluded that the calf euthanased on day 7 post-infection had exhibited the initial stages of a severe response to infection.

Although all calves responded severely to infection, differences were observed in pyrexia and parasitological responses between calves inoculated with different stocks

of *T. annulata* and from *T. parva* (Muguga). Calves inoculated with *T. annulata* (Hisar) became pyrexic on day 4-5 post-infection whereas, calves inoculated with *T. annulata* (Doukkalla) or *T. parva* (Muguga) became pyrexic on day 9 post-infection. The duration in days to the detection of the first macroschizont was shorter for calves with *T. annulata* (Hisar) than for calves with *T. annulata* (Doukkalla) or with *T. parva* (Muguga). The duration in days to the detection of the first piroplasm was shorter for calves with *T. annulata* (Hisar) and *T. annulata* (Doukkalla) than for the calf with *T. parva* (Muguga).

The WBC and RBC responses of the calf infected with *T. annulata* (Doukkalla) differed from those of the calves infected with *T. annulata* (Hisar) described here and those reported previously (Preston *et al.* 1992a). This calf exhibited a moderate leucopenic response with a five-fold increase in the numbers of monocytes from preinfection numbers. A mild anaemia was detected by the small decline in the numbers of RBC and PCV which coincided with a piroplasm parasitaemia of 9%. A macroschizont parasitosis in the draining lymph node greater than 5% was recorded which coincided with a marked increase in the number of hyperplastic cells.

The findings obtained with the calf infected with *T. parva* (Muguga) were similar to those reported in previous studies, except that infection in this animal was prolonged (Morrison *et al.* 1981a). This calf exhibited a severe leucopenic response which was sustained for 7 days prior to euthanasia. A mild anaemia was detected by the small decline in the numbers of RBC and PCV which coincided with a piroplasm parasitaemia of 13%. A macroschizont parasitosis in the draining lymph node greater than 5% was recorded which coincided with a marked increase in the number of hyperplastic cells.

A role for the macroschizont in the clinical symptoms associated with both *T. annulata* and *T. parva* (Muguga) infections was indicated by a severe macroschizont parasitosis accompanied by a severe pyrexia and leucopenia. The absence of detectable intra-erythrocytic piroplasms in the blood and liver smears of calves succumbing to *T. annulata* (Tova) infection (Pipano, Weisman & Benado 1974) provides some evidence of a role for the macroschizonts in the clinical symptoms

associated with *T. annulata* infections at least. A role for the piroplasm in the pathogenesis of anaemia (Preston *et al.* 1992a) was indicated by the direct relation found between the numbers of RBC, PCV and piroplasm parasitaemia observed in all the calves both those infected with *T. annulata* and that infected with *T. parva* (Muguga).

The results showed that PBM from all the calves inoculated with *T. annulata* (Hisar) produced NO over the course of infection. Levels of NO recorded in cultures of PBM harvested at intervals for the calf euthanased on day 14 post-infection were very similar but decreased on day 8 post-infection. Levels of NO recorded in cultures of PBM harvested at intervals for the other calves increased on day 5 post-infection and decreased on day 8 post-infection. The complete reduction in levels of NO_2^- produced in the cultures which included L-NMMA confirmed that this compound was a degradation product of NO and reflected the specific production of NO by the PBM. Incubation with BoIFN-γ did not markedly affect NO production. It was therefore concluded that PBM harvested from calves undergoing infection with *T. annulata* (Hisar) synthesized NO spontaneously *in vitro*. The results resembled those obtained by previous studies (Visser *et al.* 1995) where PBM harvested at intervals from cattle undergoing infection with *T. annulata* and *T. parva* synthesized NO spontaneously *in vitro*.

Although a lack of knowledge limits discussion of the potential role of NO in the pathogenesis of infection with *T. annulata* or *T. parva*, this molecule may be responsible for some of the symptoms and lesions described here which resembled those attributed to NO activity in other diseases (Clark, Rockett & Cowden 1991; Lopez-Belmonte *et al.* 1993). That is, NO activity may contribute to the mucosal damage and haemorrhage detected in calves infected with *T. annulata* or *T. parva* (Uilenberg 1981a; Irvin & Cunningham 1981); to the lymphocytolysis detected in *T. parva* (Morrison *et al.* 1981a); to the comatose state which sometimes accompanies the terminal stages of *T. annulata* (Srivastava & Sharma 1976) and *T. parva* (Giles *et al.* 1978) infections.

3.6 CONCLUSION

It was concluded that the tissues collected for the subsequent pathological studies had been obtained from calves responding severely to infection. Calves infected with *T. annulata* (Hisar) were euthanased during the initial stages of pyrexia, peak pyrexia and the nadir of disease. Calves infected with *T. annulata* (Doukkalla) and *T. parva* (Muguga) were euthanased during the nadir of disease. With the exception of the calf infected with *T. annulata* (Doukkalla), all other calves had responded in a characteristic manner to infection with either *T. annulata* (Hisar) (Preston *et al.* 1992a) or *T. parva* (Muguga) (Irvin & Morrison 1987). All the calves, with the exception of the calf euthanased during the early stages of infection, exhibited symptoms associated with an 'acute' (lethal) form of infection.

CHAPTER FOUR

PATHOLOGY OF BOVINE THEILERIOSES

4.1 INTRODUCTION

The macroscopic and microscopic pathology of selected lymphoid and other non-lymphoid organs was examined in calves infected with *T. annulata* or *T. parva* (Muguga). The organs were initially selected on the basis of: the distribution of the macroscopic lesions seen at the post-mortem examination of calf 41B; their physiological importance, and, in the case of lymph nodes, their distance from the site of inoculation. Additional organs, i.e. the brain, the pituitary gland, the hepatic lymph node and skin lesions were examined from subsequent calves.

The thymus and the spleen and the following lymph nodes were selected for particular attention from all animals: the prescapular lymph node (LN) which drained the site of inoculation and the contralateral prescapular LN; the draining and contralateral precrural LNs which were the LNs furthest away from the site of inoculation; the mesenteric LN which drained the gut and the hepatic LN which drained the liver. The organs of physiological importance were the kidney, liver, abomasum, lung, brain and heart. The adrenal and pituitary glands were of interest as endocrine glands.

The progressive development of lesions in calves infected with *T. annulata* (Hisar) was investigated by examining organs obtained during the initial stages of pyrexia, peak pyrexia and the nadir of disease. The tissue of calves infected with *T. annulata* (Doukkalla) or *T. parva* (Muguga) were examined during the nadir of disease.

4.2 EXPERIMENTAL DESIGN

A post-mortem examination was conducted on calves (Chapter 3) infected with *T. annulata* or *T. parva* (Muguga). Pilot studies were conducted on a calf which had been inoculated with sporozoites of *T. annulata* (Hisar). This calf provided tissues for sampling on day 12 post-infection to assess the lesions during the nadir of disease. Three calves were then inoculated with sporozoites of *T. annulata* (Hisar) to provide: tissues for sampling on days 7, 12 and 14 post-infection to assess the lesions

during the initial stages of pyrexia, peak pyrexia and nadir of disease respectively. A calf inoculated with sporozoites of *T. annulata* (Doukkalla) from another study provided tissues for sampling on day 24 post-infection to assess the lesions of a different stock of *T. annulata* during the nadir of disease. During the course of the work a calf which had been inoculated with sporozoites of *T. parva* (Muguga) from another study became available. This calf provided tissues for sampling on day 21 post-infection and was used to assess the lesions of a different species of *Theileria* during the nadir of disease.

The organs were examined for macroscopic lesions including oedema and haemorrhage from the selected organs. Samples of tissues were fixed in formaldehyde for processing by conventional haematoxylin and eosin staining techniques for the examination of their microscopic lesions. Samples of tissues from healthy normal cattle, obtained from the Gorgie abattoir by the chief meat inspector Mr. Alan Cameron, were treated similarly to provide control material from uninfected animals. The tissue sections were examined for microscopic lesions, including necrosis and haemorrhage, and their cellular components, in particular lymphoid cells and macrophages, assessed.

4.3 MATERIALS & METHODS

4.3.1 COLLECTION OF TISSUES POST-MORTEM

The organs were collected immediately following euthanasia of the calves by intravenous barbiturate Euthatal (Rhone Merieux) @1ml/1.4kg body weight *in extremis*. Macroscopic lesions were recorded and samples of tissue were removed from the following lymphoid and non-lymphoid organs: the draining and contralateral prescapular LNs, draining and contralateral precrural LNs, mesenteric and hepatic LNs, spleen, thymus, kidney, liver, abomasum, lung, brain stem, cerebellum, cerebral hemispheres, heart, skin, adrenal and pituitary glands.

4.3.2 FIXATION, PROCESSING & SECTIONING OF TISSUES EMBEDDED IN PARAFFIN WAX

Several samples ($1cm^3$) were removed from each of the organs and fixed as soon as possible in 10% neutral buffered formaldehyde (pH 7.4) for 24 hours and processed in a vacuum impregnation processor (Mile Scientific). This process conducted by

staff at the University of Edinburgh Pathology Department involved the dehydration of tissues through ascending percentages of alcohol (50% to absolute alcohol) to xylene prior to the tissues being embedded in paraffin wax. Paraffin tissue sections 3μm in thickness were cut on a rotary microtome (Leitz 1512), floated on water heated to 56^{0}C and mounted onto poly-l-lysine (Sigma) coated slides [Appendix V]. Sections were air-dried at 56^{0}C for 24 hours and stored in slide boxes.

4.3.3 STAINING OF PARAFFIN TISSUE SECTIONS BY HAEMATOXYLIN & EOSIN

The paraffin tissue sections were dewaxed in histoclear (Raymond A Lamb), rehydrated through alcohol to water, stained in Harris's haematoxylin (Raymond A Lamb), differentiated in acid/alcohol, blued up in Scott's tap water, stained in eosin-Y (Raymond A Lamb), dehydrated through alcohol to histoclear and mounted in DPX permanent mounting medium (BDH) [Appendix VI & VII].

4.3.4 ASSESSMENT OF MICROSCOPIC PATHOLOGY

Several tissue sections from each organ were examined at 200 x magnification using a Nikon S. Ke II microscope. Structural changes were recorded in the organs which included assessment of the following: lymphoid follicle morphology; lymphoid cell depletion; granuloma formation; medullary cord disruption; medullary sinus disruption; disruptive cellular infiltrate; oedema; congestion.

The numbers of lymphoid cells, macrophages, foamy macrophages and eosinophils as compared to numbers in uninfected tissue sections were recorded on the following subjective scale: nc no change; + small increase; ++ moderate increase; +++ large increase; - small decrease; -- moderate decrease; --- large decrease. The damage detected in these tissue sections which was due to necrosis or haemorrhage was assessed on a subjective scale as follows: - no damage; * mild damage; ** moderate damage; *** extensive damage.

Since the macroschizont-infected cells were difficult to detect in tissue sections unless stained by immunocytochemical techniques, as described below, no attempt was made to assess the distribution of the parasites at this stage of the work.

4.4 RESULTS

4.4.1 MACROSCOPIC POST-MORTEM FINDINGS

No macroscopic lesions were observed in lymphoid or non-lymphoid organs of the uninfected normal cattle, but a variety of lesions were observed in the organs of the infected animals.

4.4.1.1 MACROSCOPIC LESIONS IN A CALF (41B) INFECTED WITH T. ANNULATA (HISAR) AS A PILOT STUDY

On day 12 post-infection during the terminal stages of disease in calf 41B [Table 4.1A] the draining prescapular LN was oedematous and extensive areas of haemorrhage were detected on its surface. The contralateral prescapular LN, draining and contralateral precrural LNs and mesenteric LN were all oedematous and haemorrhagic, but to a lesser degree than the draining prescapular LN. The spleen was friable and enlarged. Several petechial haemorrhages were seen on the surface of the thymus and lung. Ulceration of the abomasum was observed. Haemorrhages were found on the surfaces of the kidney, liver and adrenal gland.

4.4.1.2 MACROSCOPIC LESIONS IN CALVES (55C, 19 & 20) EXAMINED AT INTERVALS AFTER INFECTION WITH T. ANNULATA (HISAR)

On day 7 post-infection during the initial stages of pyrexia in calf 55C [Table 4.1A] the draining prescapular LN was enlarged and petechial haemorrhages were detected on its surface. Several petechial haemorrhages were seen on the hepatic LN and thymus. Macroscopic lesions were not found in the contralateral prescapular LN, draining and contralateral precrural LNs and mesenteric LN or the spleen, kidney, liver, abomasum, lung, brain stem, cerebellum, cerebral hemispheres, heart, adrenal or pituitary glands. Although no apparent lesions were detected in the brain, brain tissues were processed specifically to look for parasites, see below.

On day 12 post-infection at the peak of pyrexia in calf 19 [Table 4.1A] the draining prescapular LN was oedematous and extensive areas of haemorrhage were detected. Several petechial haemorrhages were seen on the surface of the contralateral prescapular LN, draining and contralateral precrural LNs, mesenteric and hepatic LNs and thymus. The spleen was friable. The hepatic LN, liver and lung were enlarged. Surface haemorrhages and petechial haemorrhages occurred on the kidney,

ORGAN	CALF			
	41B (day 12 post-infection)	55C (day 7 post-infection)	19 (day 12 post-infection)	20 (day 14 post-infection)
Prescapular LN (draining)	oedema & haemorrhage	petechial haemorrhage & enlarged	oedema & haemorrhage	oedema & haemorrhage
Prescapular LN (contralateral)	oedema & haemorrhage	no lesions	petechial haemorrhage	oedema & haemorrhage
Precrural LN (draining)	oedema & haemorrhage	no lesions	petechial haemorrhage	oedema & haemorrhage
Precrural LN (contralateral)	oedema & haemorrhage	no lesions	petechial haemorrhage	oedema & haemorrhage
Mesenteric LN	oedema & haemorrhage	no lesions	petechial haemorrhage	oedema & haemorrhage
Hepatic LN	nd	petechial haemorrhage	petechial haemorrhage & enlarged	oedema & haemorrhage
Spleen	friable & enlarged	no lesions	friable	friable
Thymus	petechial haemorrhage	petechial haemorrhage	petechial haemorrhage	petechial haemorrhage
Kidney	haemorrhage	no lesions	petechial haemorrhage, haemorrhage & enlarged	haemorrhage
Liver	haemorrhage	no lesions	petechial haemorrhage, haemorrhage & enlarged	white 'infarcts'
Abomasum	ulceration	no lesions	haemorrhage	ulceration
Lung	petechial haemorrhage	no lesions	petechial haemorrhage, haemorrhage & enlarged	petechial haemorrhage
Brain stem	nd	no lesions	no lesions	no lesions
Cerebellum	nd	no lesions	no lesions	no lesions
Cerebral hemisphere	nd	no lesions	no lesions	no lesions
Heart	nd	no lesions	no lesions	no lesions
Adrenal gland	haemorrhage	no lesions	petechial haemorrhage & haemorrhage	oedema & haemorrhage
Pituitary gland	nd	no lesions	no lesions	no lesions

LN Lymph node
nd Not done

Table 4.1A Macroscopic lesions in the organs of calf 41B (at nadir of disease) and in organs assessed during the initial stages of pyrexia (calf 55C), peak pyrexia (calf 19) and at nadir of disease (calf 20) in calves infected with *T. annulata* (Hisar)

liver, lung and adrenal gland. Areas of haemorrhage were found on the abomasum. No macroscopic lesions were seen in the brain stem, cerebellum, cerebral hemispheres, heart or pituitary gland.

On day 14 post-infection at the nadir of disease in calf 20 [Table 4.1A] the draining prescapular LN was oedematous and extensive areas of haemorrhage were detected (Figure 4.1). The contralateral prescapular LN, draining (Figure 4.2) and contralateral precrural LNs, mesenteric and hepatic LNs and adrenal gland (Figure 4.3) were oedematous and haemorrhagic, but to a lesser degree than the draining prescapular LN. The spleen was friable. Several surface petechial haemorrhages were observed on the thymus (Figure 4.4) and lung (Figure 4.5). Surface haemorrhages were seen on the kidney (Figure 4.6) and liver (Figure 4.7). White "infarcts" were found on the surface of the liver (Figure 4.8). Several ulcers were seen in the abomasum (Figure 4.9). No macroscopic lesions were found in the brain stem, cerebellum, cerebral hemispheres, heart or pituitary gland.

4.4.1.3 MACROSCOPIC LESIONS IN A CALF (861) DURING THE TERMINAL STAGES OF INFECTION WITH T. ANNULATA (DOUKKALLA)

On day 24 post-infection during the terminal stages of disease in calf 861 [Table 4.1B] the draining prescapular LN was oedematous and extensive areas of haemorrhage were detected. The contralateral prescapular LN, draining and contralateral precrural LNs and mesenteric LN were oedematous and haemorrhagic, but to a lesser degree than the draining prescapular LN. White "infarcts" were observed on the surfaces of the liver and lung. The abomasum was extensively ulcerated. Nodular skin lesions were seen on the surfaces of the prescapular and groin regions of the animal. No macroscopic lesions were found in the spleen, thymus, kidney or adrenal gland.

4.4.1.4 MACROSCOPIC LESIONS IN A CALF (8) DURING THE TERMINAL STAGES OF INFECTION WITH T. PARVA (MUGUGA)

On day 21 post-infection during the terminal stages of disease in calf 8 [Table 4.1B] the draining prescapular LN was oedematous and extensive areas of haemorrhage were detected. The contralateral prescapular LN, draining and contralateral precrural

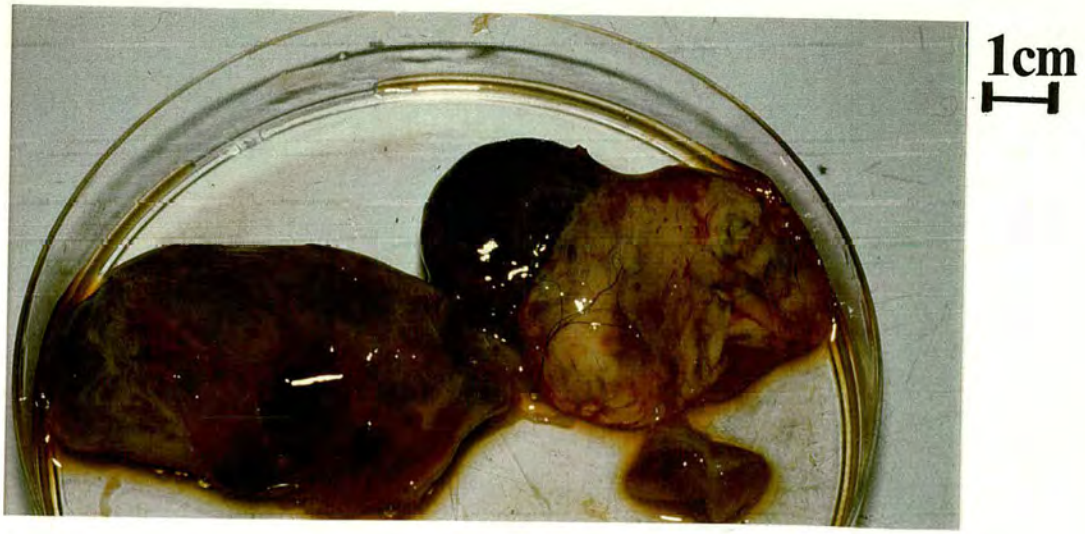

Figure 4.1 Extensive haemorrhage and oedema in the draining prescapular lymph node of the calf infected with *T. annulata* (Hisar) on day 14 post-infection at the nadir of disease.

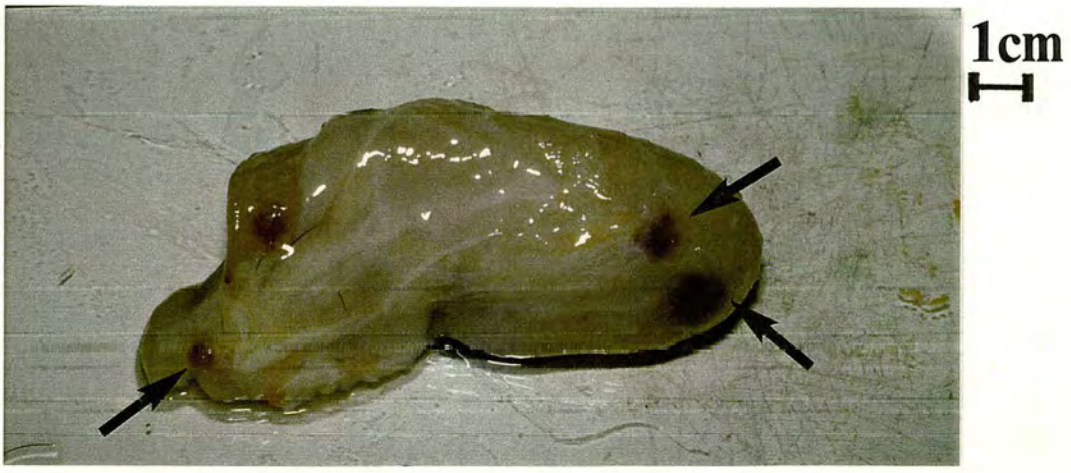

Figure 4.2 Haemorrhages (arrows) in the draining precrural lymph node of the calf infected with *T. annulata* (Hisar) on day 14 post-infection at the nadir of disease.

Figure 4.3 Oedematous adrenal gland of the calf infected with *T. annulata* (Hisar) on day 14 post-infection at the nadir of disease.

Figure 4.4 Petechial haemorrhages (arrows) in the thymus of the calf infected with *T. annulata* (Hisar) on day 14 post-infection at the nadir of disease.

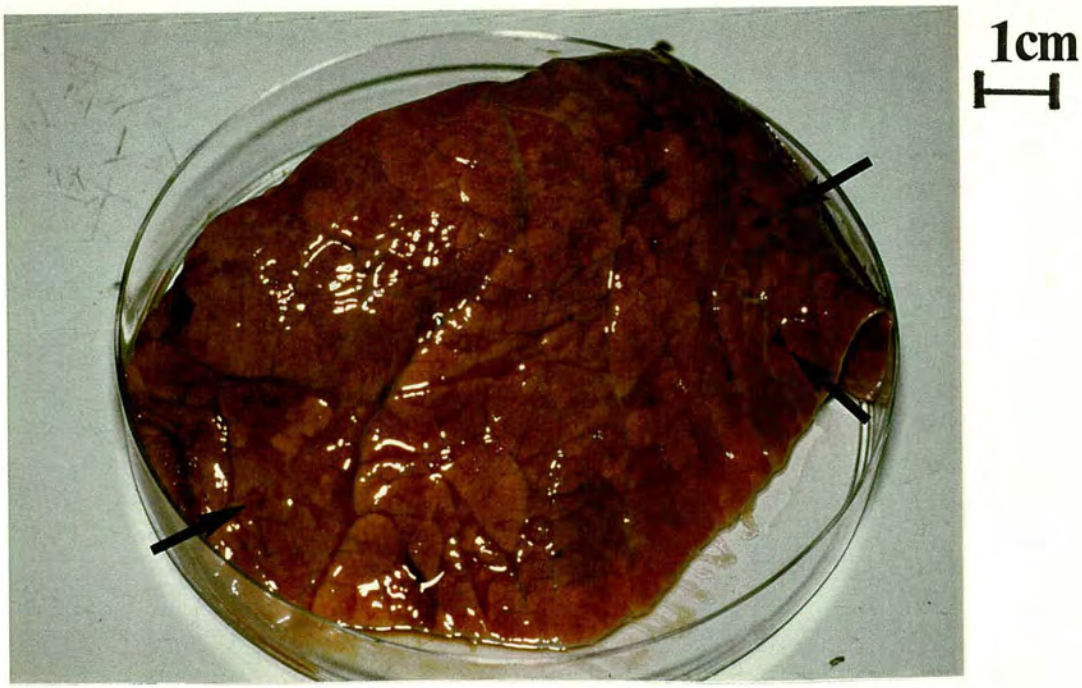

Figure 4.5 Petechial haemorrhages (arrows) in the lung of the calf infected with *T. annulata* (Hisar) on day 14 post-infection at the nadir of disease.

Figure 4.6 Petechial haemorrhages (arrows) in the kidney of the calf infected with *T. annulata* (Hisar) on day 14 post-infection at the nadir of disease.

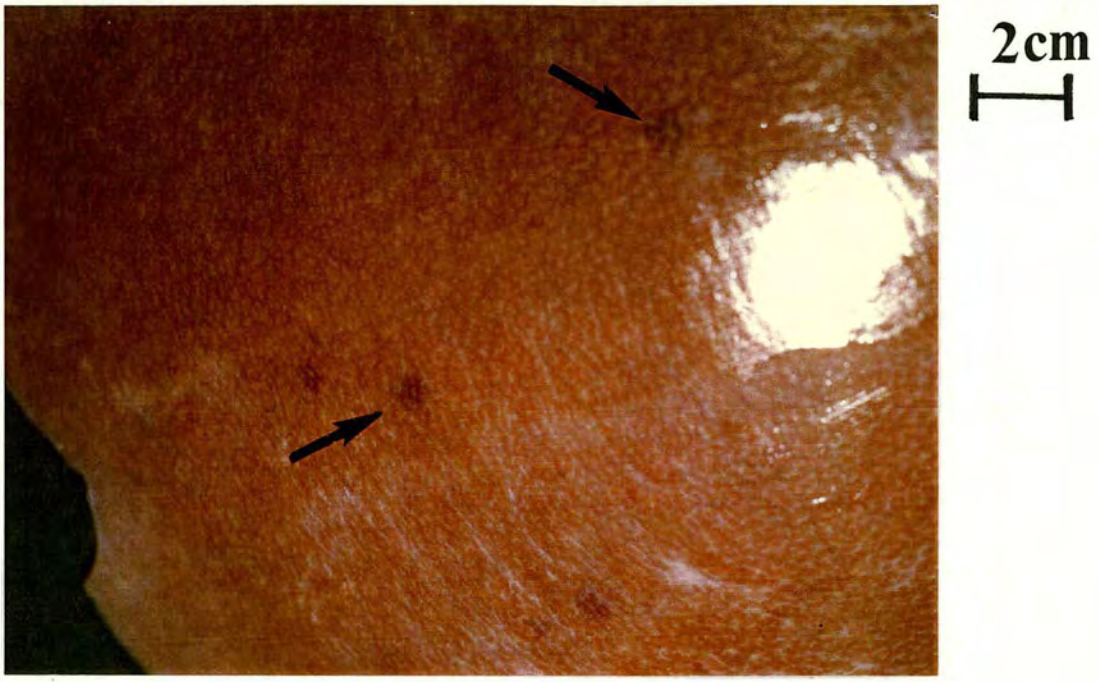

Figure 4.7 Petechial haemorrhages (arrows) in the liver of the calf infected with *T. annulata* (Hisar) on day 14 post-infection at the nadir of disease.

Figure 4.8 White "infarcts" (arrow) in the liver of the calf infected with *T. annulata* (Hisar) on day 14 post-infection at the nadir of disease.

Figure 4.9 Ulcers (arrows) in the abomasum of the calf infected with *T. annulata* (Hisar) on day 14 post-infection at the nadir of disease.

ORGAN	CALF	
	861 (day 24 post-infection)	8 (day 21 post-infection)
Prescapular LN (draining)	oedema & haemorrhage	oedema & haemorrhage
Prescapular LN (contralateral)	oedema & haemorrhage	oedema & haemorrhage
Precrural LN (draining)	oedema & haemorrhage	oedema & haemorrhage
Precrural LN (contralateral)	oedema & haemorrhage	oedema & haemorrhage
Mesenteric LN	oedema & haemorrhage	oedema & haemorrhage
Hepatic LN	nd	oedema & haemorrhage
Spleen	no lesions	no lesions
Thymus	no lesions	no lesions
Kidney	no lesions	no lesions
Liver	white 'infarcts'	no lesions
Abomasum	ulceration	no lesions
Lung	white 'infarcts'	no lesions
Brain stem	nd	nd
Cerebellum	nd	nd
Cerebral hemisphere	nd	nd
Heart	nd	no lesions
Skin	nodular	nd
Adrenal gland	no lesions	no lesions
Pituitary gland	nd	nd

LN Lymph node
nd Not done

Table 4.1B Macroscopic lesions in the organs of calf 861 (at nadir of disease) infected with *T. annulata* (Doukkalla) and in the organs of calf 8 (at nadir of disease) infected with *T. parva* (Muguga)

LNs, mesenteric and hepatic LNs were oedematous and haemorrhagic, but to a lesser degree than the draining prescapular LN. No macroscopic lesions were found on the spleen, thymus, kidney, liver, abomasum, lung, heart or adrenal gland.

The above observations on the macroscopic lesions led to the organs being processed for further study, as described below.

4.4.2 MICROSCOPIC PATHOLOGICAL FINDINGS

A normal tissue architecture as described by Banks (1993) and Burkitt, Young & Heath (1993) was observed in the following organs from normal uninfected cattle: the prescapular LN (Figure 4.10), precrural LN, mesenteric LN, spleen (Figure 4.11), thymus (Figure 4.12), kidney (Figure 4.13), liver (Figure 4.14), abomasum (Figure 4.15), lung (Figure 4.16) and adrenal gland (Figure 4.17). No areas of necrosis or haemorrhage were detected.

4.4.2.1 MICROSCOPIC LESIONS IN A CALF (41B) INFECTED WITH T. ANNULATA (HISAR) AS A PILOT STUDY

In contrast to the organs taken from normal uninfected cattle, a variety of lesions were found in the infected animals. On day 12 post-infection during the terminal stages of disease in calf 41B [Table 4.2A] the most adversely affected organ was the draining prescapular LN. Lymphoid cellular depletion and extensive areas of diffuse necrosis and haemorrhage were observed throughout the cortex, paracortex and medulla of this lymph node. The medullary cords and sinuses were severely disrupted. Lymphoid cellular depletion was observed in other lymphoid organs, in particular the paracortex of the contralateral prescapular LN, draining precrural LN and mesenteric LN, the white pulp of the spleen and cortex of the thymus. Lymphoid follicles were absent from the draining and contralateral prescapular LNs and reduced in size with small germinal centres in the draining and contralateral precrural LNs. Normal active follicles were seen in the mesenteric LN. Macrophages and foamy macrophages were increased in number throughout all the lymph nodes, spleen and thymus. Small granulomas were seen in the paracortex of the contralateral prescapular LN and draining precrural LN. The medullary cords of the draining precrural LN were disrupted. Sinus hyperplasia was seen in all the lymph

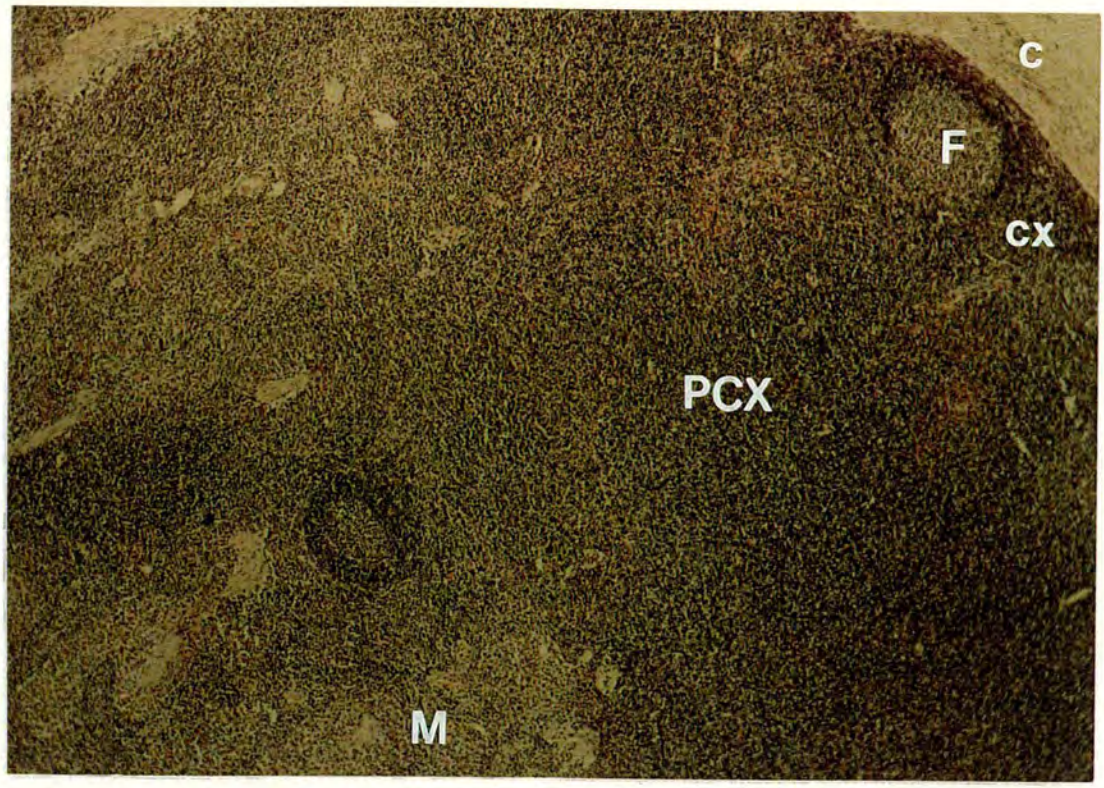

Figure 4.10 Section showing the capsule (C), cortex (CX), lymphoid follicles (F), paracortex (PCX) and medulla (M) of the prescapular lymph node of the normal, uninfected animal, (x40: H&E).

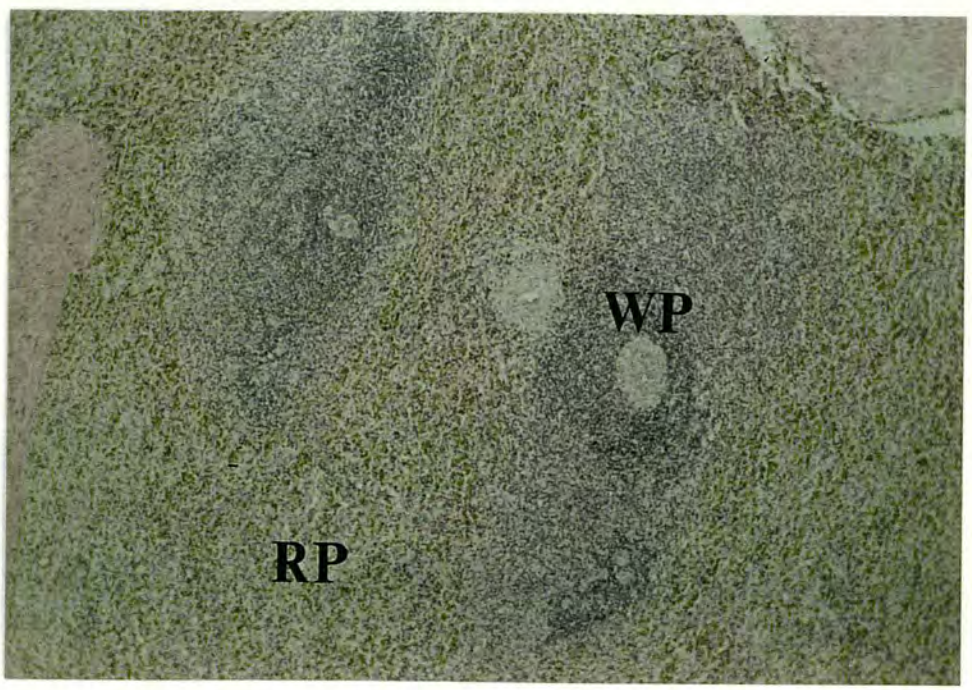

Figure 4.11 Section showing the white pulp (WP) and red pulp (RP) of the spleen of the normal, uninfected animal, (x40: H&E).

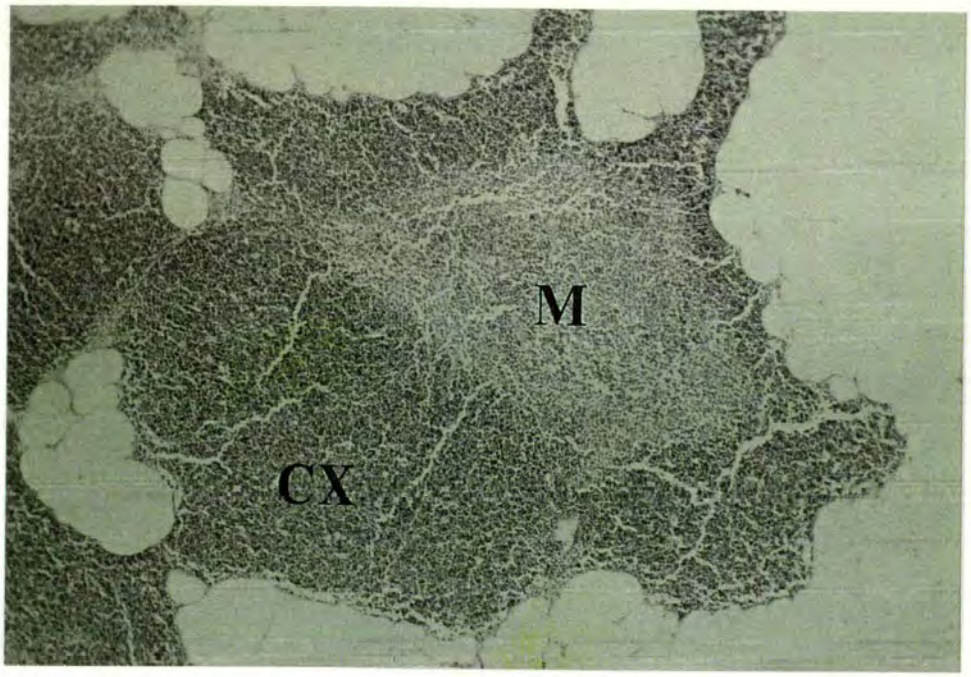

Figure 4.12 Section showing the cortex (CX) and medulla (M) of the thymus of the normal, uninfected animal, (x40: H&E).

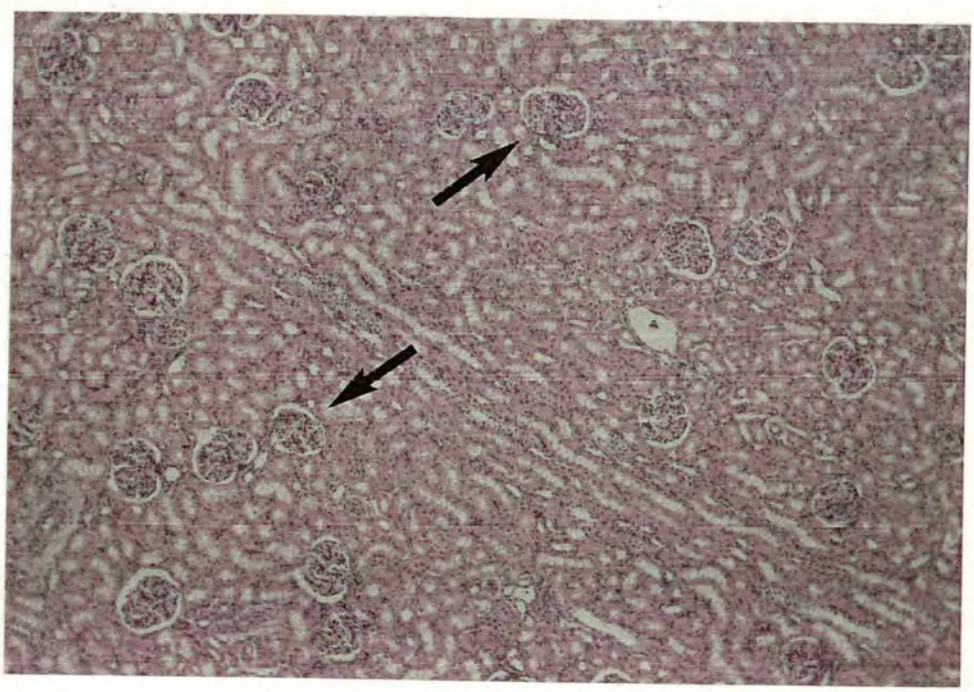

Figure 4.13 Section showing the glomeruli (arrows) in the cortex of the kidney of the normal, uninfected animal, (x40: H&E).

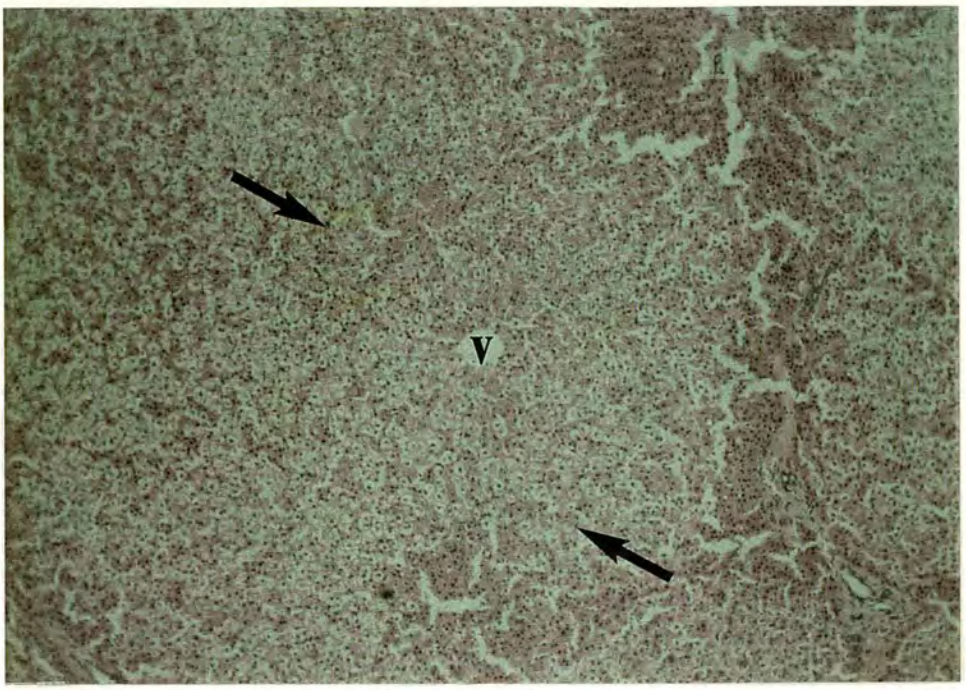

Figure 4.14 Section showing the central venule (V) and hepatocytes (arrows) of the hepatic lobule of the liver of the normal, uninfected animal, (x40: H&E).

Figure 4.15 Section showing the abomasum of the normal, uninfected animal, (x40: H&E).

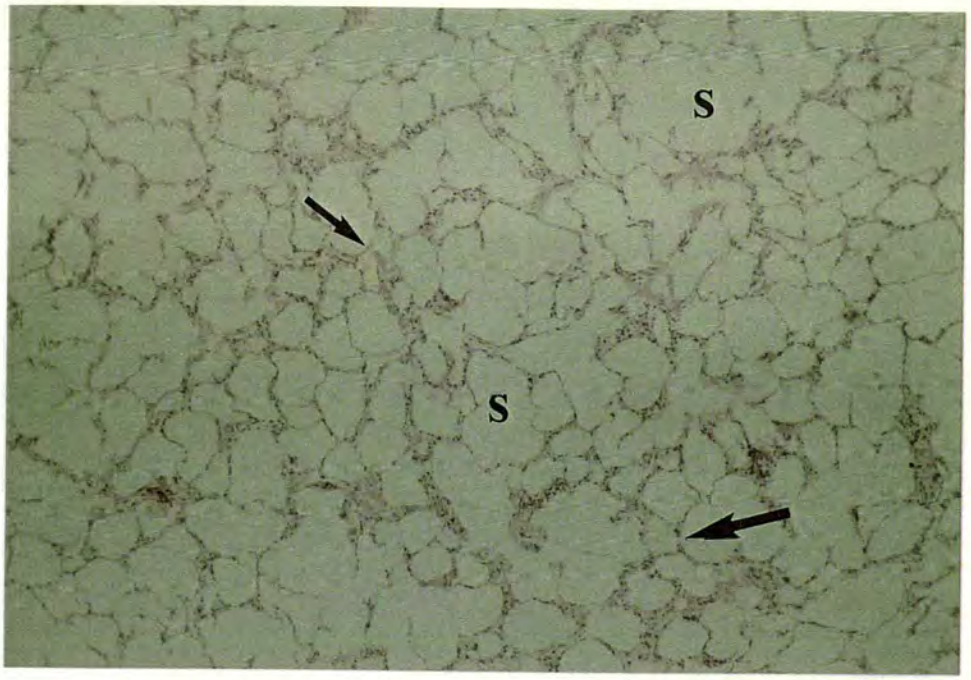

Figure 4.16 Section showing the alveolar spaces (S) and alveolar walls (arrows) of the lung of the normal, uninfected animal, (x40: H&E).

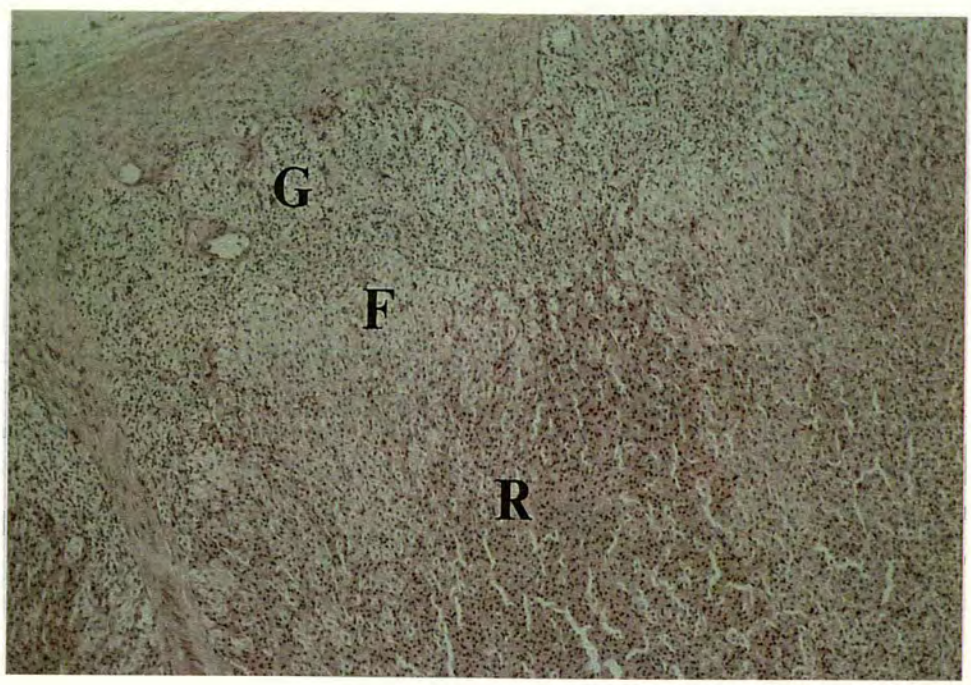

Figure 4.17 Section showing the zona glomerulosa (G), zona fasciculata (F) and zona reticularis (R) of the cortex of the adrenal gland of the normal, uninfected animal, (x40: H&E).

ORGAN	AREA	LC	MA	FMA	N	H	FEATURES	CHANGES
Prescapular LN (draining)	CX	-	+	+	***	*	Follicles	Absent
	PCX	--	+	+	***	**	Cellular depletion of LC	Throughout LN
	MC	--	--	+	***	**	Granulomas	Absent
	MS	-	-	+	***	**	MC	Disrupted
							MS	Disrupted
							Other	Severe disruption of LN architecture
Prescapular LN (contralateral)	CX	-	nc	+	-	-	Follicles	Absent
	PCX	-	+	+	-	-	Cellular depletion of LC	CX & PCX
	MC	nc	+	+	*	-	Granulomas	PCX
	MS	nc	++	+	-	-	MC	nc
							MS	Filled with mainly uninfected cells / sinus hyperplasia
							Other	Enlarged medulla
Precrural LN (draining)	CX	-	++	++	-	-	Follicles	Follicles with small germinal centres
	PCX	--	++	++	-	*	Cellular depletion of LC	CX, PCX & MC
	MC	-	-	+	-	-	Granulomas	PCX
	MS	nc	++	+	-	-	MC	Disrupted
							MS	Filled with mainly uninfected cells / sinus hyperplasia
							Other	Enlarged medulla
Precrural LN (contralateral)	CX	nc	nc	++	-	-	Follicles	Follicles with small germinal centres
	PCX	nc	+	++	-	-	Cellular depletion of LC	Absent
	MC	+	+	+	-	-	Granulomas	Absent
	MS	nc	++	+	-	-	MC	Prominent
							MS	Filled with mainly uninfected cells / sinus hyperplasia
							Other	Enlarged medulla
Mesenteric LN	CX	nc	nc	++	-	-	Follicles	Normal active follicles
	PCX	-	++	++	-	-	Cellular depletion of LC	PCX
	MC	+	+	+	-	-	Granulomas	Absent
	MS	nc	++	+	-	-	MC	Prominent
							MS	Filled with mainly uninfected cells / sinus hyperplasia
							Other	Enlarged medulla
Spleen	WP	--	+	++	-	-	Cellular depletion of LC in WP	Present
	RP	nc	+	++	-	-	Congestion of RP	Present
Thymus	CX	--	+	+	-	*	Cellular depletion of LC in CX	Present
	MED	nc	++	++	-	**		

nc No change
- Small decrease
-- Moderate decrease
--- Large decrease

+ Small increase
++ Moderate increase
+++ Large increase

- No damage
* Mild damage
** Moderate damage
*** Extensive damage

LC Lymphoid cells
FMA Foamy macrophages
MA Macrophages
N Necrosis
H Haemorrhage
LN Lymph node
CX Cortex
PCX Paracortex
MED Medulla
MC Medullary cords
MS Medullary sinuses
WP White pulp
RP Red pulp

Table 4.2A Microscopic lesions in a calf (41B) infected with *T. annulata* (Hisar) as a pilot study

ORGAN	AREA	LC	MA	FMA	N	H	FEATURES	CHANGES
Kidney	CX	+	+	+	-	-	Disruptive cellular infiltrate in CX	Present
	MED	nc	nc	+	-	-	Oedema of tubules	Present
Liver	PT	+	+	+	-	-	Disruptive cellular infiltrate	Present
							Oedema of hepatic cells	Present
Abomasum	LAP	++	++	++	-	-	Disruptive cellular infiltrate	Present
Lung	AW	+	++	+	+	+	Thickened AW	Present
	BRO	nc	nc	nc	-	-	Congestion of BRO	Absent

nc No change
- Small decrease
-- Moderate decrease
--- Large decrease

+ Small increase
++ Moderate increase
+++ Large increase

- No damage
* Mild damage
** Moderate damage
*** Extensive damage

LC Lymphoid cells
FMA Foamy macrophages
MA Macrophages
N Necrosis
H Haemorrhage

CX Cortex
MED Medulla
PT Portal tracts
LAP Lamina propria
AW Alveolar walls
BRO Bronchioles

Table 4.2A Continued

nodes, except for the draining prescapular LN. The medullary sinuses of these lymph nodes were filled with large numbers of uninfected macrophages. No change in the numbers of eosinophils in the lymphoid organs were detected (Table 4.2B), except for a small decrease in the numbers of eosinophils in the spleen. Increased numbers of lymphoid cells, macrophages and foamy macrophages were seen in the cortex of the kidney, portal tracts of the liver, lamina propria of the abomasum and alveolar walls of the lung. A small increase in the numbers of eosinophils was detected in the kidney (Table 4.2B), whereas a small decrease in the numbers of eosinophils was detected in the liver and abomasum. The numbers of eosinophils in the lung were unchanged.

4.4.2.2 MICROSCOPIC LESIONS IN CALVES (55C, 19 & 20) EXAMINED AT INTERVALS AFTER INFECTION WITH T. ANNULATA (HISAR)

On day 7 post-infection during the initial stages of pyrexia in calf 55C [Table 4.2C] the most adversely affected organ was the draining prescapular LN. Lymphoid cellular depletion was detected in the paracortex accompanied by increased numbers of macrophages and foamy macrophages (Figure 4.18). Lymphoid follicles in this lymph node were reduced in size with small germinal centres (Figure 4.18). Focal necrosis and haemorrhage (Figure 4.19) were also detected. Sinus hyperplasia was seen and the medullary sinuses were filled with large numbers of uninfected macrophages (Figure 4.20). Lymphoid cellular depletion was seen in the paracortex of the contralateral prescapular LN, hepatic LN and the white pulp of the spleen. Lymphoid follicles were reduced in size with small germinal centres in the contralateral prescapular LN and draining precrural LN, but normal active follicles were detected in the contralateral precrural LN, mesenteric and hepatic LNs. Increased numbers of macrophages were seen in the other lymphoid organs, with the exception of the thymus (Figure 4.21). Increased numbers of foamy macrophages were seen throughout all the lymph nodes, spleen and thymus. Sinus hyperplasia was seen in the contralateral prescapular LN, draining and contralateral precrural LNs, mesenteric and hepatic LNs and the medullary sinuses were filled with large number of uninfected macrophages. No disruption of the medullary cords was seen. Small granulomas were detected in the draining and contralateral prescapular LNs and the hepatic LN. No change in the numbers of eosinophils in the lymphoid organs was

ORGAN	CALF					
	41B	55C	19	20	861	8
Prescapular LN (draining)	nc	nc	+++	nc	nc	nc
Prescapular LN (contralateral)	nc	nc	nc	nc	nc	nc
Precrural LN (draining)	nc	nc	nc	nc	nc	-
Precrural LN (contralateral)	nc	nc	nc	nc	nc	-
Mesenteric LN	nc	nc	nc	nc	nc	nc
Hepatic LN	nd	nc	+	nc	nd	nc
Spleen	-	-	nc	-	-	--
Thymus	nc	nc	nc	nc	nc	-
Kidney	+	nc	+	+	nc	nc
Liver	-	nc	nc	nc	nc	-
Abomasum	-	-	-	-	nc	-
Lung	nc	nc	nc	nc	nc	nc
Brain stem	nd	nc	nc	nc	nd	nd
Cerebellum	nd	nc	nc	nc	nd	nd
Cerebral hemisphere	nd	nc	nc	nc	nd	nd
Heart	nd	nc	nc	nc	nd	nc
Skin	nd	nd	nd	nd	nc	nd
Adrenal gland	nd	nc	nc	nc	nd	nc
Pituitary gland	nd	nc	nc	nc	nd	nd

nc No change
- Small decrease
-- Moderate decrease
--- Large decrease

+ Small increase
++ Moderate increase
+++ Large increase
nd Not done

Table 4.2B Numbers of eosinophils in the tissue sections of calves (41B, 55C, 19 & 20) infected with *T. annulata* (Hisar), a calf (861) infected with *T. annulata* (Doukkalla) and a calf (8) infected with *T. parva* (Muguga)

ORGAN	AREA	LC	MA	FMA	N	H	FEATURES	CHANGES
Prescapular LN (draining)	CX	nc	+	++	-	-	Follicles	Follicles with small germinal centres
	PCX	--	+++	++	**	*	Cellular depletion of LC	PCX
	MC	+	+	-	**	**	Granulomas	PCX
	MS	nc	+++	-	**	**	MC	Prominent
							MS	Filled with mainly uninfected cells / sinus hyperplasia
							Other	Enlarged medulla
Prescapular LN (contralateral)	CX	nc	+	++	-	-	Follicles	Follicles with small germinal centres
	PCX	-	++	++	-	-	Cellular depletion of LC	PCX
	MC	+	+	+	-	-	Granulomas	PCX
	MS	nc	++	++	-	-	MC	Prominent
							MS	Filled with mainly uninfected cells / sinus hyperplasia
							Other	Enlarged medulla
Precrural LN (draining)	CX	nc	nc	++	-	-	Follicles	Follicles with small germinal centres
	PCX	nc	nc	++	-	*	Cellular depletion of LC	Absent
	MC	nc	+	+	-	*	Granulomas	Absent
	MS	nc	+	+	-	-	MC	nc
							MS	Filled with mainly uninfected cells / mild sinus hyperplasia
							Other	
Precrural LN (contralateral)	CX	nc	nc	++	-	-	Follicles	Normal active follicles
	PCX	nc	nc	++	-	-	Cellular depletion of LC	Absent
	MC	nc	nc	+	-	-	Granulomas	Absent
	MS	nc	+	+	-	-	MC	nc
							MS	Filled with mainly uninfected cells / mild sinus hyperplasia
							Other	
Mesenteric LN	CX	+	nc	++	-	-	Follicles	Normal active follicles
	PCX	nc	nc	++	-	-	Cellular depletion of LC	Absent
	MC	nc	+	+	-	-	Granulomas	Absent
	MS	nc	+	+	-	-	MC	nc
							MS	Filled with mainly uninfected cells / mild sinus hyperplasia
							Other	
Hepatic LN	CX	nc	nc	++	-	-	Follicles	Normal active follicles
	PCX	-	+	++	-	-	Cellular depletion of LC	PCX
	MC	+	+	+	-	-	Granulomas	PCX
	MS	+	+	++	-	-	MC	Prominent
							MS	Filled with mainly uninfected cells / sinus hyperplasia
							Other	Enlarged medulla
Spleen	WP	-	+	+	-	-	Cellular depletion of LC in WP	Present
	RP	nc	+	+	-	-	Congestion of RP	Present
Thymus	CX	nc	nc	nc	-	*	Cellular depletion of LC in CX	Absent
	MED	nc	nc	+	-	*		

nc No change
- Small decrease
-- Moderate decrease
--- Large decrease

+ Small increase
++ Moderate increase
+++ Large increase

- No damage
* Mild damage
** Moderate damage
*** Extensive damage

LC Lymphoid cells
FMA Foamy macrophages
MA Macrophages
N Necrosis
H Haemorrhage
CX Cortex
PCX Paracortex
MED Medulla
MC Medullary cords
MS Medullary sinuses
LN Lymph node
WP White pulp
RP Red pulp

Table 4.2C Microscopic lesions in a calf (55C) infected with *T. annulata* (Hisar) on day 7 post-infection

ORGAN	AREA	LC	MA	FMA	N	H	FEATURES	CHANGES
Kidney	CX	+	+	nc	-	-	Disruptive cellular infiltrate in CX	Present
	MED	nc	nc	nc	-	-	Oedema of tubules	Absent
Liver	PT	+	+	nc	-	-	Disruptive cellular infiltrate	Present
							Oedema of hepatic cells	Absent
Abomasum	LAP	+	nc	nc	-	-	Disruptive cellular infiltrate	Present
Lung	AW	+	nc	nc	-	-	Thickened AW	Present
	BRO	nc	nc	nc	-	-	Congestion of BRO	Present
Brain stem	GEN	nc	nc	nc	-	-	Disruptive cellular infiltrate	Absent: Normal architecture
Cerebellum	GEN	nc	nc	nc	-	-	Disruptive cellular infiltrate	Absent: Normal architecture
Cerebral hemisphere	GEN	nc	nc	nc	-	-	Disruptive cellular infiltrate	Absent: Normal architecture
Heart	GEN	nc	nc	nc	-	-	Disruptive cellular infiltrate	Absent: Normal architecture
Adrenal gland	ZG	nc	nc	nc	-	-	Disruptive cellular infiltrate	Absent: Normal architecture
	ZF	nc	nc	nc	-	-		
	ZR	nc	nc	nc	-	-		
	MED	nc	nc	nc	-	-		
Anterior Pituitary gland	GEN	nc	nc	nc	-	-	Disruptive cellular infiltrate	Absent: Normal architecture

nc No change
- Small decrease
-- Moderate decrease
--- Large decrease

+ Small increase
++ Moderate increase
+++ Large increase

- No damage
* Mild damage
** Moderate damage
*** Extensive damage

LC Lymphoid cells
FMA Foamy macrophages
MA Macrophages
N Necrosis
H Haemorrhage
GEN General
CX Cortex
MED Medulla
PT Portal tracts
LAP Lamina propria
AW Alveolar walls
BRO Bronchioles
ZG Zona glomerulosa
ZF Zona fasciculata
ZR Zona reticularis

Table 4.2C Continued

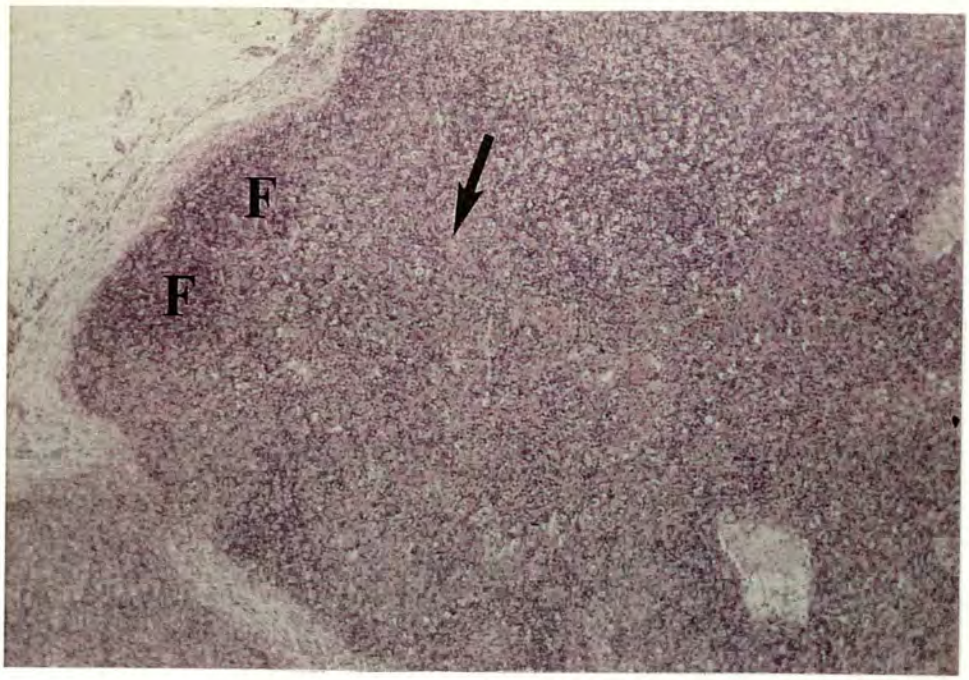

Figure 4.18 Section showing the sheets of macrophages and foamy macrophages (arrow) in the paracortex of the draining prescapular lymph node of the calf infected with *T. annulata* (Hisar) on day 7 post-infection during the initial stages of pyrexia. Note the lymphoid follicles (F) reduced in size with small germinal centres, (x40: H&E).

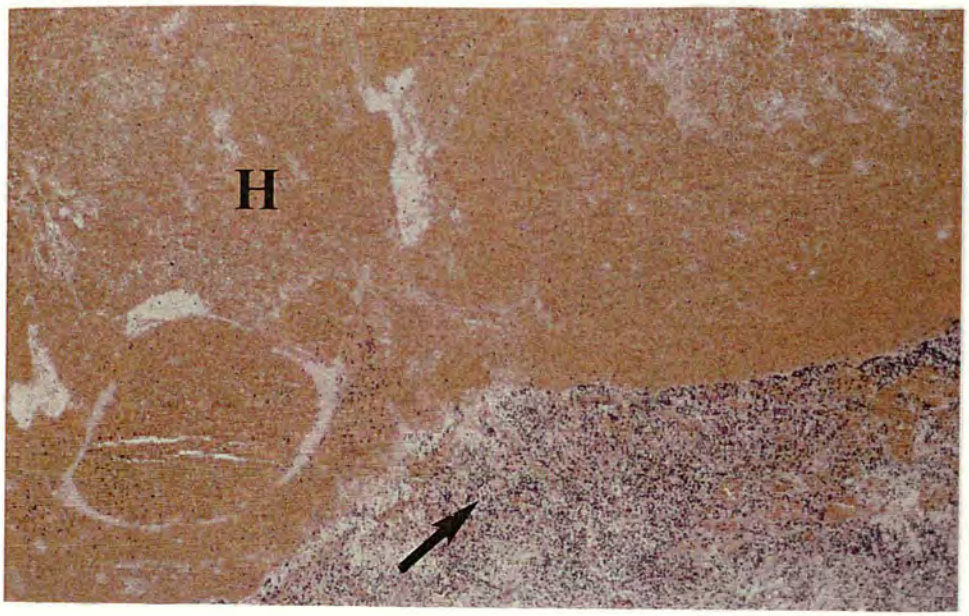

Figure 4.19 Section showing the extensive haemorrhage (H) and necrosis (arrow) in the paracortex of the draining prescapular lymph node of the calf infected with *T. annulata* (Hisar) on day 7 post-infection during the initial stages of pyrexia, (x40: H&E).

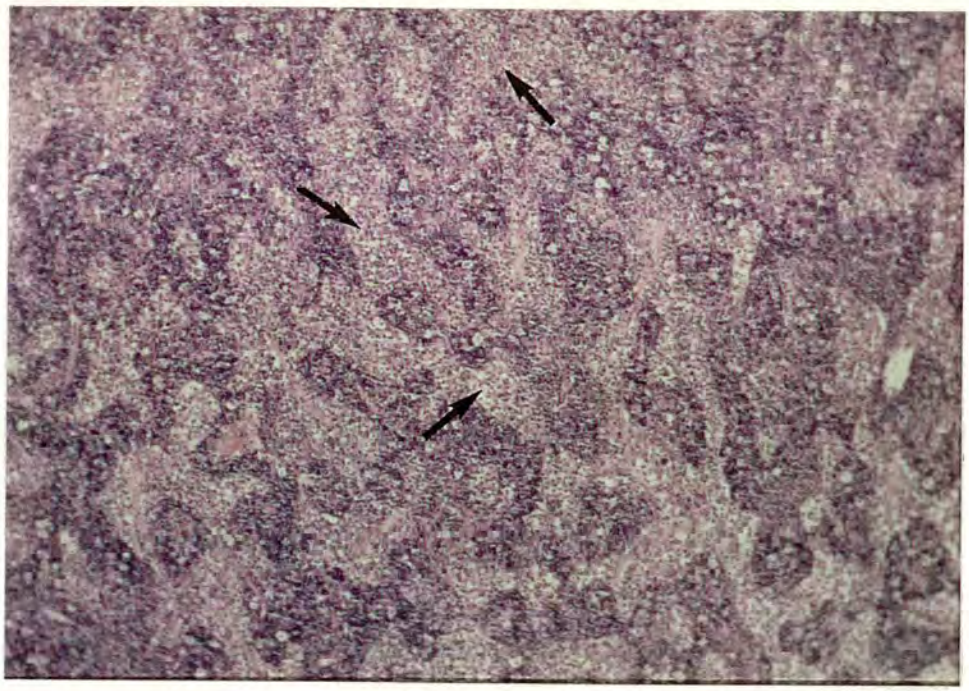

Figure 4.20 Section showing sinus hyperplasia in the medulla of the draining prescapular lymph node of the calf infected with *T. annulata* (Hisar) on day 7 post-infection during the initial stages of pyrexia. Note the medullary sinuses filled with macrophages (arrows) and the prominent medullary cords (MC), (x100: H&E).

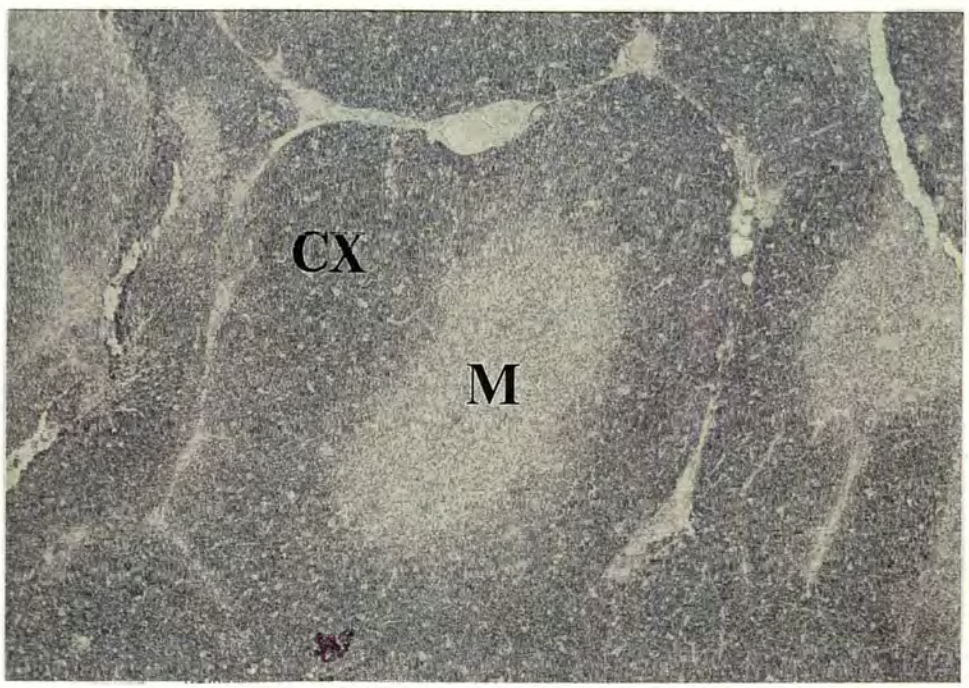

Figure 4.21 Section showing the normal architecture of the cortex (CX) and medulla (M) of the thymus of the calf infected with *T. annulata* (Hisar) on day 7 post-infection during the initial stages of pyrexia, (x40: H&E).

detected (Table 4.2B), except for a small decrease in the numbers of eosinophils in the spleen. Increased numbers of lymphoid cells and/or macrophages, but not foamy macrophages, were seen in the cortex of the kidney, portal tracts of the liver, lamina propria of the abomasum and alveolar walls of the lung. A normal architecture was seen in the brain, heart, adrenal and pituitary glands. No change in the numbers of eosinophils in the non-lymphoid organs was detected (Table 4.2B), except for a small decrease in the numbers of eosinophils in the abomasum.

On day 12 post-infection at the peak of pyrexia in calf 19 [Table 4.2D] the draining prescapular LN was still the most adversely affected organ. Lymphoid cellular depletion, increased numbers of macrophages and foamy macrophages, and multifocal granulomas (Figure 4.22) were detected throughout this lymph node. The granulomas were accompanied by large numbers of macrophages, eosinophils and parasitised cells (Figure 4.23). Sinus hyperplasia was seen and medullary sinuses were filled with large numbers of uninfected macrophages. Focal necrosis and diffuse haemorrhage were detected. Lymphoid cellular depletion was found in the remaining LNs, particularly in the paracortex of the contralateral prescapular LN, draining and contralateral precrural LNs, mesenteric and hepatic LNs. Lymphoid cellular depletion was also seen in the white pulp of the spleen and cortex of the thymus (Figure 4.24). Lymphoid follicles of all the lymph nodes were reduced in size with small germinal centres. Increased numbers of macrophages, accompanied by foamy macrophages in most cases, occurred in all the lymph nodes, spleen and thymus. Granulomas were also detected in the paracortex of the draining precrural LN. Sinus hyperplasia was seen in the other lymph nodes and the medullary sinuses were filled with large numbers of uninfected macrophages. The medullary cords of all the lymph nodes were disrupted, except for the contralateral prescapular LN. No change in the numbers of eosinophils in the lymphoid organs were detected (Table 4.2B), except for a large increase in the numbers of eosinophils in the draining prescapular LN and a small increase in the hepatic LN. Increased numbers of lymphoid cells and macrophages, also accompanied by foamy macrophages in most cases, were seen in the cortex of the kidney, portal tracts of the liver, lamina propria of the abomasum, alveolar walls of the lung and cortex of the adrenal gland. A normal architecture was still seen in the brain and heart. No change in the numbers

ORGAN	AREA	LC	MA	FMA	N	H	FEATURES	CHANGES
Prescapular LN (draining)	CX	-	++	+	-	-	Follicles	Follicles with small germinal centres
	PCX	--	+++	+	*	*	Cellular depletion of LC	Throughout LN
	MC	--	--	+	*	*	Granulomas	Throughout LN
	MS	-	+++	+	*	*	MC	Disrupted
							MS	Filled with mainly uninfected cells / sinus hyperplasia
							Other	Enlarged medulla
Prescapular LN (contralateral)	CX	nc	++	++	-	-	Follicles	Follicles with small germinal centres
	PCX	--	++	++	*	*	Cellular depletion of LC	PCX
	MC	+	+	+	-	-	Granulomas	Absent
	MS	nc	++	++	-	-	MC	Prominent
							MS	Filled with mainly uninfected cells / sinus hyperplasia
							Other	Enlarged medulla
Precrural LN (draining)	CX	nc	+	++	*	-	Follicles	Follicles with small germinal centres
	PCX	--	++	++	*	-	Cellular depletion of LC	PCX, MC & MS
	MC	-	-	+	*	-	Granulomas	PCX
	MS	-	++	++	*	-	MC	Disrupted
							MS	Filled with mainly uninfected cells / sinus hyperplasia
							Other	Enlarged medulla
Precrural LN (contralateral)	CX	-	+	++	*	-	Follicles	Follicles with small germinal centres
	PCX	--	++	++	*	-	Cellular depletion of LC	Throughout LN
	MC	-	-	+	*	-	Granulomas	Absent
	MS	-	++	++	*	-	MC	Disrupted
							MS	Filled with mainly uninfected cells / sinus hyperplasia
							Other	Enlarged medulla
Mesenteric LN	CX	+	nc	++	*	-	Follicles	Follicular hyperplasia
	PCX	-	+	++	*	*	Cellular depletion of LC	PCX, MC & MS
	MC	-	-	+	*	*	Granulomas	Absent
	MS	-	++	++	*	*	MC	Disrupted
							MS	Filled with mainly uninfected cells / sinus hyperplasia
							Other	Enlarged medulla
Hepatic LN	CX	-	+	++	*	-	Follicles	Follicles with small germinal centres
	PCX	--	++	++	*	-	Cellular depletion of LC	Throughout LN
	MC	-	-	+	*	-	Granulomas	Absent
	MS	-	++	++	*	-	MC	Disrupted
							MS	Filled with mainly uninfected cells / sinus hyperplasia
							Other	Enlarged medulla
Spleen	WP	-	+	nc	-	-	Cellular depletion of LC in WP	Present
	RP	nc	+	nc	-	-	Congestion of RP	Present
Thymus	CX	-	nc	nc	-	*	Cellular depletion of LC in CX	Present
	MED	nc	++	+	-	*		

nc No change
- Small decrease
-- Moderate decrease
--- Large decrease

+ Small increase
++ Moderate increase
+++ Large increase

- No damage
* Mild damage
** Moderate damage
*** Extensive damage

LC Lymphoid cells
FMA Foamy macrophages
MA Macrophages
N Necrosis
H Haemorrhage
CX Cortex
PCX Paracortex
MED Medulla
MC Medullary cords
MS Medullary sinuses
LN Lymph node
WP White pulp
RP Red pulp

Table 4.2D Microscopic lesions in a calf (19) infected with *T. annulata* (Hisar) on day 12 post-infection

ORGAN	AREA	LC	MA	FMA	N	H	FEATURES	CHANGES
Kidney	CX	+	nc	nc	-	-	Disruptive cellular infiltrate in CX	Present
	MED	nc	nc	nc	-	-	Oedema of tubules	Present
Liver	PT	+	+	+	*	*	Disruptive cellular infiltrate	Present
							Oedema of hepatic cells	Absent
Abomasum	LAP	+	+	++	-	-	Disruptive cellular infiltrate	Present
Lung	AW	+	+	nc	*	-	Thickened AW	Present
	BRO	nc	nc	nc	-	-	Congestion of BRO	Present
Brain stem	GEN	nc	nc	nc	-	-	Disruptive cellular infiltrate	Absent: Normal architecture
Cerebellum	GEN	nc	nc	nc	-	-	Disruptive cellular infiltrate	Absent: Normal architecture
Cerebral hemisphere	GEN	nc	nc	nc	-	-	Disruptive cellular infiltrate	Absent: Normal architecture
Heart	GEN	nc	nc	nc	-	-	Disruptive cellular infiltrate	Absent: Normal architecture
Adrenal gland	ZG	nc	nc	nc	-	-	Disruptive cellular infiltrate	Present
	ZF	+	+	nc	-	-		
	ZR	nc	nc	nc	-	-		
	MED	nc	nc	nc	-	-		
Anterior Pituitary gland	GEN	nc	nc	nc	-	-	Disruptive cellular infiltrate	Absent: Normal architecture

nc No change
- Small decrease
-- Moderate decrease
--- Large decrease

+ Small increase
++ Moderate increase
+++ Large increase

- No damage
* Mild damage
** Moderate damage
*** Extensive damage

LC Lymphoid cells
FMA Foamy macrophages
MA Macrophages
N Necrosis
H Haemorrhage
GEN General
CX Cortex
MED Medulla
PT Portal tracts
LAP Lamina propria
AW Alveolar walls
BRO Bronchioles
ZG Zona glomerulosa
ZF Zona fasciculata
ZR Zona reticularis

Table 4.2D Continued

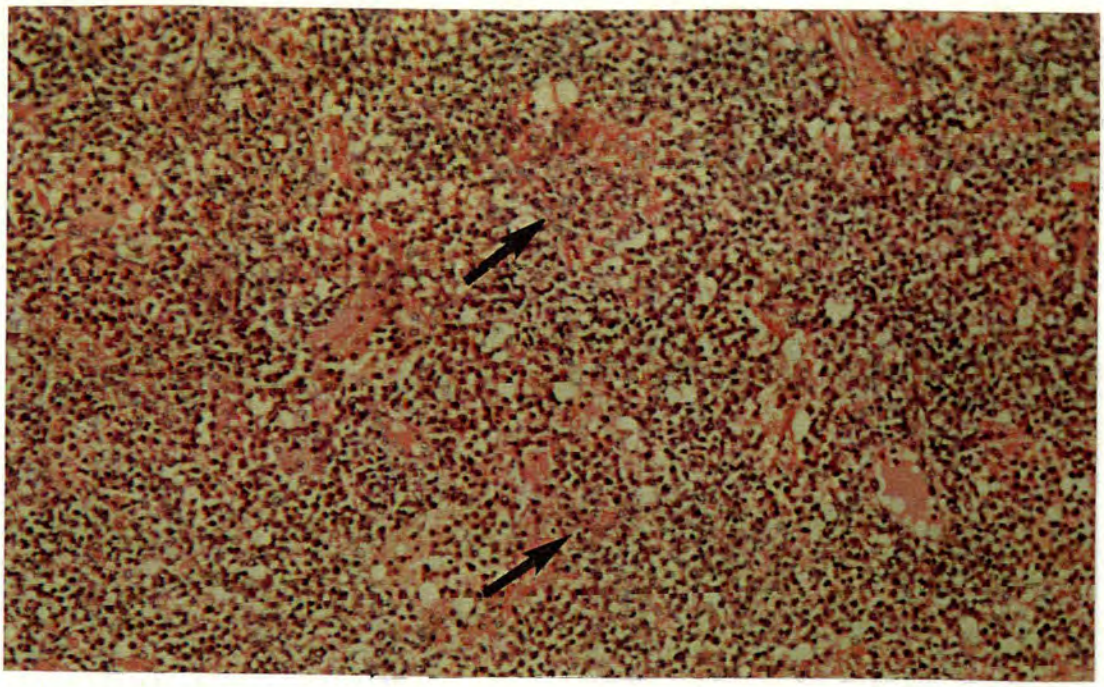

Figure 4.22 Section showing multifocal granulomas (arrows) distributed throughout the paracortex of the draining prescapular lymph node of the calf infected with *T. annulata* (Hisar) on day 12 post-infection at the peak of pyrexia, (x100: H&E).

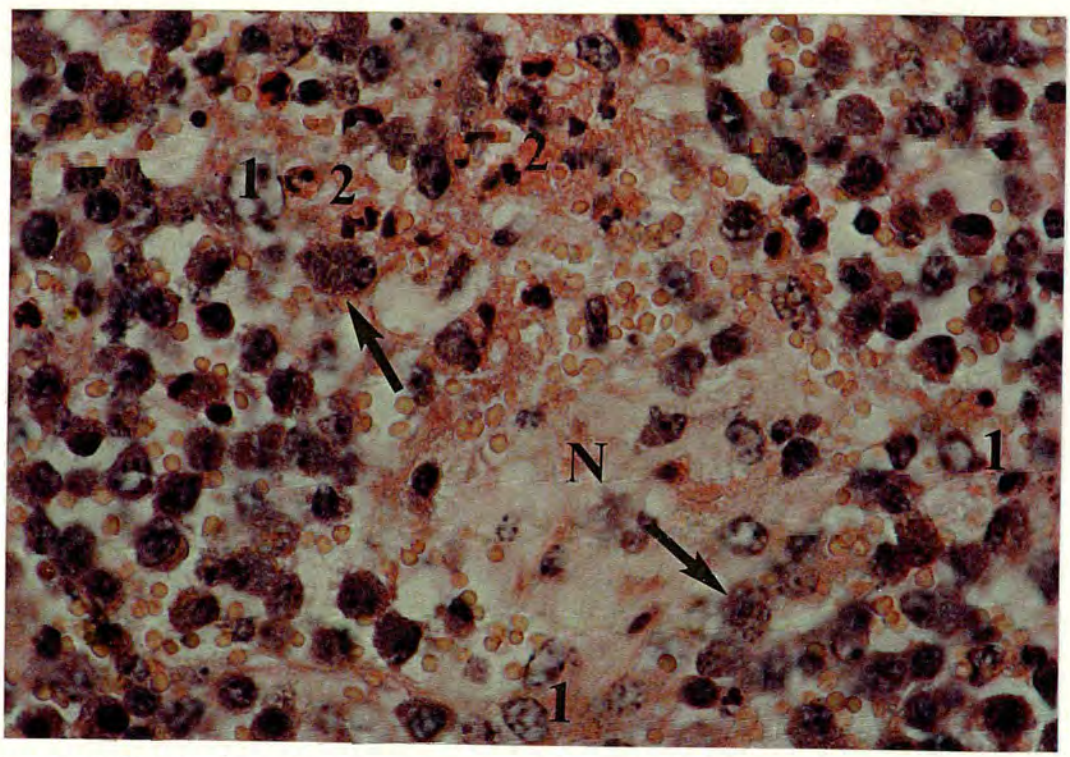

Figure 4.23 Section showing a granuloma with localised tissue necrosis (N) accompanied by large numbers of macrophages (1), eosinophils (2) and parasitised cells (arrows) in the paracortex of the draining prescapular lymph node of the calf infected with *T. annulata* (Hisar) on day 12 post-infection at the peak of pyrexia, (x500: H&E).

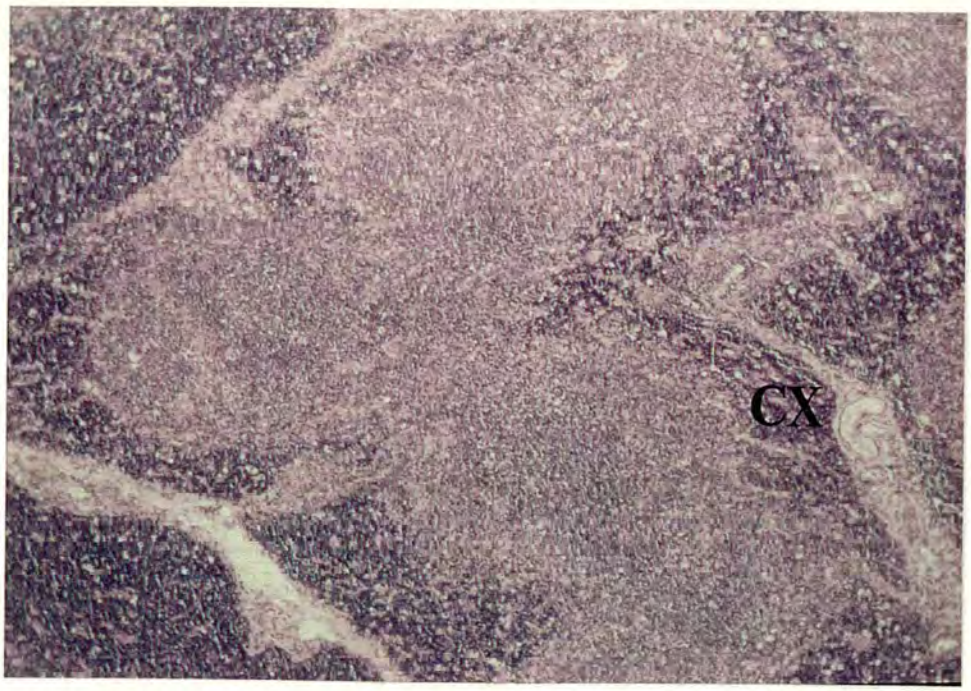

Figure 4.24 Section showing the lymphoid cellular depletion in the cortex (CX) of the thymus of the calf infected with *T. annulata* (Hisar) on day 12 post-infection at the peak of pyrexia, (x40: H&E).

Figure 4.25 Section showing the extensive necrosis (arrows) throughout the paracortex of the draining prescapular lymph node of the calf infected with *T. annulata* (Hisar) on day 14 post-infection at the nadir of disease, (x40: H&E).

of eosinophils in the non-lymphoid organs was detected (Table 4.2B), except for a small increase in the numbers of eosinophils in the kidney and a small decrease in the abomasum.

On day 14 post-infection during the nadir of disease in calf 20 [Table 4.2E] the draining prescapular LN was still the most adversely affected organ. Extensive necrosis (Figures 25 & 26) and haemorrhage were detected throughout this lymph node, lymphoid follicles were absent and depletion of both lymphoid cells and macrophages was detected. Lymphoid cellular depletion was found in the other lymphoid organs, particularly in the paracortex of the contralateral prescapular LN, draining and contralateral precrural LNs, mesenteric and hepatic LNs, the white pulp of the spleen and cortex of the thymus (Figure 4.27). The lymphoid follicles of these lymph nodes were either absent or reduced in size with small germinal centres. Increased numbers of macrophages, but not foamy macrophages, were seen in these lymphoid organs. No granulomas were detected. Sinus hyperplasia was seen in all the lymph nodes, except for the draining prescapular LN, and the medullary sinuses were filled with large numbers of uninfected macrophages. The medullary cords of the draining and contralateral prescapular LNs and mesenteric LN were disrupted. No change in the numbers of eosinophils in the lymphoid organs was detected (Table 4.2B), except for a small decrease in the numbers of eosinophils in the spleen. Increased numbers of lymphoid cells and macrophages, but not foamy macrophages, were seen in the cortex of the kidney (Figure 4.28), portal tracts of the liver (Figure 4.29), lamina propria of the abomasum, alveolar walls of the lung (Figure 4.30) and cortex of the adrenal gland. A normal architecture was still seen in the brain and heart. No change in the numbers of eosinophils in the non-lymphoid organs was detected (Table 4.2B), except for a small increase in the numbers of eosinophils in the kidney and a small decrease in the abomasum.

4.4.2.3 MICROSCOPIC LESIONS IN A CALF (861) DURING THE TERMINAL STAGES OF INFECTION WITH T. ANNULATA (DOUKKALLA)

On day 24 post-infection during the terminal stages of disease in calf 861 [Table 4.2F] the most adversely affected organ was the draining prescapular LN with extensive necrosis and haemorrhage observed throughout the cortex (Figures 4.31 &

ORGAN	AREA	LC	MA	FMA	N	H	FEATURES	CHANGES
Prescapular LN (draining)	CX	--	--	nc	**	***	Follicles	Absent
	PCX	--	--	nc	**	***	Cellular depletion of LC	Throughout LN
	MC	--	--	nc	**	***	Granulomas	Absent
	MS	--	--	nc	***	***	MC	Disrupted
							MS	Disrupted
							Other	Severe disruption of LN architecture
Prescapular LN (contralateral)	CX	-	+	nc	-	-	Follicles	Follicles with small germinal centres
	PCX	--	++	nc	*	*	Cellular depletion of LC	Throughout LN
	MC	-	-	nc	*	*	Granulomas	Absent
	MS	-	++	nc	**	**	MC	Disrupted
							MS	Filled with mainly uninfected cells / sinus hyperplasia
							Other	Enlarged medulla
Precrural LN (draining)	CX	-	+	nc	**	*	Follicles	Follicles with small germinal centres
	PCX	--	+	nc	**	*	Cellular depletion of LC	CX & PCX
	MC	nc	+	nc	-	-	Granulomas	Absent
	MS	nc	+	nc	-	-	MC	nc
							MS	Filled with mainly uninfected cells / sinus hyperplasia
							Other	Enlarged medulla
Precrural LN (contralateral)	CX	-	nc	nc	*	*	Follicles	Follicles with small germinal centres
	PCX	--	+	nc	**	*	Cellular depletion of LC	CX & PCX
	MC	+	+	nc	-	-	Granulomas	Absent
	MS	nc	+	nc	-	-	MC	Prominent
							MS	Filled with mainly uninfected cells / sinus hyperplasia
							Other	Enlarged medulla
Mesenteric LN	CX	nc	nc	nc	-	-	Follicles	Normal active follicles
	PCX	-	+	nc	**	*	Cellular depletion of LC	PCX & MC
	MC	-	-	nc	-	-	Granulomas	Absent
	MS	nc	+	nc	**	*	MC	Disrupted
							MS	Filled with mainly uninfected cells / mild sinus hyperplasia
							Other	
Hepatic LN	CX	-	+	nc	-	-	Follicles	Follicles with small germinal centres
	PCX	--	++	nc	*	-	Cellular depletion of LC	CX & PCX
	MC	+	+	nc	-	-	Granulomas	Absent
	MS	nc	+	nc	-	-	MC	Prominent
							MS	Filled with mainly uninfected cells / sinus hyperplasia
							Other	Enlarged medulla
Spleen	WP	-	+	nc	-	-	Cellular depletion of LC in WP	Present
	RP	nc	nc	nc	-	-	Congestion of RP	Present
Thymus	CX	-	nc	nc	*	-	Cellular depletion of LC in CX	Present
	MED	nc	+	nc	**	*		

nc No change
- Small decrease
-- Moderate decrease
--- Large decrease

+ Small increase
++ Moderate increase
+++ Large increase

- No damage
* Mild damage
** Moderate damage
*** Extensive damage

LC Lymphoid cells
FMA Foamy macrophages
MA Macrophages
N Necrosis
H Haemorrhage
CX Cortex
PCX Paracortex
MED Medulla
MC Medullary cords
MS Medullary sinuses
LN Lymph node
WP White pulp
RP Red pulp

Table 4.2E Microscopic lesions in a calf (20) infected with *T. annulata* (Hisar) on day 14 post-infection

ORGAN	AREA	LC	MA	FMA	N	H	FEATURES	CHANGES
Kidney	CX	+	+	nc	-	-	Disruptive cellular infiltrate in CX	Present
	MED	nc	nc	nc	-	-	Oedema of tubules	Present
Liver	PT	+	+	nc	*	-	Disruptive cellular infiltrate	Present
							Oedema of hepatic cells	Absent
Abomasum	LAP	+	+	nc	-	-	Disruptive cellular infiltrate	Present
Lung	AW	+	+	nc	*	*	Thickened AW	Present
	BRO	nc	nc	nc	-	-	Congestion of BRO	Absent
Brain stem	GEN	nc	nc	nc	-	-	Disruptive cellular infiltrate	Absent: Normal architecture
Cerebellum	GEN	nc	nc	nc	-	-	Disruptive cellular infiltrate	Absent: Normal architecture
Cerebral hemisphere	GEN	nc	nc	nc	-	-	Disruptive cellular infiltrate	Absent: Normal architecture
Heart	GEN	nc	nc	nc	-	-	Disruptive cellular infiltrate	Absent: Normal architecture
Adrenal gland	ZG	+	+	nc	*	*	Disruptive cellular infiltrate	Present
	ZF	+	+	nc	*	*		
	ZR	+	+	nc	*	*		
	MED	nc	nc	nc	-	-		
Anterior Pituitary gland	GEN	nc	nc	nc	-	-	Disruptive cellular infiltrate	Absent: Normal architecture

nc No change
- Small decrease
-- Moderate decrease
--- Large decrease

+ Small increase
++ Moderate increase
+++ Large increase

- No damage
* Mild damage
** Moderate damage
*** Extensive damage

LC Lymphoid cells
FMA Foamy macrophages
MA Macrophages
N Necrosis
H Haemorrhage
GEN General
CX Cortex
MED Medulla
PT Portal tracts
LAP Lamina propria
AW Alveolar walls
BRO Bronchioles
ZG Zona glomerulosa
ZF Zona fasciculata
ZR Zona reticularis

Table 4.2E Continued

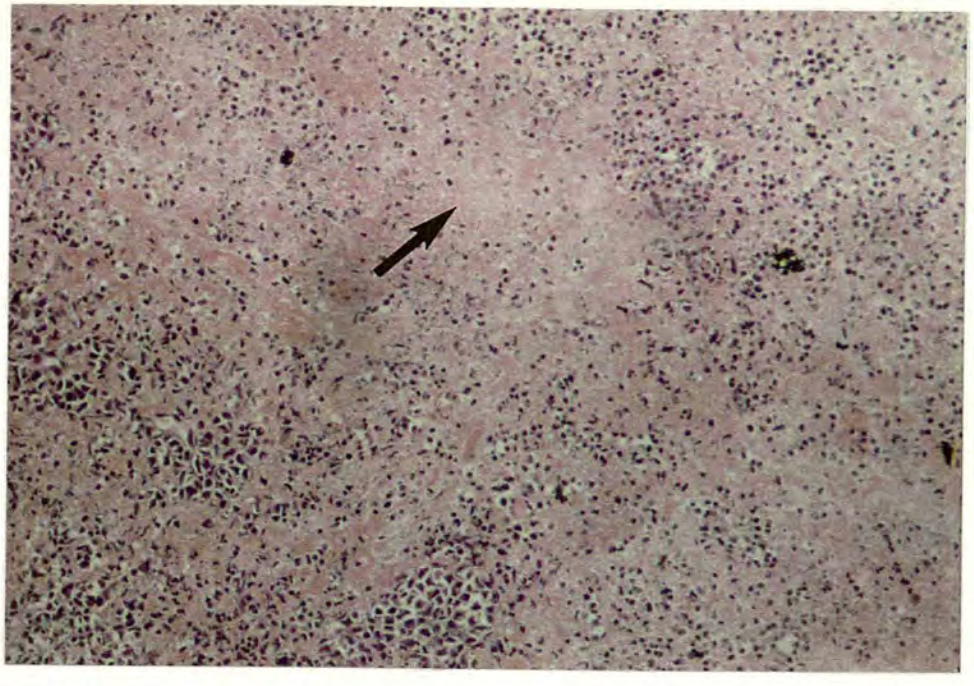

Figure 4.26 Section showing the necrosis (arrow) in the paracortex of the draining prescapular lymph node of the calf infected with *T. annulata* (Hisar) on day 14 post-infection at the nadir of disease, (x100: H&E).

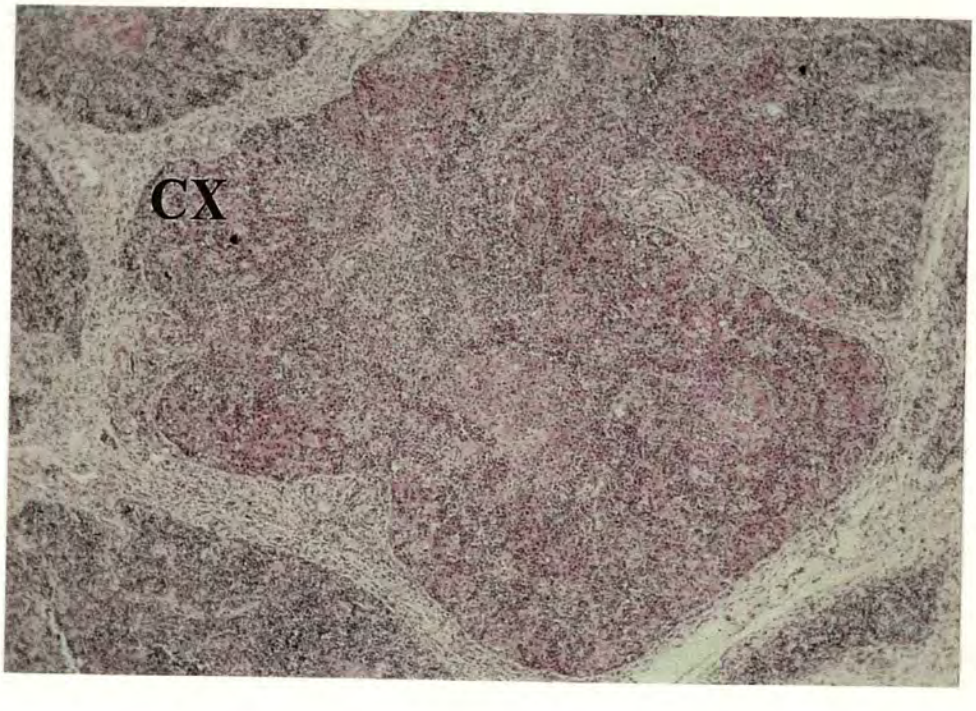

Figure 4.27 Section showing the lymphoid cellular depletion in the cortex (CX) of the thymus of the calf infected with *T. annulata* (Hisar) on day 14 post-infection at the nadir of disease, (x40: H&E).

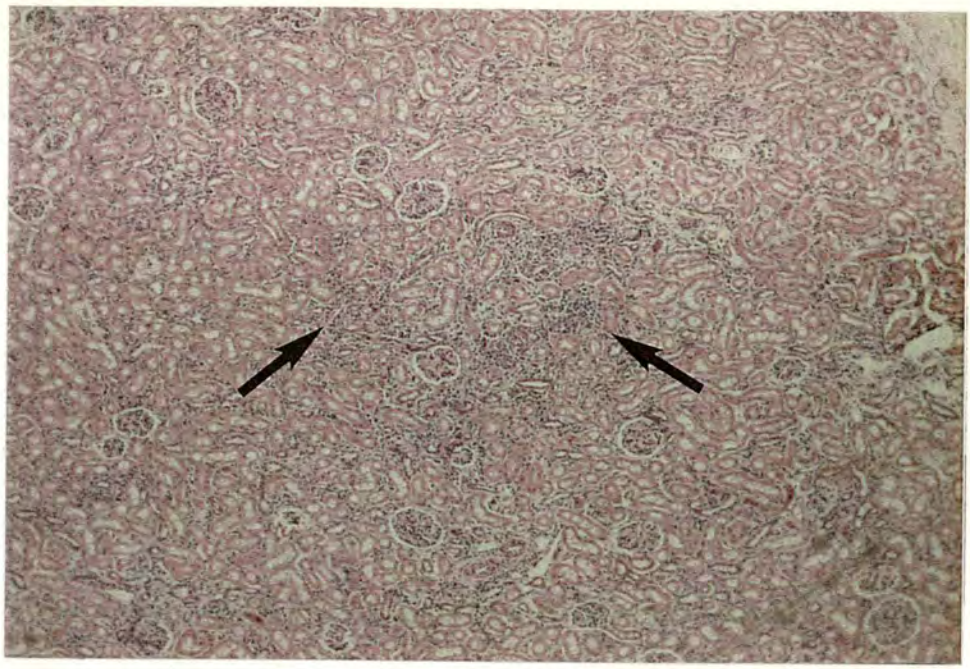

Figure 4.28 Section showing the infiltration of lymphocytes and macrophages (arrows) in the cortex of the kidney of the calf infected with *T. annulata* (Hisar) on day 14 post-infection at the nadir of disease, (x40: H&E).

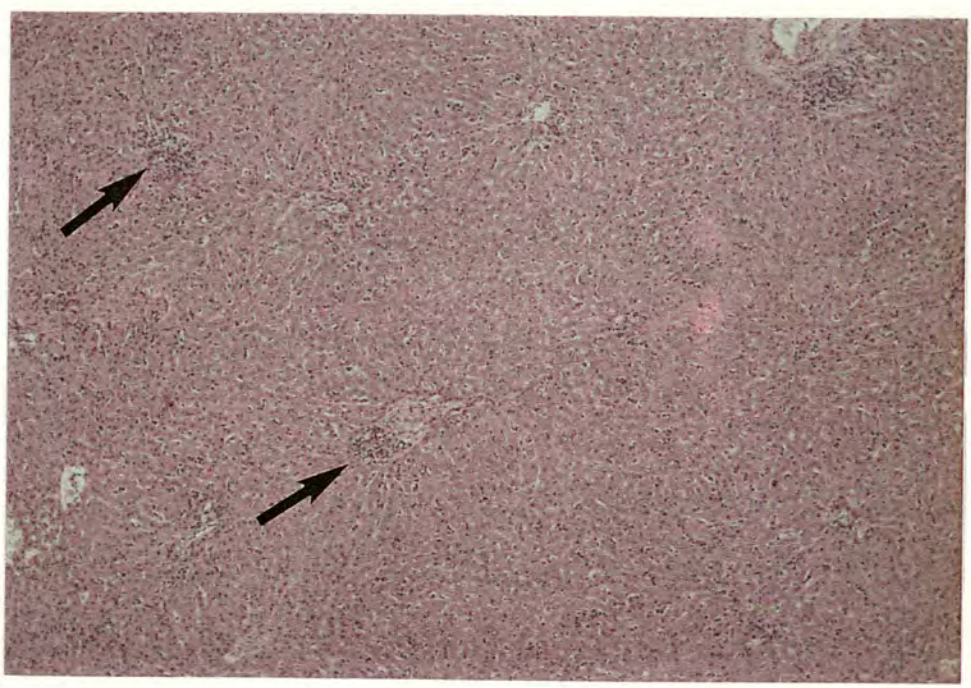

Figure 4.29 Section showing the infiltration of lymphocytes and macrophages (arrows) in the liver of the calf infected with *T. annulata* (Hisar) on day 14 post-infection at the nadir of disease, (x40: H&E).

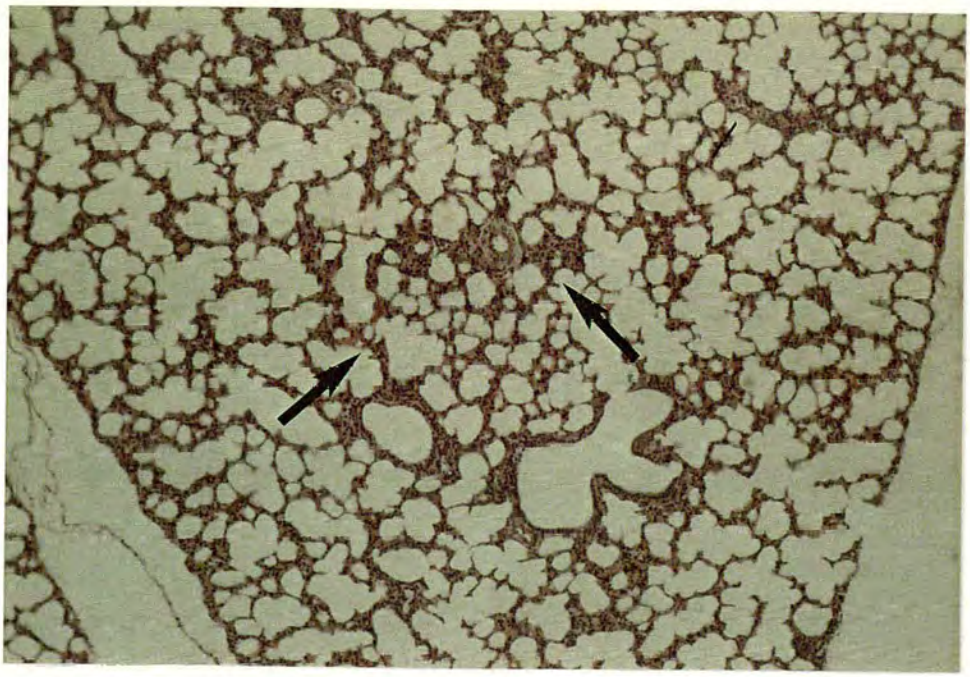

Figure 4.30 Section showing the thickened alveolar walls (arrows) of the lung of the calf infected with *T. annulata* (Hisar) on day 14 post-infection at the nadir of disease, (x40: H&E).

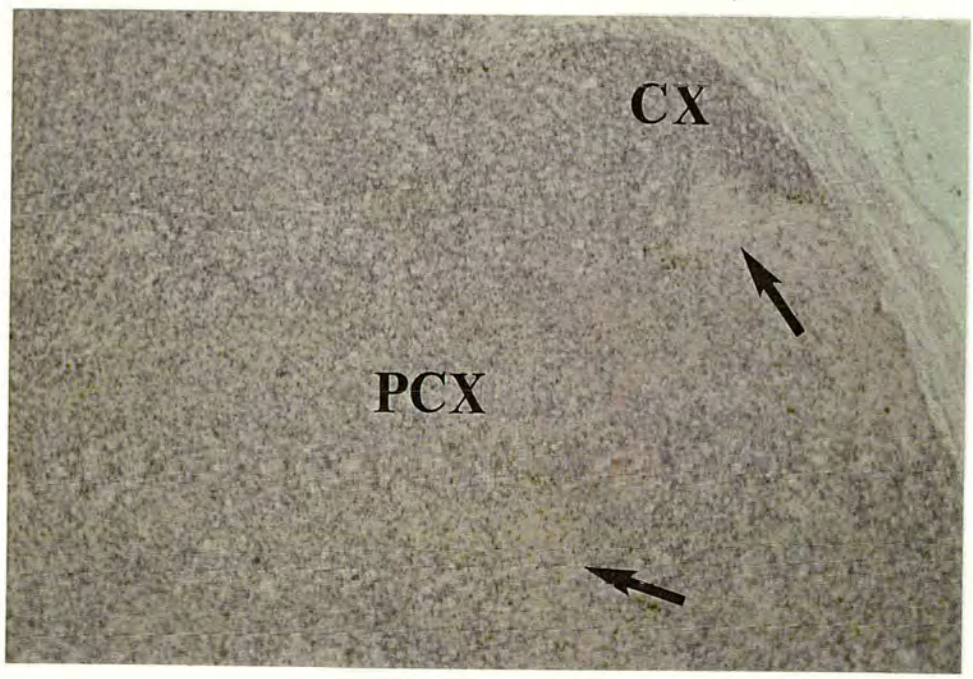

Figure 4.31 Section showing the extensive necrosis (arrows) throughout the cortex (CX) and paracortex (PCX) of the draining prescapular lymph node of the calf infected with *T. annulata* (Doukkalla) on day 24 post-infection during the terminal stages of disease, (x40: H&E).

ORGAN	AREA	LC	MA	FMA	N	H	FEATURES	CHANGES
Prescapular LN (draining)	CX	--	+	++	**	*	Follicles	Absent
	PCX	--	+	++	**	**	Cellular depletion of LC	Throughout LN
	MC	-	-	+	**	*	Granulomas	Absent
	MS	-	+	++	***	*	MC	Disrupted
							MS	Disrupted
							Other	Extensive disruption of LN architecture
Prescapular LN (contralateral)	CX	-	+	++	*	*	Follicles	Absent
	PCX	--	+++	++	*	*	Cellular depletion of LC	CX & PCX
	MC	nc	+	+	-	*	Granulomas	Absent
	MS	nc	++	++	-	-	MC	nc
							MS	Filled with mainly uninfected cells / sinus hyperplasia
							Other	Enlarged medulla
Precrural LN (draining)	CX	-	+	++	*	*	Follicles	Absent
	PCX	-	++	++	*	*	Cellular depletion of LC	CX & PCX
	MC	nc	+	+	-	-	Granulomas	Absent
	MS	nc	++	++	-	-	MC	nc
							MS	Filled with mainly uninfected cells / sinus hyperplasia
							Other	Enlarged medulla
Precrural LN (contralateral)	CX	-	++	++	-	*	Follicles	Absent
	PCX	--	++	++	-	*	Cellular depletion of LC	CX, PCX & MC
	MC	-	-	+	-	*	Granulomas	Absent
	MS	nc	++	++	-	*	MC	Disrupted
							MS	Filled with mainly uninfected cells / sinus hyperplasia
							Other	Enlarged medulla
Mesenteric LN	CX	-	+	++	**	**	Follicles	Normal active follicles
	PCX	-	++	++	*	*	Cellular depletion of LC	CX & PCX
	MC	nc	nc	+	-	-	Granulomas	Absent
	MS	nc	++	++	-	-	MC	nc
							MS	Filled with mainly uninfected cells / sinus hyperplasia
							Other	Enlarged medulla
Spleen	WP	nc	nc	++	-	-	Cellular depletion of LC in WP	Absent
	RP	nc	nc	+	-	-	Congestion of RP	Present
Thymus	CX	--	+	+	*	*	Cellular depletion of LC in CX	Present
	MED	nc	++	++	**	*		

nc No change
- Small decrease
-- Moderate decrease
--- Large decrease

+ Small increase
++ Moderate increase
+++ Large increase

- No damage
* Mild damage
** Moderate damage
*** Extensive damage

LC Lymphoid cells
FMA Foamy macrophages
MA Macrophages
N Necrosis
H Haemorrhage
LN Lymph node
CX Cortex
PCX Paracortex
MED Medulla
MC Medullary cords
MS Medullary sinuses
WP White pulp
RP Red pulp

Table 4.2F Microscopic lesions in a calf (861) infected with *T. annulata* (Doukkalla) on day 24 post-infection

ORGAN	AREA	LC	MA	FMA	N	H	FEATURES	CHANGES
Kidney	CX	+	+	+	-	-	Disruptive cellular infiltrate in CX	Present
	MED	nc	nc	nc	-	-	Oedema of tubules	Present
Liver	PT	+	+	nc	-	-	Disruptive cellular infiltrate	Present
							Oedema of hepatic cells	Absent
Abomasum	LAP	+	++	+++	*	*	Disruptive cellular infiltrate	Present
Lung	AW	+	+	+	-	-	Thickened AW	Present
	BRO	nc	nc	nc	-	-	Congestion of BRO	Absent
Skin	SDER	nc	+++	++	**	**	Disruptive cellular infiltrate	Present

nc No change
- Small decrease
-- Moderate decrease
--- Large decrease

+ Small increase
++ Moderate increase
+++ Large increase

- No damage
* Mild damage
** Moderate damage
*** Extensive damage

LC Lymphoid cells
FMA Foamy macrophages
MA Macrophages
N Necrosis
H Haemorrhage

CX Cortex
MED Medulla
PT Portal tracts
LAP Lamina propria
AW Alveolar walls
BRO Bronchioles
SDER Superficial dermis

Table 4.2F Continued

4.32), paracortex and medulla. Lymphoid follicles were absent and lymphoid cellular depletion was detected throughout this lymph node. Lymphoid cellular depletion was seen in the other lymphoid organs, with the exception of the spleen, in particular the paracortex of the contralateral prescapular LN, draining and contralateral precrural LNs, mesenteric LN and the cortex of the thymus (Figure 4.33). Lymphoid follicles were absent from these lymph nodes, except normal active follicles were detected in the mesenteric LN. Increased numbers of macrophages and foamy macrophages were found in all the lymph nodes, and the thymus. Increased numbers of foamy macrophages were detected in the spleen. No granulomas were detected. Sinus hyperplasia was seen in all the lymph nodes, except for the draining prescapular LN, and the medullary sinuses were filled with large numbers of uninfected macrophages. The medullary cords of the draining prescapular LN and contralateral precrural LN were disrupted. No change in the numbers of eosinophils in the lymphoid organs was detected (Table 4.2B), except for a small decrease in the numbers of eosinophils in the spleen. Increased numbers of lymphoid cells and macrophages, accompanied in many cases by foamy macrophages, were seen in the cortex of the kidney, portal tracts of the liver, lamina propria of the abomasum and alveolar walls of the lung. Increased numbers of macrophages and foamy macrophages were also seen in the superficial dermis of the skin associated with a diffuse necrosis and haemorrhage (Figure 4.34). No change in the numbers of eosinophils in the non-lymphoid organs was detected (Table 4.2B).

4.4.2.4 MICROSCOPIC LESIONS IN A CALF (8) DURING THE TERMINAL STAGES OF INFECTION WITH T. PARVA (MUGUGA)

On day 21 post-infection during the terminal stages of disease in calf 8 [Table 4.2G] the most adversely affected organ was the draining prescapular LN. A diffuse lymphocytic hyperplasia was detected in the paracortex (Figures 4.35 & 4.36) of this lymph node, lymphoid follicles were absent and extensive areas of necrosis (Figure 4.37) and haemorrhage were seen. Lymphoid cellular depletion was observed in the other lymphoid organs, in particular the paracortex of the contralateral prescapular LN, draining and contralateral precrural LNs, mesenteric and hepatic LNs, the white pulp of the spleen and cortex of the thymus (Figure 4.38). In these lymph nodes lymphoid follicles were absent, except normal active follicles were detected in the

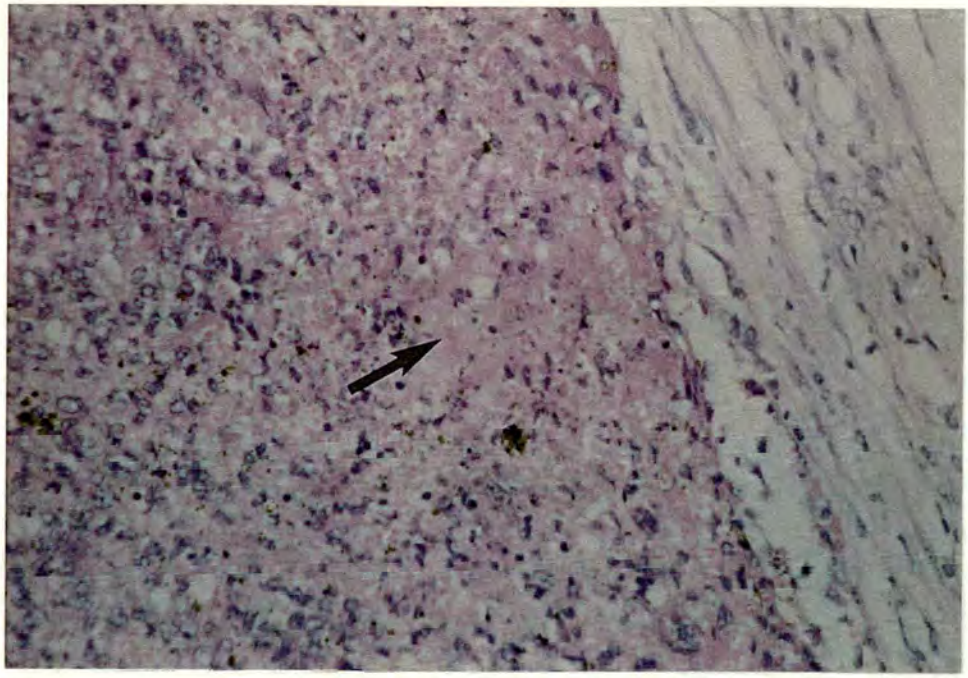

Figure 4.32 Section showing the necrosis (arrow) in the cortex of the draining prescapular lymph node of the calf infected with *T. annulata* (Doukkalla) on day 24 post-infection during the terminal stages of disease, (x250: H&E).

Figure 4.33 Section showing the lymphoid cellular depletion in the cortex (CX) of the thymus of the calf infected with *T. annulata* (Doukkalla) on day 24 post-infection during the terminal stages of disease, (x40: H&E).

Figure 4.34 Section showing macrophages, foamy macrophages (arrows) and necrosis (N) in the superficial dermis of the skin of the calf infected with *T. annulata* (Doukkalla) on day 24 post-infection during the terminal stages of disease, (x40: H&E).

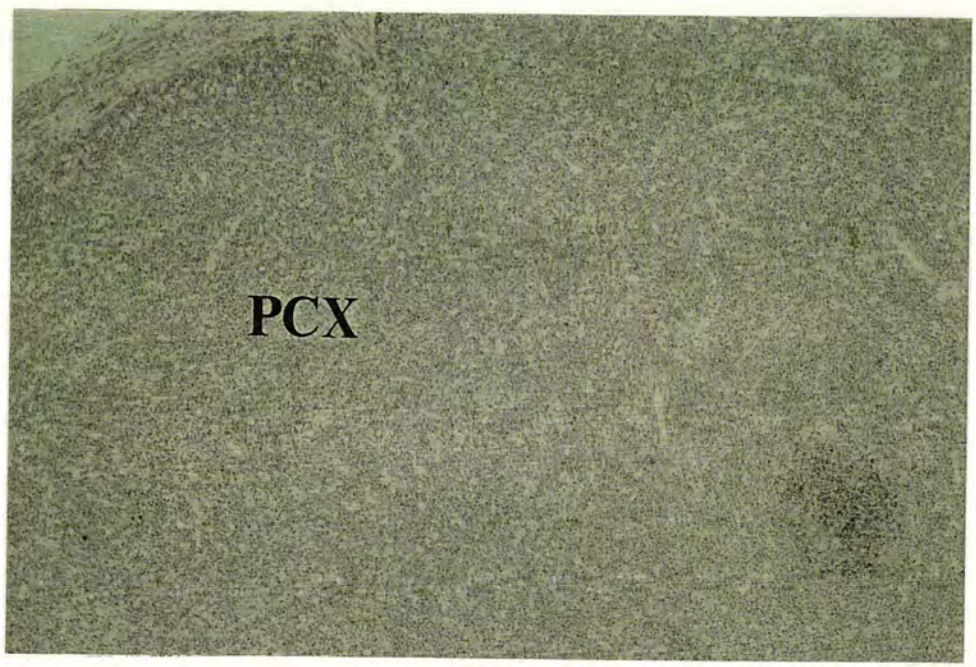

Figure 4.35 Section showing the diffuse lymphocytic hyperplasia throughout the paracortex (PCX) of the draining prescapular lymph node of the calf infected with *T. parva* (Muguga) on day 21 post-infection during the terminal stages of disease, (x40: H&E).

ORGAN	AREA	LC	MA	FMA	N	H	FEATURES	CHANGES
Prescapular LN (draining)	CX	+	nc	nc	-	-	Follicles	Absent
	PCX	+++	nc	+	*	-	Cellular depletion of LC	Absent
	MC	nc	nc	nc	**	**	Granulomas	Absent
	MS	nc	+	nc	**	**	MC	nc
							MS	nc
							Other	Lymphoproliferation in PCX
Prescapular LN (contralateral)	CX	-	nc	nc	-	-	Follicles	Absent
	PCX	--	nc	nc	-	-	Cellular depletion of LC	CX & PCX
	MC	nc	nc	nc	-	-	Granulomas	Absent
	MS	nc	nc	+	-	-	MC	nc
							MS	nc
							Other	
Precrural LN (draining)	CX	-	nc	nc	-	-	Follicles	Absent
	PCX	--	nc	nc	-	-	Cellular depletion of LC	CX & PCX
	MC	nc	nc	nc	-	-	Granulomas	Absent
	MS	nc	nc	+	-	-	MC	nc
							MS	nc
							Other	
Precrural LN (contralateral)	CX	-	nc	nc	-	-	Follicles	Absent
	PCX	--	nc	nc	-	-	Cellular depletion of LC	CX & PCX
	MC	nc	nc	nc	-	-	Granulomas	Absent
	MS	nc	+	+	-	-	MC	nc
							MS	nc
							Other	
Mesenteric LN	CX	nc	nc	nc	-	-	Follicles	Normal active follicles
	PCX	nc	nc	+	-	-	Cellular depletion of LC	Absent
	MC	nc	nc	nc	-	-	Granulomas	Absent
	MS	nc	+	+	-	-	MC	nc
							MS	nc
							Other	
Hepatic LN	CX	-	nc	nc	-	-	Follicles	Absent
	PCX	--	+	+	-	-	Cellular depletion of LC	CX & PCX
	MC	nc	+	nc	-	-	Granulomas	Absent
	MS	nc	++	+	-	-	MC	nc
							MS	Filled with mainly uninfected cells / sinus hyperplasia
							Other	
Spleen	WP	-	+	nc	-	-	Cellular depletion of LC in WP	Present
	RP	nc	nc	nc	-	-	Congestion of RP	Present
Thymus	CX	--	nc	nc	-	-	Cellular depletion of LC in CX	Present
	MED	nc	++	nc	**	-		

nc No change
- Small decrease
-- Moderate decrease
--- Large decrease

+ Small increase
++ Moderate increase
+++ Large increase

- No damage
* Mild damage
** Moderate damage
*** Extensive damage

LC Lymphoid cells
FMA Foamy macrophages
MA Macrophages
N Necrosis
H Haemorrhage
LN Lymph node
CX Cortex
PCX Paracortex
MED Medulla
MC Medullary cords
MS Medullary sinuses
WP White pulp
RP Red pulp

Table 4.2G Microscopic lesions in a calf (8) infected with *T. parva* (Muguga) on day 21 post-infection

ORGAN	AREA	LC	MA	FMA	N	H	FEATURES	CHANGES
Kidney	CX	+	+	nc	-	-	Disruptive cellular infiltrate in CX	Present
	MED	nc	nc	nc	-	-	Oedema of tubules	Present
Liver	PT	nc	nc	nc	-	-	Disruptive cellular infiltrate	Absent: Normal architecture
							Oedema of hepatic cells	Absent
Abomasum	LAP	nc	nc	nc	-	-	Disruptive cellular infiltrate	Absent: Normal architecture
Lung	AW	+	+	+	-	-	Thickened AW	Present
	BRO	nc	nc	nc	-	-	Congestion of BRO	Absent
Heart	GEN	nc	nc	nc	-	-	Disruptive cellular infiltrate	Absent: Normal architecture
Adrenal gland	ZG	nc	nc	nc	-	-	Disruptive cellular infiltrate	Absent: Normal architecture
	ZF	nc	nc	nc	-	-		
	ZR	nc	nc	nc	-	-		
	MED	nc	nc	nc	-	-		

nc No change
- Small decrease
-- Moderate decrease
--- Large decrease

+ Small increase
++ Moderate increase
+++ Large increase

- No damage
* Mild damage
** Moderate damage
*** Extensive damage

LC Lymphoid cells
FMA Foamy macrophages
MA Macrophages
N Necrosis
H Haemorrhage
GEN General

CX Cortex
MED Medulla
PT Portal tracts
LAP Lamina propria
AW Alveolar walls
BRO Bronchioles
ZG Zona glomerulosa
ZF Zona fasciculata
ZR Zona reticularis

Table 4.2G Continued

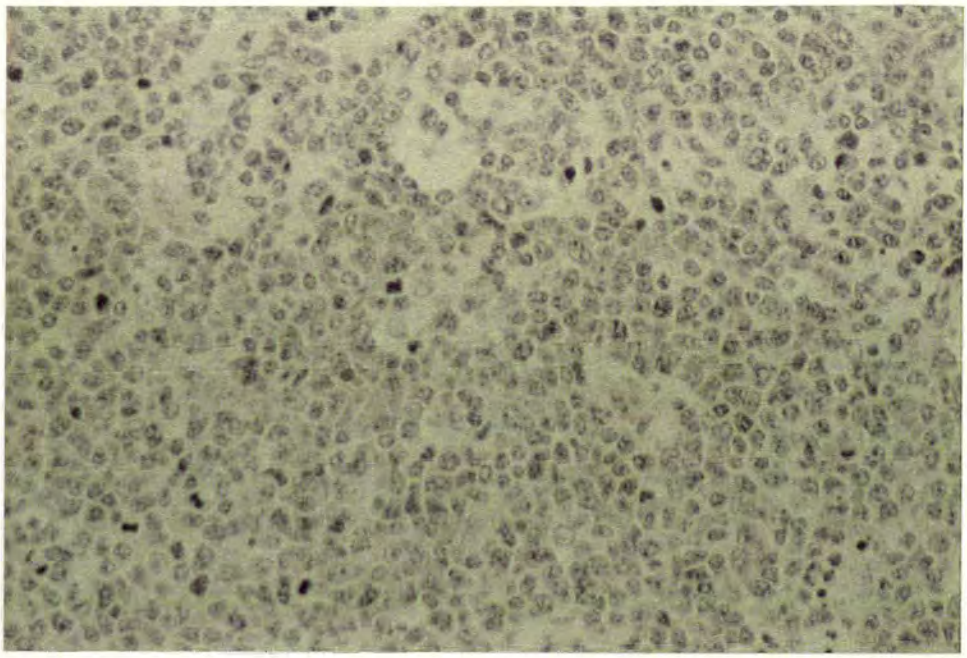

Figure 4.36 Section showing the diffuse lymphocytic hyperplasia in the paracortex of the draining prescapular lymph node of the calf infected with *T. parva* (Muguga) on day 21 post-infection during the terminal stages of disease, (x250: H&E).

Figure 4.37 Section showing the extensive necrosis (N) throughout the medulla of the draining prescapular lymph node of the calf infected with *T. parva* (Muguga) on day 21 post-infection during the terminal stages of disease, (x40: H&E).

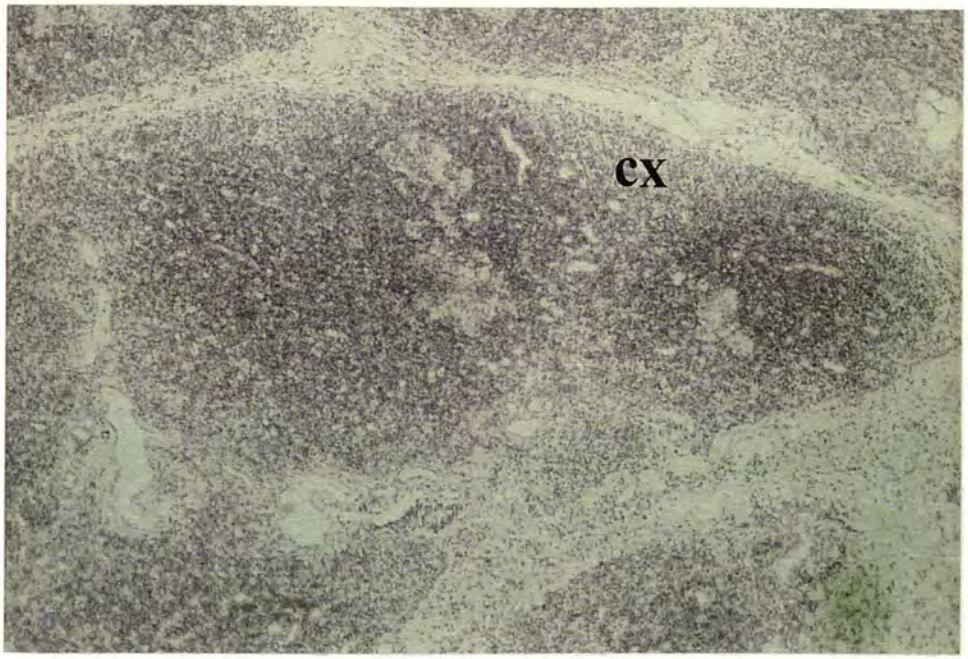

Figure 4.38 Section showing the lymphoid cellular depletion in the cortex (CX) of the thymus of the calf infected with *T. parva* (Muguga) on day 21 post-infection during the terminal stages of disease, (x40: H&E).

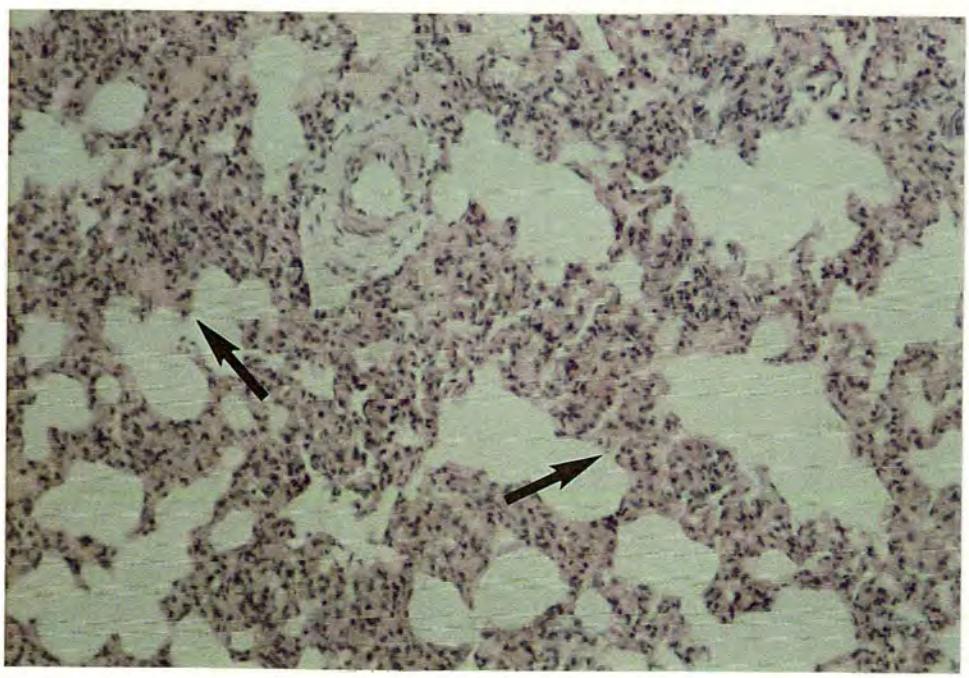

Figure 4.39 Section showing the thickened alveolar walls (arrows) in the lung of the calf infected with *T. parva* (Muguga) on day 21 post-infection during the terminal stages of disease, (x100: H&E).

mesenteric LN. Increased numbers of macrophages were seen in the lymphoid organs, with the exception of the contralateral prescapular LN and draining precrural LN, particularly in the medullary sinuses of the draining prescapular LN, contralateral precrural LN, mesenteric and hepatic LNs, the white pulp of the spleen and medulla of the thymus. Increased numbers of foamy macrophages were seen throughout all the lymph nodes. No granulomas were detected. Sinus hyperplasia was detected in the hepatic LN and the medullary sinuses were filled with large numbers of uninfected macrophages. No disruption of the medullary cords was detected. A decrease in the numbers of eosinophils was detected in the draining and contralateral precrural LNs, the spleen and thymus (Table 4.2B), whereas no change in the numbers of eosinophils was seen in the draining and contralateral prescapular LNs, mesenteric and hepatic LNs. Increased numbers of lymphoid cells and macrophages were seen in the cortex of the kidney and alveolar walls of the lung (Figure 4.39). Foamy macrophages were also seen in the alveolar walls of the lung. A normal architecture was seen in the liver, abomasum, heart and adrenal gland. No change in the numbers of eosinophils in the non-lymphoid organs was detected (Table 4.2B), except for a small decrease in the numbers of eosinophils in the liver and abomasum.

4.5 DISCUSSION

The macroscopic and microscopic investigations of lymphoid and non-lymphoid organs in calves infected with *T. annulata* or *T. parva* (Muguga) showed that extensive pathological responses had been elicited by both infections.

Macroscopic and microscopic lesions were seen in the superficial and internal lymph nodes, spleen, thymus, kidney, liver, abomasum, lung, adrenal gland and skin of calves infected with *T. annulata*. These observations in cattle infected with parasite stocks from India and North Africa resembled those obtained by previous studies on cattle lethally infected with parasite stocks from Russia (Dschunkowsky & Luhs 1904), North Africa (Sergent *et al.* 1945) and India (Gill *et al.* 1977; Baharsefat *et al.* 1977; Srivastava & Sharma 1981; Manickam *et al.* 1984).

Macroscopic lesions were seen in the superficial and internal lymph nodes of the calf infected with *T. parva* and microscopic lesions were recorded in the thymus and lung. These observations resembled those obtained by previous studies on cattle lethally infected with *T. parva* (Barnett 1960; De Kock 1957; DeMartini & Moulton 1973), except that macroscopic and microscopic lesions were absent in the majority of the non-lymphoid organs from the calf of this study.

The most striking macroscopic pathological response detected in calves infected with *T. annulata* or *T. parva* (Muguga) was the extensive oedema and haemorrhage in the superficial and internal lymph nodes, in particular the prescapular LN draining the site of inoculation. Lesions were not restricted to the lymph node draining the site of inoculation, although it was the most extensively damaged lymph node, but were found throughout the remaining superficial and internal lymph nodes and non-lymphoid organs of the body.

A progressive development of macroscopic and microscopic lesions occurred in calves infected with *T. annulata* (Hisar) examined during the initial stages of pyrexia, peak pyrexia and the nadir of disease. During the initial stages of pyrexia (day 7 post-infection) lesions were observed in the superficial and internal lymph nodes and the organs containing lymphoid tissues. By the peak of pyrexia (day 12 post-infection) and the nadir of disease (day 14 post-infection) extensive lesions were observed in the superficial and internal lymph nodes, the organs containing lymphoid tissues and the majority of the non-lymphoid organs.

Among the most striking microscopic pathological responses observed in calves infected with *T. annulata* or *T. parva* (Muguga) were the regression and disappearance of lymphoid follicles, the extensive lymphoid cellular depletion in the paracortex of the lymphoid organs and the disruptive cellular infiltrate throughout the non-lymphoid organs. These findings resembled those reported in previous studies with calves lethally infected with *T. annulata* (Gill *et al.* 1977; Baharsefat *et al.* 1977; Srivastava & Sharma 1981) or *T. parva* (Barnett 1960; De Kock 1957; DeMartini & Moulton 1973).

A novel microscopic pathological response was observed in the lymph nodes of calves infected with *T. annulata* (Hisar), in particular the draining prescapular LN. The early stages of a paracortical granulomatous response were detected in the draining prescapular LN during the initial stages of disease. As infection progressed a more advanced paracortical hyperplastic granulomatous response was observed throughout the lymph node involving large numbers of macrophages, eosinophils and parasitised cells. By the nadir of disease extensive areas of cellular depletion, disorganisation and degeneration were detected throughout the lymph node and there were no signs of a granulomatous response. This response was interesting since many of the pathological effects which involve T cell mediated immunity in microbial and parasitic diseases are associated with a granulomatous response (Ridley & Wise 1964; Ridley 1979).

Large numbers of eosinophils were seen throughout the draining prescapular LN obtained during the peak of pyrexia. These eosinophils were apparently recruited to this lymph node however haematological investigations (Chapter 3) did not detect large numbers of eosinophils in the blood of this animal. It is known that eosinophils are attracted by products released from T cells (Secor 1990) and by chemotactic and stimulatory substances released by some granulomas (James & Colley 1978). Importantly, eosinophils have cytotoxic capabilities (Roitt, Brostoff & Male 1989).

The extensive lymphoid cellular destruction seen in the paracortex of the lymph nodes and cortex of the thymus of both the *T. annulata* and *T. parva* (Muguga) infected animals may contribute to the clinical responses seen in *T. annulata* and *T. parva* infections. Other studies have suggested that lymphopoietic exhaustion in both *T. annulata* and *T. parva* infected animals may lead to a deficient immune response resulting in immunosuppression (Wagner *et al.* 1975; Sharpe & Langley 1983). The absence of detectable cytotoxic cells in the blood or lymph nodes from cattle succumbing to *T. annulata* infection as compared to animals that recovered (Preston *et al.* 1983) provides some evidence for immunosuppression in *T. annulata* at least.

A large increase in the number of macrophages was found in the medulla of the lymph nodes of cattle infected with *T. annulata* or *T. parva* (Muguga), as had been

reported previously for cattle infected with *T. annulata* (Gill *et al.* 1977) or *T. parva* (Barnett 1960; De Kock 1957). The presence of such large numbers of macrophages was interesting since macrophages, obtained from a naive calf, cultured with *T. annulata* (Hisar) macroschizont-infected cells have previously been shown to synthesise TNF-α (Preston *et al.* 1993), a cytokine which has been found to induce pyrexia, cachexia (Beutler & Cerami 1986) and leucopenia (Ulich *et al.* 1987) in other animals as well as NO (Visser *et al.* 1995), a compound known to mediate mucosal damage and haemorrhage (Lopez-Belmonte *et al.* 1993). Macrophages may therefore be the source of detrimental factors (toxins) suggested to be responsible for the extensive tissue necrosis and haemorrhage observed in both *T. annulata* (Neitz 1957) and *T. parva* (Barnett 1960) infections.

A diffuse paracortical lymphocytic hyperplasia was detected in the draining prescapular LN obtained during the terminal stages of disease from the *T. parva* (Muguga) infected animal. However, there was no evidence to suggest a granulomatous response had occurred in this or any of the other lymph nodes during the earlier stages of disease and there were no signs of the extensive degeneration of cells associated with the granulomatous response like that detected in the lymph nodes during the latter stages of disease with *T. annulata* (Hisar). Nor have previous studies reported a granulomatous response (Barnett 1960; De Kock 1957; DeMartini & Moulton 1973). The possible reasons for the different pathology elicited by both *T. annulata* and *T. parva* infections will be considered later.

Additional microscopic pathological responses recorded in the calves infected with *T. annulata* of this study resembled those found during previous studies on *T. annulata* infected animals (Gill *et al.* 1977; Baharsefat *et al.* 1977; Srivastava & Sharma 1981; Manickam *et al.* 1984). These pathological responses included lymphoid infiltration in the cortex of the kidney, portal tracts of the liver and superficial dermis of the skin, congestion of the red pulp of the spleen and extensive ulceration of the abomasum. No microscopic lesions were detected in the heart or brain from the calves in this study and a lymphoid infiltration in the cortex of the adrenal gland was found.

If the infections in all the calves had been permitted to run their course the ultimate cause of death may have been attributed to the widespread destruction of the lymphoid and haemopoietic organs. Although, respiratory failure due to pulmonary oedema has been reported to be the main cause of death in *T. annulata* and *T. parva* infected animals (Neitz 1957; De Kock 1957).

4.6 CONCLUSION

Many of the physiologically important lymphoid and non-lymphoid organs in calves infected with *T. annulata* or *T. parva* (Muguga) exhibited a wide range of tissue damage. Among the most striking microscopic findings detected in both the *T. annulata* and *T. parva* (Muguga) infected animals was a progressive regression and degeneration of lymphoid follicles, depletion of lymphoid cells in the lymphoid organs and a disruptive cellular infiltrate in the non-lymphoid organs. A progressive granulomatous response was detected in the draining prescapular LN of the *T. annulata* (Hisar) infected animals. In contrast, a diffuse lymphocytic hyperplasia was detected in the draining prescapular LN of the *T. parva* (Muguga) infected animal. Further investigations were conducted to determine the distribution of the parasite, particularly in relation to the tissue damage recorded in this work.

CHAPTER FIVE

DISTRIBUTION OF PARASITES IN CALVES WITH BOVINE THEILERIOSES

5.1 INTRODUCTION

As described above (Chapter 4) lymphoid and non-lymphoid organs of calves infected with *T. annulata* or *T. parva* (Muguga) exhibited a wide range of microscopic lesions. The most interesting findings were: the regression and degeneration of lymphoid follicles and the extensive depletion of lymphoid cells in the lymphoid organs of both the *T. annulata* and *T. parva* (Muguga) infected animals; the formation of granulomas in the lymph nodes obtained during the initial stages of pyrexia and at peak pyrexia from *T. annulata* (Hisar) infected animals; the diffuse lymphocytic hyperplasia detected in the draining prescapular lymph node of the *T. parva* (Muguga) infected animal.

The work described below was intended to examine the extent of parasite dissemination throughout the lymphoid and non-lymphoid organs of these calves and to assess the role of parasites in tissue damage.

5.2 EXPERIMENTAL DESIGN

Parasite distribution was assessed in tissues fixed, processed for embedding in paraffin wax and sectioned as described in chapter 4 (4.3.2), and impression smears prepared as described below. Material was prepared from the organs of calves infected with *T. annulata* or *T. parva* (Muguga), as listed in chapter 4 (4.3.1). Samples of tissues from normal cattle, obtained from the abattoir, were treated similarly to provide control material from uninfected animals.

The overall dissemination of macroschizonts, microschizonts and piroplasms throughout the organs in calves infected with *T. annulata* or *T. parva* (Muguga) was assessed using impression smears stained with Giemsa's stain. The specific locations of macroschizonts and microschizonts in these organs were assessed using tissue sections immunocytochemically labelled with MAb 1C7, which recognises *T. annulata* macroschizont-infected cells, or MAb 4, which recognises *T. parva*

(Muguga) macroschizont- and microschizont-infected cells and counterstained with Harris's haematoxylin. The relationship between parasites and tissue damage was analysed by comparing the distribution of the parasites to the tissue damage, as recorded previously in chapter 4.

5.3 MATERIALS & METHODS

5.3.1 FIXATION & STAINING OF IMPRESSION SMEARS

Several impression smears were made as soon as possible from the samples of tissue removed from the organs. The air-dried slides were either fixed in methanol (BDH) for 2-3 minutes (for subsequent staining with Giemsa's stain) or fixed in acetone (BDH) for 5-10 minutes (for subsequent immunocytochemical staining). The fixed impression smears were air-dried at room temperature and stored in slide boxes. The impression smears were stained with Giemsa's stain as described [Appendix I].

5.3.2 ASSESSMENT OF IMPRESSION SMEARS

Several smears were examined under oil immersion at 1000 x magnification using a Nikon S. Ke II microscope. The number of macroschizont-infected cells (Figure 5.1) and microschizont-infected cells (Figure 5.2) detected in 200 cells, and the number of intra-erythrocytic piroplasms (Figure 5.3) detected in 100 erythrocytes were recorded as a percentage according to the following formula: number of infected cells/total number of cells x 100. Macroschizonts appeared as bodies containing few, large nuclei within the cytoplasm of the infected cells and microschizonts appeared as intra-cytoplasmic bodies containing numerous relatively smaller nuclei, as described previously in section 2.4. Three separate counts from the impression smears from each organ were made and the mean percentages were recorded.

5.3.3 STAINING OF PARAFFIN TISSUE SECTIONS WITH ANTIBODIES & AVIDIN/BIOTIN COMPLEX (ABC) HORSERADISH PEROXIDASE (HRP) IMMUNOCYTOCHEMICAL TECHNIQUES

Several tissue sections were immunocytochemically labelled using methods described previously (Hsu, Raine & Fanger 1981) [Appendix VIII & IX] and counterstained with Harris's haematoxylin. In brief, dewaxed paraffin tissue sections were incubated with hydrogen peroxide to inactivate any endogenous peroxidase which may be visualised by the chromogen substrate leading to disruptive levels of

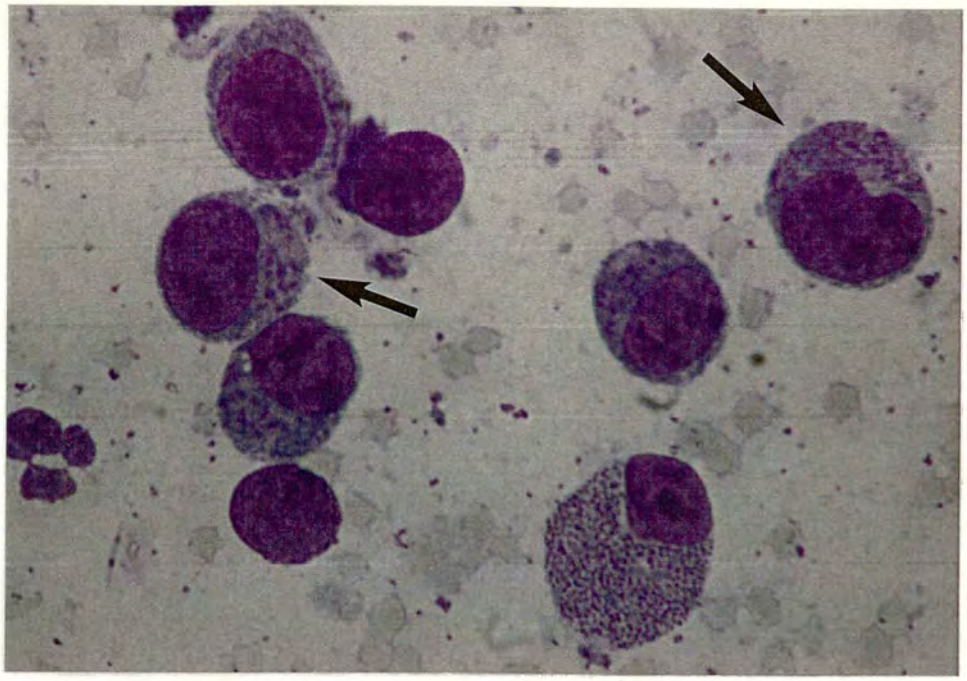

Figure 5.1 Macroschizont-infected cells (arrows) in the impression smear of the draining prescapular lymph node of the calf infected with *T. annulata* (Hisar) on day 12 post-infection at the peak of pyrexia, (x1000: Giemsa's stain).

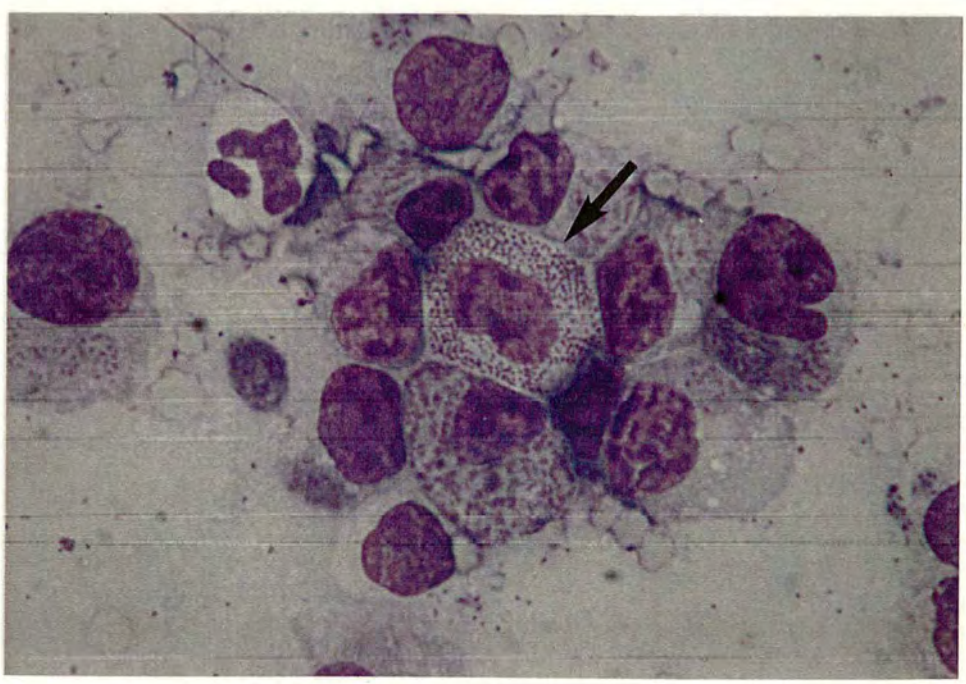

Figure 5.2 Microschizont-infected cell (arrow) in the impression smear of the draining prescapular lymph node of the calf infected with *T. annulata* (Hisar) on day 12 post-infection at the peak of pyrexia, (x1000: Giemsa's stain).

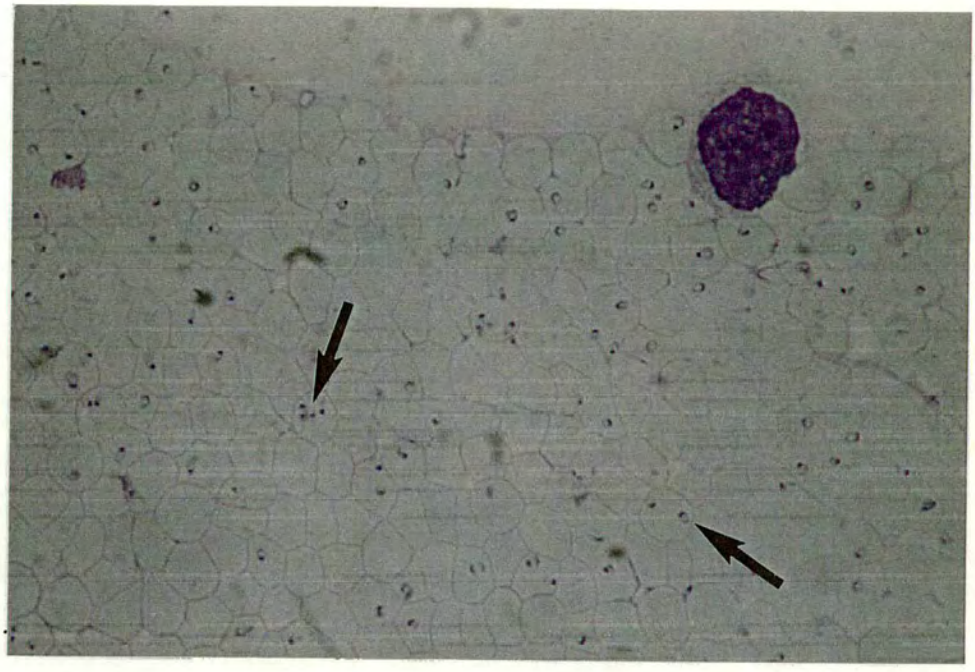

Figure 5.3 Intra-erythrocytic piroplasms (arrows) in the impression smear of the spleen of the calf infected with *T. annulata* (Hisar) on day 12 post-infection at the peak of pyrexia, (x1000: Giemsa's stain).

background staining. Tissue sections were then treated with trypsin to expose surface antigens prior to incubation with primary antibodies as surface antigens are often masked by fixation of tissues in formaldehyde (personal communication Mr. John Lauder). The primary antibodies were then labelled by incubating the sections with biotinylated secondary antibodies which were subsequently identified by reacting with the avidin/biotin horseradish peroxidase complex (ABC/HRP). Positive reactions were then visualised by incubation with 3, 3' diaminobenzidine tetrahydrochloride (DAB; DAKO) substrate. Prior to incubation with secondary antibody, tissue sections were incubated with normal serum from the same species as the secondary antibody was raised in. This step was required to block any non-specific background staining which may have been elicited to the secondary antibody. Negative controls for non-specific staining with test antibodies comprised tissue sections treated with normal serum from the same species the secondary antibody had been raised in instead of the test antibody. Positive controls for the test antibody, using tissue sections known to be positive for the test antibody, were used to ensure the solutions being used were active.

T. annulata macroschizonts were detected by hybridoma supernatants of MAb 1C7 (Shiels *et al.* 1986; Glascodine, Tetley, Tait, Brown & Shiels 1990) (diluted 1:2 in normal rabbit serum (SAPU)) *T. annulata* microschizonts were recognised by Harris's haematoxylin counterstain. *T. parva* (Muguga) macroschizonts and microschizonts were detected by hybridoma supernatants of MAb 4 (donated by ILRI) (diluted 1:50 in normal rabbit serum (SAPU)). Biotinylated rabbit anti-mouse secondary antibody (DAKO) (diluted 1:400 in normal rabbit serum (SAPU)) and normal rabbit serum (diluted 1:5 in tris-buffered saline) controls were used in the immunocytochemical labelling techniques conducted on both the *T. annulata* and *T. parva* tissue sections. Immunocytochemically labelled schizont-infected cells were stained brown in colour. Macroschizonts stained with Harris's haematoxylin appeared as bodies containing few, large nuclei within the cytoplasm of the infected cells, whereas microschizonts stained with Harris's haematoxylin appeared as intra-cytoplasmic bodies containing numerous relatively smaller nuclei.

5.3.4 ASSESSMENT OF IMMUNOCYTOCHEMICALLY LABELLED PARAFFIN TISSUE SECTIONS

Several tissue sections were examined at 200 x magnification using a Nikon S. Ke II microscope and the total numbers of macroschizont- and microschizont-infected cells were recorded on the following subjective scale: - no schizont-infected cells; + small numbers of schizont-infected cells (<10 per field); ++ moderate numbers of schizont-infected cells (10-50 per field); +++ large numbers of schizont-infected cells (>50 per field). The results were decided upon after scanning the whole section.

Parasite distribution was compared to the tissue damage recorded previously (4.3.4), i.e. tissue damage associated with necrosis or haemorrhage (subjective scale: - no damage; * mild damage; ** moderate damage; *** extensive damage) and the identification of structural changes (including the following: lymphoid follicle morphology; lymphoid cell depletion; granuloma formation; medullary cord disruption; medullary sinus disruption; disruptive cellular infiltrate; oedema; congestion).

5.4 RESULTS

5.4.1 OVERALL PARASITE DISTRIBUTION IN INFECTED CATTLE AS ASSESSED BY IMPRESSION SMEARS

5.4.1.1 PARASITE DISTRIBUTION IN A CALF (41B) INFECTED WITH T. ANNULATA (HISAR) AS A PILOT STUDY

On day 12 post-infection during the terminal stages of disease in calf 41B [Figure 5.4] macroschizont-infected cells were found in all lymphoid organs, i.e. the lymph nodes, spleen and thymus, and all non-lymphoid organs, i.e. the kidney, liver and lung. The largest numbers recorded were in the draining prescapular LN (68%). Microschizont-infected cells were found in all lymphoid and non-lymphoid organs, with the exception of the contralateral prescapular LN and spleen. The largest numbers recorded were in the mesenteric LN (5%). Intra-erythrocytic piroplasms were found in all lymphoid and non-lymphoid organs. The largest numbers recorded were in the kidney and lung (75%).

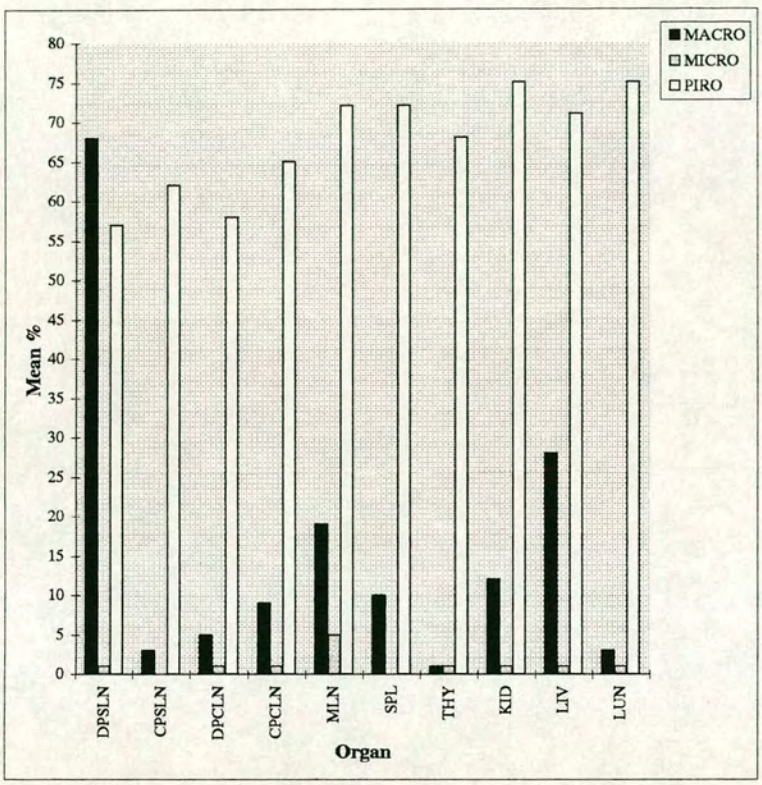

DPSLN Draining prescapular lymph node
CPSLN Contralateral prescapular lymph node
DPCLN Draining precrural lymph node
CPCLN Contralateral precrural lymph node
MLN Mesenteric lymph node
SPL Spleen
THY Thymus
KID Kidney
LIV Liver
LUN Lung

Figure 5.4 Parasite distribution in impression smears of a calf (41B) infected with *T. annulata* (Hisar) as a pilot study

5.4.1.2 PARASITE DISTRIBUTION IN CALVES (55C, 19 & 20) EXAMINED AT INTERVALS AFTER INFECTION WITH T. ANNULATA (HISAR)

On day 7 post-infection during the initial stages of pyrexia in calf 55C [Figure 5.5A] macroschizont-infected cells were found in most lymphoid organs, i.e. the majority of lymph nodes and the spleen, but only in the lung and heart of the non-lymphoid organs. The largest numbers recorded were in the lung (3%). By day 12 post-infection at the peak of pyrexia [Figure 5.5B] and day 14 post-infection during the nadir of disease [Figure 5.5C] in calves 19 and 20 respectively, they were seen in all lymphoid organs, i.e. the lymph nodes, spleen and thymus, and in all non-lymphoid organs, with the exception of the heart. The largest numbers recorded were in the draining prescapular LN on day 12 post-infection (41%) and on day 14 post-infection (12%).

On day 7 post-infection during the initial stages of pyrexia in calf 55C [Figure 5.5A] microschizont-infected cells were not detected in any organs. By day 12 post-infection at the peak of pyrexia [Figure 5.5B] and day 14 post-infection during the nadir of disease [Figure 5.5C] in calves 19 and 20 respectively, they were found in all lymphoid organs, but in only a minority of non-lymphoid organs, i.e. the liver, abomasum and adrenal gland. The largest numbers recorded were in the hepatic LN on day 12 post-infection (2%) and the draining and contralateral prescapular LNs on day 14 post-infection (1%).

On day 7 post-infection during the initial stages of pyrexia in calf 55C [Figure 5.5A] intra-erythrocytic piroplasms were only detected in the contralateral prescapular LN and draining precrural LN. The largest numbers recorded were in the contralateral prescapular LN (7%). By day 12 post-infection at the peak of pyrexia [Figure 5.5B] and day 14 post-infection during the nadir of disease [Figure 5.5C] in calves 19 and 20 respectively, they were found in all lymphoid and non-lymphoid organs. The largest numbers recorded were in the spleen on day 12 post-infection (41%) and the heart on day 14 post-infection (68%).

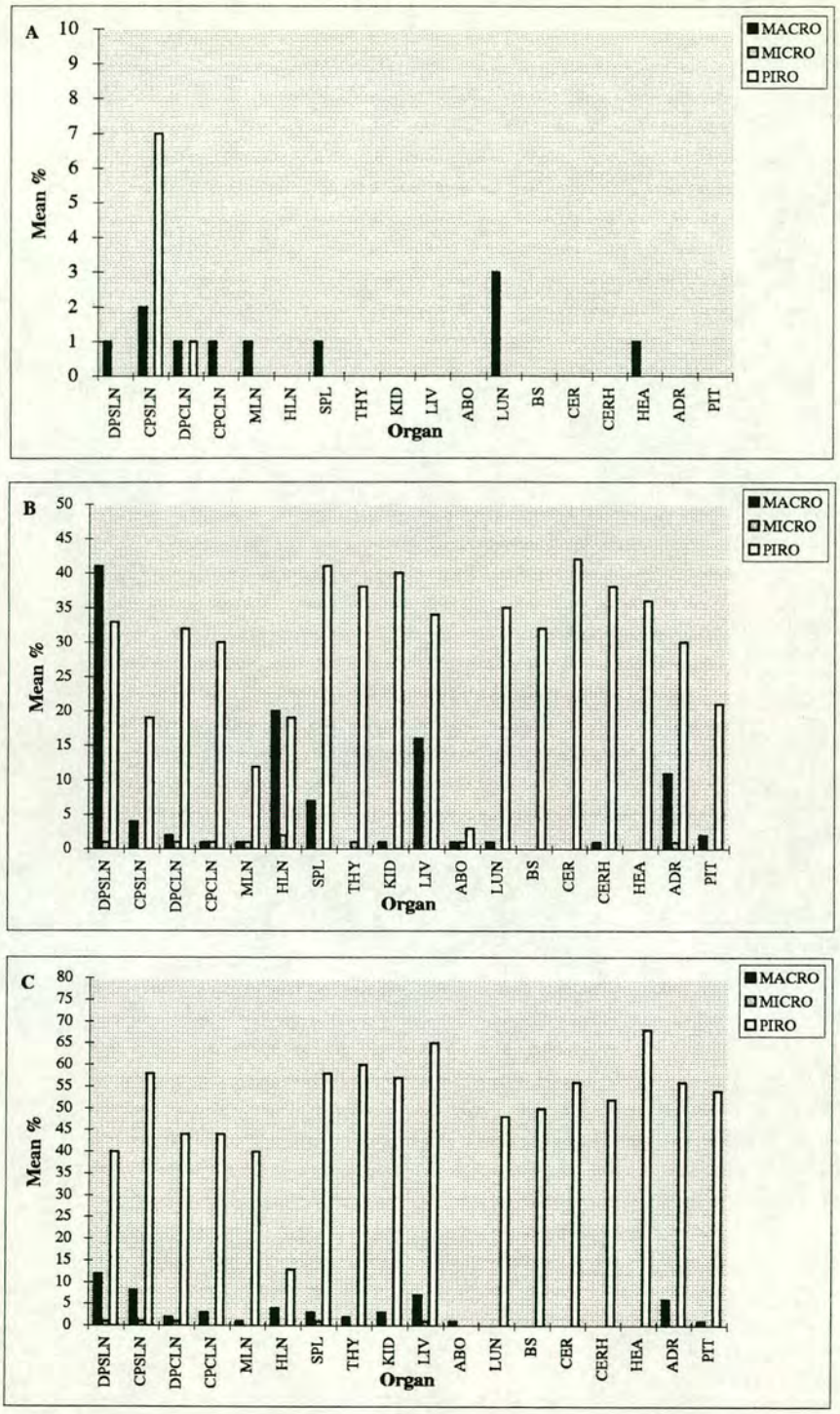

DPSLN Draining prescapular lymph node
CPSLN Contralateral prescapular lymph node
DPCLN Draining precrural lymph node
CPCLN Contralateral precrural lymph node
MLN Mesenteric lymph node
HLN Hepatic lymph node
SPL Spleen
THY Thymus
KID Kidney
LIV Liver
ABO Abomasum
LUN Lung
BS Brain stem
CER Cerebellum
CERH Cerebral hemisphere
HEA Heart
ADR Adrenal gland
PIT Pituitary gland

Figure 5.5 Parasite distribution in impression smears of calves (55C (A), 19 (B) & 20 (C)) examined at intervals after infection with *T. annulata* (Hisar)

5.4.1.3 PARASITE DISTRIBUTION IN A CALF (861) DURING THE TERMINAL STAGES OF INFECTION WITH T. ANNULATA (DOUKKALLA)

On day 24 post-infection during the terminal stages of disease in calf 861 [Figure 5.6A] macroschizont-infected cells were found in all lymphoid organs, i.e. the lymph nodes, spleen and thymus, and all non-lymphoid organs, with the exception of the kidney. The largest numbers recorded were in the draining prescapular LN (85%). Microschizont-infected cells were only detected in the draining prescapular LN and draining precrural LN. The largest numbers recorded were in the draining prescapular and precrural LNs (1%). Intra-erythrocytic piroplasms were found in all lymphoid and non-lymphoid organs. The largest numbers recorded were in the draining precrural LN (24%).

5.4.1.4 PARASITE DISTRIBUTION IN A CALF (8) DURING THE TERMINAL STAGES OF INFECTION WITH T. PARVA (MUGUGA)

On day 21 post-infection during the terminal stages of disease in calf 8 [Figure 5.6B] macroschizont-infected cells were detected in all lymphoid organs, i.e. the lymph nodes, spleen and thymus, and all non-lymphoid organs, with the exception of the abomasum and adrenal gland. The largest numbers recorded were in the draining prescapular LN (31%). Microschizont-infected cells were found in all lymphoid organs, with the exception of the thymus, but only a minority of non-lymphoid organs namely the liver and lung. The largest numbers recorded were in the draining precrural LN (4%). Intra-erythrocytic piroplasms were detected in all lymphoid and non-lymphoid organs. The largest numbers recorded were in the spleen (23%).

5.4.2 DISTRIBUTION OF SCHIZONT-INFECTED CELLS (MACROSCHIZONT & MICROSCHIZONT) IN RELATION TO TISSUE DAMAGE AS ASSESSED BY IMMUNOCYTOCHEMICALLY LABELLED PARAFFIN TISSUE SECTIONS

Tissue sections were immunocytochemically labelled with MAb 1C7, which recognises *T. annulata* macroschizont-infected cells, or MAb 4, which recognises *T. parva* (Muguga) macroschizont- and microschizont-infected cells and counterstained with Harris's haematoxylin. Immunocytochemically labelled schizont-infected cells were stained brown in colour. Macroschizonts stained with Harris's haematoxylin appeared as bodies containing few, large nuclei within the cytoplasm of the infected

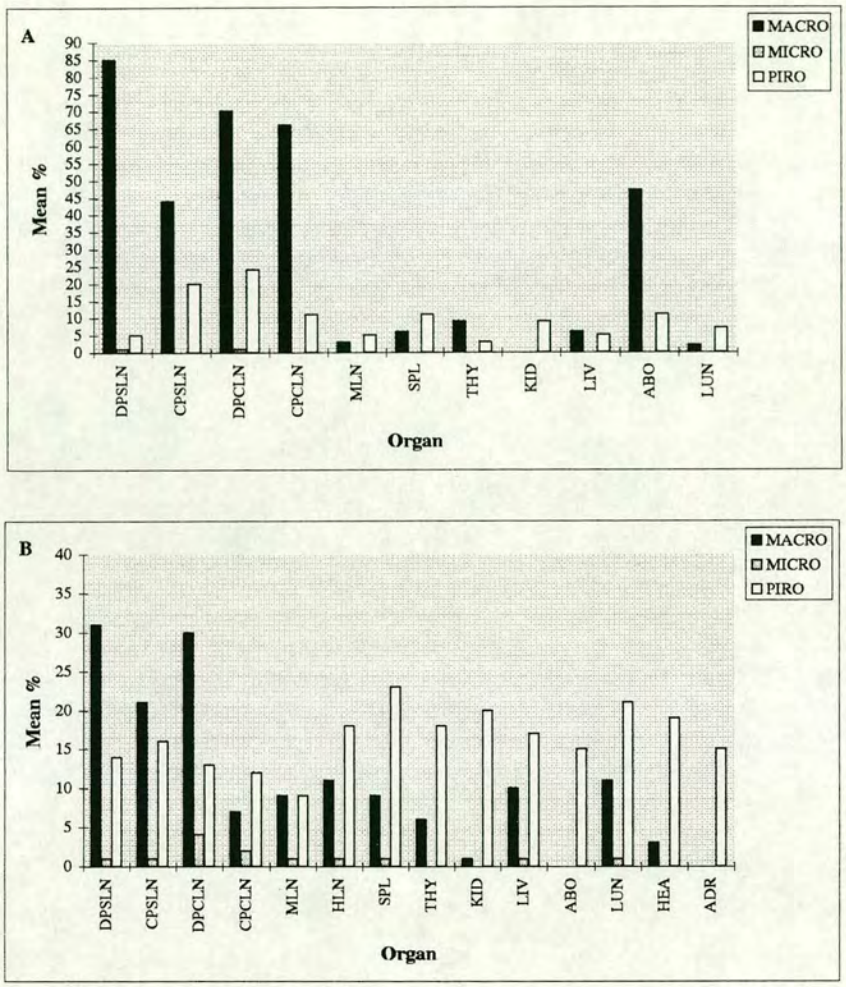

DPSLN Draining prescapular lymph node
CPSLN Contralateral prescapular lymph node
DPCLN Draining precrural lymph node
CPCLN Contralateral precrural lymph node
MLN Mesenteric lymph node
HLN Hepatic lymph node
SPL Spleen
THY Thymus
KID Kidney
LIV Liver
ABO Abomasum
LUN Lung
HEA Heart
ADR Adrenal gland

Figure 5.6 Parasite distribution in impression smears of a calf (861 (A)) infected with *T. annulata* (Doukkalla) and a calf (8 (B)) infected with *T. parva* (Muguga)

cells, whereas microschizonts stained with Harris's haematoxylin appeared as intra-cytoplasmic bodies containing numerous relatively smaller nuclei.

5.4.2.1 DISTRIBUTION OF SCHIZONT-INFECTED CELLS IN UNINFECTED CONTROL CATTLE

Tissue sections did not contain any structures which resembled the macroschizont- or microschizont-infected cells found in tissues of infected animals. The lymphoid and non-lymphoid organs showed a normal tissue architecture as described by Banks (1993) and Burkitt *et al.* (1993).

5.4.2.2 DISTRIBUTION OF SCHIZONT-INFECTED CELLS IN A CALF (41B) INFECTED WITH T. ANNULATA (HISAR) AS A PILOT STUDY

On day 12 post-infection during the terminal stages of disease in calf 41B [Table 5.1A] large numbers of macroschizont- and microschizont-infected cells occurred throughout the draining prescapular LN accompanied by extensive lymphoid cellular depletion and disruption of tissue architecture. Lymphoid follicles of this lymph node were absent. Macroschizont- and microschizont-infected cells were detected throughout the other lymphoid organs, i.e. the remaining lymph nodes, spleen (Figure 5.7) and thymus. In these lymph nodes lymphoid cellular depletion was seen in the paracortex, with the exception of the contralateral precrural LN, and sinus hyperplasia was detected. Lymphoid follicles in these lymph nodes were either absent or reduced in size with small germinal centres, with the exception of the mesenteric LN. Granulomas were seen in the paracortex of the contralateral prescapular LN and draining precrural LN. Lymphoid cellular depletion was also seen in the white pulp of the spleen and cortex of the thymus. The red pulp of the spleen was congested. Macroschizont- and microschizont-infected cells occurred throughout all the non-lymphoid organs, i.e. the kidney, liver, abomasum (Figure 5.8) and lung. A disruptive cellular infiltrate was seen in these organs, with the exception of the lung. Oedema occurred in the kidney and liver and a diffuse necrosis and haemorrhage was seen in the thickened alveolar walls of the lung.

ORGAN	AREA	SIC	N	H	FEATURES	CHANGES
Prescapular LN (draining)	CX	++	***	*	Follicles	Absent
	PCX	+++	***	**	Cellular depletion of LC	Throughout LN
	MC	+	***	**	Granulomas	Absent
	MS	+	***	**	MC	Disrupted
					MS	Disrupted
					Other	Severe disruption of LN architecture
Prescapular LN (contralateral)	CX	+	-	-	Follicles	Absent
	PCX	+	-	-	Cellular depletion of LC	CX & PCX
	MC	+	*	-	Granulomas	PCX
	MS	+	-	-	MC	nc
					MS	Filled with mainly uninfected cells / sinus hyperplasia
					Other	Enlarged medulla
Precrural LN (draining)	CX	+	-	-	Follicles	Follicles with small germinal centres
	PCX	+	-	*	Cellular depletion of LC	CX, PCX & MC
	MC	+	-	-	Granulomas	PCX
	MS	+	-	-	MC	Disrupted
					MS	Filled with mainly uninfected cells / sinus hyperplasia
					Other	Enlarged medulla
Precrural LN (contralateral)	CX	++	-	-	Follicles	Follicles with small germinal centres
	PCX	++	-	-	Cellular depletion of LC	Absent
	MC	+	-	-	Granulomas	Absent
	MS	+	-	-	MC	Prominent
					MS	Filled with mainly uninfected cells / sinus hyperplasia
					Other	Enlarged medulla
Mesenteric LN	CX	++	-	-	Follicles	Normal active follicles
	PCX	++	-	-	Cellular depletion of LC	PCX
	MC	+	-	-	Granulomas	Absent
	MS	+	-	-	MC	Prominent
					MS	Filled with mainly uninfected cells / sinus hyperplasia
					Other	Enlarged medulla
Spleen	WP	+++	-	-	Cellular depletion of LC in WP	Present
	RP	+++	-	-	Congestion of RP	Present
Thymus	CX	+	-	*	Cellular depletion of LC in CX	Present
	MED	++	-	**		

nd None detected
\+ Small numbers of schizont-infected cells
++ Moderate numbers of schizont-infected cells
+++ Large numbers of schizont-infected cells

\- No damage
* Mild damage
** Moderate damage
*** Extensive damage

SIC Schizont-infected cells
N Necrosis
H Haemorrhage
LN Lymph node
LC Lymphoid cells
CX Cortex
PCX Paracortex
MED Medulla
MC Medullary cords
MS Medullary sinuses
WP White pulp
RP Red pulp
nc No change

Table 5.1A Distribution of schizont-infected cells detected by MAb 1C7 and Harris's haematoxylin in a calf (41B) infected with *T.annulata* (Hisar) as a pilot study

ORGAN	AREA	SIC	N	H	FEATURES	CHANGES
Kidney	CX	++	-	-	Disruptive cellular infiltrate in CX	Present
	MED	++	-	-	Oedema of tubules	Present
Liver	PT	++	-	-	Disruptive cellular infiltrate	Present
					Oedema of hepatic cells	Present
Abomasum	LAP	+++	-	-	Disruptive cellular infiltrate	Present
Lung	AW	++	+	+	Thickened AW	Present
	BRO	+	-	-	Congestion of BRO	Absent

nd None detected
+ Small numbers of schizont-infected cells
++ Moderate numbers of schizont-infected cells
+++ Large numbers of schizont-infected cells

- No damage
* Mild damage
** Moderate damage
*** Extensive damage

SIC Schizont-infected cells
N Necrosis
H Haemorrhage
CX Cortex
MED Medulla

PT Portal tracts
LAP Lamina propria
AW Alveolar wall
BRO Bronchiole

Table 5.1A Continued

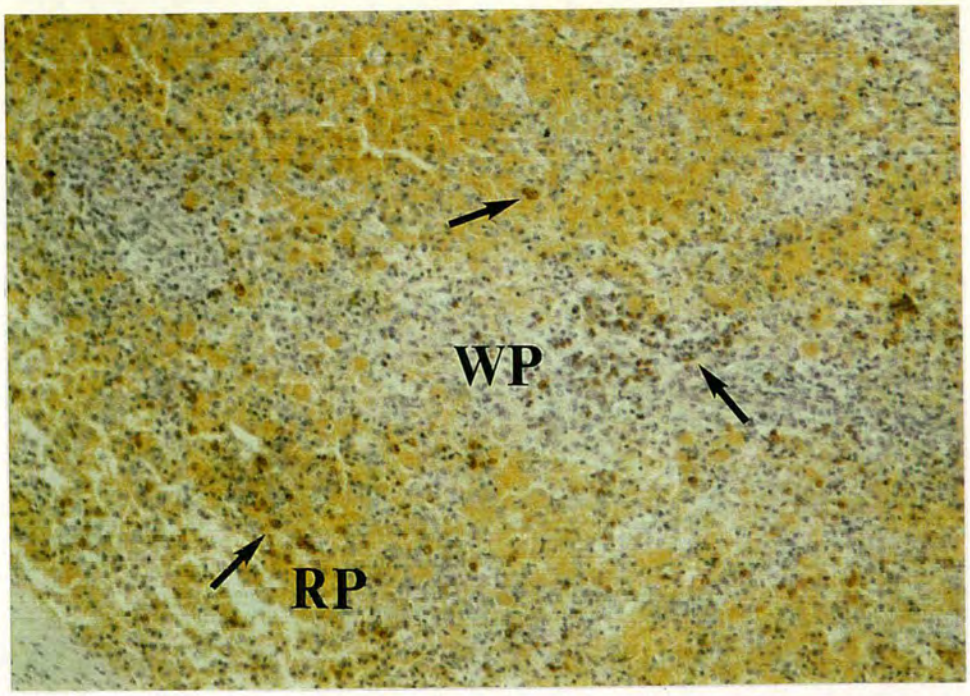

Figure 5.7 Section showing macroschizont-infected cells (arrows) in the white pulp (WP) and red pulp (RP) of the spleen of the calf infected with *T. annulata* (Hisar) on day 12 post-infection during the terminal stages of disease, (x100: MAb 1C7 & DAB).

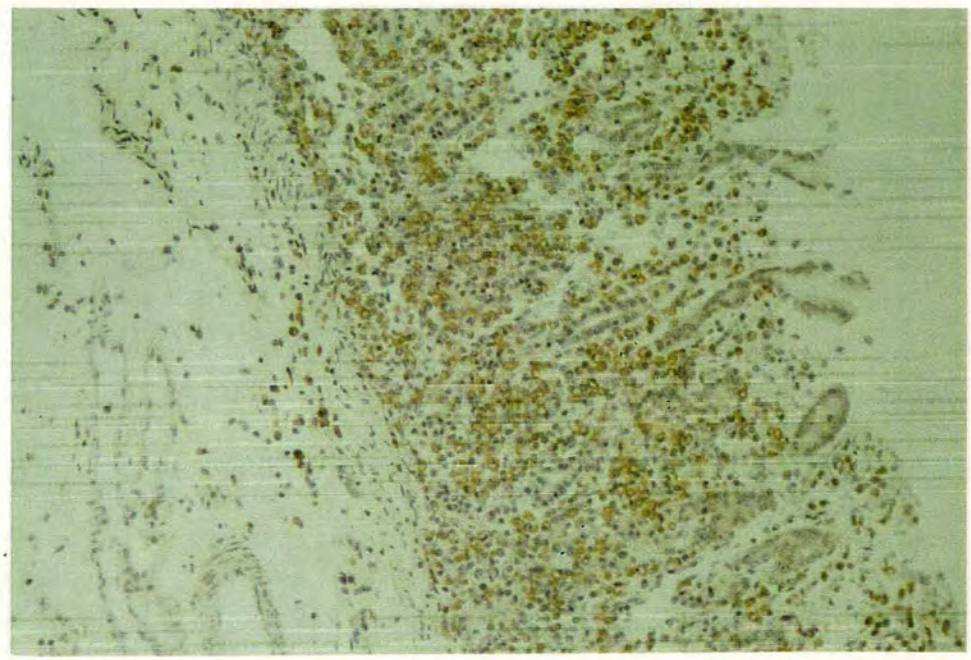

Figure 5.8 Section showing macroschizont-infected cells (brown) in the abomasum of the calf infected with *T. annulata* (Hisar) on day 12 post-infection during the terminal stages of disease, (x100: MAb 1C7 & DAB).

5.4.2.3 DISTRIBUTION OF SCHIZONT-INFECTED CELLS IN CALVES (55C, 19 & 20) EXAMINED AT INTERVALS DURING INFECTION WITH T. ANNULATA (HISAR)

On day 7 post-infection during the initial stages of pyrexia in calf 55C [Table 5.1B] small numbers of macroschizont-infected cells occurred only in the medulla of all the lymph nodes (Figure 5.9), with the exception of the hepatic LN, both the white and red pulp of the spleen and the medulla of the thymus. Lymphoid cellular depletion was seen in the paracortex of the draining and contralateral prescapular LNs and the hepatic LN, and sinus hyperplasia was detected in all the lymph nodes. Lymphoid follicles reduced in size with small germinal centres were seen in the draining and contralateral prescapular LNs and the draining precrural LN. Granulomas were seen in the paracortex of the draining and contralateral prescapular LNs and the hepatic LN. Lymphoid cellular depletion was also seen in the white pulp of the spleen. The red pulp of the spleen was congested. Macroschizont-infected cells occurred throughout most non-lymphoid organs, i.e. the kidney, liver, abomasum, lung, adrenal and pituitary glands. A disruptive cellular infiltrate was seen in these organs, with the exception of the lung, adrenal and pituitary glands. The alveolar walls of the lung were thickened and the bronchioles were congested.

On day 12 post-infection at the peak of pyrexia in calf 19 [Table 5.1C] large numbers of macroschizont- and microschizont-infected cells occurred throughout the draining prescapular LN (Figure 5.10A) accompanied by lymphoid cellular depletion and sinus hyperplasia. Lymphoid follicles of this lymph node were reduced in size with small germinal centres and granulomas (Figure 5.10B) were seen throughout. Macroschizont- and microschizont-infected cells were detected throughout the other lymphoid organs, i.e. the remaining lymph nodes, spleen and thymus. In these lymph nodes lymphoid cellular depletion was seen in the paracortex and sinus hyperplasia was detected. Lymphoid follicles in these lymph nodes were reduced in size with small germinal centres, with the exception of the mesenteric LN where follicular hyperplasia was seen. Granulomas were also seen in the paracortex of the draining precrural LN. Lymphoid cellular depletion was also seen in the white pulp of the spleen and cortex of the thymus. The red pulp of the spleen was congested. Macroschizont- and microschizont-infected cells occurred throughout most non-lymphoid organs, i.e. the kidney, liver, abomasum, lung and adrenal gland.

ORGAN	AREA	SIC	N	H	FEATURES	CHANGES
Prescapular LN (draining)	CX	nd	-	-	Follicles	Follicles with small germinal centres
	PCX	nd	**	*	Cellular depletion of LC	PCX
	MC	+	**	**	Granulomas	PCX
	MS	+	**	**	MC	Prominent
					MS	Filled with mainly uninfected cells / sinus hyperplasia
					Other	Enlarged medulla
Prescapular LN (contralateral)	CX	nd	-	-	Follicles	Follicles with small germinal centres
	PCX	nd	-	-	Cellular depletion of LC	PCX
	MC	+	-	-	Granulomas	PCX
	MS	+	-	-	MC	Prominent
					MS	Filled with mainly uninfected cells / sinus hyperplasia
					Other	Enlarged medulla
Precrural LN (draining)	CX	nd	-	-	Follicles	Follicles with small germinal centres
	PCX	nd	-	*	Cellular depletion of LC	Absent
	MC	+	-	*	Granulomas	Absent
	MS	+	-	-	MC	nc
					MS	Filled with mainly uninfected cells / mild sinus hyperplasia
					Other	
Precrural LN (contralateral)	CX	nd	-	-	Follicles	Normal active follicles
	PCX	nd	-	-	Cellular depletion of LC	Absent
	MC	+	-	-	Granulomas	Absent
	MS	+	-	-	MC	nc
					MS	Filled with mainly uninfected cells / mild sinus hyperplasia
					Other	
Mesenteric LN	CX	nd	-	-	Follicles	Normal active follicles
	PCX	nd	-	-	Cellular depletion of LC	Absent
	MC	+	-	-	Granulomas	Absent
	MS	+	-	-	MC	nc
					MS	Filled with mainly uninfected cells / mild sinus hyperplasia
					Other	
Hepatic LN	CX	nd	-	-	Follicles	Normal active follicles
	PCX	nd	-	-	Cellular depletion of LC	PCX
	MC	nd	-	-	Granulomas	PCX
	MS	nd	-	-	MC	Prominent
					MS	Filled with mainly uninfected cells / sinus hyperplasia
					Other	Enlarged medulla
Spleen	WP	+	-	-	Cellular depletion of LC in WP	Present
	RP	+	-	-	Congestion of RP	Present
Thymus	CX	nd	-	*	Cellular depletion of LC in CX	Absent
	MED	+	-	*		

nd None detected
\+ Small numbers of schizont-infected cells
++ Moderate numbers of schizont-infected cells
+++ Large numbers of schizont-infected cells

\- No damage
* Mild damage
** Moderate damage
*** Extensive damage

SIC Schizont-infected cells
N Necrosis
H Haemorrhage
LN Lymph node
LC Lymphoid cells
CX Cortex
PCX Paracortex
MED Medulla
MC Medullary cords
MS Medullary sinuses
WP White pulp
RP Red pulp
nc No change

Table 5.1B Distribution of schizont-infected cells detected by MAb 1C7 and Harris's haematoxylin in a calf (55C) infected with *T.annulata* (Hisar) on day 7 post-infection

ORGAN	AREA	SIC	N	H	FEATURES	CHANGES
Kidney	CX	+	-	-	Disruptive cellular infiltrate in CX	Present
	MED	nd	-	-	Oedema of tubules	Absent
Liver	PT	+	-	-	Disruptive cellular infiltrate	Present
					Oedema of hepatic cells	Absent
Abomasum	LAP	+	-	-	Disruptive cellular infiltrate	Present
Lung	AW	+	-	-	Thickened AW	Present
	BRO	nd	-	-	Congestion of BRO	Present
Brain stem	GEN	nd	-	-	Disruptive cellular infiltrate	Absent: Normal architecture
Cerebellum	GEN	nd	-	-	Disruptive cellular infiltrate	Absent: Normal architecture
Cerebral hemisphere	GEN	nd	-	-	Disruptive cellular infiltrate	Absent: Normal architecture
Heart	GEN	nd	-	-	Disruptive cellular infiltrate	Absent: Normal architecture
Adrenal gland	ZG	+	-	-	Disruptive cellular infiltrate	Absent: Normal architecture
	ZF	+	-	-		
	ZR	nd	-	-		
	MED	nd	-	-		
Anterior Pituitary gland	GEN	+	-	-	Disruptive cellular infiltrate	Absent: Normal architecture

nd None detected
+ Small numbers of schizont-infected cells
++ Moderate numbers of schizont-infected cells
+++ Large numbers of schizont-infected cells

- No damage
* Mild damage
** Moderate damage
*** Extensive damage

SIC Schizont-infected cells
N Necrosis
H Haemorrhage
GEN General
CX Cortex
MED Medulla
PT Portal tracts
LAP Lamina propria
AW Alveolar wall
BRO Bronchiole
ZG Zona glomerulosa
ZF Zona fasciculata
ZR Zona reticularis

Table 5.1B Continued

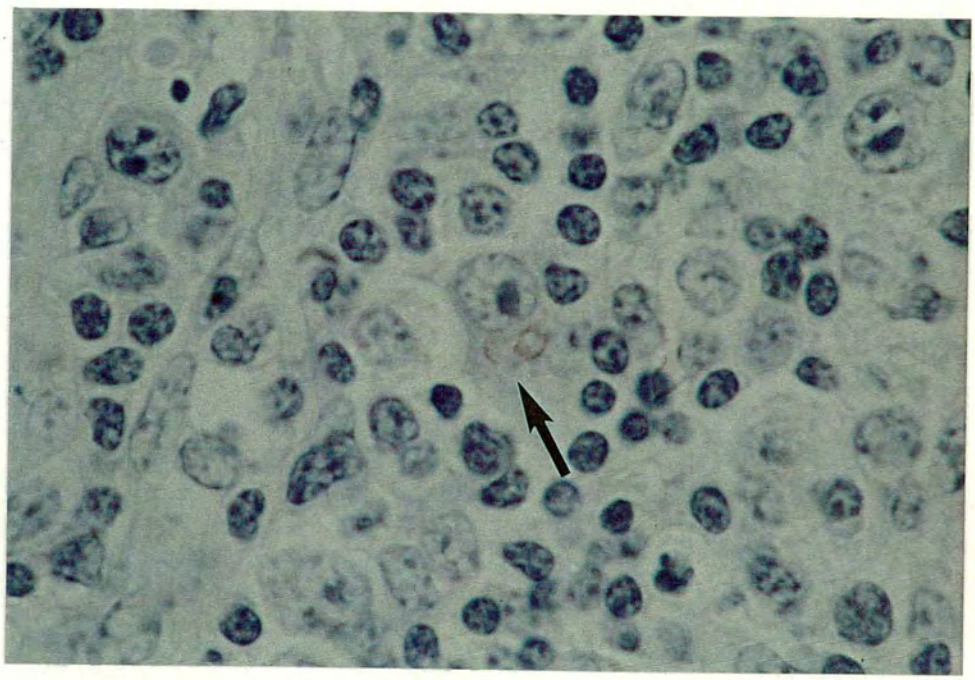

Figure 5.9 Section showing a macroschizont-infected cell (arrow) in the medullary sinuses of the draining prescapular lymph node of the calf infected with *T. annulata* (Hisar) on day 7 post-infection during the initial stages of pyrexia, (x1000: MAb 1C7 & DAB).

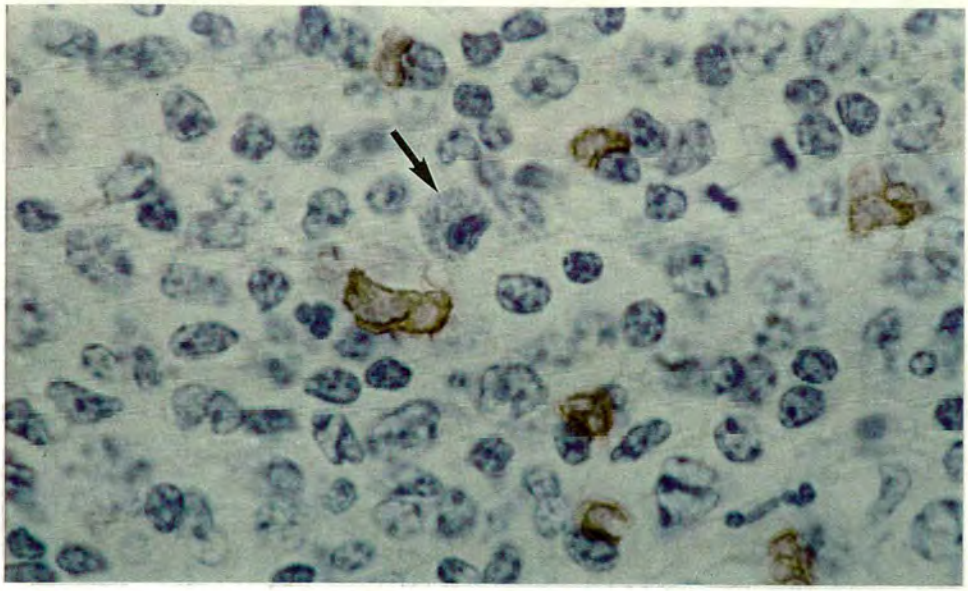

Figure 5.10A Section showing macroschizont-infected cells (brown) and a microschizont-infected cell (arrow) in the paracortex of the draining prescapular lymph node of the calf infected with *T. annulata* (Hisar) on day 12 post-infection at the peak of pyrexia, (x1000: MAb 1C7 & DAB).

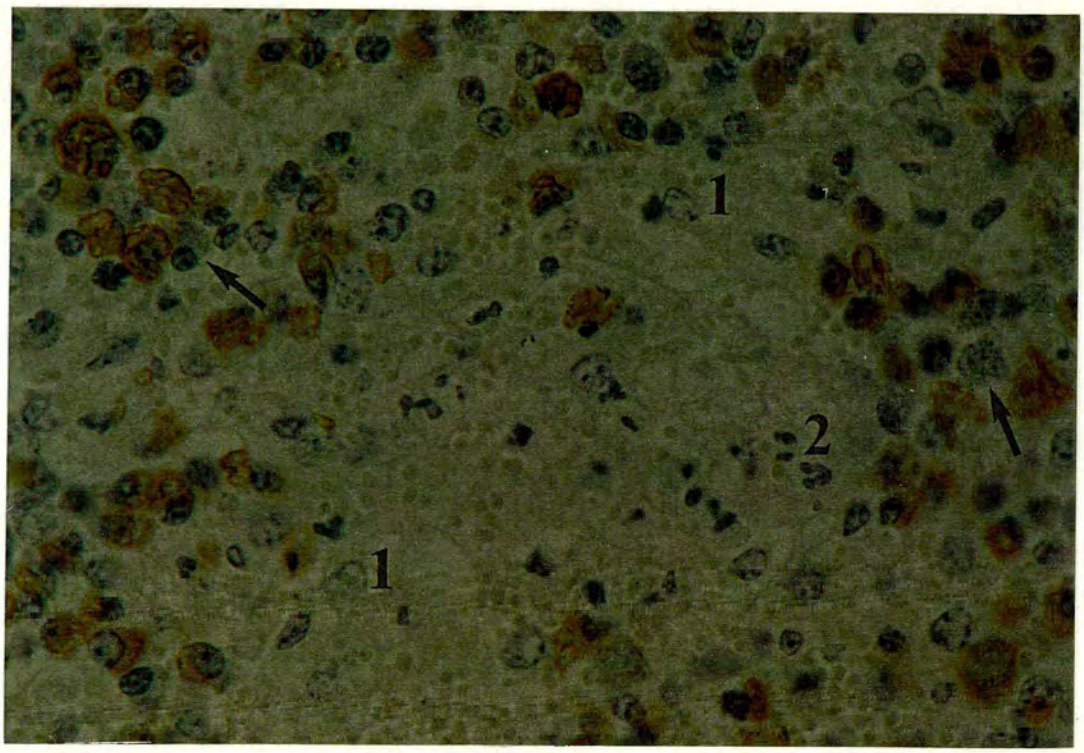

Figure 5.10B Section showing a granuloma accompanied by large numbers of macroschizont-infected cells (brown), microschizont-infected cells (arrows), macrophages (1) and eosinophils (2) in the paracortex of the draining prescapular lymph node of the calf infected with *T. annulata* (Hisar) on day 12 post-infection at the peak of pyrexia, (x500: MAb 1C7 & DAB).

ORGAN	AREA	SIC	N	H	FEATURES	CHANGES
Prescapular LN (draining)	CX	+	-	-	Follicles	Follicles with small germinal centres
	PCX	++	*	*	Cellular depletion of LC	Throughout LN
	MC	+	*	*	Granulomas	Throughout LN
	MS	+++	*	*	MC	Disrupted
					MS	Filled with mainly uninfected cells / sinus hyperplasia
					Other	Enlarged medulla
Prescapular LN (contralateral)	CX	+	-	-	Follicles	Follicles with small germinal centres
	PCX	+	*	*	Cellular depletion of LC	PCX
	MC	+	-	-	Granulomas	Absent
	MS	+	-	-	MC	Prominent
					MS	Filled with mainly uninfected cells / sinus hyperplasia
					Other	Enlarged medulla
Precrural LN (draining)	CX	+	*	-	Follicles	Follicles with small germinal centres
	PCX	+	*	-	Cellular depletion of LC	PCX, MC & MS
	MC	+	*	-	Granulomas	PCX
	MS	+	*	-	MC	Disrupted
					MS	Filled with mainly uninfected cells / sinus hyperplasia
					Other	Enlarged medulla
Precrural LN (contralateral)	CX	+	*	-	Follicles	Follicles with small germinal centres
	PCX	+	*	-	Cellular depletion of LC	Throughout LN
	MC	+	*	-	Granulomas	Absent
	MS	+	*	-	MC	Disrupted
					MS	Filled with mainly uninfected cells / sinus hyperplasia
					Other	Enlarged medulla
Mesenteric LN	CX	+	*	-	Follicles	Follicular hyperplasia
	PCX	+	*	*	Cellular depletion of LC	PCX, MC & MS
	MC	+	*	*	Granulomas	Absent
	MS	+	*	*	MC	Disrupted
					MS	Filled with mainly uninfected cells / sinus hyperplasia
					Other	Enlarged medulla
Hepatic LN	CX	+	*	-	Follicles	Follicles with small germinal centres
	PCX	+	*	-	Cellular depletion of LC	Throughout LN
	MC	+	*	-	Granulomas	Absent
	MS	+	*	-	MC	Disrupted
					MS	Filled with mainly uninfected cells / sinus hyperplasia
					Other	Enlarged medulla
Spleen	WP	++	-	-	Cellular depletion of LC in WP	Present
	RP	++	-	-	Congestion of RP	Present
Thymus	CX	nd	-	*	Cellular depletion of LC in CX	Present
	MED	+	-	*		

nd None detected
+ Small numbers of schizont-infected cells
++ Moderate numbers of schizont-infected cells
+++ Large numbers of schizont-infected cells

- No damage
* Mild damage
** Moderate damage
*** Extensive damage

SIC Schizont-infected cells
N Necrosis
H Haemorrhage
LN Lymph node
LC Lymphoid cells
CX Cortex
PCX Paracortex
MED Medulla
MC Medullary cords
MS Medullary sinuses
WP White pulp
RP Red pulp
nc No change

Table 5.1C Distribution of schizont-infected cells detected by MAb 1C7 and Harris's haematoxylin in a calf (19) infected with *T.annulata* (Hisar) on day 12 post-infection

ORGAN	AREA	SIC	N	H	FEATURES	CHANGES
Kidney	CX	+	-	-	Disruptive cellular infiltrate in CX	Present
	MED	nd	-	-	Oedema of tubules	Present
Liver	PT	++	*	*	Disruptive cellular infiltrate	Present
					Oedema of hepatic cells	Absent
Abomasum	LAP	+	-	-	Disruptive cellular infiltrate	Present
Lung	AW	+	*	-	Thickened AW	Present
	BRO	+	-	-	Congestion of BRO	Present
Brain stem	GEN	nd	-	-	Disruptive cellular infiltrate	Absent: Normal architecture
Cerebellum	GEN	nd	-	-	Disruptive cellular infiltrate	Absent: Normal architecture
Cerebral hemisphere	GEN	nd	-	-	Disruptive cellular infiltrate	Absent: Normal architecture
Heart	GEN	nd	-	-	Disruptive cellular infiltrate	Absent: Normal architecture
Adrenal gland	ZG	+	-	-	Disruptive cellular infiltrate	Present
	ZF	++	-	-		
	ZR	++	-	-		
	MED	+	-	-		
Anterior Pituitary gland	GEN	++	-	-	Disruptive cellular infiltrate	Absent: Normal architecture

nd None detected
+ Small numbers of schizont-infected cells
++ Moderate numbers of schizont-infected cells
+++ Large numbers of schizont-infected cells

- No damage
* Mild damage
** Moderate damage
*** Extensive damage

SIC Schizont-infected cells
N Necrosis
H Haemorrhage
GEN General
CX Cortex
MED Medulla
PT Portal tracts
LAP Lamina propria
AW Alveolar wall
BRO Bronchiole
ZG Zona glomerulosa
ZF Zona fasciculata
ZR Zona reticularis

Table 5.1C Continued

Macroschizont-infected cells alone were detected in the pituitary gland. A disruptive cellular infiltrate was seen in these organs, with the exception of the lung and pituitary gland. Oedema occurred in the kidney and a diffuse necrosis and haemorrhage was seen in the liver. The alveolar walls of the lung were thickened and the bronchioles were congested.

On day 14 post-infection during the nadir of disease in calf 20 [Table 5.1D] large numbers of macroschizont- and microschizont-infected cells occurred throughout the draining prescapular LN (Figure 5.11) accompanied by lymphoid cellular depletion and extensive disruption of tissue architecture. Lymphoid follicles of this lymph node were absent. Macroschizont- and microschizont-infected cells were detected throughout the other lymphoid organs, i.e. the remaining lymph nodes, spleen (Figure 5.12) and thymus. In these lymph nodes lymphoid cellular depletion was seen in the paracortex and sinus hyperplasia was detected. Lymphoid follicles in these lymph nodes were reduced in size with small germinal centres, with the exception of the mesenteric LN. No granulomas were seen. Lymphoid cellular depletion was also seen in the white pulp of the spleen and cortex of the thymus. The red pulp of the spleen was congested. Macroschizont- and microschizont-infected cells occurred throughout most non-lymphoid organs, i.e. the kidney (Figure 5.13), liver, lung (Figure 5.14) and adrenal gland (Figures 5.15 & 5.16). Macroschizont-infected cells alone were detected in the abomasum, heart and pituitary gland (Figure 5.17). A disruptive cellular infiltrate was seen in these organs, with the exception of the lung and pituitary gland. Oedema occurred in the kidney and the alveolar walls of the lung were thickened.

5.4.2.4 DISTRIBUTION OF SCHIZONT-INFECTED CELLS IN A CALF (861) DURING THE TERMINAL STAGES OF INFECTION WITH T. ANNULATA (DOUKKALLA)

On day 24 post-infection during the terminal stages of disease in calf 861 [Table 5.1E] large numbers of macroschizont- and microschizont-infected cells occurred throughout the draining prescapular LN accompanied by lymphoid cellular depletion and extensive disruption of tissue architecture. Lymphoid follicles of this lymph node were absent. Macroschizont- and microschizont-infected cells were detected throughout the other lymphoid organs, i.e. the remaining lymph nodes and the

ORGAN	AREA	SIC	N	H	FEATURES	CHANGES
Prescapular LN (draining)	CX	++	**	***	Follicles	Absent
	PCX	+++	**	***	Cellular depletion of LC	Throughout LN
	MC	+	**	***	Granulomas	Absent
	MS	+++	***	***	MC	Disrupted
					MS	Disrupted
					Other	Severe disruption of LN architecture
Prescapular LN (contralateral)	CX	+	-	-	Follicles	Follicles with small germinal centres
	PCX	+	*	*	Cellular depletion of LC	Throughout LN
	MC	+	*	*	Granulomas	Absent
	MS	++	**	**	MC	Disrupted
					MS	Filled with mainly uninfected cells / sinus hyperplasia
					Other	Enlarged medulla
Precrural LN (draining)	CX	+	**	*	Follicles	Follicles with small germinal centres
	PCX	++	**	*	Cellular depletion of LC	CX & PCX
	MC	+	-	-	Granulomas	Absent
	MS	+	-	-	MC	nc
					MS	Filled with mainly uninfected cells / sinus hyperplasia
					Other	Enlarged medulla
Precrural LN (contralateral)	CX	+	*	*	Follicles	Follicles with small germinal centres
	PCX	++	**	*	Cellular depletion of LC	CX & PCX
	MC	+	-	-	Granulomas	Absent
	MS	+	-	-	MC	Prominent
					MS	Filled with mainly uninfected cells / sinus hyperplasia
					Other	Enlarged medulla
Mesenteric LN	CX	+	-	-	Follicles	Normal active follicles
	PCX	+	**	*	Cellular depletion of LC	PCX & MC
	MC	+	-	-	Granulomas	Absent
	MS	++	**	*	MC	Disrupted
					MS	Filled with mainly uninfected cells / mild sinus hyperplasia
					Other	
Hepatic LN	CX	+	-	-	Follicles	Follicles with small germinal centres
	PCX	+	*	-	Cellular depletion of LC	CX & PCX
	MC	+	-	-	Granulomas	Absent
	MS	+	-	-	MC	Prominent
					MS	Filled with mainly uninfected cells / sinus hyperplasia
					Other	Enlarged medulla
Spleen	WP	++	-	-	Cellular depletion of LC in WP	Present
	RP	++	-	-	Congestion of RP	Present
Thymus	CX	+	*	-	Cellular depletion of LC in CX	Present
	MED	++	**	*		

nd None detected
\+ Small numbers of schizont-infected cells
++ Moderate numbers of schizont-infected cells
+++ Large numbers of schizont-infected cells

\- No damage
* Mild damage
** Moderate damage
*** Extensive damage

SIC Schizont-infected cells
N Necrosis
H Haemorrhage
LN Lymph node
LC Lymphoid cells
CX Cortex
PCX Paracortex
MED Medulla
MC Medullary cords
MS Medullary sinuses
WP White pulp
RP Red pulp
nc No change

Table 5.1D Distribution of schizont-infected cells detected by MAb 1C7 and Harris's haematoxylin in a calf (20) infected with *T.annulata* (Hisar) on day 14 post-infection

ORGAN	AREA	SIC	N	H	FEATURES	CHANGES
Kidney	CX	+	-	-	Disruptive cellular infiltrate in CX	Present
	MED	nd	-	-	Oedema of tubules	Present
Liver	PT	++	*	-	Disruptive cellular infiltrate	Present
					Oedema of hepatic cells	Absent
Abomasum	LAP	+	-	-	Disruptive cellular infiltrate	Present
Lung	AW	+	*	*	Thickened AW	Present
	BRO	nd	-	-	Congestion of BRO	Absent
Brain stem	GEN	nd	-	-	Disruptive cellular infiltrate	Absent: Normal architecture
Cerebellum	GEN	nd	-	-	Disruptive cellular infiltrate	Absent: Normal architecture
Cerebral hemisphere	GEN	nd	-	-	Disruptive cellular infiltrate	Absent: Normal architecture
Heart	GEN	+	-	-	Disruptive cellular infiltrate	Absent: Normal architecture
Adrenal gland	ZG	+	*	*	Disruptive cellular infiltrate	Present
	ZF	++	*	*		
	ZR	++	*	*		
	MED	+	-	-		
Anterior Pituitary gland	GEN	++	-	-	Disruptive cellular infiltrate	Absent: Normal architecture

nd None detected
+ Small numbers of schizont-infected cells
++ Moderate numbers of schizont-infected cells
+++ Large numbers of schizont-infected cells

- No damage
* Mild damage
** Moderate damage
*** Extensive damage

SIC Schizont-infected cells
N Necrosis
H Haemorrhage
GEN General
CX Cortex
MED Medulla
PT Portal tracts
LAP Lamina propria
AW Alveolar wall
BRO Bronchiole
ZG Zona glomerulosa
ZF Zona fasciculata
ZR Zona reticularis

Table 5.1D Continued

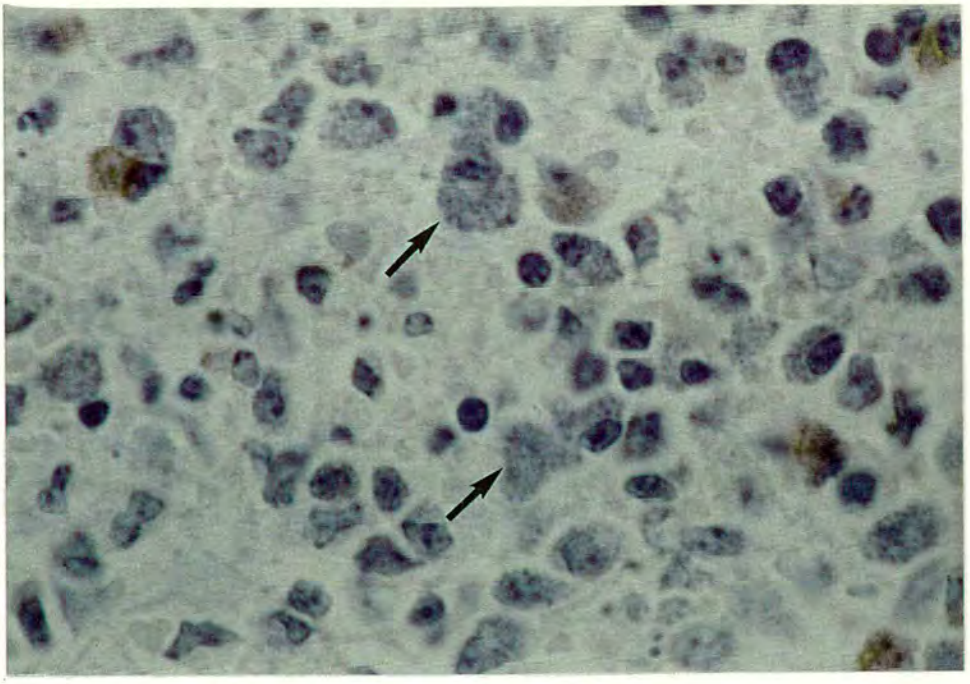

Figure 5.11 Section showing macroschizont-infected cells (brown) and microschizont-infected cells (arrows) in the medullary sinuses of the draining prescapular lymph node of the calf infected with *T. annulata* (Hisar) on day 14 post-infection at the nadir of disease, (x1000: MAb 1C7 & DAB).

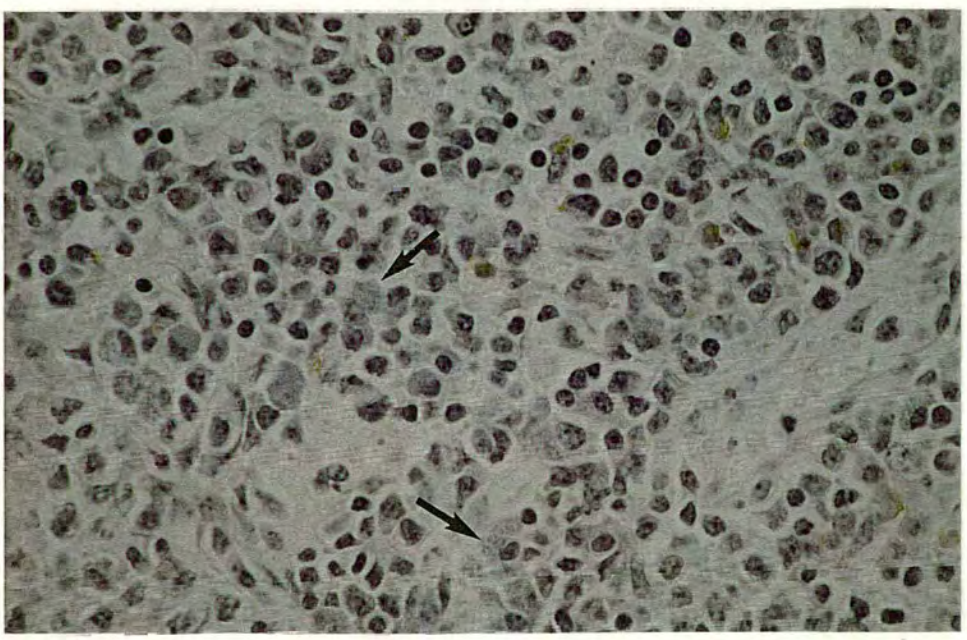

Figure 5.12 Section showing macroschizont-infected cells (brown) and microschizont-infected cells (arrows) in the white pulp of the spleen of the calf infected with *T. annulata* (Hisar) on day 14 post-infection at the nadir of disease, (x500: MAb 1C7 & DAB).

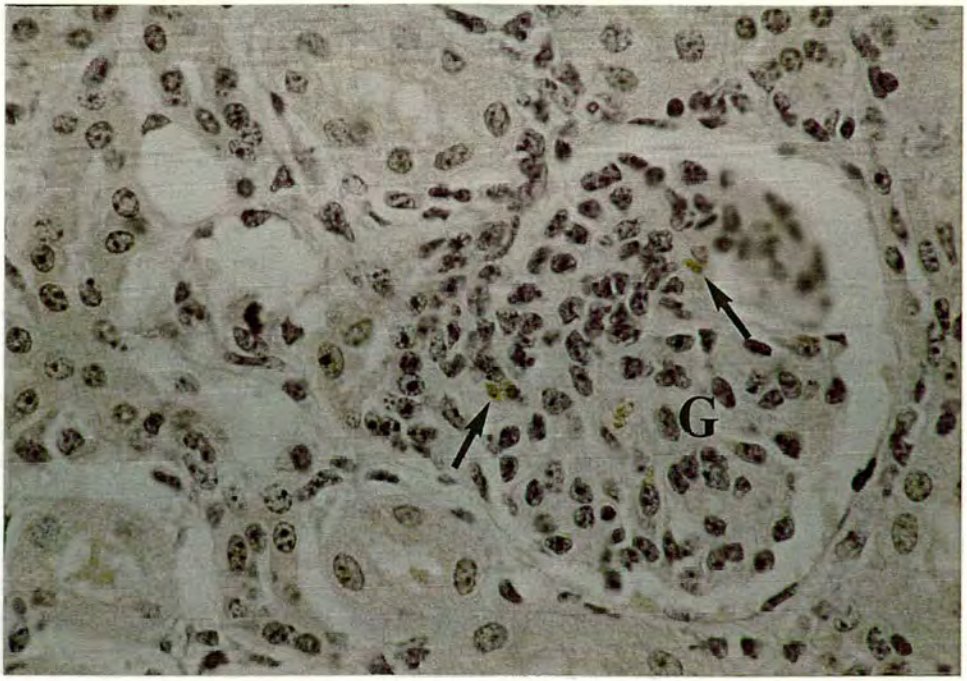

Figure 5.13 Section showing macroschizont-infected cells (arrows) in one of the glomeruli (G) of the cortex of the kidney of the calf infected with *T. annulata* (Hisar) on day 14 post-infection at the nadir of disease, (x500: MAb 1C7 & DAB).

Figure 5.14 Section showing macroschizont-infected cells (arrows) in the alveolar walls of the lung of the calf infected with *T. annulata* (Hisar) on day 14 post-infection at the nadir of disease, (x500: MAb 1C7 & DAB).

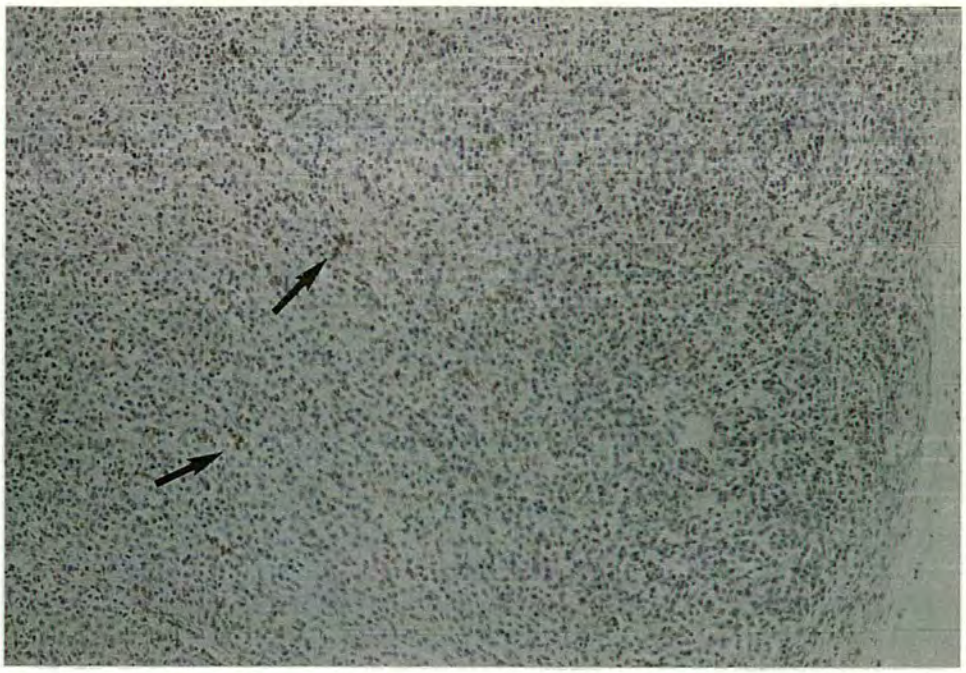

Figure 5.15 Section showing macroschizont-infected cells (arrows) throughout the cortex of the adrenal gland of the calf infected with *T. annulata* (Hisar) on day 14 post-infection at the nadir of disease, (x100: MAb 1C7 & DAB).

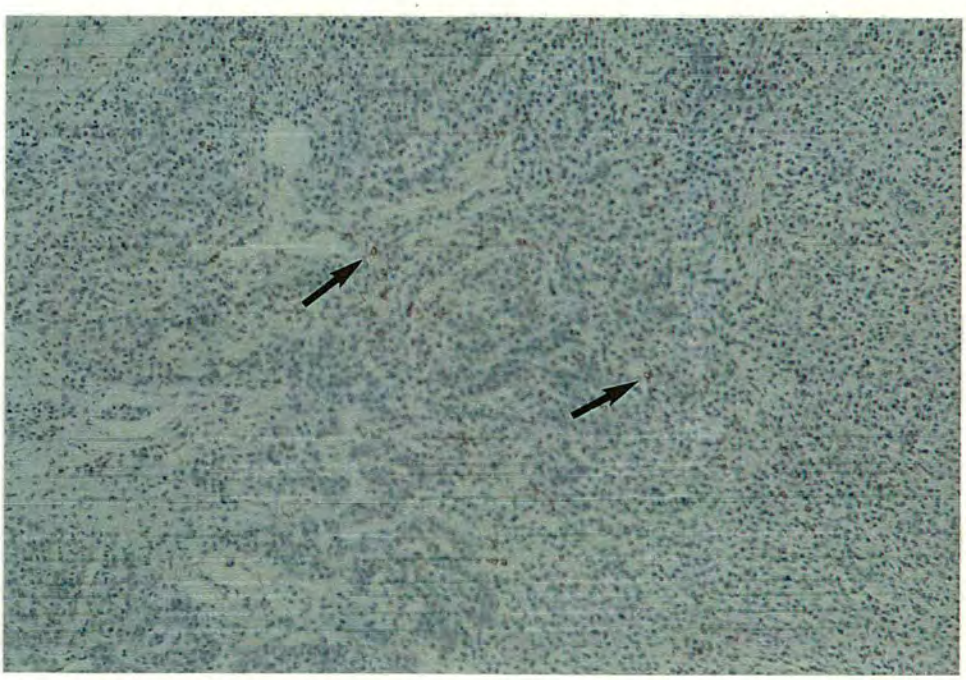

Figure 5.16 Section showing macroschizont-infected cells (arrows) in the medulla of the adrenal gland of the calf infected with *T. annulata* (Hisar) on day 14 post-infection at the nadir of disease, (x100: MAb 1C7 & DAB).

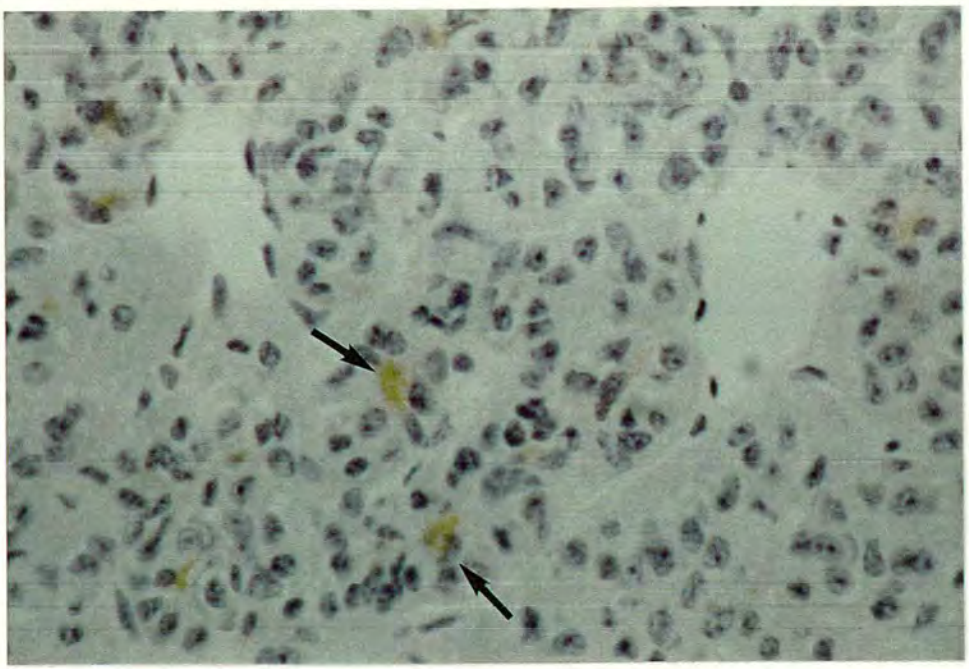

Figure 5.17 Section showing macroschizont-infected cells (arrows) in the pituitary gland of the calf infected with *T. annulata* (Hisar) on day 14 post-infection at the nadir of disease, (x500: MAb 1C7 & DAB).

Figure 5.18 Section showing macroschizont-infected cells (arrows) in the superficial dermis of the skin of the calf infected with *T. annulata* (Doukkalla) on day 24 post-infection during the terminal stages of disease, (x100: MAb 1C7 & DAB).

ORGAN	AREA	SIC	N	H	FEATURES	CHANGES
Prescapular LN (draining)	CX	++	**	*	Follicles	Absent
	PCX	+++	**	**	Cellular depletion of LC	Throughout LN
	MC	+	**	*	Granulomas	Absent
	MS	+++	***	*	MC	Disrupted
					MS	Disrupted
					Other	Extensive disruption of LN architecture
Prescapular LN (contralateral)	CX	+	*	*	Follicles	Absent
	PCX	+	*	*	Cellular depletion of LC	CX & PCX
	MC	+	-	*	Granulomas	Absent
	MS	+	-	-	MC	nc
					MS	Filled with mainly uninfected cells / sinus hyperplasia
					Other	Enlarged medulla
Precrural LN (draining)	CX	+	*	*	Follicles	Absent
	PCX	+	*	*	Cellular depletion of LC	CX & PCX
	MC	+	-	-	Granulomas	Absent
	MS	+	-	-	MC	nc
					MS	Filled with mainly uninfected cells / sinus hyperplasia
					Other	Enlarged medulla
Precrural LN (contralateral)	CX	++	-	*	Follicles	Absent
	PCX	++	-	*	Cellular depletion of LC	CX, PCX & MC
	MC	+	-	*	Granulomas	Absent
	MS	+	-	*	MC	Disrupted
					MS	Filled with mainly uninfected cells / sinus hyperplasia
					Other	Enlarged medulla
Mesenteric LN	CX	+	**	**	Follicles	Normal active follicles
	PCX	+	*	*	Cellular depletion of LC	CX & PCX
	MC	+	-	-	Granulomas	Absent
	MS	+	-	-	MC	nc
					MS	Filled with mainly uninfected cells / sinus hyperplasia
					Other	Enlarged medulla
Spleen	WP	+	-	-	Cellular depletion of LC in WP	Absent
	RP	+	-	-	Congestion of RP	Present
Thymus	CX	+	*	*	Cellular depletion of LC in CX	Present
	MED	+++	**	*		

nd None detected
+ Small numbers of schizont-infected cells
++ Moderate numbers of schizont-infected cells
+++ Large numbers of schizont-infected cells

- No damage
* Mild damage
** Moderate damage
*** Extensive damage

SIC Schizont-infected cells
N Necrosis
H Haemorrhage
LN Lymph node
LC Lymphoid cells
CX Cortex
PCX Paracortex
MED Medulla
MC Medullary cords
MS Medullary sinuses
WP White pulp
RP Red pulp
nc No change

Table 5.1E Distribution of schizont-infected cells detected by MAb 1C7 and Harris's haematoxylin in a calf (861) infected with *T.annulata* (Doukkalla) on day 24 post-infection

ORGAN	AREA	SIC	N	H	FEATURES	CHANGES
Kidney	CX	+	-	-	Disruptive cellular infiltrate in CX	Present
	MED	+	-	-	Oedema of tubules	Present
Liver	PT	+	-	-	Disruptive cellular infiltrate	Present
					Oedema of hepatic cells	Absent
Abomasum	LAP	+	*	*	Disruptive cellular infiltrate	Present
Lung	AW	+	-	-	Thickened AW	Present
	BRO	nd	-	-	Congestion of BRO	Absent
Skin	SDER	+++	**	**	Disruptive cellular infiltrate	Present

nd None detected
+ Small numbers of schizont-infected cells
++ Moderate numbers of schizont-infected cells
+++ Large numbers of schizont-infected cells

SIC Schizont-infected cells
N Necrosis
H Haemorrhage
CX Cortex
MED Medulla

PT Portal tracts
LAP Lamina propria
AW Alveolar wall
BRO Bronchiole
SDER Superficial dermis

- No damage
* Mild damage
** Moderate damage
*** Extensive damage

Table 5.1E Continued

thymus. Macroschizont-infected cells alone were seen in both the white and red pulp of the spleen. In these lymph nodes lymphoid cellular depletion was seen in the paracortex and sinus hyperplasia was detected. Lymphoid follicles in these lymph nodes were absent, with the exception of the mesenteric LN. No granulomas were seen. Lymphoid cellular depletion was also seen in the cortex of the thymus and the red pulp of the spleen was congested. Macroschizont-infected cells occurred throughout most non-lymphoid organs, i.e. the kidney, abomasum and skin (Figures 5.18 & 5.19). Microschizont-infected cells were also seen in these organs. Macroschizont-infected cells alone were recorded in the liver and lung. A disruptive cellular infiltrate was seen in these organs, with the exception of the lung. Oedema occurred in the kidney and the alveolar walls of the lung were thickened. An extensive diffuse necrosis and haemorrhage was also seen in the skin.

5.4.2.5 DISTRIBUTION OF SCHIZONT-INFECTED CELLS IN A CALF (8) DURING THE TERMINAL STAGES OF INFECTION WITH T. PARVA (MUGUGA)

On day 21 post-infection during the terminal stages of disease in calf 8 [Table 5.1F] large numbers of macroschizont- and microschizont-infected cells occurred throughout the draining prescapular LN (Figure 5.20) accompanied by a diffuse lymphocytic hyperplasia. Lymphoid follicles of this lymph node were absent. Macroschizont- and microschizont-infected cells were detected throughout the other lymphoid organs, with the exception of the mesenteric and hepatic LNs and the thymus where macroschizont-infected cells alone were recorded. In these lymph nodes lymphoid cellular depletion was seen in the cortex and paracortex, with the exception of the mesenteric LN. Sinus hyperplasia was detected in the hepatic LN. Lymphoid follicles in these lymph nodes were absent, with the exception of the mesenteric LN. No granulomas were seen. Lymphoid cellular depletion was also seen in the white pulp of the spleen and cortex of the thymus. The red pulp of the spleen was congested. Macroschizont-infected cells alone occurred throughout most non-lymphoid organs, with the exception of the lung where both macroschizont- and microschizont-infected cells were recorded. A disruptive cellular infiltrate and oedema were seen in the kidney. The alveolar walls of the lung were thickened.

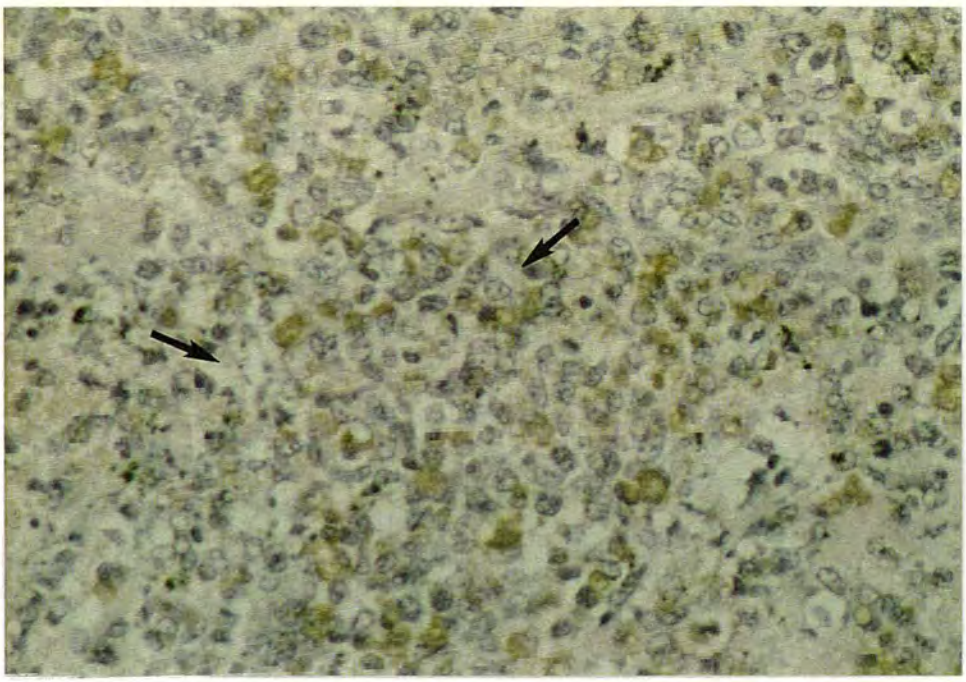

Figure 5.19 Section showing macroschizont-infected cells (brown) in the superficial dermis of the skin of the calf infected with *T. annulata* (Doukkalla) on day 24 post-infection during the terminal stages of disease. Note the foamy macrophages (arrows), (x250: MAb 1C7 & DAB).

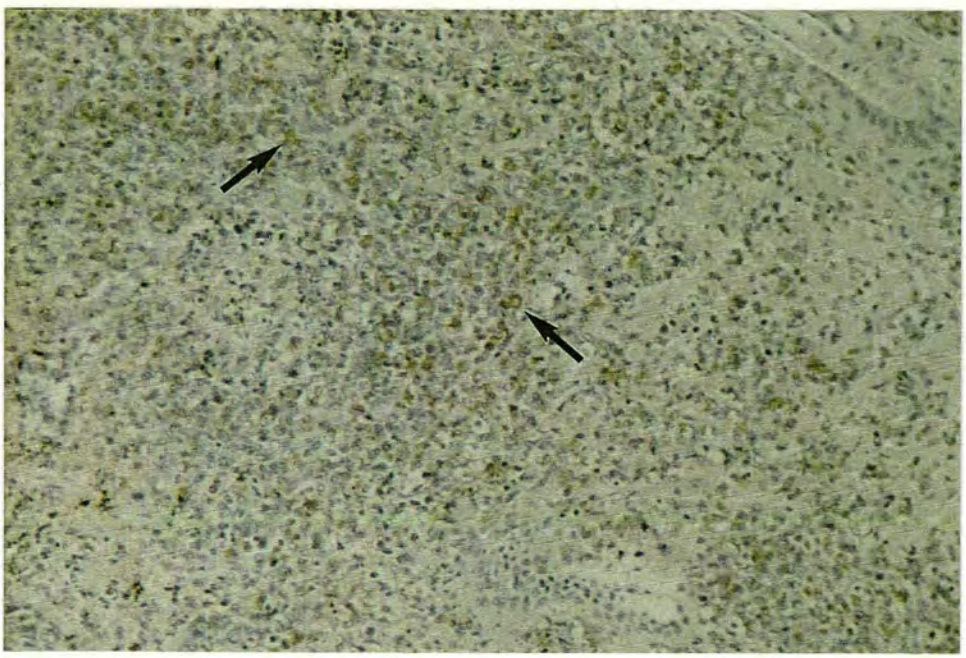

Figure 5.20 Section showing macroschizont-infected cells (arrows) in the medulla of the draining prescapular lymph node of the calf infected with *T. parva* (Muguga) on day 21 post-infection during the terminal stages of disease, (x100: MAb 1C7 & DAB).

ORGAN	AREA	SIC	N	H	FEATURES	CHANGES
Prescapular LN (draining)	CX	+++	-	-	Follicles	Absent
	PCX	+++	*	-	Cellular depletion of LC	Absent
	MC	+++	**	**	Granulomas	Absent
	MS	+++	**	**	MC	nc
					MS	nc
					Other	Lymphoproliferation in PCX
Prescapular LN (contralateral)	CX	+	-	-	Follicles	Absent
	PCX	+	-	-	Cellular depletion of LC	CX & PCX
	MC	+	-	-	Granulomas	Absent
	MS	+	-	-	MC	nc
					MS	nc
					Other	
Precrural LN (draining)	CX	+	-	-	Follicles	Absent
	PCX	+	-	-	Cellular depletion of LC	CX & PCX
	MC	+	-	-	Granulomas	Absent
	MS	+	-	-	MC	nc
					MS	nc
					Other	
Precrural LN (contralateral)	CX	+	-	-	Follicles	Absent
	PCX	+	-	-	Cellular depletion of LC	CX & PCX
	MC	+	-	-	Granulomas	Absent
	MS	+	-	-	MC	nc
					MS	nc
					Other	
Mesenteric LN	CX	+	-	-	Follicles	Normal active follicles
	PCX	+	-	-	Cellular depletion of LC	Absent
	MC	+	-	-	Granulomas	Absent
	MS	+	-	-	MC	nc
					MS	nc
					Other	
Hepatic LN	CX	+	-	-	Follicles	Absent
	PCX	+	-	-	Cellular depletion of LC	CX & PCX
	MC	+	-	-	Granulomas	Absent
	MS	+	-	-	MC	nc
					MS	Filled with mainly uninfected cells / sinus hyperplasia
					Other	
Spleen	WP	+	-	-	Cellular depletion of LC in WP	Present
	RP	+	-	-	Congestion of RP	Present
Thymus	CX	+	-	-	Cellular depletion of LC in CX	Present
	MED	++	**	-		

nd None detected
+ Small numbers of schizont-infected cells
++ Moderate numbers of schizont-infected cells
+++ Large numbers of schizont-infected cells

- No damage
* Mild damage
** Moderate damage
*** Extensive damage

SIC Schizont-infected cells
N Necrosis
H Haemorrhage
LN Lymph node
LC Lymphoid cells
CX Cortex
PCX Paracortex
MED Medulla
MC Medullary cords
MS Medullary sinuses
WP White pulp
RP Red pulp
nc No change

Table 5.1F Distribution of schizont-infected cells detected by MAb 4 and Harris's haematoxylin in a calf (8) infected with *T.parva* (Muguga) on day 21 post-infection

ORGAN	AREA	SIC	N	H	FEATURES	CHANGES
Kidney	CX	+	-	-	Disruptive cellular infiltrate in CX	Present
	MED	+	-	-	Oedema of tubules	Present
Liver	PT	+	-	-	Disruptive cellular infiltrate	Absent: Normal architecture
					Oedema of hepatic cells	Absent
Abomasum	LAP	nd	-	-	Disruptive cellular infiltrate	Absent: Normal architecture
Lung	AW	+	-	-	Thickened AW	Present
	BRO	nd	-	-	Congestion of BRO	Absent
Heart	GEN	+	-	-	Disruptive cellular infiltrate	Absent: Normal architecture
Adrenal gland	ZG	nd	-	-	Disruptive cellular infiltrate	Absent: Normal architecture
	ZF	nd	-	-		
	ZR	nd	-	-		
	MED	nd	-	-		

nd None detected
+ Small numbers of schizont-infected cells
++ Moderate numbers of schizont-infected cells
+++ Large numbers of schizont-infected cells

- No damage
* Mild damage
** Moderate damage
*** Extensive damage

SIC Schizont-infected cells
N Necrosis
H Haemorrhage
GEN General
CX Cortex
MED Medulla

PT Portal tracts
LAP Lamina propria
AW Alveolar wall
BRO Bronchiole
ZG Zona glomerulosa
ZF Zona fasciculata
ZR Zona reticularis

Table 5.1F Continued

5.5 DISCUSSION

Investigation of the distribution of macroschizonts, microschizonts and piroplasms in the organs of calves infected with *T. annulata* or *T. parva* (Muguga) showed parasites were not restricted to the lymph node which drained the site of inoculation, but occurred throughout the organs examined. This finding resembled those of previous studies on cattle infected with parasite stocks of *T. annulata* from Russia (Dschunkowsky & Luhs 1904), India (Gill *et al.* 1977; Baharsefat *et al.* 1977) and North Africa (Sergent *et al.* 1945) and *T. parva* (Steck 1928; Neitz 1957; Barnett 1960).

During the early stages of disease, only macroschizont-infected cells were detected in the medullary areas of the lymphoid organs from the calf infected with *T. annulata* (Hisar). In contrast, during the terminal stages of disease both macroschizont- and microschizont-infected cells were seen throughout the various compartments of the lymphoid organs from calves infected with *T. annulata* or *T. parva* (Muguga), i.e. the cortex, paracortex and medulla of the lymph nodes, both the white and red pulp of the spleen and the cortex and medulla of the thymus. Previous studies on cattle infected with *T. parva* had reported that macroschizont- and microschizont-infected cells were more numerous in T dependent areas than B dependent areas of lymphoid organs (Barnett 1960; reviewed by Irvin & Morrison 1987), but the B dependent areas of the lymphoid organs from the *T. parva* infected calf of this study had been destroyed.

The route of dissemination for *T. annulata* has not been studied. Studies on the initial stages of disease with *T. parva* describe the systemic dissemination of the parasites to various lymphoid and non-lymphoid organs, as taking place either via the lymphatic system or via the blood stream from the site of inoculation (Barnett 1960; DeMartini & Mouton 1973; Emery 1981). The ability of *T. parva* to disseminate throughout the organs of the body has been suggested as a contributing factor to the host's inability to elicit an effective immune response to infection. It was proposed that if the parasites were confined to the draining prescapular lymph node immune responses might be more effective at controlling the subsequent multiplication of the parasitised cells (Emery & Morrison 1980).

Macroschizonts and microschizonts occurred in more lymphoid and non-lymphoid organs as infection progressed in calves infected with *T. annulata* (Hisar). Their dissemination was accompanied by the extensive progressive tissue damage of lymphoid and non-lymphoid organs as recorded in chapter 4. These findings resembled those reported in previous studies (Sergent *et al.* 1945; Neitz 1957). Piroplasms were also detected in more lymphoid and non-lymphoid organs as infection progressed. They were found in all the organs by the terminal stages of disease- both in erythrocytes within blood vessels and within erythrocytes which had haemorrhaged into the organs. Their dissemination was accompanied by an increasingly severe anaemic response (PCV of 32%, 23% & 14% on days 7, 12 & 14 post-infection respectively) as recorded in chapter 3. Interestingly intra-erythrocytic piroplasms have been reported to contribute to anaemia in cattle infected with *T. annulata* (Hooshmand-Rad 1976; Preston *et al.* 1992a). It was concluded that all stages of the parasite (macroschizonts, microschizonts and piroplasms) were involved in pathogenesis with *T. annulata* (Hisar).

In contrast in *T. parva* infections the macroschizont appears to be the main pathogenic stage and the disease progresses more rapidly than that of *T. annulata* (Irvin & Morrison 1987). In this study neither infection with the Doukkalla stock of *T. annulata* nor *T. parva* (Muguga) followed the usual course of disease. In the *T. annulata* (Doukkalla) calf a large number of macroschizont-infected cells and a small number of intra-erythrocytic piroplasms were accompanied by extensive tissue damage and a mild anaemic response (PCV of 23% on day 23 post-infection) as recorded in chapters 3 and 4. In the *T. parva* (Muguga) infected calf a small number of macroschizont-infected cells and a small number of intra-erythrocytic piroplasms were accompanied by less extensive tissue damage and a mild anaemic response (PCV of 25% on day 21 post-infection) as recorded in chapters 3 and 4.

5.6 CONCLUSION

A wide range of lymphoid and non-lymphoid organs in calves infected with *T. annulata* or *T. parva* (Muguga) contained schizont-infected cells (macroschizont and microschizont) which by the terminal stages of disease were not confined to any particular internal compartment. In both *T. annulata* and *T. parva* (Muguga) infected

animals, in most of the lymphoid and non-lymphoid organs schizont-infected cells were accompanied by tissue damage indicating a role for these stages of the parasite in pathogenesis. In order to identify the phenotype of the schizont-infected cells and to assess the cellular responses elicited by the schizont-infected cells more precisely in the *T. annulata* or *T. parva* (Muguga) infected animals, studies were then conducted to identify antibodies for use in conventional immunocytochemical techniques.

CHAPTER SIX

SCREENING OF ANTIBODIES FOR PHENOTYPIC ANALYSIS OF SCHIZONT-INFECTED CELLS

6.1 INTRODUCTION

This chapter describes the screening of a panel of monoclonal antibodies to parasite antigens and bovine leucocyte surface markers. This work was done to identify the reagents required to identify the phenotype of the schizont-infected cells and the cellular responses elicited by schizont-infected cells in *T. annulata* or *T. parva* (Muguga) infected animals.

6.2 EXPERIMENTAL DESIGN

Monoclonal antibodies were assessed on sections of tissues prepared from various lymphoid and non-lymphoid organs obtained during the terminal stages of disease from the calf 41B infected with *T. annulata* (Hisar) which had provided the material used in the pilot studies described above. The following samples of tissues from normal cattle obtained from the abattoir were treated similarly to provide control material from uninfected animals: the prescapular, precrural and mesenteric LNs, spleen, thymus, kidney, liver, abomasum, lung and adrenal gland.

Immunocytochemical techniques were used to assess the antibodies on material fixed and processed in the following different ways: (i) formaldehyde-fixed paraffin tissue sections; (ii) acetone-fixed impression smears (iii) acetone-fixed cryostat tissue sections. The immunocytochemical techniques were modified to optimise the potential use of antibodies in subsequent pathological investigations.

6.3 MATERIALS & METHODS

6.3.1 PREPARATION OF PARAFFIN TISSUE SECTIONS & IMPRESSION SMEARS

Several tissue sections were prepared as described in chapter 4 (4.3.2) and several impression smears as described in chapter 5 (5.3.1) from the following organs: the prescapular, precrural and mesenteric LNs, spleen, thymus, kidney, liver, abomasum, lung and adrenal gland, with the exception of the hepatic LN, brain stem, cerebellum, cerebral hemispheres, heart, skin and pituitary gland.

6.3.2 PREPARATION OF CRYOSTAT TISSUE SECTIONS

Several samples ($0.5cm^3$) were removed from each of the organs listed above (6.3.1) and mounted as soon as possible in OCT mounting medium (Raymond A Lamb), snap frozen in liquid nitrogen and stored at -70^0C. Cryostat sections 6μm in thickness were cut on a Cambridge rotary microtome which had been incorporated into a Brights cryostat. Sections were mounted onto poly-l-lysine (Sigma) coated slides [Appendix V] and air-dried at room temperature for 2 hours prior to fixation in ice cold acetone (BDH) for 10 minutes. Sections were stored at -70^0C.

6.3.3 ABC/HRP & ABC/ALKALINE PHOSPHATASE (AP) IMMUNOCYTOCHEMICAL TECHNIQUES

6.3.3.1 ASSESSMENT ON PARAFFIN TISSUE SECTIONS USING TRYPSIN TREATMENT TO EXPOSE SURFACE ANTIGENS

Antibodies [Table 6.1] which recognise parasite or bovine leucocyte surface markers were assessed on several formaldehyde-fixed paraffin tissue sections using the ABC/HRP [Appendix VIII & IX] & ABC/AP [Appendix X & XI] immunocytochemical techniques.

Negative controls for non-specific staining with test antibodies comprised tissue sections treated with normal serum from the same species as the secondary antibody had been raised in instead of the test antibody. Positive controls for the test antibody, i.e. tissue sections obtained from samples of organs previously shown to be positive for the test antibody, were used to ensure the solutions being used were active.

Information on the primary antibodies used, their presentation and optimal dilution, and the reagents required for their use in ABC/HRP & ABC/AP immunocytochemical techniques, i.e. blocking serum and secondary antibodies are given in Table 6.2.

6.3.3.2 ASSESSMENT ON PARAFFIN TISSUE SECTIONS USING MICROWAVE ANTIGEN RETRIEVAL TECHNIQUES TO EXPOSE SURFACE ANTIGENS

The ABC/HRP & ABC/AP immunocytochemical techniques as described above 6.3.3.1 were used on several formaldehyde-fixed paraffin tissue sections, except the use of trypsin treatment to expose surface antigens was now replaced by microwave

Antibody	Source	Antibody specificity	Reference
EU1	EU	Anti-macroschizont	-
EU106	EU	Anti-macroschizont	Sutherland, Shiels, Jackson, Brown, Brown, Tait & Preston (1993)
1E11	WUMP	Anti-macroschizont	Shiels *et al.* (1986)
VPM30	WUMP	Anti-ovine B cells	-
CD45RA	DAKO	Anti-human B cells	Norton & Isaacson (1989)
anti-IgM	SAPU	Anti-human B cells	-
CD2	SAPU	Anti-human T cells & NK cells	-
CC42	ECACC	Anti-bovine T cells & NK cells	Howard & Naessens (1993)
CD3	DAKO	Human T cells	Ramos-Vara *et al*. (1994)
CD3	SAPU	Anti-human T cells	-
MM1A	WSU	Anti-bovine T cells	Howard & Naessens (1993)
IL-A21	ILRAD	Anti-bovine class II MHC restricted T cells	Morrison (personal communication)
VPM36	WUMP	Anti-ovine class II MHC restricted T cells	-
CC8	ECACC	Anti-bovine class II MHC restricted T cells	-
cl 197	ECACC	Anti-bovine gamma delta T cells	-
J5	ECACC	Anti-bovine T cell activation factor	Naessens, Newson, Bensaid, Teale, Magondu & Black (1985)
SBU-T8	WUMP	Anti-ovine class I MHC restricted T cells	-
VPM19	WUMP	Anti-ovine class I MHC restricted T cells	-
IL-A15	ILRAD	Anti-bovine monocytes, granulocytes & NK cells	Splitter & Morrison (1991)
IL-A24	ILRAD	Anti-bovine monocytes & granulocytes	Howard & Naessens (1993)
VPM65	WUMP	Anti-ovine monocytes	-
CD68	DAKO	Anti-human macrophages	Kelly, Bliss, Morton, Burns & McGee (1988)
cl 218	ECACC	Anti-human adhesion molecule	-
Du 1-29	ECACC	Anti-human adhesion molecule	-

SAPU Scottish Antibody Production Unit
ILRAD International Laboratory for Research in Animal Diseases
ECACC European Cell and American Culture Collection
CC Institute for Animal Health, Compton

EU Edinburgh University
WSU Washington State University, USA
WUMP Welcome Unit of Molecular Parasitology, University of Glasgow
- No references available

Table 6.1 Assessment of anti-parasite and leucocyte antibodies on bovine tissue sections using immunocytochemical techniques

PRIMARY ANTIBODY	PRESENTATION	DILUTIONS	BLOCKING SERUM	SECONDARY ANTIBODY
EU1	Monoclonal (supernatant)	Neat	Rabbit	Rabbit anti-mouse-biot
EU106	Monoclonal (supernatant)	Neat	Rabbit	Rabbit anti-mouse-biot
1E11	Monoclonal (supernatant)	Neat	Rabbit	Rabbit anti-mouse-biot
VPM30	Monoclonal (supernatant)	Neat	Rabbit	Rabbit anti-mouse-biot
CD45RA	Monoclonal (supernatant)	1:25;1:50	Rabbit	Rabbit anti-mouse-biot
anti-IgM	Monoclonal (supernatant)	1:10;1:50;1:100	Rabbit	Rabbit anti-mouse-biot
CD2	Monoclonal (purified)	1:10;1:50;1:100	Rabbit	Rabbit anti-mouse-biot
CC42	Monoclonal (supernatant)	Neat	Rabbit	Rabbit anti-mouse-biot
CD3[1]	Polyclonal (affinity-isolated)	1:100	Goat	Goat anti-rabbit-biot
CD3[2]	Monoclonal (purified)	1:10;1:50;1:100	Rabbit	Rabbit anti-mouse-biot
MM1A	Monoclonal (supernatant)	Neat	Rabbit	Rabbit anti-mouse-biot
IL-A21	Monoclonal (supernatant)	Neat	Rabbit	Rabbit anti-mouse-biot
VPM36	Monoclonal (supernatant)	Neat	Rabbit	Rabbit anti-mouse-biot
CC8	Monoclonal (supernatant)	Neat	Rabbit	Rabbit anti-mouse-biot
cl 197	Monoclonal (supernatant)	Neat	Rabbit	Rabbit anti-mouse-biot
J5	Monoclonal (supernatant)	Neat	Rabbit	Rabbit anti-mouse-biot
SBU-T8	Monoclonal (supernatant)	Neat	Rabbit	Rabbit anti-mouse-biot
VPM19	Monoclonal (supernatant)	Neat	Rabbit	Rabbit anti-mouse-biot
IL-A15	Monoclonal (supernatant)	Neat	Rabbit	Rabbit anti-mouse-biot
IL-A24	Monoclonal (supernatant)	Neat	Rabbit	Rabbit anti-mouse-biot
VPM65	Monoclonal (supernatant)	Neat	Rabbit	Rabbit anti-mouse-biot
CD68	Monoclonal (supernatant)	Neat	Rabbit	Rabbit anti-mouse-biot
cl 218	Monoclonal (supernatant)	Neat	Rabbit	Rabbit anti-mouse-biot
Du 1-29	Monoclonal (supernatant)	Neat	Rabbit	Rabbit anti-mouse-biot

biot Biotinylated
1 CD3 (DAKO)
2 CD3 (SAPU)

Table 6.2 Primary antibodies and the reagents required for their use in immunocytochemical techniques

antigen retrieval techniques (Shi, Key & Kalra 1991) [Appendix XII]. In brief, dewaxed tissue sections were placed in citrate buffer and heated in a conventional microwave oven on high power to expose surface antigens.

6.3.3.3 ASSESSMENT ON CRYOSTAT TISSUE SECTIONS

The ABC/HRP & ABC/AP immunocytochemical techniques as described in 6.3.3.1 were used on several acetone-fixed cryostat tissue sections, except the dewaxation and rehydration of tissue sections were not required. Pretreatment to expose surface antigens was excluded since formaldehyde had not been used as a fixative. Acetone-fixed cryostat tissue sections are more fragile than formaldehyde-fixed paraffin tissue sections. Glucose oxidase [Appendix XIII] was therefore used to inactivate endogenous peroxidase (Andrew & Jasani 1987) (prior to step 19 of the ABC/HRP immunocytochemical techniques) instead of hydrogen peroxide, as this substance can have a deleterious effect upon cell surface markers and membranes (personal communication Mr. John Lauder).

6.3.3.4 ASSESSMENT ON IMPRESSION SMEARS

The ABC/HRP & ABC/AP immunocytochemical techniques as described in 6.3.3.1 were used on several acetone-fixed impression smears, except the dewaxation and rehydration of impression smears were not required. Pretreatment to expose surface antigens was excluded since acetone, instead of formaldehyde, had been used as a fixative.

6.4 RESULTS

6.4.1 ASSESSMENT OF ANTIBODIES USING ABC/HRP & ABC/AP IMMUNOCYTOCHEMICAL TECHNIQUES

6.4.1.1 ANTIBODIES IDENTIFIED FOR USE ON PARAFFIN TISSUE SECTIONS

Assessment of antibodies [Table 6.1] which recognise parasite and bovine leucocyte surface markers using the ABC/HRP [Appendix VIII & IX] and ABC/AP [Appendix X & XI] immunocytochemical techniques identified only two antibodies which were positive on formaldehyde-fixed paraffin tissue sections. These were the MAb IL-A15 (Splitter & Morrison 1991) which recognises CD11b, the C3bi complement receptor, on monocytes, granulocytes and NK cells (Figure 6.1) and the polyclonal antibody A452 (DAKO) (Ramos-Vara, Miller, Lopez, Prats & Brevik 1994) which

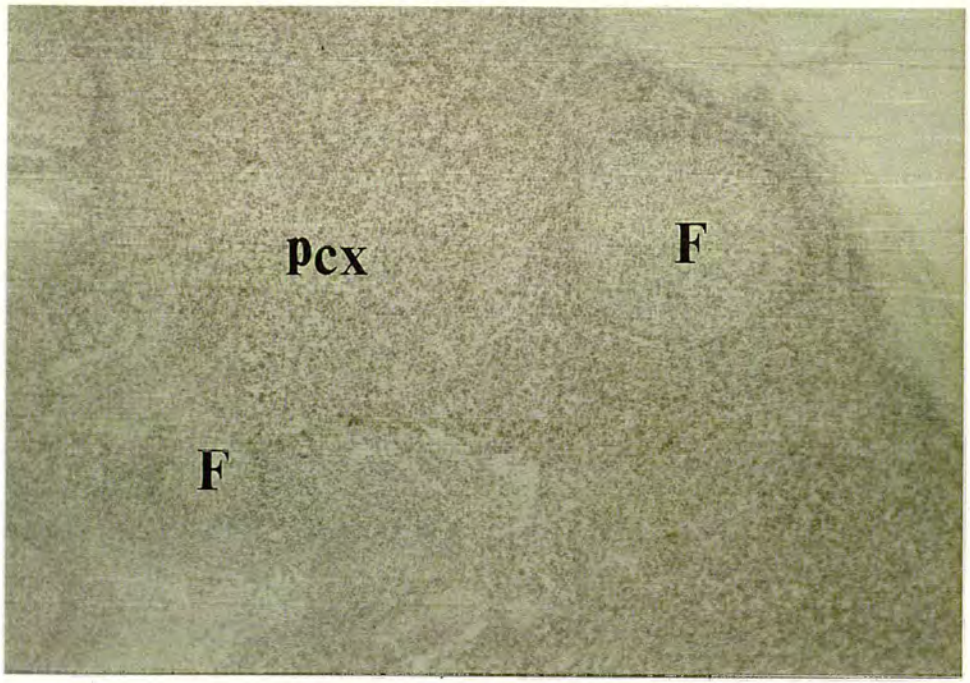

Figure 6.1 Section showing CD11b^{+} cells (pink) in the lymphoid follicles (F) and paracortex (PCX) of the prescapular lymph node of the normal, uninfected animal, (x40: MAb IL-A15 & Vector Red).

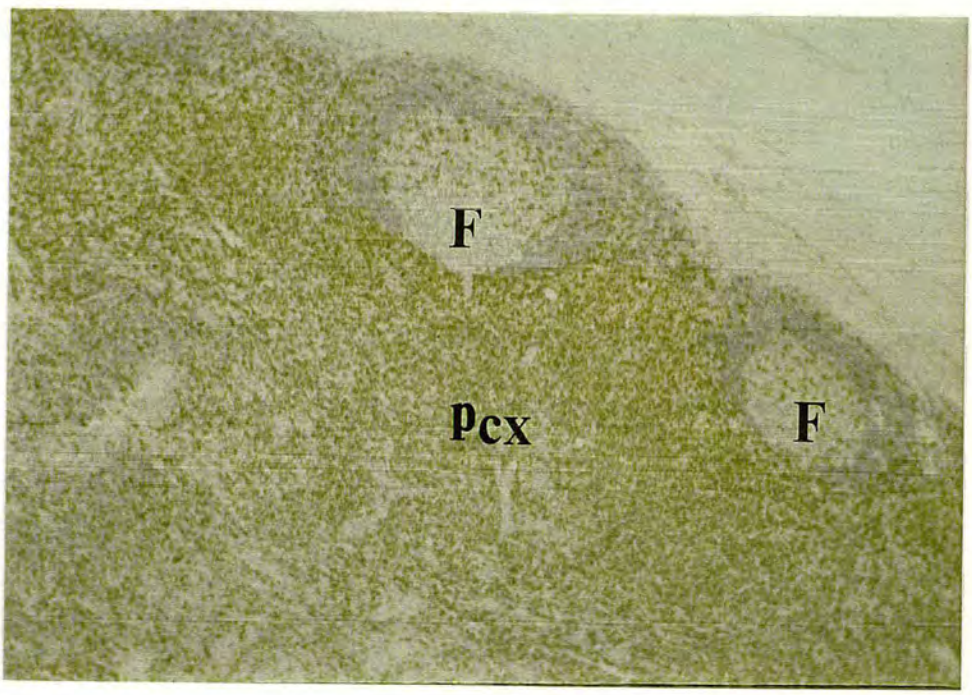

Figure 6.2 Section showing CD3^{+} cells (brown) in the lymphoid follicles (F) and paracortex (PCX) of the prescapular lymph node of the normal, uninfected animal, (x40: polyclonal antibody A452 & DAB).

recognises CD3 on T cells (Figure 6.2). The remaining antibodies gave negative results. Alteration of the incubation time for trypsin treatment did not expose additional surface markers for identification with antibodies.

6.4.1.2 ASSESSMENT ON PARAFFIN TISSUE SECTIONS USING MICROWAVE ANTIGEN RETRIEVAL TECHNIQUES

The use of microwave antigen retrieval techniques to expose surface markers which had previously not been exposed with trypsin treatment, did not identify any additional positive antibodies which could be used on formaldehyde-fixed paraffin tissue sections.

6.4.1.3 ASSESSMENT ON CRYOSTAT TISSUE SECTIONS

Additional positive antibodies were not identified using cryopreserved tissues. Instead, the morphology of the tissues was severely disrupted and high levels of background staining were seen (Figure 6.3). These factors made it impossible to use acetone-fixed cryostat tissue sections for subsequent pathological investigations on bovine tissues.

6.4.1.4 ASSESSMENT ON IMPRESSION SMEARS

No additional positive antibodies were identified using acetone-fixed impression smears. Instead, high levels of background staining were observed which made it impossible to use acetone-fixed impression smears to investigate schizont-infected cell phenotype.

6.4.1.5 MODIFICATION OF IMMUNOCYTOCHEMICAL TECHNIQUES

The following modifications of the immunocytochemical techniques were used in attempts to reduce the high levels of background staining: changing the species of secondary antibody used to eliminate any cross-reactivity between species; introducing additional blocking steps to eliminate any excess secondary antibody or avidin/biotin receptors; introducing detergent washes to remove any 'sticky' non-specific compounds. Unfortunately, none of these modifications to the ABC/HRP immunocytochemical techniques proved successful.

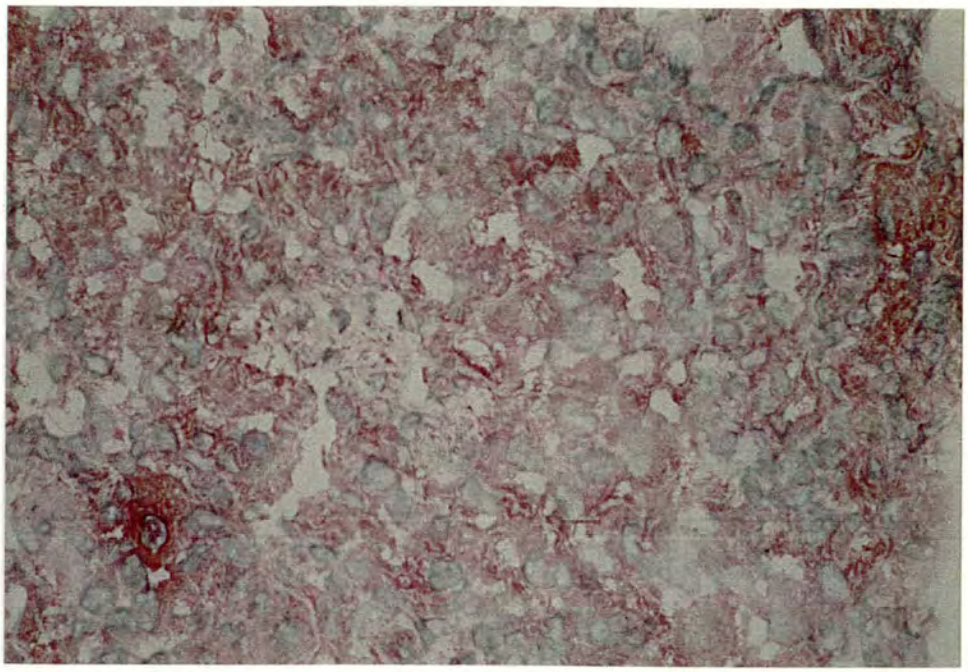

Figure 6.3 Cryostat section showing the severe disruption of tissue morphology and the high levels of background staining (pink) in the prescapular lymph node of the normal, uninfected animal, (x500: MAb IL-A15 & Vector Red).

6.5 DISCUSSION

Formaldehyde-fixed paraffin tissue sections provided the high quality of tissue morphology required for analysis by antibodies recognising parasite or bovine leucocyte antigens, but unfortunately relatively few antibodies worked on the formaldehyde-fixed tissues. Although the identification of a large range of antibodies for use with immunocytochemical techniques was not possible, two interesting antibodies were identified for subsequent use, i.e. MAb IL-A15 and the polyclonal antibody A452, which identify cells of the myeloid and T cell lineages respectively.

The manner in which tissues were processed appeared to act as a serious constraint to using antibodies to parasite and bovine leucocyte antigens on tissues from bovine lymphoid and non-lymphoid organs. Formaldehyde fixation of tissues either masked antigens, which could not be exposed by enzyme digestion or heat pretreatment, or completely destroyed them. Cryopreservation of tissues, for subsequent fixation in the less harmful fixative acetone, caused additional problems of extensive disruption of cellular morphology possibly due to freezing and thawing. Acetone-fixed impression smears could not be assessed because of the disruptive levels of background staining possibly due to the presence of large amounts of tissue debris. Any attempts to solve these problems were unsuccessful. Ultimately, it was difficult to standardise the conditions in which the immunocytochemical techniques were carried out. The temperature and humidity of the working environment may have altered the chemical interactions involved in the immunocytochemical techniques and may ultimately have affected the viability of the test antibodies. Since so many steps were carried out during the immunocytochemical techniques it was difficult to isolate problems within the system.

As described in the following chapters the two positive antibodies, MAb IL-A15 and polyclonal antibody A452, were then used to investigate the phenotype of the schizont-infected cells and the cellular responses elicited by schizont-infected cells in *T. annulata* or *T. parva* (Muguga) infected animals.

CHAPTER SEVEN

PHENOTYPIC ANALYSIS OF SCHIZONT-INFECTED CELLS

7.1 INTRODUCTION

The identity of the cells inhabited by macroschizonts and microschizonts in infected cattle was still unclear at the time this project began. With only one exception (Howard *et al.* 1993) attempts using flow cytometry and antibodies to bovine leucocyte antigens to identity the cells inhabited by *T. annulata* (Spooner *et al.* 1988; Spooner *et al.* 1989; Glass *et al.* 1989) and *T. parva* (Baldwin *et al.* 1988; Morrison *et al.* 1989) had concentrated on phenotyping *in vitro* derived macroschizont-infected, transformed cell lines. This chapter describes the use of MAb IL-A15 and polyclonal antibody A452 together with the two MAbs (1C7 & 4) which detected schizont antigens, of *T. annulata* and *T. parva* (Muguga) respectively, to characterise the phenotype of macroschizont- and microschizont-infected cells in tissues from lymphoid and non-lymphoid organs of *T. annulata* or *T. parva* (Muguga) infected calves.

7.2 EXPERIMENTAL DESIGN

The phenotype of schizont-infected cells was examined with antibodies which identified parasite (MAb 1C7 & MAb 4) and bovine leucocyte antigens (MAb IL-A15 & polyclonal antibody A452) using ABC immunocytochemical techniques and Harris's haematoxylin counterstain on paraffin tissue sections. Samples of tissues from normal cattle, obtained from the abattoir, were treated similarly to provide control uninfected material.

7.3 MATERIALS & METHODS

7.3.1 PARAFFIN TISSUE SECTIONS

Several tissue sections were prepared as described in chapter 4 from the following lymphoid and non-lymphoid organs of calves 41B, 55C, 19, 20, 861 and 8: the draining and contralateral prescapular LNs, draining and contralateral precrural LNs, mesenteric and hepatic LNs, spleen, thymus, kidney, liver, abomasum, lung, brain stem, cerebellum, cerebral hemispheres, heart, skin, adrenal and pituitary glands.

7.3.2 ABC IMMUNOCYTOCHEMICAL TECHNIQUES USED WITH ANTIBODIES 1C7, 4, IL-A15 & A452

The following antibodies were used: (i) MAb 1C7 (Shiels *et al.* 1986) which identifies *T. annulata* macroschizonts; (ii) MAb 4 (donated by ILRI) which recognises *T. parva* (Muguga) macroschizonts and microschizonts; (iii) MAb IL-A15 (Splitter & Morrison 1991) which identifies CD11b, the C3bi complement receptor, found most widely on macrophages, monocytes, granulocytes, dendritic cells, B cells and NK cells (Howard & Naessens 1993); (iv) polyclonal antibody A452 (DAKO) (Ramos-Vara *et al.* 1994) which identifies T (CD3) cells.

Double staining [Appendix XIV] was carried out using the ABC/HRP system to detect MAb 1C7 and the ABC/AP system to detect MAb IL-A15 on the same tissue section. Double staining immunocytochemical techniques were not possible with combinations of MAb 1C7 and polyclonal antibody A452, MAbs 4 and IL-A15 or MAb 4 and polyclonal antibody A452 due to the obscuring levels of background staining which prevented interpretation of the results. This problem was overcome using single staining immunocytochemical techniques with polyclonal antibody A452 [Appendix VIII & IX] or MAb IL-A15 [Appendix X & XI] and Harris's haematoxylin counterstain, instead of MAbs 1C7 and 4, for the identification of schizont-infected cells. In brief, single staining with MAb 1C7, MAb 4 and polyclonal antibody A452 involved incubation in ABC/HRP (DAKO) prior to visualisation by DAB (DAKO). Endogenous peroxidase activity was inactivated with hydrogen peroxide [Appendix IX]. Single staining with MAb IL-A15 involved incubation in ABC/AP (DAKO) prior to visualisation by Vector Red (Vector) [Appendix X & XI]. Endogenous phosphatase activity was inactivated with levamisole solution (Vector) [Appendix XI].

In all these methods, dewaxed tissue sections were treated in trypsin prior to incubation with primary antibody. The following list gives the optimal conditions for the reagents used for phenotyping schizont-infected cells: MAb 1C7 (diluted 1:2 in rabbit serum); MAb 4 (diluted 1:50 in rabbit serum); MAb IL-A15 (diluted 1:2 in rabbit serum); polyclonal antibody A452 (diluted 1:200 in goat serum), prior to incubation in secondary antibody: biotinylated rabbit anti-mouse (DAKO) (diluted

1:400 in rabbit serum) for use with MAb 1C7, MAb 4 and MAb IL-A15; biotinylated goat anti-rabbit (DAKO) (diluted 1:500 in goat serum) for use with polyclonal antibody A452. Non-specific binding of secondary antibody was prevented with rabbit serum (SAPU) for use with MAb 1C7, MAb 4 and MAb IL-A15 and goat serum (SAPU) for use with polyclonal antibody A452. Controls for non-specific binding of the primary antibodies comprised tissue sections treated as above except normal rabbit serum, for use with MAb 1C7, MAb 4 and MAb IL-A15, and normal goat serum, for use with polyclonal antibody A452, were substituted for the primary antibodies.

7.3.3 ASSESSMENT OF IMMUNOCYTOCHEMICALLY LABELLED PARAFFIN TISSUE SECTIONS

Several tissue sections were examined at 1000 x magnification using a Nikon S. Ke II microscope and the numbers of stained schizont-infected cells ($CD11b^+$ or $CD3^+$) were recorded. In slides stained with MAbs IL-A15 and 1C7, macroschizont-infected cells ($1C7^+$) and microschizont-infected cells ($1C7^-$) were counted. In slides stained with MAb IL-A15 or polyclonal antibody A452, all schizonts (macroschizonts and microschizonts), detected by Harris's haematoxylin, were counted. The percentages of $CD11b^+$ and $CD3^+$ schizont-infected cells in the organs were subsequently calculated according to the following formula: Number of stained ($CD11b^+$ or $CD3^+$) parasitised cells / Total number of parasitised cells x 100.

7.4 RESULTS

7.4.1 PHENOTYPIC ANALYSIS OF MACROSCHIZONT- & MICROSCHIZONT-INFECTED CELLS

The sections were examined to see if the macroschizont-infected cells ($1C7^+$) and microschizont-infected cells ($1C7^-$) (Figure 7.1) were stained by either MAb IL-A15 ($CD11b^+$) or polyclonal antibody A452 ($CD3^+$).

The surfaces of cells infected with *T. annulata* at all stages of differentiation-from macroschizont to microschizont-were stained with MAb IL-A15, but not with polyclonal antibody A452. Such stained parasitised cells occurred in the lymphoid organs, i.e. the prescapular LNs, precrural LNs, mesenteric and hepatic LNs, spleen, thymus, as well as in the reticulo-endothelial tissues of the kidney, liver, abomasum,

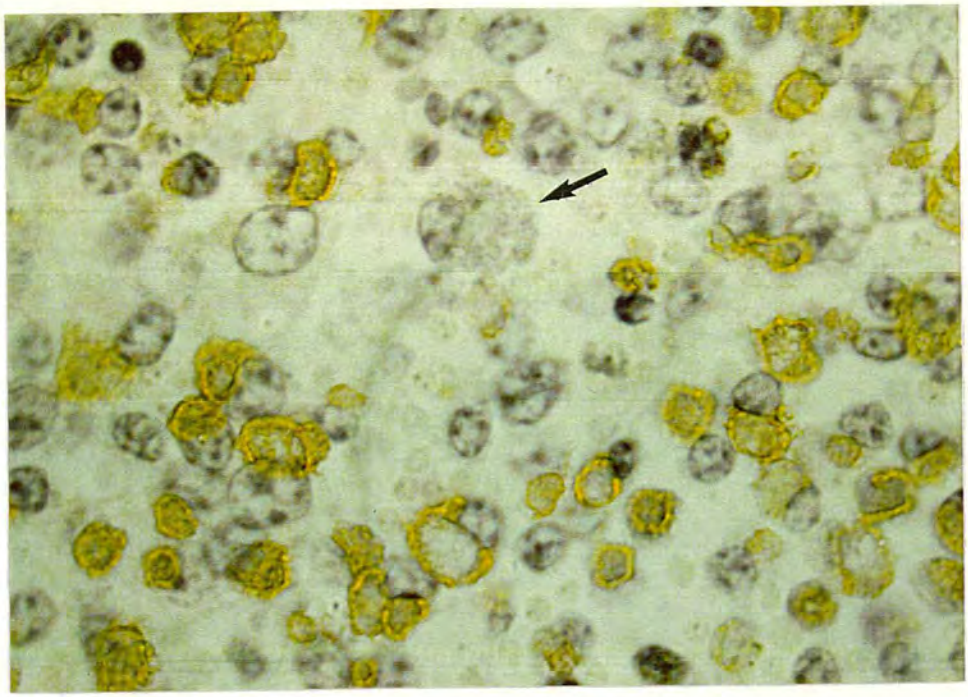

Figure 7.1 Section showing $1C7^+$ macroschizont-infected cells (brown) and a $1C7^-$ microschizont-infected cell (arrow) in the paracortex of the draining prescapular lymph node of the calf infected with *T. annulata* (Hisar) on day 12 post-infection during the terminal stages of disease, (x1000: MAb 1C7 & DAB).

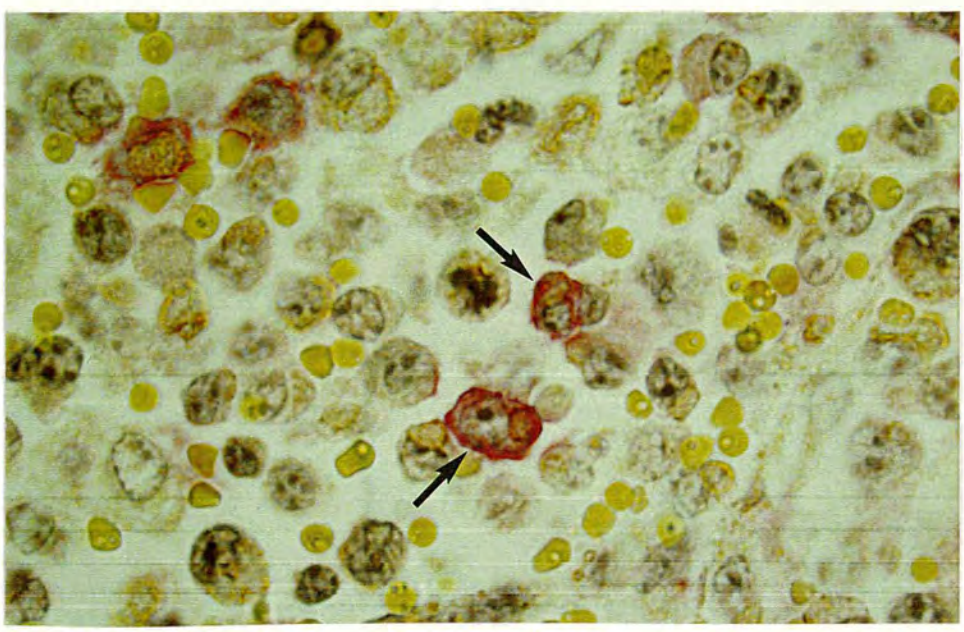

Figure 7.2 Section showing $1C7^+/CD11b^+$ macroschizont-infected cells (arrows) in the paracortex of the draining prescapular lymph node of the calf infected with *T. annulata* (Hisar) on day 12 post-infection during the terminal stages of disease. Note the $CD11b^+$ macroschizonts within the cytoplasm of the host cells (arrows), (x1000: MAb 1C7 & DAB; MAb IL-A15 & Vector Red).

lung, adrenal and pituitary glands. These findings are illustrated by the results obtained when sections prepared from the prescapular lymph node draining the site of inoculation of calf 41B on day 12 after infection were double stained with MAb IL-A15 and MAb 1C7. Both the paracortical and medullary regions of this lymph node contained macroschizont-infected cells ($1C7^+$ schizonts) and microschizont-infected cells ($1C7^-$ schizonts). Both $1C7^+$ (macro) schizont-infected, $CD11b^+$ cells (Figure 7.2) and $1C7^-$ (micro) schizont-infected, $CD11b^+$ cells (Figure 7.3) were found in the paracortex. Not all the parasitised cells seen in this area were stained by MAb IL-A15: $1C7^+$ (macro) schizont-infected, $CD11b^-$ cells and $1C7^-$ (micro) schizont-infected, $CD11b^-$ cells (Figure 7.4) occurred as well. Some $1C7^+$ (macro) schizont-infected, $CD11b^+$ cells were seen to be undergoing mitosis (Figure 7.5). Parasitised cells with similar staining patterns for MAbs IL-A15 and 1C7 were also found in the medulla: e.g. $1C7^+$ (macro) schizont-infected, $CD11b^+$ cells; $1C7^+$ (macro) schizont-infected cells, $CD11b^-$ cells; $1C7^-$ (micro) schizont-infected, $CD11b^-$ cells (Figure 7.6). In a number of instances, MAb IL-A15 coated the outer rim of schizonts lying within the cytoplasm of the host cells as well as the walls of the parasitised host cells (Figures 7.2 & 7.6). Uninfected macrophage-like $CD11b^+$ cells were also noted (Figure 7.6).

In contrast the surfaces of cells infected with *T. parva* (Muguga) at all stages of differentiation-from macroschizont to microschizont-were stained with either MAb IL-A15 or polyclonal antibody A452. Such stained parasitised cells occurred in the lymphoid organs, i.e. the prescapular LNs, precrural LNs and hepatic LN, thymus, as well as in the reticulo-endothelial tissues of the liver and lung. These findings are illustrated by the results obtained when sections prepared from the prescapular lymph node draining the site of inoculation of calf 8 on day 21 after infection were single stained with either MAb IL-A15 or polyclonal antibody A452 and counterstained with Harris's haematoxylin. Both the paracortical and medullary regions of this lymph node contained macroschizont-infected cells and microschizont-infected cells. Both macroschizont-infected, $CD11b^+$ cells, microschizont-infected, $CD11b^+$ cells (Figure 7.7), macroschizont-infected, $CD3^+$ cells and microschizont-infected, $CD3^+$ cells (Figure 7.8) were found in the paracortex and medulla. Not all the parasitised cells seen in these areas were stained

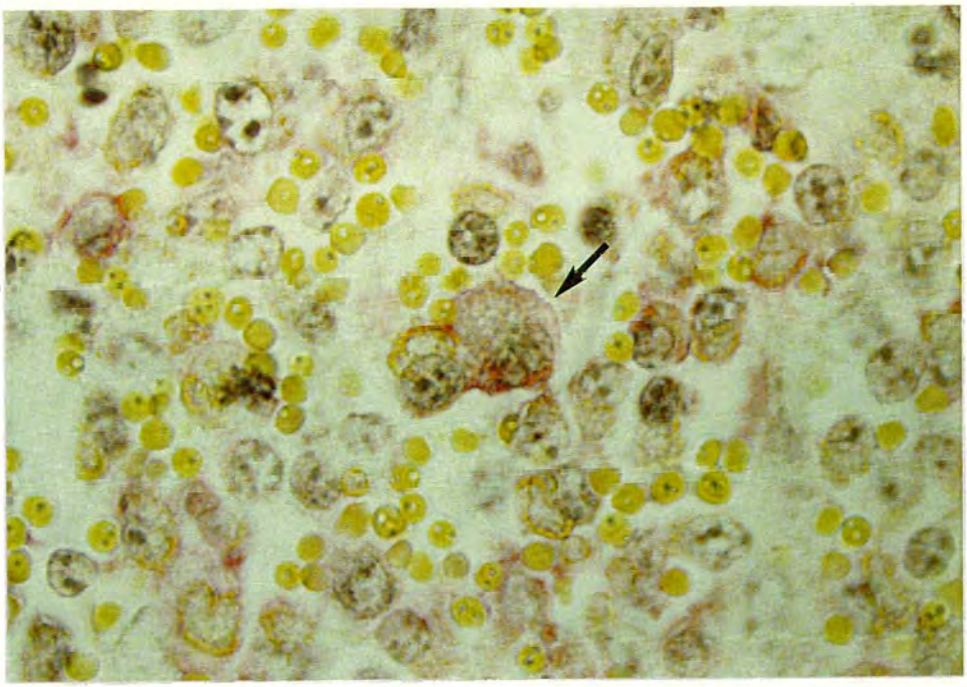

Figure 7.3 Section showing a $1C7^{-}/CD11b^{+}$ microschizont-infected cell (arrow) in the paracortex of the draining prescapular lymph node of the calf infected with *T. annulata* (Hisar) on day 12 post-infection during the terminal stages of disease, (x1000: MAb 1C7 & DAB; MAb IL-A15 & Vector Red).

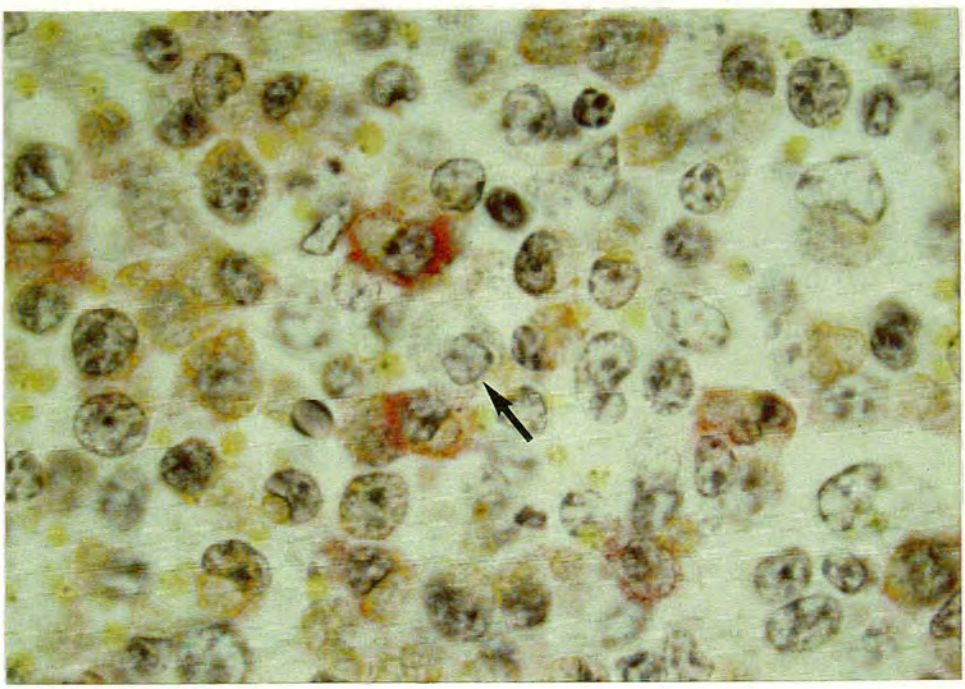

Figure 7.4 Section showing a $1C7^{-}/CD11b^{-}$ microschizont-infected cell (arrow) in the paracortex of the draining prescapular lymph node of the calf infected with *T. annulata* (Hisar) on day 12 post-infection during the terminal stages of disease, (x1000: MAb 1C7 & DAB; MAb IL-A15 & Vector Red).

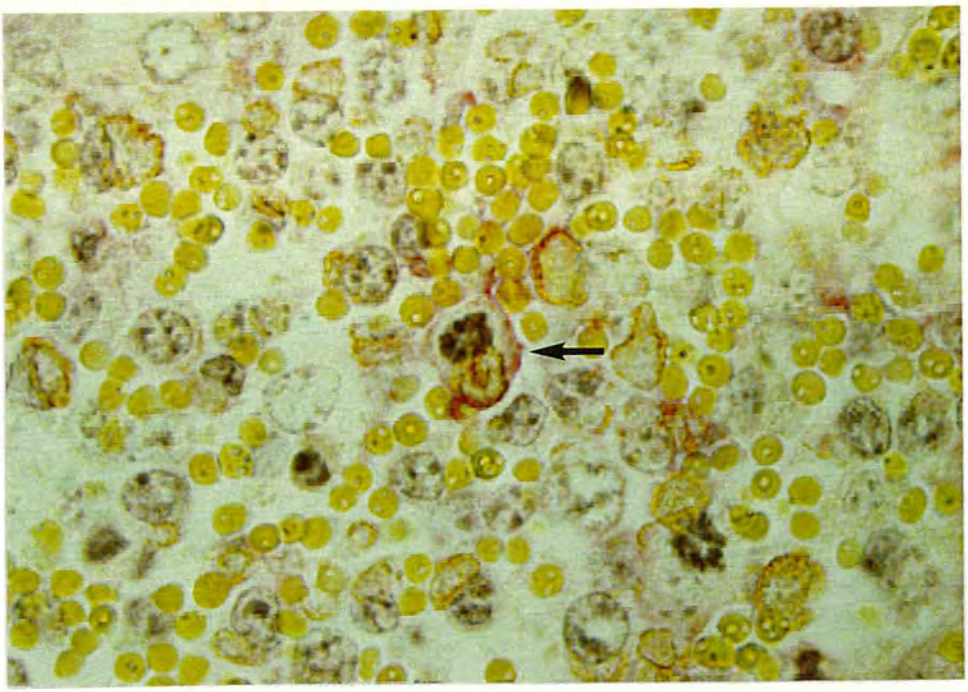

Figure 7.5 Section showing a $1C7^{+}/CD11b^{+}$ macroschizont-infected cell (arrow) undergoing mitosis in the paracortex of the draining prescapular lymph node of the calf infected with *T. annulata* (Hisar) on day 12 post-infection during the terminal stages of disease, (x1000: MAb 1C7 & DAB; MAb IL-A15 & Vector Red).

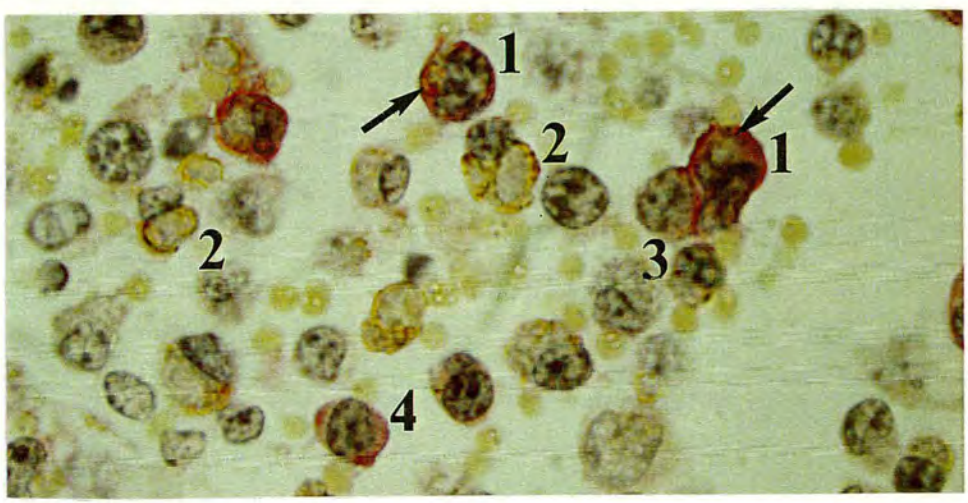

Figure 7.6 Section showing the following: $1C7^{+}/CD11b^{+}$ macroschizont-infected cells (1); $1C7^{+}/CD11b^{-}$ macroschizont-infected cells (2); a $1C7^{-}/CD11b^{-}$ microschizont-infected cell (3); an uninfected macrophage-like $CD11b^{+}$ cell (4) in the paracortex of the draining prescapular lymph node of the calf infected with *T. annulata* (Hisar) on day 12 post-infection during the terminal stages of disease. Note the $CD11b^{+}$ macroschizonts within the cytoplasm of the host cells (arrows), (x1000: MAb 1C7 & DAB; MAb IL-A15 & Vector Red).

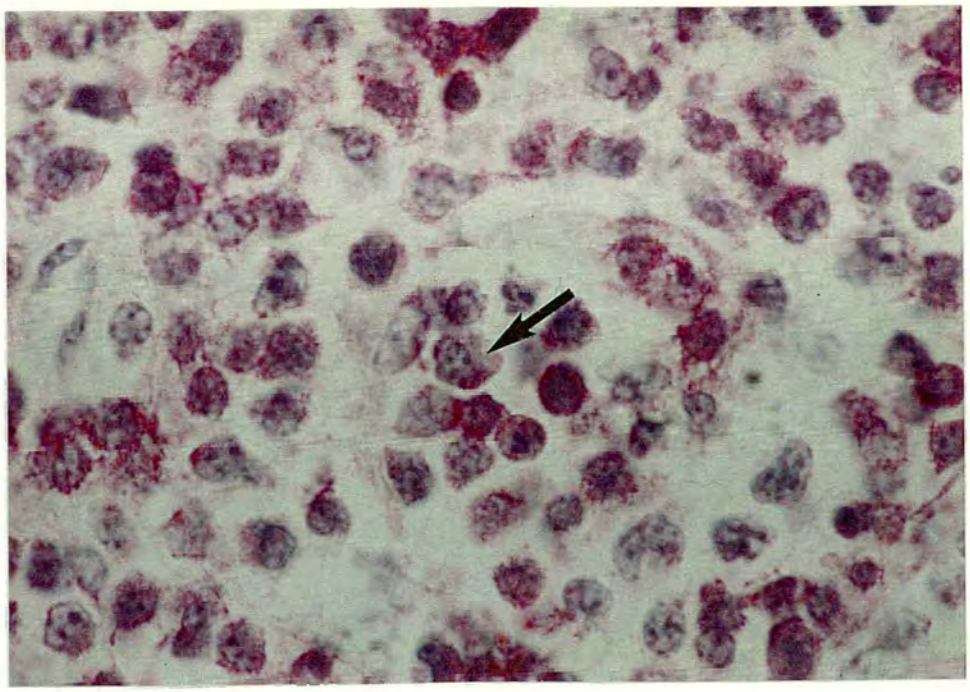

Figure 7.7 Section showing a $CD11b^+$ microschizont-infected cell (arrow) in the medulla of the draining prescapular lymph node of the calf infected with *T. parva* (Muguga) on day 21 post-infection during the terminal stages of disease, (x1000: MAb IL-A15 & Vector Red).

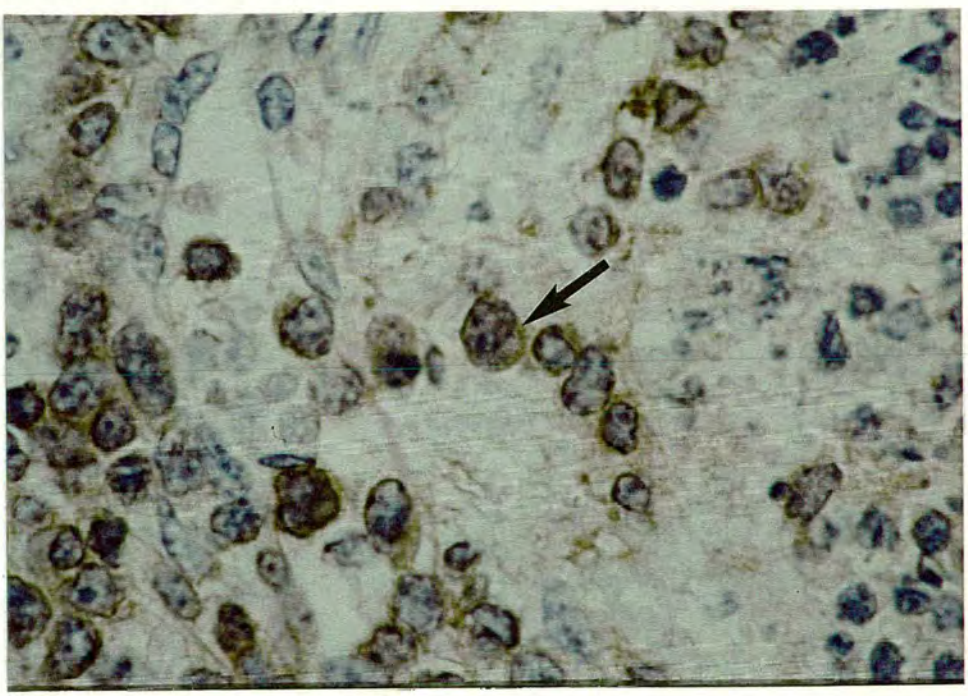

Figure 7.8 Section showing a $CD3^+$ microschizont-infected cell (arrow) in the medulla of the draining prescapular lymph node of the calf infected with *T. parva* (Muguga) on day 21 post-infection during the terminal stages of disease, (x1000: polyclonal antibody A452 & DAB).

by MAb IL-A15 or polyclonal antibody A452: macroschizont-infected, $CD11b^-$ cells, microschizont-infected, $CD11b^-$ cells, macroschizont-infected, $CD3^-$ cells and microschizont-infected, $CD3^-$ cells occurred as well.

7.4.2 DISTRIBUTION OF $CD11B^+$ & $CD3^+$ SCHIZONT-INFECTED CELLS

The distribution of $CD11b^+$ and $CD3^+$ schizont-infected cells was investigated by counting the numbers of such cells in the tissues of all the infected animals. The tissue sections of the lymphoid and non-lymphoid organs of the uninfected, normal cattle did not contain any structures which resembled the macroschizont- or microschizont-infected cells.

7.4.2.1 DISTRIBUTION OF $CD11B^+$ & $CD3^+$ SCHIZONT-INFECTED CELLS IN A CALF (41B) INFECTED WITH T. ANNULATA (HISAR) AS A PILOT STUDY

On day 12 post-infection during the terminal stages of disease in calf 41B [Table 7.1A] $CD11b^+$ schizont-infected cells were seen in all lymphoid organs, i.e. the draining and contralateral prescapular LNs, draining and contralateral precrural LNs, mesenteric LN, spleen and thymus (total $CD11b^+$ schizont-infected cells at 45%) and all non-lymphoid organs, except the kidney (total $CD11b^+$ schizont-infected cells at 30%). $CD3^+$ schizont-infected cells were not found in any of the lymphoid or non-lymphoid organs.

7.4.2.2 DISTRIBUTION OF $CD11B^+$ & $CD3^+$ SCHIZONT-INFECTED CELLS IN CALVES (55C, 19 & 20) EXAMINED AT INTERVALS AFTER INFECTION WITH T. ANNULATA (HISAR)

On day 7 post-infection during the initial stages of pyrexia in calf 55C [Table 7.1B] $CD11b^+$ schizont-infected cells were only seen in the draining prescapular LN and spleen (total $CD11b^+$ schizont-infected cells at 33%) and were not found in any of the non-lymphoid organs. $CD3^+$ schizont-infected cells were not found in lymphoid or non-lymphoid organs.

On day 12 post-infection at the peak of pyrexia in calf 19 [Table 7.1C] $CD11b^+$ schizont-infected cells were now seen in all lymphoid organs, i.e. the draining and contralateral prescapular LNs, draining and contralateral precrural LNs, mesenteric and hepatic LNs, spleen and thymus (total $CD11b^+$ schizont-infected cells at 42%)

ORGAN	Total SIC	$SIC^+/CD11b^+$
Prescapular LN (draining)	126	70
Prescapular LN (contralateral)	4	2
Precrural LN (draining)	33	14
Precrural LN (contralateral)	16	6
Mesenteric LN	60	8
Spleen	24	17
Thymus	27	14
TOTAL	290	131
% $SIC^+/CD11b^+$		**45**

ORGAN	Total SIC	$SIC^+/CD3^+$
Prescapular LN (draining)	100	0
Prescapular LN (contralateral)	2	0
Precrural LN (draining)	16	0
Precrural LN (contralateral)	6	0
Mesenteric LN	8	0
Spleen	10	0
Thymus	1	0
TOTAL	143	0
% $SIC^+/CD3^+$		**0**

ORGAN	Total SIC	$SIC^+/CD11b^+$
Kidney	nd	nd
Liver	51	7
Abomasum	100	44
Lung	24	2
TOTAL	175	53
% $SIC^+/CD11b^+$		**30**

ORGAN	Total SIC	$SIC^+/CD3^+$
Kidney	23	0
Liver	40	0
Abomasum	40	0
Lung	4	0
TOTAL	107	0
% $SIC^+/CD3^+$		**0**

LN Lymph node
SIC Schizont-infected cells
nd None detected

Table 7.1A % $CD11b^+$ & $CD3^+$ schizont-infected cells in tissue sections of a calf (41B) infected with *T. annulata* (Hisar): in sections stained with MAb IL-A15, macroschizonts were identified with MAb 1C7 and microschizonts by Harris's haematoxylin; in sections stained with polyclonal antibody A452, all schizonts (macroschizonts & microschizonts) were identified with Harris's haematoxylin

ORGAN	Total SIC	SIC$^+$/ CD11b$^+$
Prescapular LN (draining)	22	10
Prescapular LN (contralateral)	nd	nd
Precrural LN (draining)	nd	nd
Precrural LN (contralateral)	nd	nd
Mesenteric LN	nd	nd
Hepatic LN	nd	nd
Spleen	20	4
Thymus	nd	nd
TOTAL	42	14
% SIC$^+$/ CD11b$^+$		**33**

ORGAN	Total SIC	SIC$^+$/ CD3$^+$
Prescapular LN (draining)	nd	nd
Prescapular LN (contralateral)	nd	nd
Precrural LN (draining)	nd	nd
Precrural LN (contralateral)	nd	nd
Mesenteric LN	nd	nd
Hepatic LN	nd	nd
Spleen	nd	nd
Thymus	nd	nd
TOTAL	0	0
% SIC$^+$/ CD3$^+$		**0**

ORGAN	Total SIC	SIC$^+$/ CD11b$^+$
Kidney	nd	nd
Liver	nd	nd
Abomasum	4	0
Lung	nd	nd
Brain stem	nd	nd
Cerebellum	nd	nd
Cerebral hemisphere	nd	nd
Heart	nd	nd
Adrenal gland	nd	nd
Anterior Pituitary gland	nd	nd
TOTAL	4	0
% SIC$^+$/ CD11b$^+$		**0**

ORGAN	Total SIC	SIC$^+$/ CD3$^+$
Kidney	nd	nd
Liver	nd	nd
Abomasum	nd	nd
Lung	nd	nd
Brain stem	nd	nd
Cerebellum	nd	nd
Cerebral hemisphere	nd	nd
Heart	nd	nd
Adrenal gland	nd	nd
Anterior Pituitary gland	nd	nd
TOTAL	0	0
% SIC$^+$/ CD3$^+$		**0**

LN Lymph node
SIC Schizont-infected cells
nd None detected

Table 7.1B % CD11b$^+$ & CD3$^+$ schizont-infected cells in tissue sections of a calf (55C) infected with *T. annulata* (Hisar): in sections stained with MAb IL-A15, macroschizonts were identified with MAb 1C7 and microschizonts by Harris's haematoxylin; in sections stained with polyclonal antibody A452, all schizonts (macroschizonts & microschizonts) were identified with Harris's haematoxylin

ORGAN	Total SIC	SIC$^+$/ CD11b$^+$
Prescapular LN (draining)	114	55
Prescapular LN (contralateral)	73	6
Precrural LN (draining)	11	4
Precrural LN (contralateral)	14	6
Mesenteric LN	10	5
Hepatic LN	44	21
Spleen	28	18
Thymus	27	21
TOTAL	321	136
% SIC$^+$/ CD11b$^+$		**42**

ORGAN	Total SIC	SIC$^+$/ CD3$^+$
Prescapular LN (draining)	105	0
Prescapular LN (contralateral)	6	0
Precrural LN (draining)	nd	nd
Precrural LN (contralateral)	4	0
Mesenteric LN	3	0
Hepatic LN	26	0
Spleen	17	0
Thymus	3	0
TOTAL	164	0
% SIC$^+$/ CD3$^+$		**0**

ORGAN	Total SIC	SIC$^+$/ CD11b$^+$
Kidney	11	7
Liver	100	75
Abomasum	106	92
Lung	14	5
Brain stem	nd	nd
Cerebellum	nd	nd
Cerebral hemisphere	nd	nd
Heart	nd	nd
Adrenal gland	45	30
Anterior Pituitary gland	nd	nd
TOTAL	276	209
% SIC$^+$/ CD11b$^+$		**76**

ORGAN	Total SIC	SIC$^+$/ CD3$^+$
Kidney	2	0
Liver	4	0
Abomasum	2	0
Lung	1	0
Brain stem	nd	nd
Cerebellum	nd	nd
Cerebral hemisphere	nd	nd
Heart	nd	nd
Adrenal gland	18	0
Anterior Pituitary gland	nd	nd
TOTAL	27	0
% SIC$^+$/ CD3$^+$		**0**

LN Lymph node
SIC Schizont-infected cells
nd None detected

Table 7.1C % CD11b$^+$ & CD3$^+$ schizont-infected cells in tissue sections of a calf (19) infected with *T. annulata* (Hisar): in sections stained with MAb IL-A15, macroschizonts were identified with MAb 1C7 and microschizonts by Harris's haematoxylin; in sections stained with polyclonal antibody A452, all schizonts (macroschizonts & microschizonts) were identified with Harris's haematoxylin

and most of the non-lymphoid organs, i.e. the kidney, liver, abomasum, lung and adrenal gland (total $CD11b^+$ schizont-infected cells at 76%). $CD3^+$ schizont-infected cells were not found in any of the lymphoid or non-lymphoid organs.

On day 14 post-infection during the nadir of disease in calf 20 [Table 7.1D] $CD11b^+$ schizont-infected cells were seen in all lymphoid organs (Figure 7.9) (total $CD11b^+$ schizont-infected cells at 73%) and most of the non-lymphoid organs, i.e. the kidney, liver, lung, adrenal (Figure 7.10) and pituitary glands (Figure 7.11) (total $CD11b^+$ schizont-infected cells at 71%). $CD3^+$ schizont-infected cells were not found in any of the lymphoid or non-lymphoid organs.

7.4.2.3 DISTRIBUTION OF $CD11B^+$ & $CD3^+$ SCHIZONT-INFECTED CELLS IN A CALF (861) DURING THE TERMINAL STAGES OF INFECTION WITH T. ANNULATA (DOUKKALLA)

On day 24 post-infection during the terminal stages of disease in calf 861 [Table 7.1E] $CD11b^+$ schizont-infected cells were seen in all lymphoid organs, i.e. the draining and contralateral prescapular LNs, draining and contralateral precrural LNs, mesenteric LN, spleen and thymus (total $CD11b^+$ schizont-infected cells at 44%) and all of the non-lymphoid organs, i.e. the kidney, liver, abomasum, lung and skin (total $CD11b^+$ schizont-infected cells at 85%). $CD3^+$ schizont-infected cells were not found in any of the lymphoid or non-lymphoid organs.

7.4.2.4 DISTRIBUTION OF $CD11B^+$ & $CD3^+$ SCHIZONT-INFECTED CELLS IN A CALF (8) DURING THE TERMINAL STAGES OF INFECTION WITH T. PARVA (MUGUGA)

On day 21 post-infection during the terminal stages of disease in calf 8 [Table 7.1F] $CD11b^+$ schizont-infected cells were seen in most lymphoid organs, i.e. the draining and contralateral prescapular LNs, draining precrural LN, hepatic LN and spleen (total $CD11b^+$ schizont-infected cells at 36%) but only one non-lymphoid organ, i.e. the liver (total $CD11b^+$ schizont-infected cells at 50%). $CD3^+$ schizont-infected cells were also found in most lymphoid organs, i.e. the draining and contralateral prescapular LNs, draining and contralateral precrural LNs and spleen (total $CD3^+$ schizont-infected cells at 84%) but only one $CD3^+$ schizont-infected cell was seen in the non-lymphoid organs, i.e. the lung.

ORGAN	Total SIC	SIC$^+$/ CD11b$^+$
Prescapular LN (draining)	114	82
Prescapular LN (contralateral)	110	72
Precrural LN (draining)	114	95
Precrural LN (contralateral)	56	44
Mesenteric LN	100	80
Hepatic LN	23	7
Spleen	31	23
Thymus	30	18
TOTAL	578	421
% SIC$^+$/ CD11b$^+$		**73**

ORGAN	Total SIC	SIC$^+$/ CD3$^+$
Prescapular LN (draining)	102	0
Prescapular LN (contralateral)	112	0
Precrural LN (draining)	19	0
Precrural LN (contralateral)	2	0
Mesenteric LN	100	0
Hepatic LN	4	0
Spleen	15	0
Thymus	34	0
TOTAL	388	0
% SIC$^+$/ CD3$^+$		**0**

ORGAN	Total SIC	SIC$^+$/ CD11b$^+$
Kidney	8	4
Liver	28	24
Abomasum	nd	nd
Lung	17	4
Brain stem	nd	nd
Cerebellum	nd	nd
Cerebral hemisphere	nd	nd
Heart	nd	nd
Adrenal gland	40	32
Anterior Pituitary gland	9	8
TOTAL	102	72
% SIC$^+$/ CD11b$^+$		**71**

ORGAN	Total SIC	SIC$^+$/ CD3$^+$
Kidney	2	0
Liver	4	0
Abomasum	nd	nd
Lung	2	0
Brain stem	nd	nd
Cerebellum	nd	nd
Cerebral hemisphere	nd	nd
Heart	nd	nd
Adrenal gland	26	0
Anterior Pituitary gland	1	0
TOTAL	35	0
% SIC$^+$/ CD3$^+$		**0**

LN Lymph node
SIC Schizont-infected cells
nd None detected

Table 7.1D % CD11b$^+$ & CD3$^+$ schizont-infected cells in tissue sections of a calf (20) infected with *T. annulata* (Hisar): in sections stained with MAb IL-A15, macroschizonts were identified with MAb 1C7 and microschizonts by Harris's haematoxylin; in sections stained with polyclonal antibody A452, all schizonts (macroschizonts & microschizonts) were identified with Harris's haematoxylin

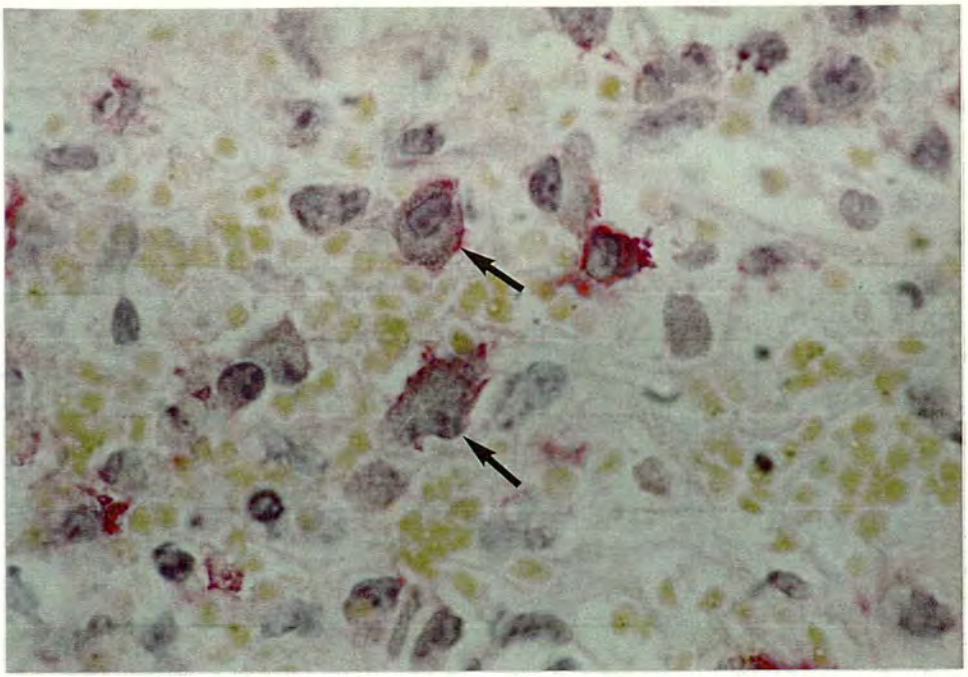

Figure 7.9 Section showing $1C7^{-}/CD11b^{+}$ microschizont-infected cells (arrows) in the medullary sinuses of the draining prescapular lymph node of the calf infected with *T. annulata* (Hisar) on day 14 post-infection at the nadir of disease. Note the extensive haemorrhage (brown), (x1000: MAb 1C7 & DAB; MAb IL-A15 & Vector Red).

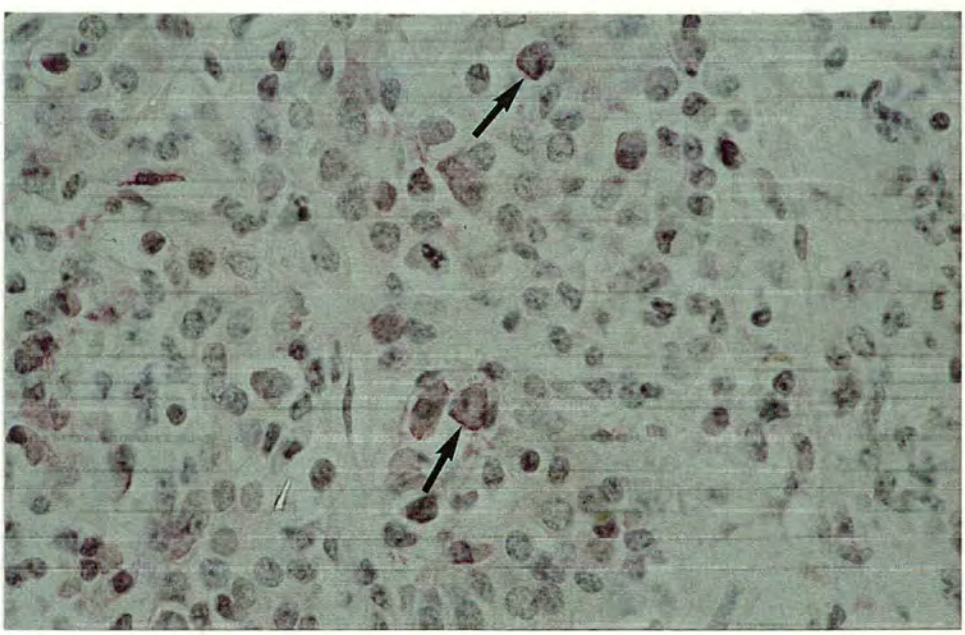

Figure 7.10 Section showing $1C7^{-}/CD11b^{+}$ microschizont-infected cells (arrows) in the medulla of the adrenal gland of the calf infected with *T. annulata* (Hisar) on day 14 post-infection at the nadir of disease, (x500: MAb 1C7 & DAB; MAb IL-A15 & Vector Red).

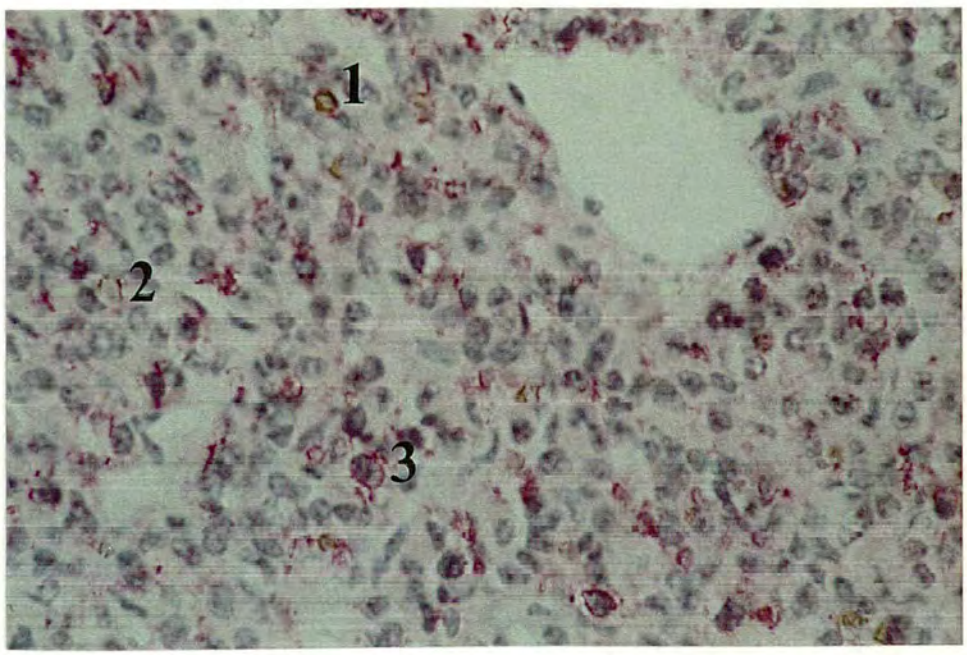

Figure 7.11 Section showing the following: a $1C7^{+}/CD11b^{+}$ macroschizont-infected cell (1); a $1C7^{+}/CD11b^{-}$ macroschizont-infected cell (2); a $1C7^{-}/CD11b^{+}$ microschizont-infected cell (3) in the pituitary gland of the calf infected with *T. annulata* (Hisar) on day 14 post-infection at the nadir of disease, (x500: MAb 1C7 & DAB; MAb IL-A15 & Vector Red).

ORGAN	Total SIC	$SIC^+/CD11b^+$
Prescapular LN (draining)	105	24
Prescapular LN (contralateral)	101	45
Precrural LN (draining)	30	9
Precrural LN (contralateral)	100	48
Mesenteric LN	14	11
Spleen	3	1
Thymus	100	60
TOTAL	453	198
% $SIC^+/CD11b^+$		**44**

ORGAN	Total SIC	$SIC^+/CD3^+$
Prescapular LN (draining)	100	0
Prescapular LN (contralateral)	6	0
Precrural LN (draining)	10	0
Precrural LN (contralateral)	40	0
Mesenteric LN	4	0
Spleen	nd	nd
Thymus	21	0
TOTAL	181	0
% $SIC^+/CD3^+$		**0**

ORGAN	Total SIC	$SIC^+/CD11b^+$
Kidney	8	6
Liver	4	4
Abomasum	15	6
Lung	1	0
Skin	106	98
TOTAL	134	114
% $SIC^+/CD11b^+$		**85**

ORGAN	Total SIC	$SIC^+/CD3^+$
Kidney	nd	nd
Liver	nd	nd
Abomasum	2	0
Lung	nd	nd
Skin	42	0
TOTAL	44	0
% $SIC^+/CD3^+$		**0**

LN Lymph node
SIC Schizont-infected cells
nd None detected

Table 7.1E % $CD11b^+$ & $CD3^+$ schizont-infected cells in tissue sections of a calf (861) infected with *T. annulata* (Doukkalla): in sections stained with MAb IL-A15, macroschizonts were identified with MAb 1C7 and microschizonts by Harris's haematoxylin; in sections stained with polyclonal antibody A452, all schizonts (macroschizonts & microschizonts) were identified with Harris's haematoxylin

ORGAN	Total SIC	SIC$^+$/ CD11b$^+$
Prescapular LN (draining)	38	10
Prescapular LN (contralateral)	30	16
Precrural LN (draining)	9	2
Precrural LN (contralateral)	1	0
Mesenteric LN	nd	nd
Hepatic LN	7	2
Spleen	4	2
Thymus	nd	nd
TOTAL	89	32
% SIC$^+$/ CD11b$^+$		**36**

ORGAN	Total SIC	SIC$^+$/ CD3$^+$
Prescapular LN (draining)	39	32
Prescapular LN (contralateral)	20	17
Precrural LN (draining)	17	15
Precrural LN (contralateral)	9	7
Mesenteric LN	nd	nd
Hepatic LN	nd	nd
Spleen	4	4
Thymus	nd	nd
TOTAL	89	75
% SIC$^+$/ CD3$^+$		**84**

ORGAN	Total SIC	SIC$^+$/ CD11b$^+$
Kidney	nd	nd
Liver	10	6
Abomasum	nd	nd
Lung	2	0
Heart	nd	nd
Adrenal gland	nd	nd
TOTAL	12	6
% SIC$^+$/ CD11b$^+$		**50**

ORGAN	Total SIC	SIC$^+$/ CD3$^+$
Kidney	nd	nd
Liver	nd	nd
Abomasum	nd	nd
Lung	1	1
Heart	nd	nd
Adrenal gland	nd	nd
TOTAL	1	1
% SIC$^+$/ CD3$^+$		**100**

LN Lymph node
SIC Schizont-infected cells
nd None detected

Table 7.1F % CD11b$^+$ & CD3$^+$ schizont-infected cells in tissue sections of a calf (8) infected with *T. parva* (Muguga): in sections stained with either MAb IL-A15 or polyclonal antibody A452, all schizonts (macroschizonts & microschizonts) were identified with Harris's haematoxylin

7.5 DISCUSSION

T. annulata schizont-infected cells at all stages of differentiation, from macroschizont- to microschizont-infected cells, expressed CD11b, the C3bi complement receptor. Such $CD11b^+$ schizont-infected cells occurred throughout the lymphoid organs, i.e. the lymph nodes, spleen and thymus and the non-lymphoid organs, i.e. the liver, kidney, abomasum, lung, skin, adrenal and pituitary glands. In contrast, the *T. annulata* schizont-infected cells did not express CD3, the T cell marker. These observations provided evidence for a myeloid origin for the schizont-infected cells, although B and NK cells could not be excluded as hosts. Importantly, these findings confirmed earlier observations (Sergent *et al.* 1945) which described schizonts as living within elements of the reticulo-endothelial system, reticular cells of the lymph nodes and spleen, Kupffer cells of the liver and histiocytes.

Since both *in vivo*-derived cell lines (Howard *et al.* 1993; Forsyth *et al.* in press) and schizont-infected cells in tissues (Forsyth *et al.* in press) express CD11b, it seems likely that the *in vivo*-derived cell lines used to prepare the attenuated cell line vaccines in current use (Pipano 1989) represent the cell types inhabited by the parasites in tissues as well as blood. The phenotypic profiles of the *in vivo*-derived cell lines recorded to date showed that the cells chosen for infection by sporozoites *in vitro* (Howard *et al.* 1993) are phenotypically similar to the cells infected *in vivo*.

The pattern of staining with the MAb IL-A15 in the uninfected, control tissues (Figure 6.1) resembled that of previous studies (Splitter & Morrison 1991). The MAb recognised large macrophage-like cells in the paracortex of prescapular, precrural and mesenteric lymph nodes, the white pulp of the spleen and alveolar walls of the lung, as well as cells in the germinal centres of the lymph nodes. These observations confirmed that the preparations of MAb IL-A15 used here had a similar specificity for bovine tissues to those used to define the MAbs reactivity (Splitter & Morrison 1991). Importantly, Harris's haematoxylin counterstain aided in the identification of cell phenotype.

CD11b has a number of functions. It serves as the membrane receptor for C3bi which acts as an opsonin for many microorganisms (Cooper 1991), is involved in

adhesion and the transmigration of blood leucocytes (Belvilacqua 1993) and promotes NK cell binding to targets (Erdei, Fust & Gergely 1991), which is interesting with respect to the findings on NK cell mediated lysis of *T. annulata* schizont-infected cells (Preston *et al.* 1983). The finding that *T. annulata* schizont-infected cells in tissues expressed CD11b, but not CD3, is therefore of relevance to three unsolved problems. These are: the nature of the cell inhabited by *T. annulata* schizonts in cattle undergoing lethal infections with *T. annulata*; the way in which *T. annulata* schizonts transfer from cell to cell, in particular during infection and immunisation with cell line vaccines; the route of dissemination of the schizont-infected cells from blood or lymph into the tissues of the infected animals.

It seems feasible that any schizonts which may have been freed from their host cells may have been opsonised either by complement and/or antibody and then linked to cells bearing the C3bi receptor. Attachment of the parasite/complement complex would thus facilitate phagocytosis of the organism by the cell. The subsequent establishment of the parasite in the cell would depend upon whether the cell bearing the C3bi receptor could support parasite proliferation. Interestingly, free schizonts of *T. parva* have been reported to activate complement *in vitro* (Shitakha, Musoke & Nyormoi; cited in Shitakha, Natulya, Musoke, Ramasamy & Buscher 1983).

Evidence for the use of C3bi and C3bi receptors in internalisation of protozoan parasites does exist. The ability of haemosporozoans of the genera *Babesia* to attach to, and subsequently penetrate mammalian erythrocytes is also directly related to their ability to recognise specific determinants on the host cell membrane. In the case of *B. rodhaini* infection, receptors dependent on the C3bi component of complement have been shown to be necessary for the penetration process (Chapman & Ward 1977). *Leishmania* species have also been shown to bind via a surface glycoprotein (metalloproteinase gp63), either directly or after opsonisation with complement, to the CR3 receptor (specific for C3bi of complement) of macrophages prior to phagocytosis (Russell & Wright 1988).

In addition, if *T. annulata*-infected cells or liberated schizonts do become opsonised with C3bi they might become attached to non-phagocytic cells which bear the C3bi

receptor, including platelets and erythrocytes, inadvertently causing lysis of these cells by activation of the membrane attack complex of the complement cascade. If this was the case, a possible explanation for the anaemia associated with animals associated with *T. annulata* may be suggested. Interestingly, lysis of platelets leads to the release of vasoactive amines, which cause considerable inflammation and tissue damage, including bronchoconstriction. Such a response may account for the damage observed in the tissues of animals infected with *T. annulata* (Chapter 4). It has been suggested that the pulmonary oedema and disseminated petechial haemorrhages seen in *T. parva* infected animals may be the direct result of the combined effects of complement activation and consumption of fibrinogen and fibrin (Shitakha *et al.* 1983). In addition, fragments of fibronectin present in the microenvironment of an inflamed site might retard macrophage removal of neutrophils undergoing apoptosis, with the release of cell contents promoting persistence of inflammation and therefore increasing the risk of permanent organ damage (Savill, Fadok, Henson & Haslett 1993).

Interestingly, HIV through its activation of complement C3bi via gp 41 appears to be able to localise on follicular dendritic cells, which are important in the development of lymphoid follicle germinal centres, in large numbers in the absence of antibody (Szakal, Kapasi, Masuda & Tew 1992). The slow depletion of follicular dendritic cells in lymph nodes of HIV infected individuals may be due to destruction of follicular dendritic cells and/or the failure of pre-follicular dendritic cells to develop into follicular dendritic cells and repopulate the lymph nodes. If *T. annulata*-infected cells or liberated schizonts activate complement *in vivo*, the findings described above may have implications for the observed destruction of lymphoid follicles in the lymph nodes of the *T. annulata* infected animals (Chapter 4).

T. parva (Muguga) schizont-infected cells at all stages of differentiation, from macroschizont to microschizont, expressed CD3, the T cell marker. In addition, a proportion of *T. parva* (Muguga) schizont-infected cells expressed CD11b, the C3bi complement receptor. Such schizont-infected cells occurred throughout lymphoid organs, including the lymph nodes and spleen and non-lymphoid organs, including the liver and lung. These observations provided evidence for a T cell origin for the

schizont-infected cells, although B and NK cells could not be excluded. Importantly, these findings confirmed earlier observations (Steck 1928, Cowdry & Danks 1933; Neitz 1957; De Kock 1957; DeMartini & Moulton 1973; Barnett 1977; Morrison *et al.* 1981a) which described schizonts as living within lymphocytes.

The different cell phenotype resided in by the *T. annulata* and *T. parva* (Muguga) macroschizonts and microschizonts may account for the different pathological responses observed in the tissues from the *T. annulata* or *T. parva* (Muguga) infected cattle as described in chapter 4. That is, many features of both *T. annulata* and *T. parva* infections are thought to be due to the secretion of IFNs by the parasitised cells and to cytokines such as IFN-γ and TNF-α produced by the host cells in response to infection (Preston *et al.* 1993). *T. annulata* has been documented to secrete type 1 IFN which downregulates lymphocyte proliferation (Balkwill 1989) whereas, *T. parva* has been documented to secrete IFN-γ (DeMartini & Baldwin 1991) which upregulates lymphoproliferation (Siegel 1988).

7.6 CONCLUSION

T. annulata schizonts (macroschizonts and microschizonts) resided within cells from the myeloid lineage which expressed CD11b, the C3bi complement receptor, but not cells from the T cell lineage which expressed CD3. In contrast, *T. parva* (Muguga) schizont-infected cells resided within cells from the T cell lineage which expressed CD3. The possibility that both *T. annulata* and *T. parva* (Muguga) schizont-infected cells resided within B and NK cells could not be excluded.

CHAPTER EIGHT

PHENOTYPIC ANALYSIS OF THE CELLULAR RESPONSES ELICITED BY SCHIZONT-INFECTED CELLS

8.1 INTRODUCTION

As described in chapter 4 identification of the exact cell types present in the tissues of the infected animals was difficult. This chapter therefore describes the use of the CD11b and CD3 markers (MAb IL-A15 & polyclonal antibody A452) to assess the identity of and the distribution of these cells particularly in relation to the schizont-infected cells.

8.2 EXPERIMENTAL DESIGN

The distribution of myeloid ($CD11b^+$) and T ($CD3^+$) cells was investigated on the same paraffin tissue sections of the lymphoid and non-lymphoid organs of normal and infected animals as had been previously examined and which had been stained with ABC immunocytochemical techniques and Harris's haematoxylin counterstain (7.3.1 & 7.3.2). The relationship between uninfected and schizont-infected cells in damaged tissues was also studied to identify the uninfected cells which had infiltrated the tissues, as opposed to schizont-infected cells.

8.3 MATERIALS & METHODS

8.3.1 ASSESSMENT OF IMMUNOCYTOCHEMICALLY LABELLED PARAFFIN TISSUE SECTIONS

Several tissue sections were examined at 200 x magnification using a Nikon S. Ke II microscope. The distribution of myeloid ($CD11b^+$) and T ($CD3^+$) cells in lymphoid and non-lymphoid organs was recorded on the following subjective scale as compared to numbers in uninfected tissue sections: nc no change; + small increase; ++ moderate increase; +++ large increase; - small decrease; - - moderate decrease; --- large decrease.

The schizont-infected cells observed in these organs at 1000 x magnification were recorded on the following subjective scale: nd none detected; * small numbers (<10 per field); ** moderate numbers (10-50 per field); *** large numbers (>50 per field).

The ratio of uninfected cells (U) to schizont-infected cells (SIC) in these organs was recorded as follows: U>SIC; U=SIC; U<SIC.

8.4 RESULTS

8.4.1 DISTRIBUTION OF CD11B$^+$ & CD3$^+$ CELLS

8.4.1.1 DISTRIBUTION OF CD11B$^+$ & CD3$^+$ CELLS IN UNINFECTED CONTROL CATTLE

CD11b$^+$ cells were seen in the lymphoid follicles, cortex, paracortex, medullary cords and sinuses of the lymph nodes (Figure 6.1), the white pulp of the spleen and alveolar walls of the lung. CD3$^+$ cells were found in the lymphoid follicles, cortex, paracortex, medullary cords and sinuses of the lymph nodes (Figure 6.2), both the white and red pulp of the spleen, the cortex and medulla of the thymus (Figure 8.1), portal tracts of the liver, lamina propria of the abomasum and alveolar walls of the lung.

8.4.1.2 DISTRIBUTION OF INFECTED & UNINFECTED CD11B$^+$ & UNINFECTED CD3$^+$ CELLS IN A CALF (41B) INFECTED WITH T. ANNULATA (HISAR) AS A PILOT STUDY

On day 12 post-infection during the terminal stages of disease in calf 41B [Table 8.1A] an increase in the number of uninfected CD11b$^+$ cells was seen in the medullary cords of all the lymph nodes and throughout the thymus (Figure 8.2). A decrease in the number of uninfected CD11b$^+$ cells was found in the paracortex of the draining and contralateral prescapular LNs. There was no change in the number of uninfected CD11b$^+$ cells seen in either the white or red pulp of the spleen. An increase in the number of uninfected CD11b$^+$ cells was seen in the portal tracts of the liver and alveolar walls of the lung. An increase in the number of infected CD11b$^+$ cells was seen in the lamina propria of the abomasum.

A decrease in the number of uninfected CD3$^+$ cells was found in the paracortex of all the lymph nodes, the white pulp of the spleen and cortex of the thymus. In contrast, an increase in the number of uninfected CD3$^+$ cells was seen in the cortex and medulla of the kidney and alveolar walls of the lung.

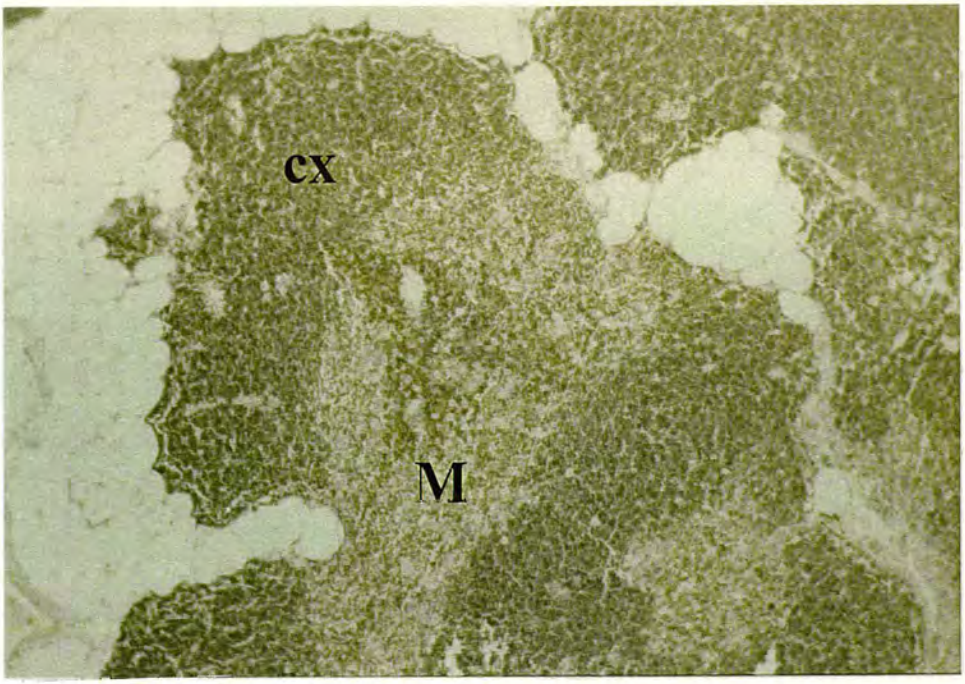

Figure 8.1 Section showing $CD3^+$ cells (brown) in the cortex (CX) and medulla (M) of the thymus of the normal, uninfected animal, (x40: polyclonal antibody A452 & DAB).

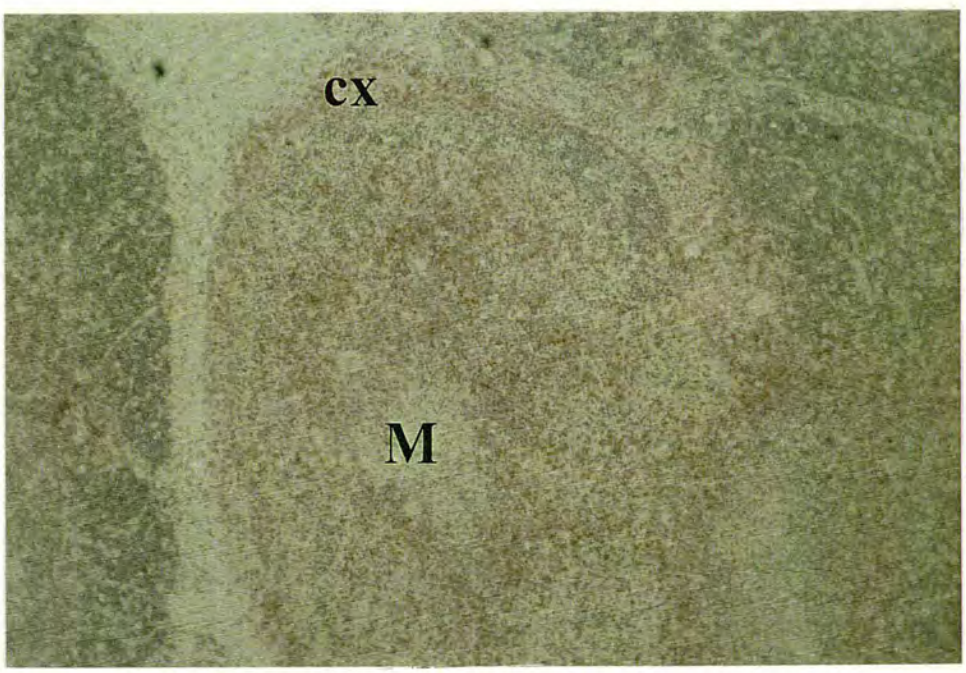

Figure 8.2 Section showing $CD11b^+$ cells (pink) in the cortex (CX) and medulla (M) of the thymus of the calf infected with *T. annulata* (Hisar) on day 12 post-infection during the terminal stages of disease, (x40: MAb IL-A15 & Vector Red).

ORGAN	AREA	CD11b$^+$	CD3$^+$	SIC	Ratio U : SIC
Prescapular LN (draining)	CX	nc	-	**	U > SIC
	PCX	-	--	***	
	MC	+	--	*	
	MS	nc	nc	*	
Prescapular LN (contralateral)	CX	nc	-	*	U > SIC
	PCX	--	--	*	
	MC	+	-	*	
	MS	nc	nc	*	
Precrural LN (draining)	CX	+	nc	*	U > SIC
	PCX	nc	-	*	
	MC	++	nc	*	
	MS	nc	nc	*	
Precrural LN (contralateral)	CX	nc	nc	**	U > SIC
	PCX	nc	-	**	
	MC	++	nc	*	
	MS	nc	nc	*	
Mesenteric LN	CX	nc	nc	**	U > SIC
	PCX	nc	--	**	
	MC	++	nc	*	
	MS	nc	nc	*	
Spleen	WP	nc	--	***	na
	RP	nc	+	***	
Thymus	CX	+	--	*	U > SIC
	MED	+++	nc	**	

ORGAN	AREA	CD11b$^+$	CD3$^+$	SIC	Ratio U : SIC
Kidney	CX	nc	+	**	na
	MED	nc	+	**	
Liver	PT	++	nc	**	U > SIC
Abomasum	LAP	+++	nc	***	U < SIC
Lung	AW	+	+	**	U > SIC
	BRO	nc	nc	*	

U Uninfected cells
SIC Schizont-infected cells
LN Lymph node
na Not applicable

CX Cortex
PCX Paracortex
MED Medulla
MC Medullary cords
MS Medullary sinuses
WP White pulp
RP Red pulp

PT Portal tracts
LAP Lamina propria
AW Alveolar walls
BRO Bronchioles

nc No change
- Small decrease
-- Moderate decrease
--- Large decrease

+ Small increase
++ Moderate increase
+++ Large increase

nd None detected
* Small numbers
** Moderate numbers
*** Large numbers

Table 8.1A Distribution of CD11b$^+$ & CD3$^+$ uninfected cells in a calf (41B) infected with *T. annulata* (Hisar) as a pilot study

8.4.1.3 DISTRIBUTION OF INFECTED & UNINFECTED CD11B$^+$ & UNINFECTED CD3$^+$ CELLS IN CALVES (55C, 19 & 20) EXAMINED AT INTERVALS AFTER INFECTION WITH T. ANNULATA (HISAR)

On day 7 post-infection during the initial stages of pyrexia in calf 55C [Table 8.1B] an increase in the number of uninfected CD11b$^+$ cells was seen in the medullary cords of all the lymph nodes (Figure 8.3), the white pulp of the spleen and the medulla of the thymus. A decrease in the number of uninfected CD11b$^+$ cells was found in the paracortex of the mesenteric LN. An increase in the number of uninfected and infected CD11b$^+$ cells was seen in the adrenal and pituitary glands.

A decrease in the number of uninfected CD3$^+$ cells was found in the cortex and paracortex of the draining prescapular LN (Figure 8.4) and the white pulp of the spleen. An increase in the number of uninfected CD3$^+$ cells was found in the cortex and medulla of the kidney, alveolar walls of the lung and the pituitary gland.

On day 12 post-infection at the peak of pyrexia in calf 19 [Table 8.1C] an increase in the number of uninfected CD11b$^+$ cells was seen in the medullary cords of all the lymph nodes, the white pulp of the spleen and throughout the thymus. An increase in the number of uninfected CD11b$^+$ cells was seen in the cortex of the kidney, portal tracts of the liver, lamina propria of the abomasum, alveolar walls of the lung, the adrenal and pituitary glands. An increase in the number of infected and uninfected CD11b$^+$ cells was seen in these organs.

A decrease in the number of uninfected CD3$^+$ cells was found in the paracortex of all the lymph nodes (Figure 8.5) and throughout the thymus (Figure 8.6). In contrast, an increase in the number of uninfected CD3$^+$ cells was seen in the red pulp of the spleen. An increase in the number of uninfected CD3$^+$ cells was also found in the cortex and medulla of the kidney, alveolar walls of the lung, the adrenal and pituitary glands.

On day 14 post-infection during the nadir of disease in calf 20 [Table 8.1D] an increase in the number of uninfected CD11b$^+$ cells was seen in the medullary cords of all the lymph nodes and throughout the spleen (Figure 8.7) and thymus (Figure

ORGAN	AREA	CD11b$^+$	CD3$^+$	SIC	Ratio U : SIC
Prescapular LN (draining)	CX	nc	-	nd	U > SIC
	PCX	nc	-	nd	
	MC	+++	nc	*	
	MS	nc	nc	*	
Prescapular LN (contralateral)	CX	nc	nc	nd	U > SIC
	PCX	nc	nc	nd	
	MC	+++	nc	*	
	MS	+	nc	*	
Precrural LN (draining)	CX	nc	nc	nd	U > SIC
	PCX	nc	nc	nd	
	MC	+++	nc	*	
	MS	nc	nc	*	
Precrural LN (contralateral)	CX	nc	nc	nd	U > SIC
	PCX	nc	nc	nd	
	MC	+++	nc	*	
	MS	+	nc	*	
Mesenteric LN	CX	nc	nc	nd	U > SIC
	PCX	-	nc	nd	
	MC	+	nc	*	
	MS	nc	nc	*	
Hepatic LN	CX	nc	nc	nd	U > SIC
	PCX	nc	nc	nd	
	MC	++	nc	nd	
	MS	nc	nc	nd	
Spleen	WP	+	-	*	U > SIC
	RP	nc	nc	*	
Thymus	CX	nc	nc	nd	U > SIC
	MED	++	nc	*	

ORGAN	AREA	CD11b$^+$	CD3$^+$	SIC	Ratio U : SIC
Kidney	CX	nc	+	*	na
	MED	nc	+	nd	
Liver	PT	nc	nc	*	na
Abomasum	LAP	nc	nc	*	na
Lung	AW	nc	+	*	na
	BRO	nc	nc	nd	
Brain stem	GEN	nc	nc	nd	na
Cerebellum	GEN	nc	nc	nd	na
Cerebral hemisphere	GEN	nc	nc	nd	na
Heart	GEN	nc	nc	nd	na
Adrenal gland	ZG	nc	nc	*	U = SIC
	ZF	+	nc	*	
	ZR	nc	nc	nd	
	MED	nc	nc	nd	
Anterior Pituitary gland	GEN	+	+	*	U = SIC

U Uninfected cells
SIC Schizont-infected cells
LN Lymph node
na Not applicable

GEN General
CX Cortex
PCX Paracortex
MED Medulla
MC Medullary cords
MS Medullary sinuses
WP White pulp
RP Red pulp

PT Portal tracts
LAP Lamina propria
AW Alveolar walls
BRO Bronchioles
ZG Zona glomerulosa
ZF Zona fasciculata
ZR Zona reticularis

nc No change
- Small decrease
-- Moderate decrease
--- Large decrease

+ Small increase
++ Moderate increase
+++ Large increase

nd None detected
* Small numbers
** Moderate numbers
*** Large numbers

Table 8.1B Distribution of CD11b$^+$ & CD3$^+$ uninfected cells in a calf (55C) infected with *T. annulata* (Hisar) on day 7 post-infection

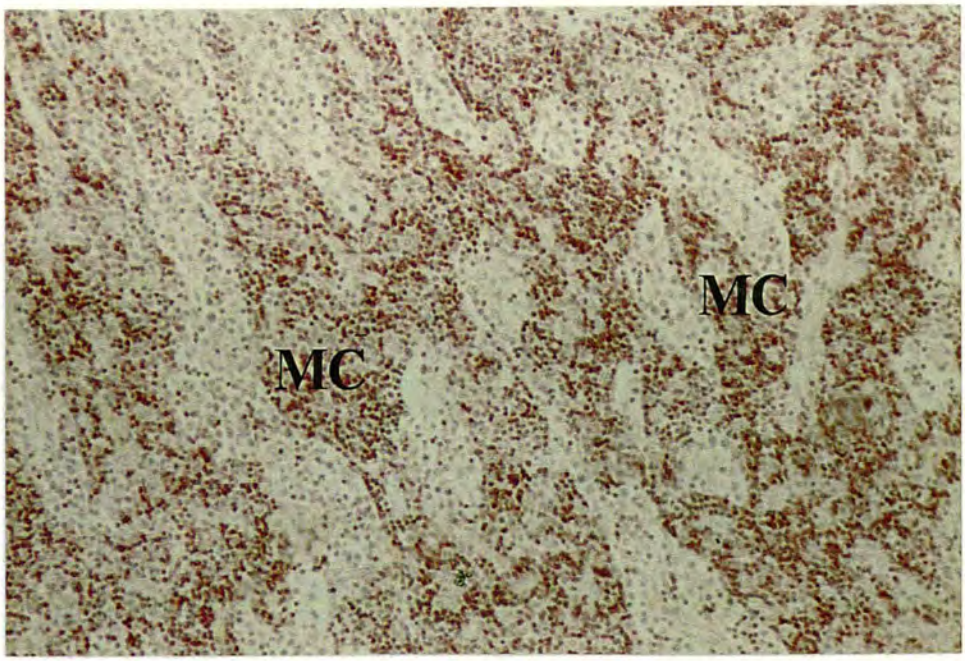

Figure 8.3 Section showing $CD11b^+$ cells (pink) in the medullary cords (MC) of the draining prescapular lymph node of the calf infected with *T. annulata* (Hisar) on day 7 post-infection during the initial stages of pyrexia, (x100: MAb IL-A15 & Vector Red).

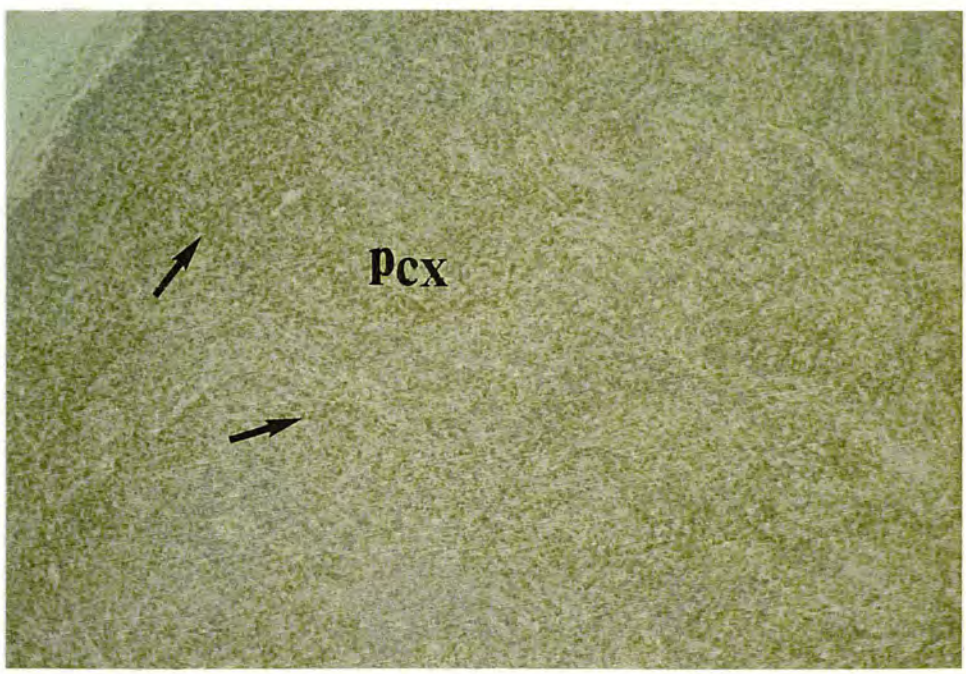

Figure 8.4 Section showing $CD3^+$ cells (arrows) in the paracortex (PCX) of the draining prescapular lymph node of the calf infected with *T. annulata* (Hisar) on day 7 post-infection during the initial stages of pyrexia, (x40: polyclonal antibody A452 & DAB).

ORGAN	AREA	CD11b$^+$	CD3$^+$	SIC	Ratio U : SIC
Prescapular LN (draining)	CX	nc	-	*	U > SIC
	PCX	nc	-	**	
	MC	+	nc	*	
	MS	nc	nc	***	
Prescapular LN (contralateral)	CX	nc	-	*	U > SIC
	PCX	nc	-	*	
	MC	+	nc	*	
	MS	nc	nc	*	
Precrural LN (draining)	CX	nc	-	*	U > SIC
	PCX	nc	-	*	
	MC	+	nc	*	
	MS	nc	nc	*	
Precrural LN (contralateral)	CX	nc	-	*	U > SIC
	PCX	nc	-	*	
	MC	+	nc	*	
	MS	nc	nc	*	
Mesenteric LN	CX	nc	-	*	U > SIC
	PCX	nc	-	*	
	MC	+	-	*	
	MS	nc	-	*	
Hepatic LN	CX	nc	nc	*	U > SIC
	PCX	nc	-	*	
	MC	+	nc	*	
	MS	nc	nc	*	
Spleen	WP	+	nc	**	U > SIC
	RP	nc	+	**	
Thymus	CX	+	--	nd	U > SIC
	MED	+++	-	*	

nc No change
- Small decrease
-- Moderate decrease
--- Large decrease

+ Small increase
++ Moderate increase
+++ Large increase

nd None detected
* Small numbers
** Moderate numbers
*** Large numbers

ORGAN	AREA	CD11b$^+$	CD3$^+$	SIC	Ratio U : SIC
Kidney	CX	+	++	*	U < SIC
	MED	nc	+	nd	
Liver	PT	+	nc	**	U < SIC
Abomasum	LAP	+	nc	*	U < SIC
Lung	AW	+	++	*	U = SIC
	BRO	nc	+	*	
Brain stem	GEN	nc	nc	nd	na
Cerebellum	GEN	nc	nc	nd	na
Cerebral hemisphere	GEN	nc	nc	nd	na
Heart	GEN	nc	nc	nd	na
Adrenal gland	ZG	nc	nc	*	U < SIC
	ZF	+	+	**	
	ZR	+	+	**	
	MED	nc	nc	*	
Anterior Pituitary gland	GEN	++	+	**	U < SIC

U Uninfected cells
SIC Schizont-infected cells
LN Lymph node
na Not applicable

GEN General
CX Cortex
PCX Paracortex
MED Medulla
MC Medullary cords
MS Medullary sinuses
WP White pulp
RP Red pulp

PT Portal tracts
LAP Lamina propria
AW Alveolar walls
BRO Bronchioles
ZG Zona glomerulosa
ZF Zona fasciculata
ZR Zona reticularis

Table 8.1C Distribution of CD11b$^+$ & CD3$^+$ uninfected cells in a calf (19) infected with *T. annulata* (Hisar) on day 12 post-infection

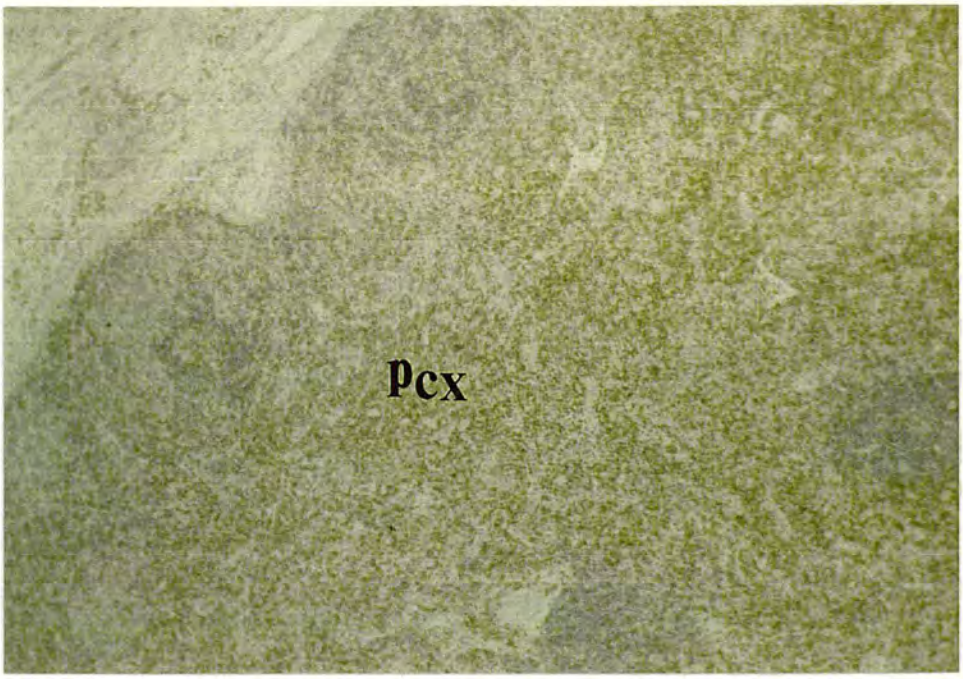

Figure 8.5 Section showing $CD3^+$ cells (brown) in the paracortex (PCX) of the draining prescapular lymph node of the calf infected with *T. annulata* (Hisar) on day 12 post-infection at the peak of pyrexia, (x40: polyclonal antibody A452 & DAB).

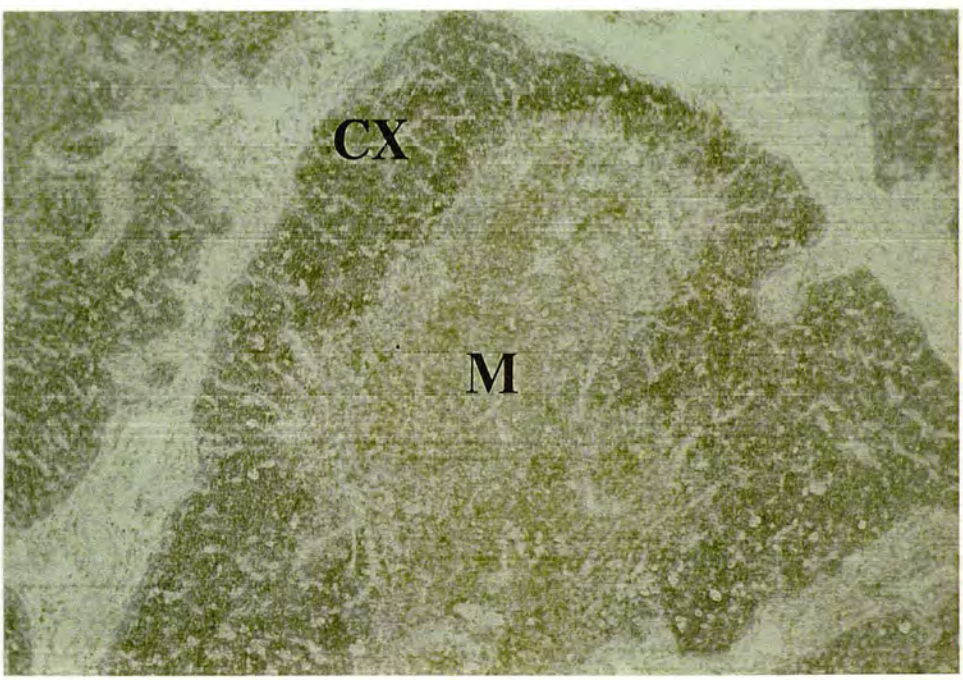

Figure 8.6 Section showing $CD3^+$ cells (brown) in the cortex (CX) and medulla (M) of the thymus of the calf infected with *T. annulata* (Hisar) on day 12 post-infection at the peak of pyrexia, (x40: polyclonal antibody A452 & DAB).

ORGAN	AREA	CD11b$^+$	CD3$^+$	SIC	Ratio U : SIC
Prescapular LN (draining)	CX	nc	-	**	U > SIC
	PCX	nc	--	***	
	MC	+	-	*	
	MS	nc	-	***	
Prescapular LN (contralateral)	CX	nc	nc	*	U > SIC
	PCX	nc	nc	*	
	MC	+	nc	*	
	MS	nc	nc	**	
Precrural LN (draining)	CX	+	nc	*	U > SIC
	PCX	nc	-	**	
	MC	+	nc	*	
	MS	nc	nc	*	
Precrural LN (contralateral)	CX	nc	nc	*	U > SIC
	PCX	nc	-	**	
	MC	+	nc	*	
	MS	nc	nc	*	
Mesenteric LN	CX	+	nc	*	U > SIC
	PCX	nc	-	*	
	MC	+	-	*	
	MS	++	nc	**	
Hepatic LN	CX	nc	nc	*	U > SIC
	PCX	nc	-	*	
	MC	+	nc	*	
	MS	nc	nc	*	
Spleen	WP	++	nc	**	U > SIC
	RP	+	+	**	
Thymus	CX	+	--	*	U > SIC
	MED	+++	nc	**	

nc No change
- Small decrease
-- Moderate decrease
--- Large decrease

+ Small increase
++ Moderate increase
+++ Large increase

nd None detected
* Small numbers
** Moderate numbers
*** Large numbers

ORGAN	AREA	CD11b$^+$	CD3$^+$	SIC	Ratio U : SIC
Kidney	CX	+	+++	*	U < SIC
	MED	nc	++	nd	
Liver	PT	nc	nc	**	na
Abomasum	LAP	nc	nc	*	na
Lung	AW	+	++	*	U = SIC
	BRO	nc	+	nd	
Brain stem	GEN	nc	nc	nd	na
Cerebellum	GEN	nc	nc	nd	na
Cerebral hemisphere	GEN	nc	nc	nd	na
Heart	GEN	nc	++	*	na
Adrenal gland	ZG	++	++	*	U = SIC
	ZF	++	+++	**	
	ZR	++	++	**	
	MED	++	+	*	
Anterior Pituitary gland	GEN	+++	++	**	U = SIC

U Uninfected cells
SIC Schizont-infected cells
LN Lymph node
na Not applicable

GEN General
CX Cortex
PCX Paracortex
MED Medulla
MC Medullary cords
MS Medullary sinuses
WP White pulp
RP Red pulp

PT Portal tracts
LAP Lamina propria
AW Alveolar walls
BRO Bronchioles
ZG Zona glomerulosa
ZF Zona fasciculata
ZR Zona reticularis

Table 8.1D Distribution of CD11b$^+$ & CD3$^+$ uninfected cells in a calf (20) infected with *T. annulata* (Hisar) on day 14 post-infection

Figure 8.7 Section showing CD11b$^+$ cells (pink) in the white pulp (WP) of the spleen of the calf infected with *T. annulata* (Hisar) on day 14 post-infection at the nadir of disease, (x40: MAb IL-A15 & Vector Red).

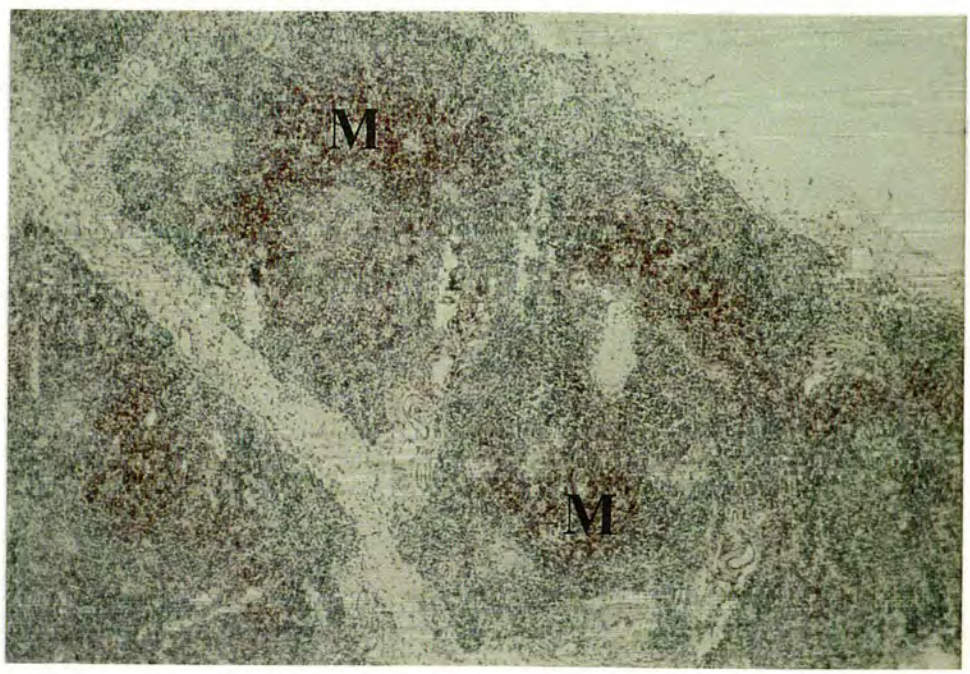

Figure 8.8 Section showing CD11b$^+$ cells (pink) in the medulla (M) of the thymus of the calf infected with *T. annulata* (Hisar) on day 14 post-infection at the nadir of disease, (x40: MAb IL-A15 & Vector Red).

8.8). An increase in the number of uninfected CD11b$^+$ cells was seen in the cortex of the kidney, alveolar walls of the lung, the adrenal and pituitary glands (Figure 8.9). An increase in the number of infected and uninfected CD11b$^+$ cells was seen in these organs.

A decrease in the number of uninfected CD3$^+$ cells was found in the paracortex of most lymph nodes (Figure 8.10) and the cortex of the thymus (Figure 8.11). An increase in the number of uninfected CD3$^+$ cells was seen in the red pulp of the spleen. An increase in the number of uninfected CD3$^+$ cells was observed in the cortex and medulla of the kidney (Figure 8.12), alveolar walls of the lung, the heart, adrenal (Figure 8.13) and pituitary glands.

8.4.1.4 DISTRIBUTION OF INFECTED & UNINFECTED CD11B$^+$ & UNINFECTED CD3$^+$ CELLS IN A CALF (861) DURING THE TERMINAL STAGES OF INFECTION WITH T. ANNULATA (DOUKKALLA)

On day 24 post-infection during the terminal stages of disease in calf 861 [Table 8.1E] an increase in the number of uninfected CD11b$^+$ cells was seen in the medullary cords of most lymph nodes, both the white and red pulp of the spleen and throughout the thymus. An increase in the number of uninfected CD11b$^+$ cells was found in the cortex and medulla of the kidney, portal tracts of the liver and alveolar walls of the lung. A marked increase in the number of uninfected CD11b$^+$ cells was seen in the lamina propria of the abomasum (Figure 8.14) and the superficial dermis of the skin (Figure 8.15). An increase in the number of infected and uninfected CD11b$^+$ cells was seen in these organs, with the exception of the lung.

A decrease in the number of uninfected CD3$^+$ cells was found in the paracortex of all the lymph nodes (Figure 8.16), the white pulp of the spleen and throughout the thymus. In contrast, an increase in the number of uninfected CD3$^+$ cells was seen in the red pulp of the spleen. An increase in the number of uninfected CD3$^+$ cells was also found in the cortex and medulla of the kidney, alveolar walls of the lung and the superficial dermis of the skin.

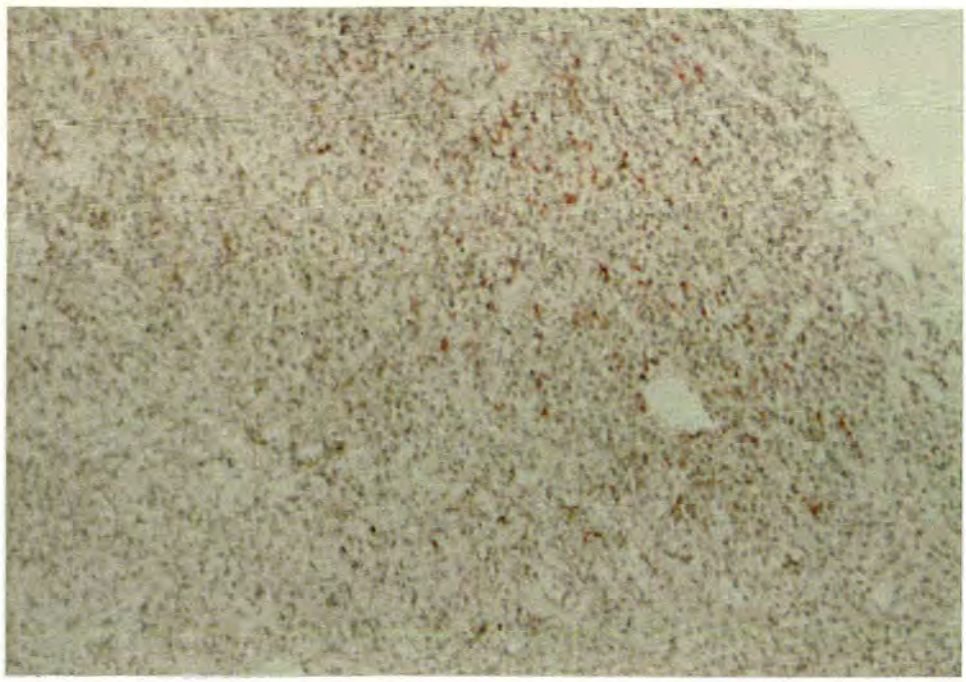

Figure 8.9 Section showing $CD11b^+$ cells (pink) in the pituitary gland of the calf infected with *T. annulata* (Hisar) on day 14 post-infection at the nadir of disease, (x100: MAb IL-A15 & Vector Red).

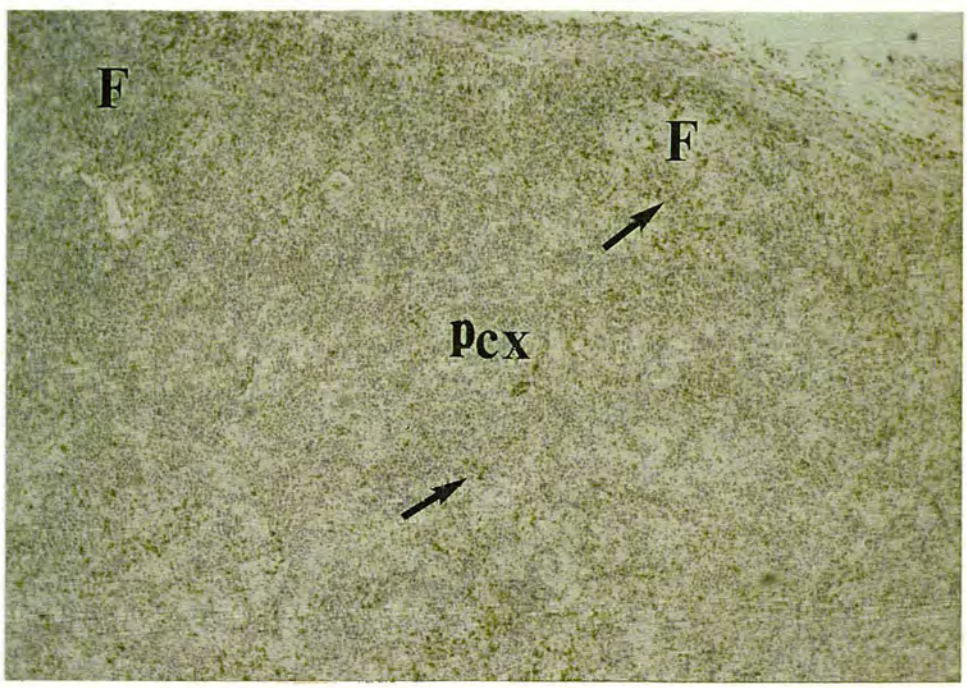

Figure 8.10 Section showing $CD3^+$ cells (arrows) in the lymphoid follicles (F) and paracortex (PCX) of the draining prescapular lymph node of the calf infected with *T. annulata* (Hisar) on day 14 post-infection at the nadir of disease, (x40: polyclonal antibody A452 & DAB).

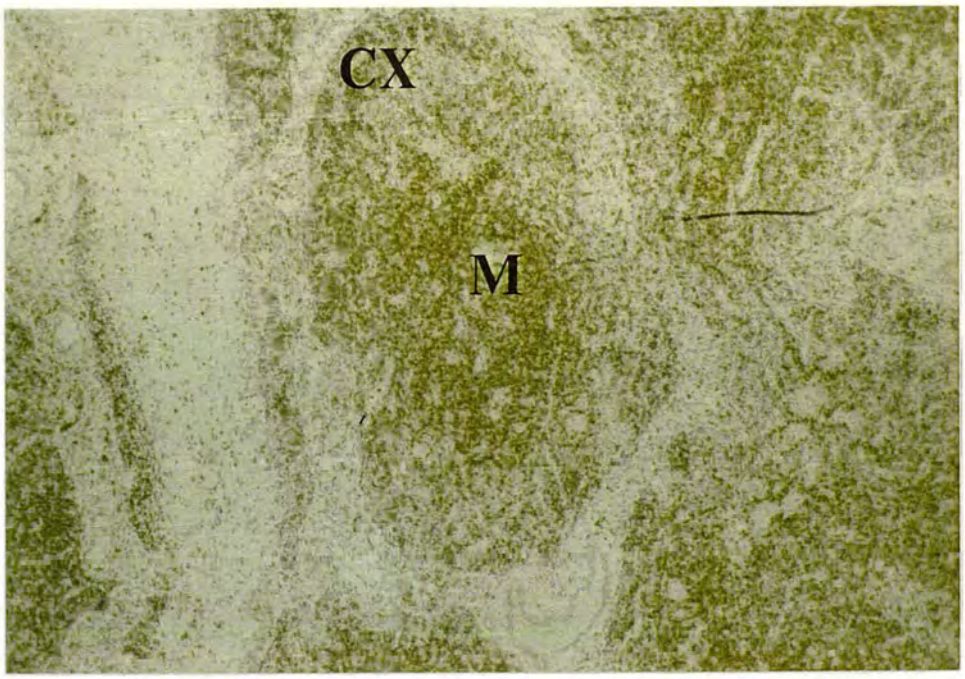

Figure 8.11 Section showing $CD3^+$ cells (brown) in the cortex (CX) and medulla (M) of the thymus of the calf infected with *T. annulata* (Hisar) on day 14 post-infection at the nadir of disease, (x40: polyclonal antibody A452 & DAB).

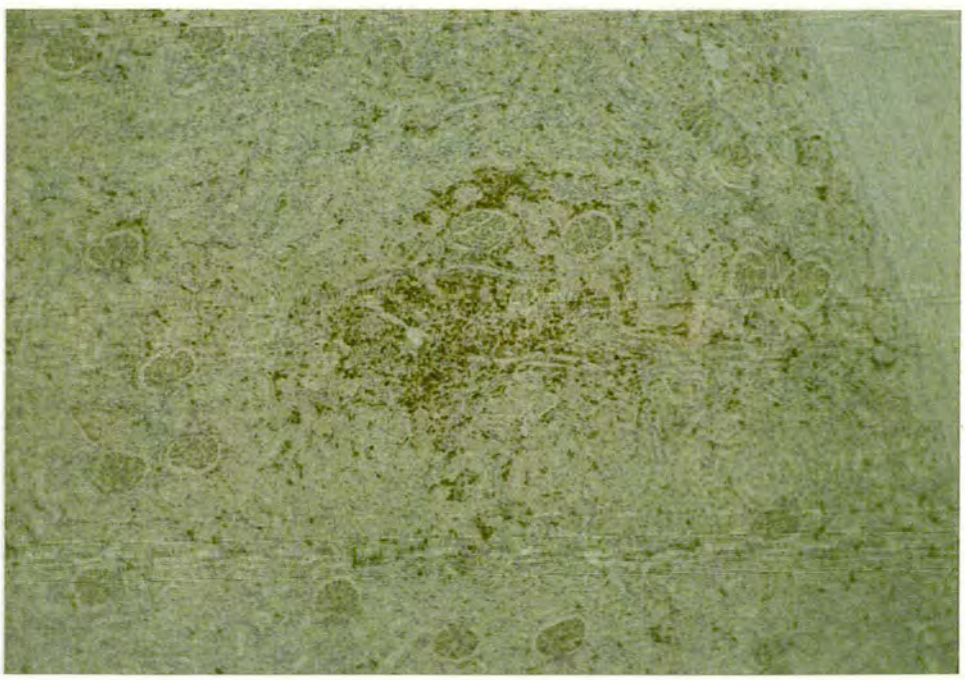

Figure 8.12 Section showing $CD3^+$ cells (brown) in the cortex of the kidney of the calf infected with *T. annulata* (Hisar) on day 14 post-infection at the nadir of disease, (x40: polyclonal antibody A452 & DAB).

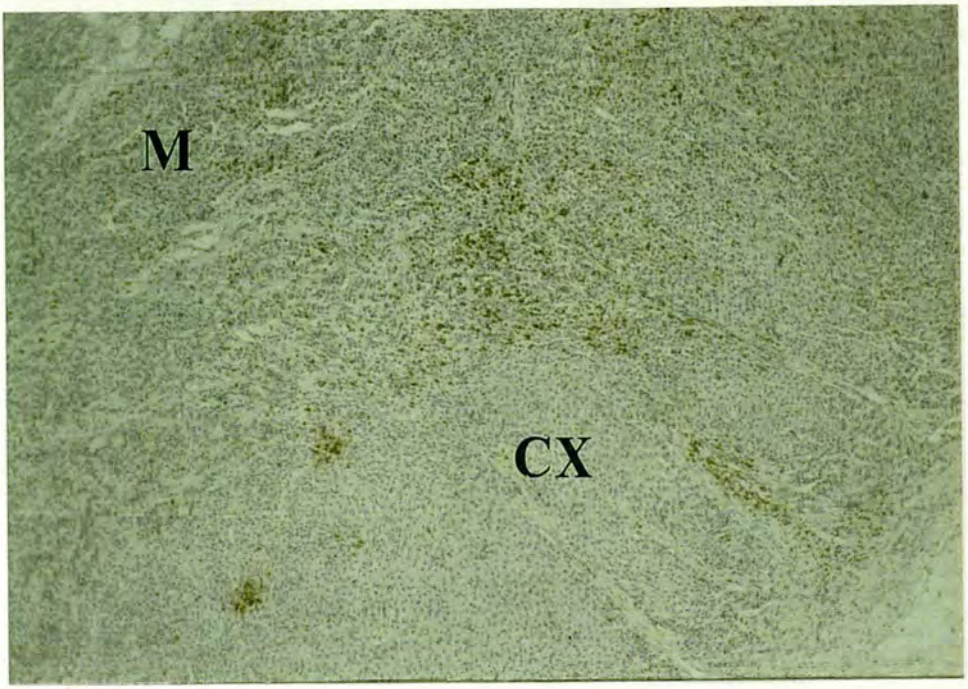

Figure 8.13 Section showing $CD3^+$ cells (brown) throughout the cortex (CX) and medulla (M) of the adrenal gland of the calf infected with *T. annulata* (Hisar) on day 14 post-infection at the nadir of disease, (x40: polyclonal antibody A452 & DAB).

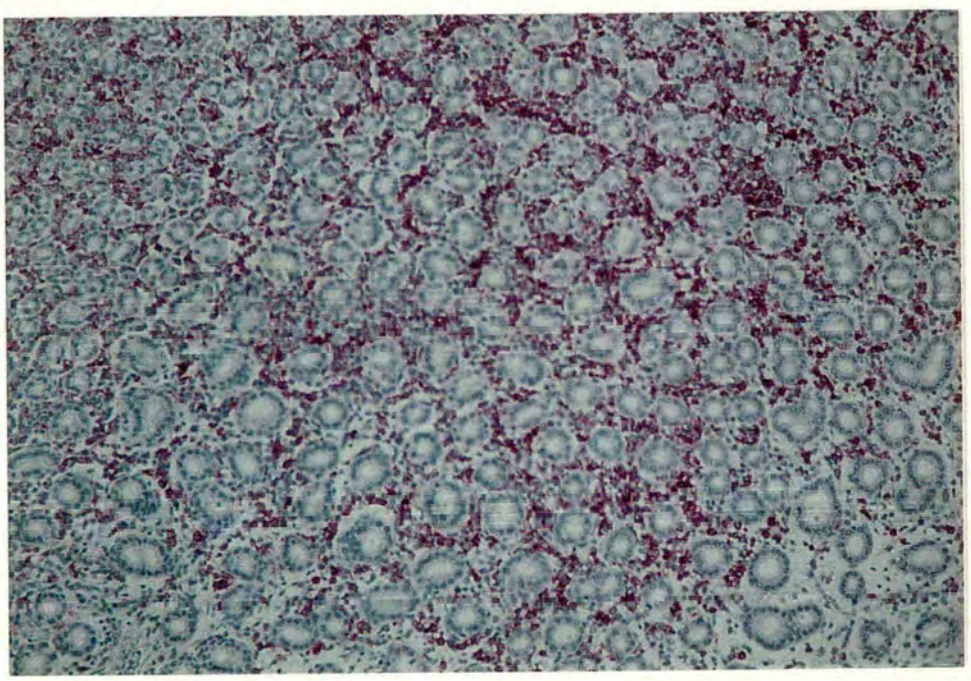

Figure 8.14 Section showing $CD11b^+$ cells (pink) in the abomasum of the calf infected with *T. annulata* (Doukkalla) on day 24 post-infection during the terminal stages of disease, (x100: MAb IL-A15 & Vector Red).

ORGAN	AREA	CD11b$^+$	CD3$^+$	SIC	Ratio U : SIC
Prescapular LN (draining)	CX	nc	-	**	U > SIC
	PCX	+	--	***	
	MC	nc	-	*	
	MS	nc	-	***	
Prescapular LN (contralateral)	CX	nc	-	*	U > SIC
	PCX	nc	--	*	
	MC	++	nc	*	
	MS	nc	nc	*	
Precrural LN (draining)	CX	nc	-	*	U > SIC
	PCX	nc	--	*	
	MC	++	nc	*	
	MS	nc	nc	*	
Precrural LN (contralateral)	CX	nc	-	**	U > SIC
	PCX	nc	--	**	
	MC	+++	nc	*	
	MS	nc	nc	*	
Mesenteric LN	CX	+	nc	*	U > SIC
	PCX	nc	--	*	
	MC	++	nc	*	
	MS	nc	nc	*	
Spleen	WP	+	-	*	U > SIC
	RP	+	+	*	
Thymus	CX	+	--	*	U > SIC
	MED	+++	--	***	

nc No change
- Small decrease
-- Moderate decrease
--- Large decrease

+ Small increase
++ Moderate increase
+++ Large increase

nd None detected
* Small numbers
** Moderate numbers
*** Large numbers

ORGAN	AREA	CD11b$^+$	CD3$^+$	SIC	Ratio U : SIC
Kidney	CX	+	++	*	U = SIC
	MED	+	++	*	
Liver	PT	+	nc	*	U = SIC
Abomasum	LAP	+++	nc	*	U < SIC
Lung	AW	+	+	*	U > SIC
	BRO	nc	nc	nd	
Skin	SDER	+++	++	***	U < SIC

U Uninfected cells
SIC Schizont-infected cells
LN Lymph node
na Not applicable

CX Cortex
PCX Paracortex
MED Medulla
MC Medullary cords
MS Medullary sinuses
WP White pulp
RP Red pulp

PT Portal tracts
LAP Lamina propria
AW Alveolar walls
BRO Bronchioles
SDER Superficial dermis

Table 8.1E Distribution of CD11b$^+$ & CD3$^+$ uninfected cells in a calf (861) infected with *T. annulata* (Doukkalla) on day 24 post-infection

Figure 8.15 Section showing $CD11b^+$ cells (pink) in the superficial dermis of the skin of the calf infected with *T. annulata* (Doukkalla) on day 24 post-infection during the terminal stages of disease, (x40: MAb IL-A15 & Vector Red).

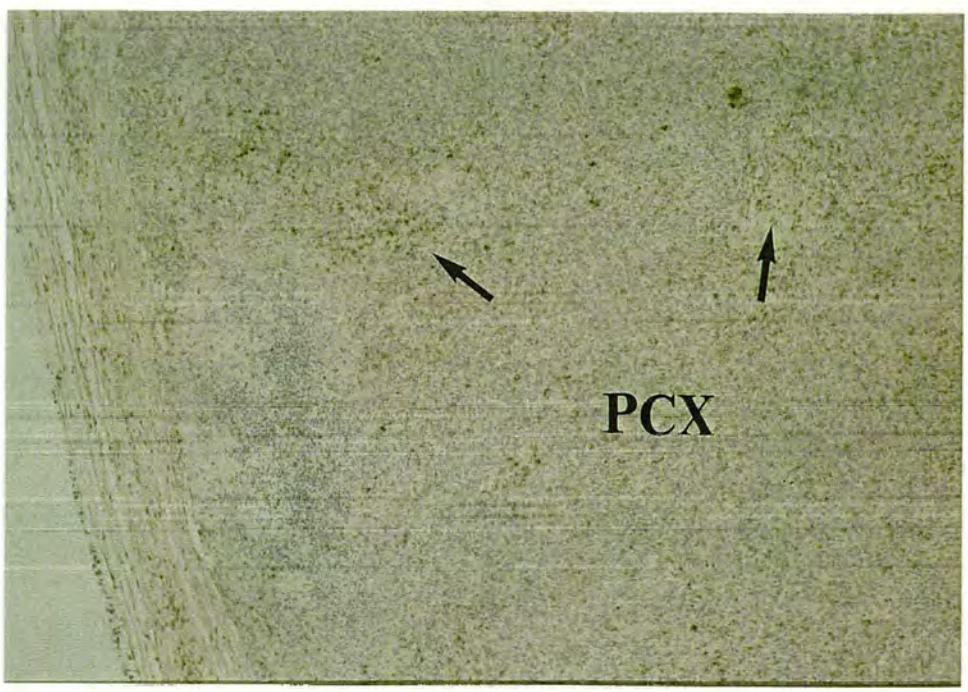

Figure 8.16 Section showing $CD3^+$ cells (arrows) in the paracortex (PCX) of the draining prescapular lymph node of the calf infected with *T. annulata* (Doukkalla) on day 24 post-infection during the terminal stages of disease, (x40: polyclonal antibody A452 & DAB).

8.4.1.5 DISTRIBUTION OF INFECTED & UNINFECTED CD11B$^+$ & CD3$^+$ CELLS IN A CALF (8) DURING THE TERMINAL STAGES OF INFECTION WITH T. PARVA (MUGUGA)

On day 21 post-infection during the terminal stages of disease in calf 8 [Table 8.1F] an increase in the number of uninfected CD11b$^+$ cells was seen in the medullary cords of all the lymph nodes (Figure 8.17), both the white and red pulp of the spleen and throughout the thymus (Figure 8.18). A decrease in the number of uninfected CD11b$^+$ cells was found in the paracortex of the draining prescapular LN. An increase in the number of uninfected CD11b$^+$ cells was found in the portal tracts of the liver, lamina propria of the abomasum and alveolar walls of the lung.

A decrease in the number of uninfected CD3$^+$ cells was found in the paracortex of all the lymph nodes (Figure 8.19), the white pulp of the spleen and throughout the thymus (Figure 8.20). In contrast, an increase in the number of uninfected CD3$^+$ cells was seen in the red pulp of the spleen. An increase in the number of uninfected CD3$^+$ cells was also found in the cortex and medulla of the kidney, alveolar walls of the lung, the heart and throughout the adrenal gland.

ORGAN	AREA	CD11b$^+$	CD3$^+$	SIC	Ratio U : SIC
Prescapular LN (draining)	CX	nc	nc	***	U > SIC
	PCX	-	--	***	
	MC	++	nc	***	
	MS	nc	nc	***	
Prescapular LN (contralateral)	CX	nc	nc	*	U > SIC
	PCX	nc	--	*	
	MC	++	nc	*	
	MS	nc	nc	*	
Precrural LN (draining)	CX	nc	nc	*	U > SIC
	PCX	nc	--	*	
	MC	++	nc	*	
	MS	nc	nc	*	
Precrural LN (contralateral)	CX	nc	nc	*	U > SIC
	PCX	nc	--	*	
	MC	+	nc	*	
	MS	nc	nc	*	
Mesenteric LN	CX	nc	nc	*	U > SIC
	PCX	nc	--	*	
	MC	++	nc	*	
	MS	nc	nc	*	
Hepatic LN	CX	nc	nc	*	U > SIC
	PCX	nc	--	*	
	MC	+	nc	*	
	MS	nc	nc	*	
Spleen	WP	++	--	*	U > SIC
	RP	+	+	*	
Thymus	CX	+	--	*	U > SIC
	MED	+++	-	**	

nc No change
- Small decrease
-- Moderate decrease
--- Large decrease

+ Small increase
++ Moderate increase
+++ Large increase

nd None detected
* Small numbers
** Moderate numbers
*** Large numbers

ORGAN	AREA	CD11b$^+$	CD3$^+$	SIC	Ratio U : SIC
Kidney	CX	nc	+	*	U > SIC
	MED	nc	+	*	
Liver	PT	++	nc	*	U > SIC
Abomasum	LAP	+	nc	nd	U > SIC
Lung	AW	+	++	*	U > SIC
	BRO	+	nc	nd	
Heart	GEN	nc	+	*	U > SIC
Adrenal gland	ZG	nc	+	nd	U > SIC
	ZF	nc	+	nd	
	ZR	nc	+	nd	
	MED	nc	+	nd	

U Uninfected cells
SIC Schizont-infected cells
LN Lymph node
na Not applicable

GEN General
CX Cortex
PCX Paracortex
MED Medulla
MC Medullary cords
MS Medullary sinuses
WP White pulp
RP Red pulp

PT Portal tracts
LAP Lamina propria
AW Alveolar walls
BRO Bronchioles
ZG Zona glomerulosa
ZF Zona fasciculata
ZR Zona reticularis

Table 8.1F Distribution of CD11b$^+$ & CD3$^+$ uninfected cells in a calf (8) infected with *T. parva* (Muguga) on day 21 post-infection

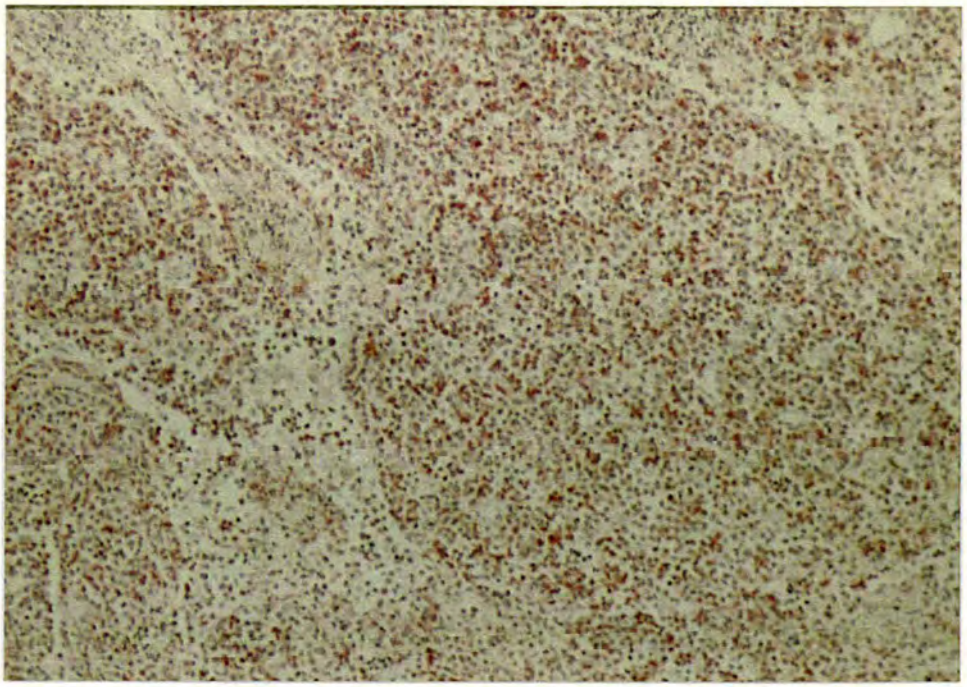

Figure 8.17 Section showing CD11b$^+$ cells (pink) in the medulla of the draining prescapular lymph node of the calf infected with *T. parva* (Muguga) on day 21 post-infection during the terminal stages of disease, (x100: MAb IL-A15 & Vector Red).

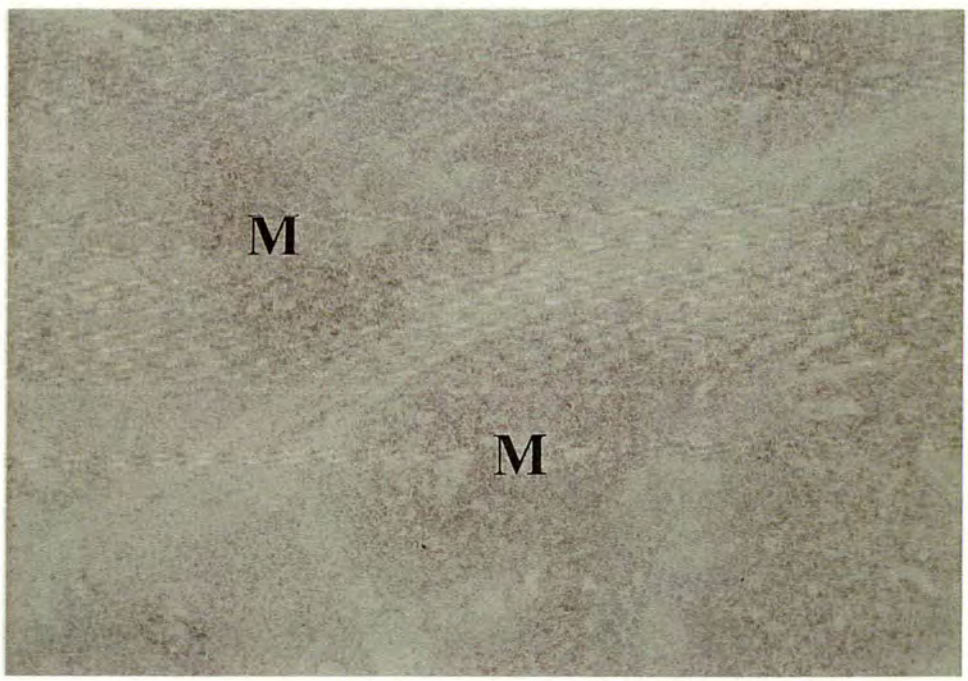

Figure 8.18 Section showing CD11b$^+$ cells (pink) in the medulla (M) of the thymus of the calf infected with *T. parva* (Muguga) on day 21 post-infection during the terminal stages of disease, (x40: MAb IL-A15 & Vector Red).

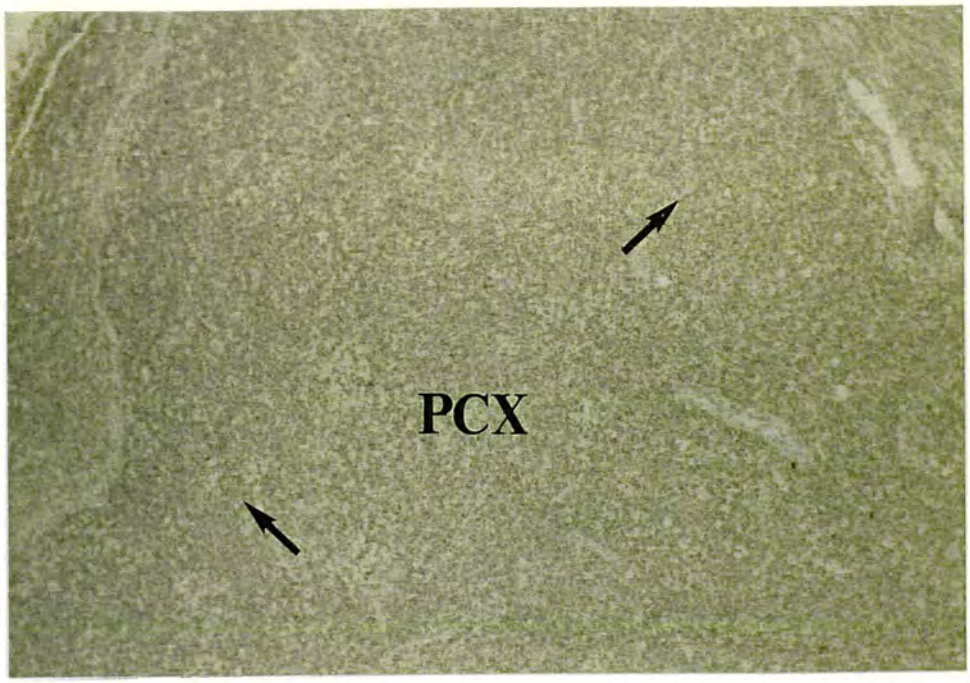

Figure 8.19 Section showing $CD3^+$ cells (arrows) in the paracortex (PCX) of the draining prescapular lymph node of the calf infected with *T. parva* (Muguga) on day 21 post-infection during the terminal stages of disease, (x40: polyclonal antibody A452 & DAB).

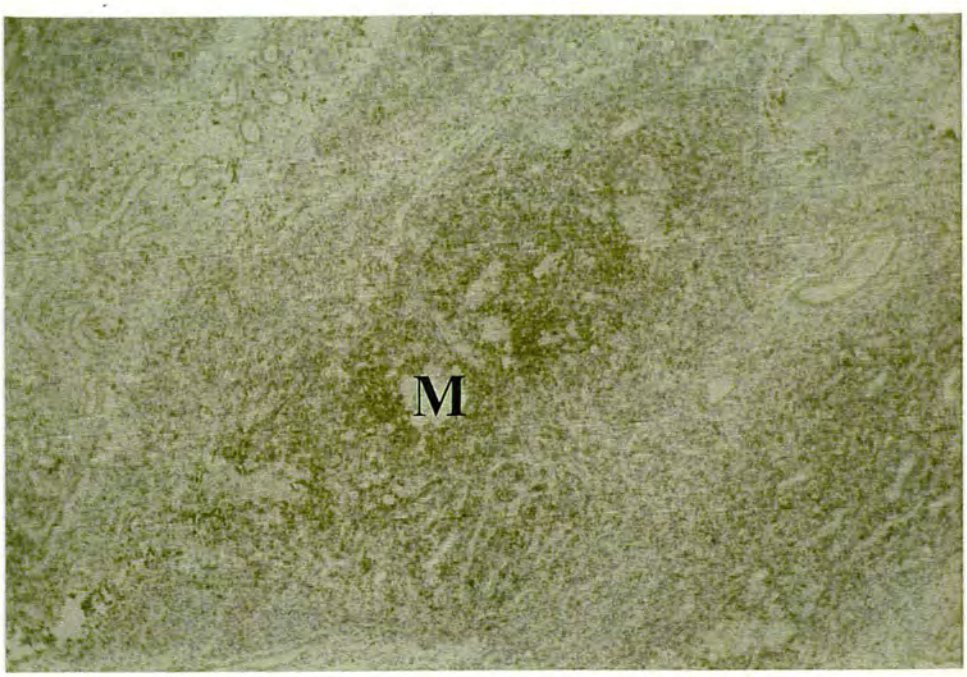

Figure 8.20 Section showing $CD3^+$ cells (brown) in the medulla (M) of the thymus of the calf infected with *T. parva* (Muguga) on day 21 post-infection during the terminal stages of disease, (x40: polyclonal antibody A452 & DAB).

8.5 DISCUSSION

The number of uninfected $CD11b^+$ cells increased in the lymphoid organs of cattle infected with *T. annulata* or *T. parva* (Muguga), in particular within the medullary cords of the lymph nodes. These $CD11b^+$ cells were small with a dense cytoplasm. In contrast, the extensive infiltration of large macrophage-like cells in the medullary sinuses of the lymph nodes in both types of infection did not stain for CD11b. Morphologically the $CD11b^+$ cells present in the medullary cords were not macrophage-like and may have been B and/or NK cells. These observations were interesting since the lymphoid follicles of most of these lymph nodes were either absent or reduced in size with small germinal centres.

The number of uninfected $CD3^+$ cells, particularly in the paracortex of the lymph nodes and the cortex of the thymus, decreased in the lymphoid organs of cattle infected with *T. annulata* or *T. parva* (Muguga). Examination of the lymphoid organs from the cattle infected with *T. annulata* (Hisar) during the initial stages of pyrexia, peak pyrexia and nadir of disease showed no signs of paracortical lymphoproliferation. These findings confirmed the occurrence of lymphoid cellular depletion as described in chapter 4 but conflicted with reports that lymphoproliferation occurs in lymph nodes of *T. annulata* infected animals (Irvin & Morrison 1987; Eisler 1988).

The number of uninfected $CD11b^+$ cells and uninfected $CD3^+$ cells increased in the non-lymphoid organs of cattle infected with *T. annulata* or *T. parva* (Muguga). This observation suggested that parasite proliferation was accompanied by the infiltration of myeloid and lymphoid cells.

The distribution of uninfected $CD11b^+$ and $CD3^+$ cells throughout the lymphoid and non-lymphoid organs of the animals infected with *T. annulata* or *T. parva* (Muguga) were similar. However, the paracortex of the draining prescapular lymph node of the two different infections contained morphologically different types of $CD11b^-$ and $CD3^-$ cells. Large numbers of macrophage-like cells ($CD11b^-/CD3^-$) were seen in the lymph nodes of the *T. annulata* infected cattle, whereas large numbers of lymphocyte-like cells ($CD11b^-/CD3^-$) were seen in the lymph node of the *T. parva*

(Muguga) infected animal. The identity of these populations of $CD11b^-$ and $CD3^-$ cells remains unknown due to the limited availability of antibodies which could stain bovine leucocyte antigens on paraffin sections of the tissues of the infected animals.

8.6 CONCLUSION

In the lymphoid organs of both the *T. annulata* and *T. parva* (Muguga) infected animals the use of MAb IL-A15 indicated that an increase in the number of B and/or NK cells occurred in the medullary cords of the lymph nodes. The use of polyclonal antibody A452 (a marker for T cells) indicated that lymphoid cellular depletion had occurred as early as day 7 as well as during the latter stages of *T. annulata* infection. No evidence of lymphoproliferation was seen in any of the lymph nodes from animals infected with *T. annulata* described here. The numerous infiltrating cells in the lymphoid organs of both the *T. annulata* and *T. parva* (Muguga) infected animals still remain unidentified. In the non-lymphoid organs of both the *T. annulata* and *T. parva* (Muguga) infected animals the number of both uninfected $CD11b^+$ and $CD3^+$ cells had increased suggesting that the non-lymphoid organs had been infiltrated with both myeloid and lymphoid cells.

CHAPTER NINE

CONTRIBUTION OF NITRIC OXIDE & APOPTOSIS TO THE PATHOLOGY OF BOVINE THEILERIOSES

9.1 INTRODUCTION

Apoptosis, also known as programmed cell death, has been increasingly recognised in pathological situations (Williams, Smith, McCarthy & Grimes 1992; Carson & Ribeiro 1993) and several of the mediators known to induce apoptosis in other systems (Deckers, Lyons, Samuel, Sanderson & Maddy 1993; Albina *et al.* 1993; Sarih *et al.* 1993) have already been demonstrated in calves undergoing bovine theileriosis. These mediators included nitric oxide (NO) (Visser *et al.* 1995; 3.4.4), tumour necrosis factor alpha (TNF-α), both produced by macrophages, and interferon gamma (IFN-γ), produced by NK cells and T cells, which is known to activate macrophages to synthesise NO and TNF-α (Preston *et al.* 1993).

The contribution of apoptosis to the pathology observed in calves undergoing severe infections with *T. annulata* or *T. parva* (Muguga) was therefore examined. Since little work had been done on apoptosis in cattle the work began by looking for appropriate techniques with which to monitor apoptosis *in vivo* and *in vitro*. The existence of techniques for the establishment and maintenance of uninfected bovine cell lines and *Theileria* infected bovine cell lines *in vitro* (Brown 1983) permitted NO and its capacity to induce apoptosis in bovine cells to be investigated *in vitro*.

9.2 EXPERIMENTAL DESIGN

Flow cytometry was assessed as a way of detecting apoptosis in suspensions of bovine peripheral blood mononuclear cells (PBM) or thymocytes. PBM were obtained from a *T. parva* (Muguga) infected calf and from an uninfected calf. The thymocytes were obtained from a normal calf. Compounds known to induce apoptosis in cells of other species were used in an attempt to induce apoptosis in suspensions of bovine PBM and thymocytes.

In situ hybridisation based on TdT-mediated-dUTP-biotin nick end labelling (TUNEL) (Gavrieli, Sherman & Ben-Sasson 1992) was assessed as a way of

detecting apoptotic cells in paraffin tissue sections of bovine tissues. Tissues were obtained from a *T. annulata* calf and from a normal calf.

The effects of NO on uninfected and *Theileria*-infected bovine cells were assessed in two ways: by analysing the induction of apoptosis in cell lines treated with S-nitroso-N-acetyl-DL-penicillamine (SNAP), a NO releasing molecule; by monitoring proliferation of cell lines treated with SNAP. Apoptosis was analysed by cytospin preparations stained with Giemsa's stain; proliferation was monitored by the incorporation of tritiated thymidine. Levels of NO (monitored as nitrite) were assessed by the Griess assay. The BL20 cell line was used to assess the effect of NO on uninfected cells; a BL20 cell line infected with *T. annulata* (Hisar) and a *T. annulata* (Ankara) cell line derived from PBM was used to assess the effect on *Theileria*-infected cell lines.

9.3 MATERIALS & METHODS

9.3.1 CALVES

The following *Bos taurus* calves were used: an uninfected 24 month old Friesian male calf (26) from Easter Bush Farm; a 4 month old Ayrshire male calf (805) from Blythbank Farm challenged with sporozoites of *T. parva* (Muguga) and assessed during the nadir of disease; a 1 month old Friesian male calf (41B; Table 3.1).

9.3.2 CELL LINES & MAINTENANCE

Three cell lines were used: a transformed bovine lymphosarcoma cell line (BL20) (Morzaria, Roeder, Roberts, Chasey & Drew 1984) which multiplies rapidly in culture; a cell line of BL20 infected with *T. annulata* (Hisar) (TaH BL20); the uncloned Ankara stock of *T. annulata* established as a macroschizont-infected cell line in PBM of calf 2 (TaAnk 2). Cell lines were established as described previously (Brown 1983) at the Institute of Cell, Animal and Population Biology, University of Edinburgh. They were maintained by routine culture in RPMI-1640 supplemented with L-glutamine (2mM), penicillin (100μg/ml), streptomycin (100μg/ml) and 20% foetal calf serum (GIBCO BRL) (complete medium) and cultured in a humidified atmosphere of 5% CO_2 in air at 37^0C (Preston *et al.* 1983).

9.3.3 ASSESSMENT OF APOPTOSIS IN BOVINE PBM & THYMOCYTES BY FLOW CYTOMETRY

In brief, apoptosis was looked for in cells from infected and uninfected calves cultured with medium alone, methylprednisolone, adenosine or SNAP. Apoptosis was detected with ethidium bromide staining and the phenotype of the apoptotic cells was identified with MAb CC42, which detected CD2, and FITC labelled sheep anti-mouse IgG. The cells undergoing the initial phase of apoptosis were observed as populations that stained faintly with ethidium bromide. Subsequent death of the cells was indicated by a characteristic bright staining with ethidium bromide. Apoptosis was examined in cells as soon as they had been isolated from the animal (Time 0) and in cells cultured *in vitro* for either 8 hours or 20 hours.

9.3.3.1 CULTURE OF PBM & THYMOCYTES

Jugular blood was taken into vacutainer tubes containing lithium heparin 14iu/ml (Becton Dickinson) for the isolation of PBM (Preston *et al.* 1993) [Appendix II]. A thymus was obtained by Mr. Alan Cameron from the Gorgie abattoir for the isolation of thymocytes [Appendix XV]. Whole cultures of PBM and thymocytes were initiated by culturing 1 x 10^7 cells/10ml (2 x 10^5 cells/200µl well) in sterile 96-well round-bottomed, microtitre plates (NUNC) in RPMI-1640 with 10% foetal calf serum (FCS) (Gibco BLR). The technique used to assess apoptosis was based upon that described by Deckers *et al.* 1993. Cells were cultured in the presence of medium alone and in the following three compounds known to induce apoptosis in murine and human cells which included: (I) methylprednisolone (Sigma), a glucocorticoid hormone (Cohen & Duke 1984; Deckers *et al.* 1993), at a final concentration of 1 x 10^{-2}M, 1 x 10^{-3}M, 1 x 10^{-4}M, 1 x 10^{-5}M and 1 x 10^{-6}M; (ii) adenosine (Sigma), a de-phosphorylated nucleotide (Szondy 1994), at a final concentration of 10mM, 5mM, 1mM, 0.5mM and 0.1mM; (iii) SNAP (Amersham Life Sciences), a compound that generates NO when added to culture medium (Ignarro, Lipton, Edwards, Baricos, Hyman, Kadowitz & Gruetter 1981; Croen 1993; Albina *et al.* 1993; Sarih *et al.* 1993), at a final concentration of 2.3mM, 1.15mM, 0.46mM, 0.23mM and 0.005mM. All samples and controls were tested in duplicate. Cultures were maintained in a humidified atmosphere of 5% CO_2 in air at 37^0C. Cell cultures were harvested at 0, 8 and 20h into 96-well round-bottomed, microtitre plates (NUNC) and stored at 4^0C until assessed.

9.3.3.2 FLOW CYTOMETRY

The microtitre plate containing cell cultures was centrifuged (MSE Mistral 3000) at 2000 g. for 4 minutes at 5^0C and the cell pellets were resuspended and washed in 200µl RPMI alone. Resuspended cells were washed in 200µl FACS medium (5% FCS/RPMI plus 0.1% sodium azide) before incubation in 50µl neat culture supernatant of an anti-pan T cell MAb CC42 (Howard & Naessens 1993) and 100µl FACS medium for 45 minutes at 4^0C. Cells were washed three times in 200µl FACS medium before incubation in 100µl sheep anti-mouse IgG-FITC (1:20) (SAPU) and 100µl ethidium bromide (1 x 10^{-6}g/ml) (Sigma) for 40 minutes at 4^0C. Cells were finally washed three times in FACS medium, resuspended in 200µl FACS medium and transfered to FACS tubes for analysis. Control wells comprised medium alone, medium with MAb CC42 and sheep anti-mouse IgG-FITC or medium with ethidium bromide.

Flow cytometric (FACS) data were obtained from a FACScan (Becton Dickinson, FACS systems) using an argon ion laser of 488nm wavelength with an output of 400mW. An electronic gate was applied before acquisition of cells to exclude electronic noise and cell debris. Cells were assessed using stored parameters demonstrated previously to be suitable for use with bovine PBM and thymocytes. Normally 10,000 cells were analysed at a rate of approximately 2000 cells per second with logarithmic amplification of fluorescence detection and side scatter; linear amplification of forward scatter. All acquisition and analysis of cells were performed using LYSIS II software. Overlap in the emission spectra of ethidium bromide and FITC was removed by electronic compensation.

Viable and apoptotic cells were distinguished by examining the forward scatter and ethidium bromide fluorescence of cells. T and B populations of apoptotic cells were assessed using FITC labelled MAb staining of ethidium bromide stained cells. Fluorescence plots of FITC fluorescence (X-axis) against ethidium bromide fluorescence (Y-axis) revealed distinct populations of cells undergoing apoptosis. Apoptosis was revealed as an increase in ethidium bromide fluorescence (Y-axis), i.e. ethidium bromide bright cells (Lyons, Samuel, Sanderson & Maddy 1992).

9.3.4 ASSESSMENT OF APOPTOSIS IN PARAFFIN TISSUE SECTIONS BY TUNEL & ABC/HRP IMMUNOCYTOCHEMICAL TECHNIQUES

In brief, the TUNEL technique [Appendix XVI] was used to identify apoptotic cells in paraffin tissue sections (Gavrieli *et al.* 1992). This technique was based upon the incorporation of biotinylated deoxyuridine (bio-dUTP) by terminal deoxynucleotidyl transferase (TdT) at sites of nuclear DNA breaks characteristic of apoptotic cell nuclei. The signal was amplified by the avidin/biotin complex (ABC) horseradish peroxidase (HRP) immunocytochemical techniques and Harris's haematoxylin counterstain which enabled apoptotic cells and other host cells to be identified by light microscopy.

9.3.4.1 TUNEL ON PARAFFIN TISSUE SECTIONS

Several paraffin tissue sections underwent proteolytic treatment with 20μg/ml proteinase K (Sigma) to expose nuclear DNA and were immersed in TdT buffer (30mM Trizma base, pH 7.2 (Sigma), 140mM sodium cacodylate (Fisons), 1mM cobalt chloride (Sigma)) prior to incubation in TdT (24e.u./μl) (Pharmacia) and biotinylated dUTP (0.3mM) (Sigma) in TdT buffer. The reaction was terminated by incubation in TB buffer (300mM sodium chloride (Sigma), 30mM sodium citrate (Fisons) prior to incubation in an avidin/biotinylated horseradish peroxidase complex (ABC/HRP) (DAKO) and visualised by peroxidase substrate chromogen 3, 3'-diaminobenzidine tetrahydrochloride (DAB) (DAKO).

9.3.5 ASSESSMENT OF APOPTOSIS IN CELL LINES EXPOSED TO NITRIC OXIDE

In brief, test cultures were exposed to SNAP and control cultures were incubated in either medium alone, medium plus sodium nitrite ($NaNO_2^-$) (Sigma) or medium plus DL-penicillamine (Sigma). These control cultures were included to confirm that any effects were due to the production of NO by SNAP and not to the nitrite (NO_2^-) ions produced by degradation of the NO so produced or to the penicillamine component of SNAP. The effects of NO on the cell cultures were analysed visually by cytospin preparations stained with Giemsa's stain and by assessing cell proliferation as monitored by the incorporation of tritiated thymidine.

9.3.5.1 CULTURE OF CELL LINES FOR THE EFFECT OF NITRIC OXIDE

Cell lines were established in complete medium (9.3.2) in 96-well flat-bottomed, microtitre plates (NUNC). The cell line BL20 was established at a concentration of $2x10^5$ cells/200µl; the cell lines TaH BL20 and TaAnk 2 at concentrations of $2x10^4$ cells/200µl. SNAP, $NaNO_2^-$ and penicillamine were made up in medium and used at three concentrations; 20µl of additive was added to the appropriate well to give the required concentration (1000µM, 200µM, 40µM). All cultures were maintained in a humidified atmosphere of 5% CO_2 in air at 37^0C. Aseptic techniques were used throughout to avoid contamination.

Three sets of plates were set up. In the first set, each cell line was cultured with the appropriate concentrations of the three additives SNAP, $NaNO_2^-$ and penicillamine and apoptosis was assessed after 3 hours and 20 hours incubation by cytospin preparations stained with Giemsa's stain (tests carried out in duplicate). In the second set, cell lines were cultured in the three additives and proliferation was assessed by the addition of tritiated thymidine (185GBq/mM methyl-^{3}H-thymidine) (Amersham Life Sciences) 18. 5KBq in 20µl medium/well. Cultures were harvested after 20 hours incubation, see below (tests carried out in six replicates). In the third set, the three additives were incubated in medium alone and the levels of NO_2^- in the wells were assessed by the Griess assay after 20 hours incubation, see below (tests carried out in six replicates).

9.3.5.2 DETECTION OF APOPTOSIS, CELL DEATH & SCHIZONTS IN CYTOSPIN PREPARATIONS

Cytospin preparations were made in duplicate using a Shandon centrifuge and fixed in absolute methanol prior to staining with Giemsa's stain [Appendix I]. Apoptosis, cell death and schizonts were assessed visually by counting 200 or more cells. Cells that had undergone apoptosis were identified by the characteristic formation of condensed bodies of nuclear material (Kerr *et al.* 1972; Wyllie *et al.* 1980). The numbers of apoptotic cells, dead cells and schizonts were expressed as percentages of the total cell counts.

9.3.5.3 ASSESSMENT OF PROLIFERATION BY THE INCORPORATION OF TRITIATED THYMIDINE

Cell cultures from 96-well round-bottomed, microtitre plates were harvested onto filter paper using a Titertek multiple cell harvester. The filter papers were air-dried and added to scintillation tubes containing 1ml of toluene (Popop (0.05g/l) plus 2, 5-Diphenyl-oxazole (6g/l) (Sigma)). The incorporation of tritium by the cells was measured as disintegrations per minute (dpm) using a liquid scintillation analyzer (TRI-CARB, 2000CA, United Technologies Packard). A reduction in the incorporation of tritium by the cells incubated with an additive as compared to incorporation by the cells incubated in medium alone was taken to mean an inhibition in proliferation. Differences in incorporation of tritium by test and control cultures were analysed by the Mann Whitney test for non-parametric data (Siegel 1976). Only when $p<0.05$ has the term significant been used in the text. Alterations in proliferation of cultures in the presence of additives as compared to proliferation in medium alone were expressed as a percentage inhibition or enhancement of growth calculated from the following formula: 100- (mean dpm plus additive/mean dpm in medium alone x100).

9.3.5.4 DETECTION OF NITRIC OXIDE PRODUCTION BY THE GRIESS ASSAY

The amount of NO_2^- produced by SNAP, $NaNO_2^-$ and penicillamine was assessed by the Griess assay (3.3.4.2), except that doubling dilutions of $NaNO_2^-$, 0 to 2000μM in culture medium were used to generate the standard curve [Appendix XVII]. Samples and standards were tested in six replicates.

9.4 RESULTS

9.4.1 ASSESSMENT OF APOPTOSIS IN BOVINE PBM & THYMOCYTES BY FLOW CYTOMETRY

No differences were observed in the levels of apoptosis recorded in cells from the uninfected and infected calves. The B cell populations of both the infected and uninfected calves cultured with medium alone were apoptotic after 8 hours and 20 hours incubation *in vitro* (Figure 9.1). The T cell population of both calves had already undergone apoptosis at time 0 (Figure 9.1).

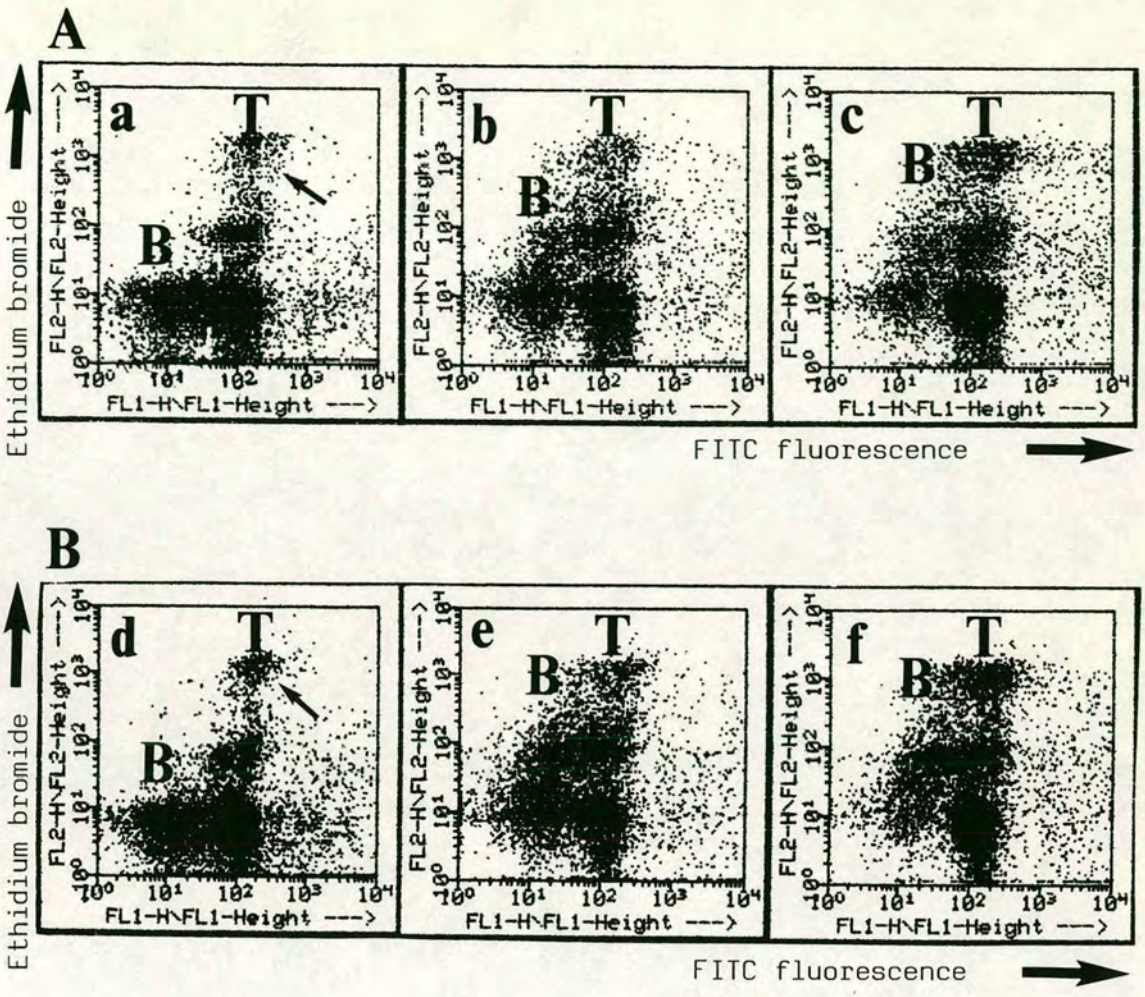

Figure 9.1 Fluorescence plots showing no difference in the levels of apoptosis recorded in populations of PBM prepared from an uninfected (A) and *T. parva* (Muguga) infected (B) calf. Cells cultured with medium alone after 0 (a, d), 8 (b, e) and 20 (c, f) hours incubation *in vitro*. B: B cell population; T: T cell population. In these figures apoptosis is revealed as an increase in ethidium bromide fluorescence (Y-axis). Note the T cell population of both calves had undergone apoptosis (arrows) at time 0.

No increase in apoptosis was observed when cells were incubated with additives known to induce apoptosis in cells of other species. Levels of apoptosis in the B and T cell populations of the infected and uninfected calves cultured with methylprednisolone, adenosine or SNAP resembled those recorded in the B or T cell populations of the infected and uninfected calves cultured with medium alone after 0, 8 hours and 20 hours incubation *in vitro* (Figure 9.2). No changes in levels of apoptosis were recorded in any of the cultures over time i.e. levels at 8 and 20 hours were the same as the level at 0 hour. Cell debris alone was recorded in thymocyte cultures from the normal calf after 0 and 20 hours incubation *in vitro* (Figure 9.3).

9.4.2 ASSESSMENT OF APOPTOSIS IN PARAFFIN TISSUE SECTIONS BY TUNEL & ABC/HRP IMMUNOCYTOCHEMICAL TECHNIQUES

The TUNEL technique was successful in detecting apoptotic cells in paraffin tissue sections (Figure 9.4). Analysis of tissue sections obtained from a calf (41B) which had responded severely to infection with *T. annulata* (Hisar) showed large numbers of apoptotic cells in the extensively damaged prescapular lymph node which drained the site of inoculation (Figure 9.5). Analysis of a prescapular lymph node obtained from a normal control showed fewer apoptotic cells in these areas of the lymph node which were positive in calf 41B (Figures 9.6 & 9.7).

9.4.3 ASSESSMENT OF APOPTOSIS, PROLIFERATION & NITRIC OXIDE PRODUCTION IN CULTURED CELL LINES

9.4.3.1 VISUAL ASSESSMENT OF APOPTOSIS, CELL DEATH & SCHIZONTS IN CELL LINES

Apoptosis (Figure 9.8), cell death (Figure 9.9) and schizonts (Figure 9.10) could be detected in cytospin preparations of cultures of uninfected (BL20) and *T. annulata* infected (TaH BL20, TaAnk 2) cell lines stained with Giemsa's stain.

9.4.3.1.1 APOPTOSIS & CELL DEATH IN BL20

Apoptosis: The percentages of cells undergoing apoptosis in cultures of BL20 after 3 hours incubation with 1000μM, 200μM and 40μM SNAP were 2%, 0% and 0% respectively (Table 9.1A). Levels in control cultures with NO_2^-, penicillamine or medium alone ranged from 0-2%.

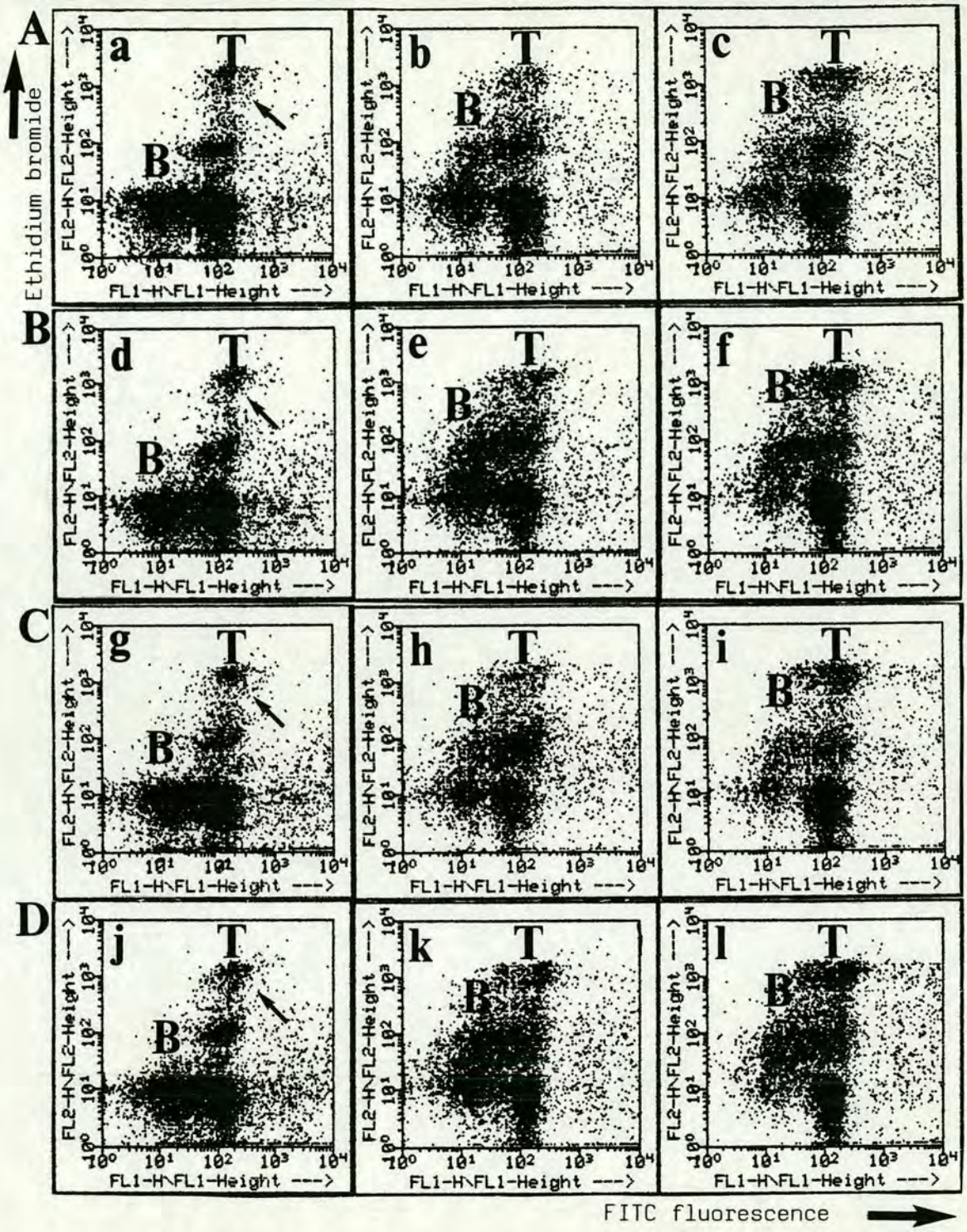

Figure 9.2 Fluorescence plots showing no difference in the levels of apoptosis recorded in populations of PBM prepared from an uninfected (A, C) and *T. parva* (Muguga) infected (B, D) calf. Cells cultured with medium alone (A, B) or methylprednisolone (C, D) after 0 (a, d, g, j), 8 (b, e, h, k) and 20 (c, f, i, l) hours incubation *in vitro*. B: B cell population; T: T cell population. In these figures apoptosis is revealed as an increase in ethidium bromide fluorescence (Y-axis). Note the T cell population of both calves had undergone apoptosis (arrows) at time 0.

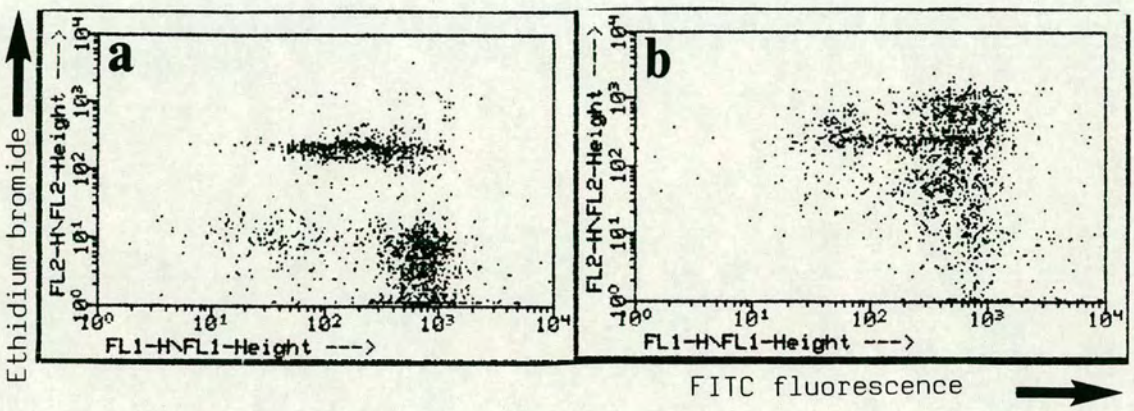

Figure 9.3 Fluorescence plots showing the cell debris recorded in the thymocyte cultures from an uninfected calf after 0 (a) and 20 (b) hours incubation *in vitro*.

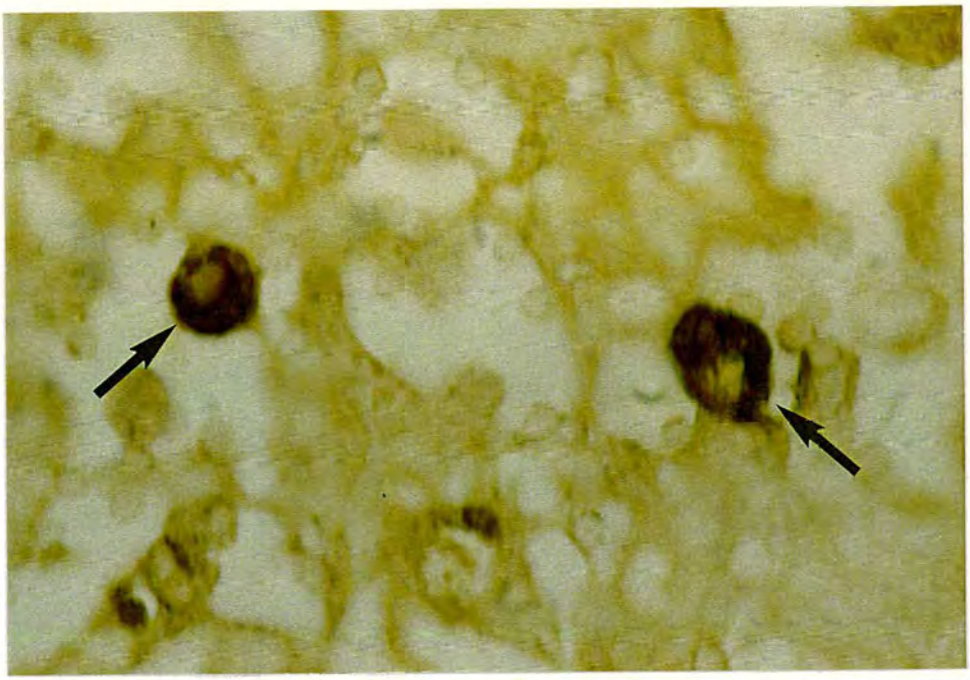

Figure 9.4 Section showing apoptotic cells (arrows) in the paracortex of the draining prescapular lymph node of the calf infected with *T. annulata* (Hisar) on day 12 post-infection during the terminal stages of disease, (x1000: TUNEL).

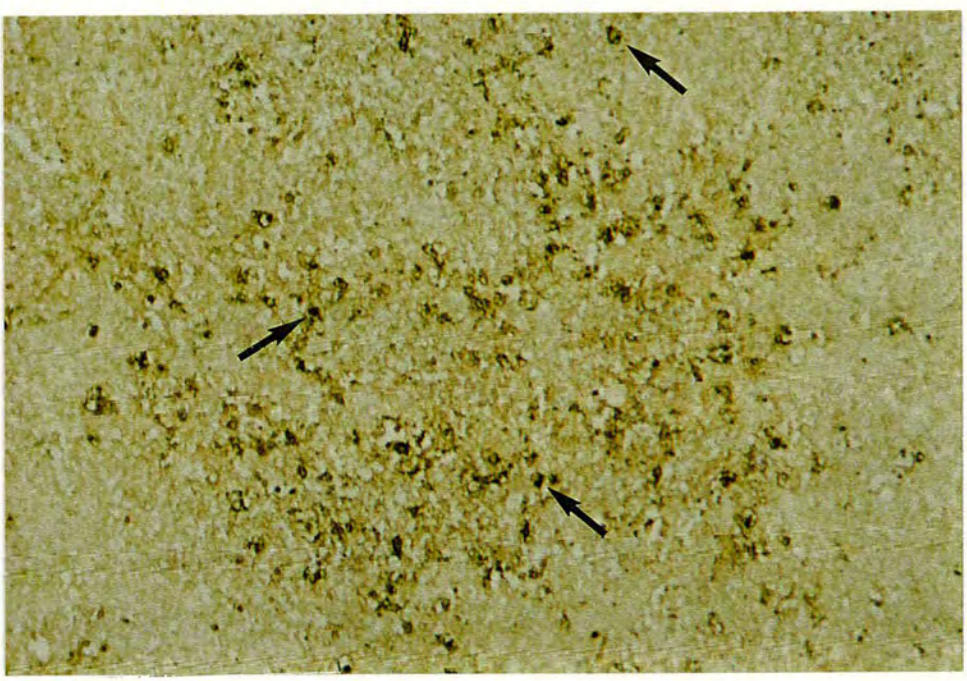

Figure 9.5 Section showing apoptotic cells (arrows) in the paracortex of the draining prescapular lymph node of the calf infected with *T. annulata* (Hisar) on day 12 post-infection during the terminal stages of disease, (x100: TUNEL).

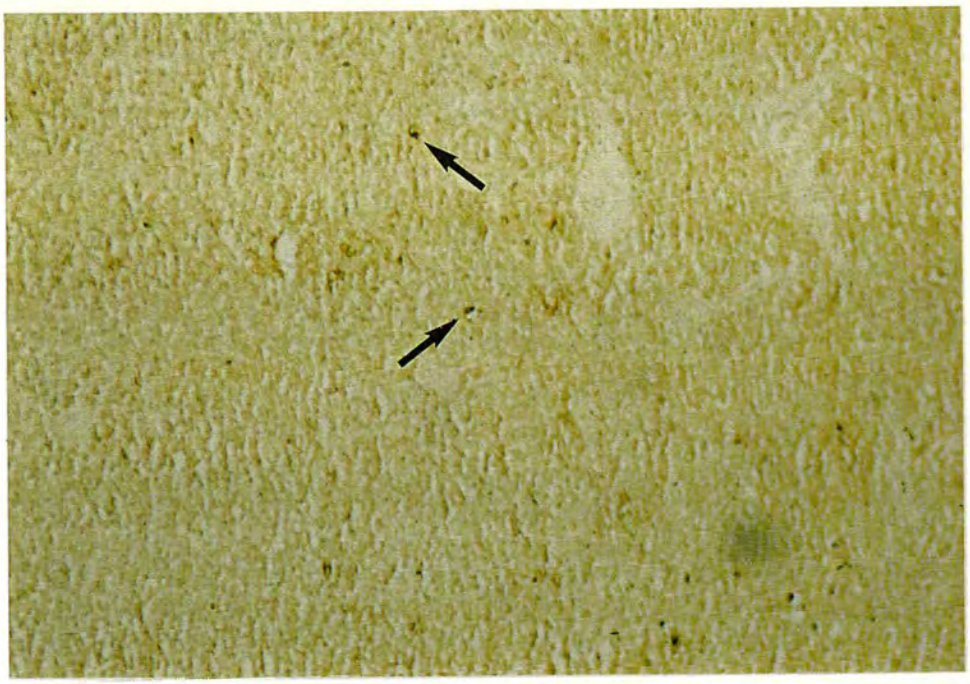

Figure 9.6 Section showing apoptotic cells (arrows) in the paracortex of the prescapular lymph node of the normal, uninfected animal, (x100: TUNEL).

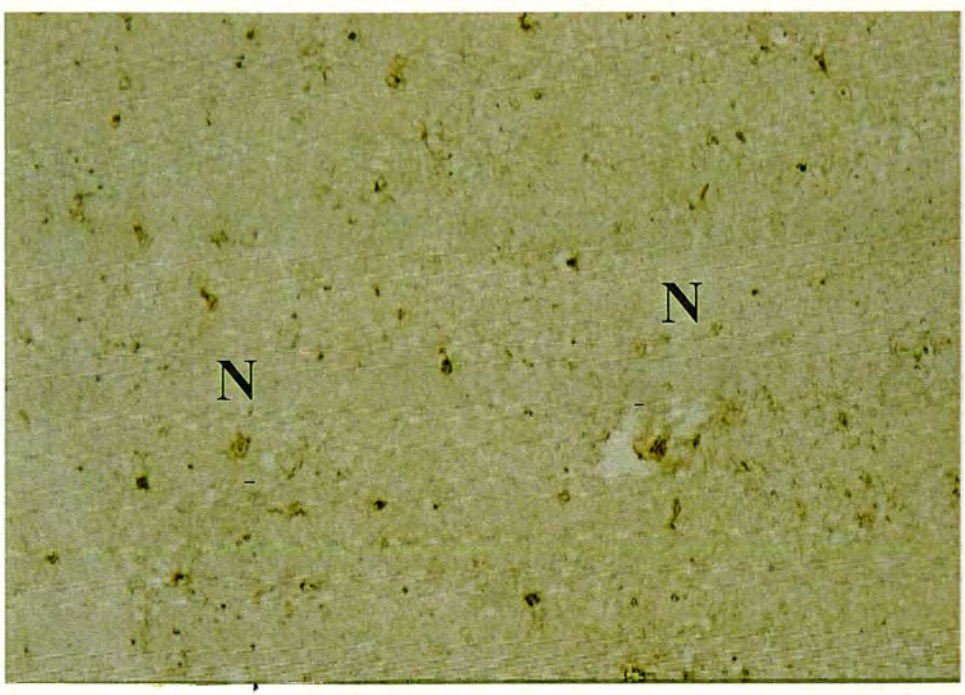

Figure 9.7 Section showing the absence of apoptotic cells in the areas of necrosis (N) in the paracortex of the draining prescapular lymph node of the calf infected with *T. annulata* (Hisar) on day 12 post-infection during the terminal stages of disease, (x100: TUNEL).

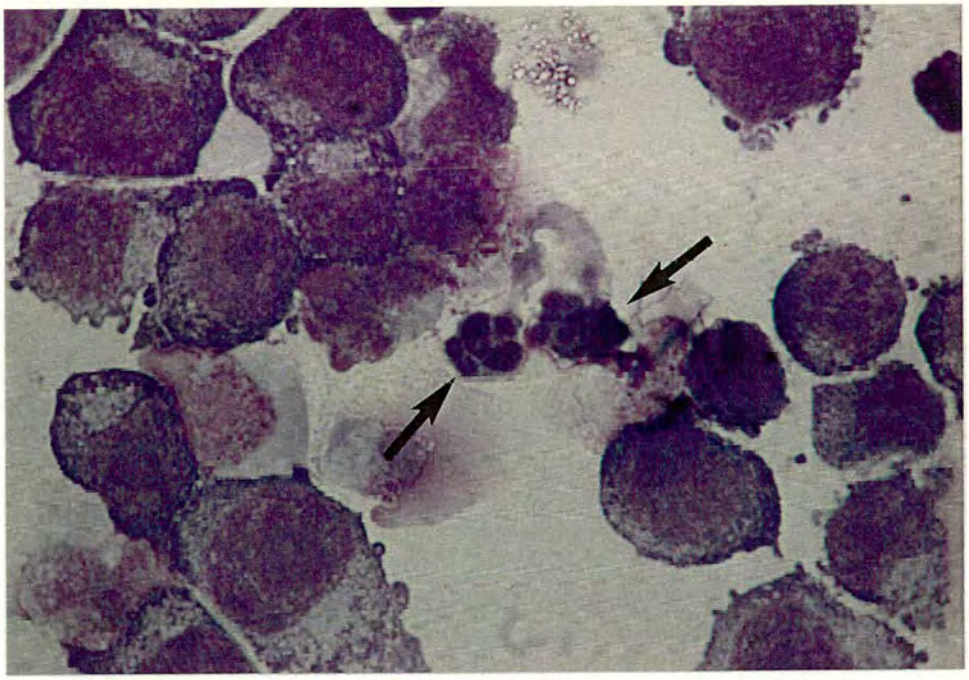

Figure 9.8 Cytospin preparation showing apoptotic cells (arrows) in the uninfected BL20 cell line culture after 20 hours incubation with medium alone, (x1000: Giemsa's stain).

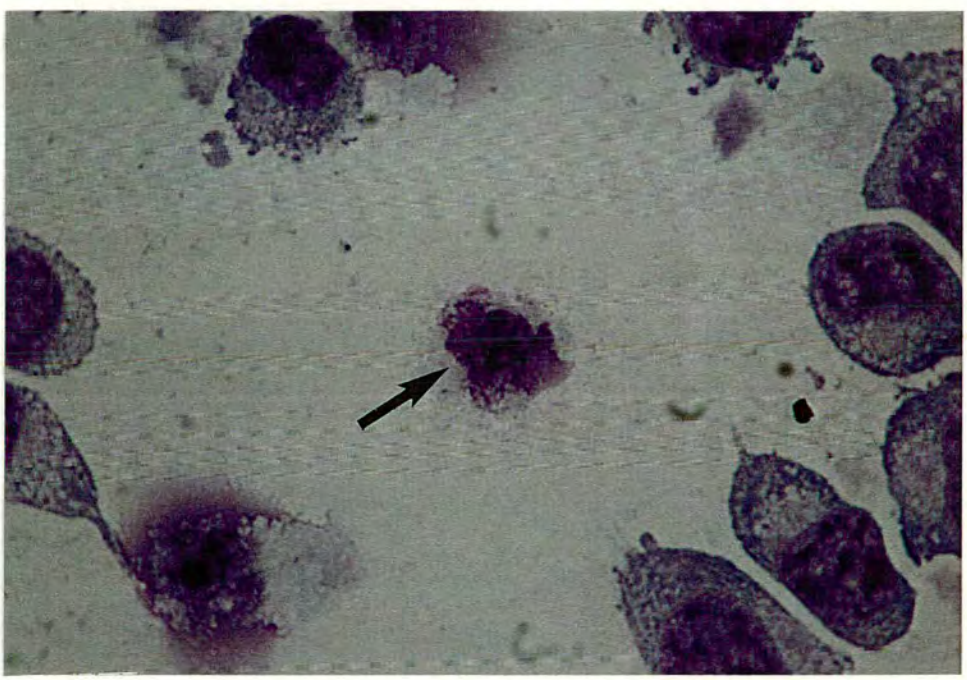

Figure 9.9 Cytospin preparation showing a dead cell (arrow) in the uninfected BL20 cell line culture after 20 hours incubation with medium alone, (x1000: Giemsa's stain).

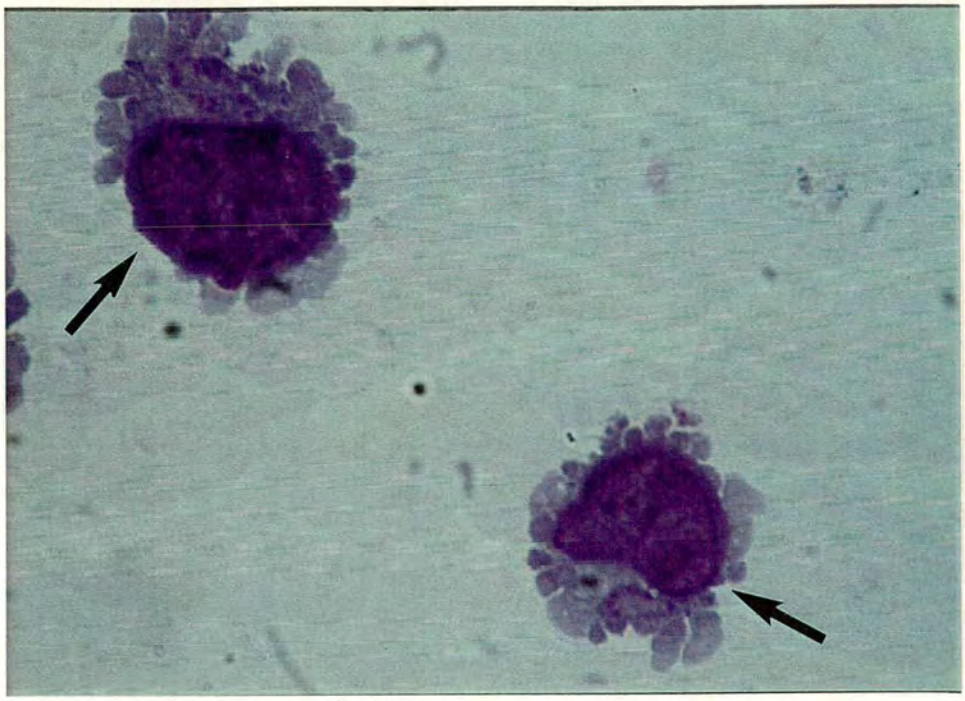

Figure 9.10 Cytospin preparation showing macroschizont-infected cells (arrows) in the TaH BL20 cell line culture after 20 hours incubation with medium alone, (x1000: Giemsa's stain).

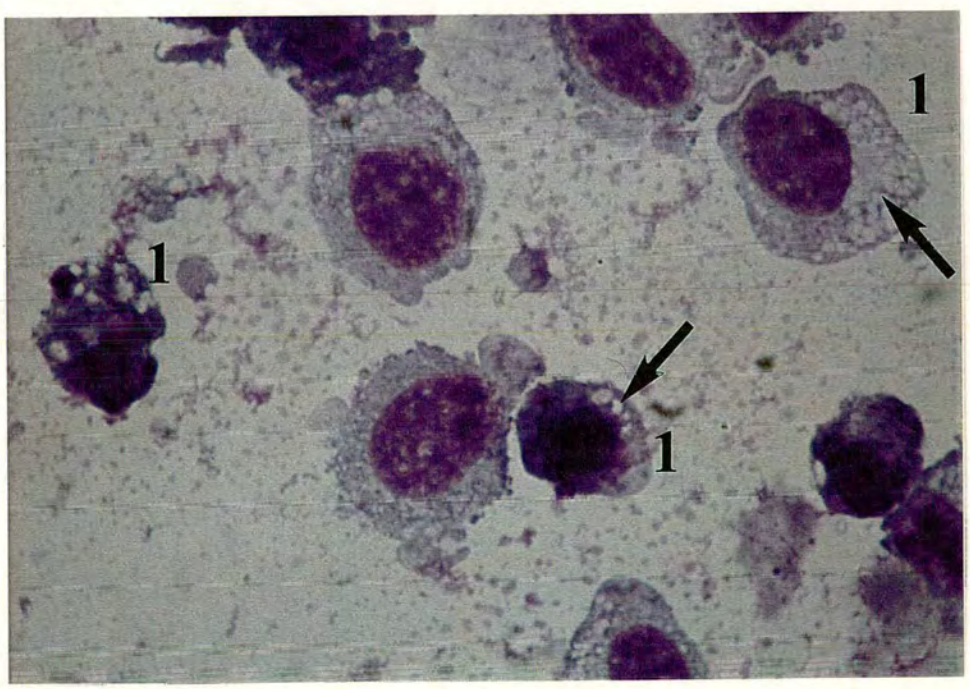

Figure 9.11 Cytospin preparation showing dead or dying cells (1) in the uninfected BL20 cell line culture after 20 hours incubation with SNAP at 1000μM. Note the vacuolation of the cytoplasm of the cells (arrows), (x1000: Giemsa's stain).

	Apoptosis			Cell Death		
μM	1000	200	40	1000	200	40
SNAP	2	0	0	1	3	5
Sodium Nitrite	2	0	0	4	8	10
Penicillamine	0	0	0	65	7	10
Medium	0			8		

Table 9.1A Mean percentage of apoptosis and cell death in cultures of BL20 after 3 hours incubation

	Apoptosis			Cell Death		
μM	1000	200	40	1000	200	40
SNAP	15	7	1	13	2	0
Sodium Nitrite	0	1	0	8	10	5
Penicillamine	1	0	0	93	12	8
Medium	0			6		

Table 9.1B Mean percentage of apoptosis and cell death in cultures of BL20 after 20 hours incubation

The percentages of cells undergoing apoptosis in cultures of this cell line after 20 hours incubation with 1000μM, 200μM and 40μM SNAP were 15%, 7% and 1% respectively (Table 9.1B). Levels in control cultures with NO_2^-, penicillamine or medium alone ranged from 0-1%.

Cell death: BL20 cultured with SNAP or penicillamine differed morphologically. BL20 cells cultured with SNAP showed a marked vacuolation of cytoplasm (Figure 9.11), whereas cells of BL20 cultured with penicillamine showed complete structural breakdown (Figure 9.12).

The percentages of dead cells detected in cultures of BL20 after 3 hours incubation with 1000μM, 200μM and 40μM SNAP were 1%, 3% and 5% respectively (Table 9.1A). Levels in control cultures with NO_2^- or medium alone ranged from 4-10%. The percentages of dead cells detected in cultures incubated with 1000μM, 200μM and 40μM penicillamine were 65%, 7% and 10% respectively.

After 20 hours incubation the percentages of dead cells detected in cultures of this cell line with 1000μM, 200μM and 40μM SNAP were 13%, 2% and 0% respectively (Table 9.1B). Levels in control cultures with NO_2^- or medium alone ranged from 5-10%. The percentages of dead cells detected in cultures incubated with 1000μM, 200μM and 40μM penicillamine were 93% 12% and 8% respectively.

9.4.3.1.2 APOPTOSIS, CELL DEATH & ALTERATION IN SCHIZONT NUMBERS IN TAH BL20

Apoptosis: The percentages of cells undergoing apoptosis in cultures of TaH BL20 after 3 hours incubation with 1000μM, 200μM and 40μM SNAP were 2%, 1% and 2% respectively (Table 9.2A). Levels in control cultures with NO_2^-, penicillamine or medium alone ranged from 1-5%.

The percentages of cells undergoing apoptosis in cultures of this cell line after 20 hours incubation with 1000μM, 200μM and 40μM SNAP were 29%, 3% and 0% respectively (Table 9.2B). Levels in control cultures with NO_2^-, penicillamine or medium alone ranged from 0-1%.

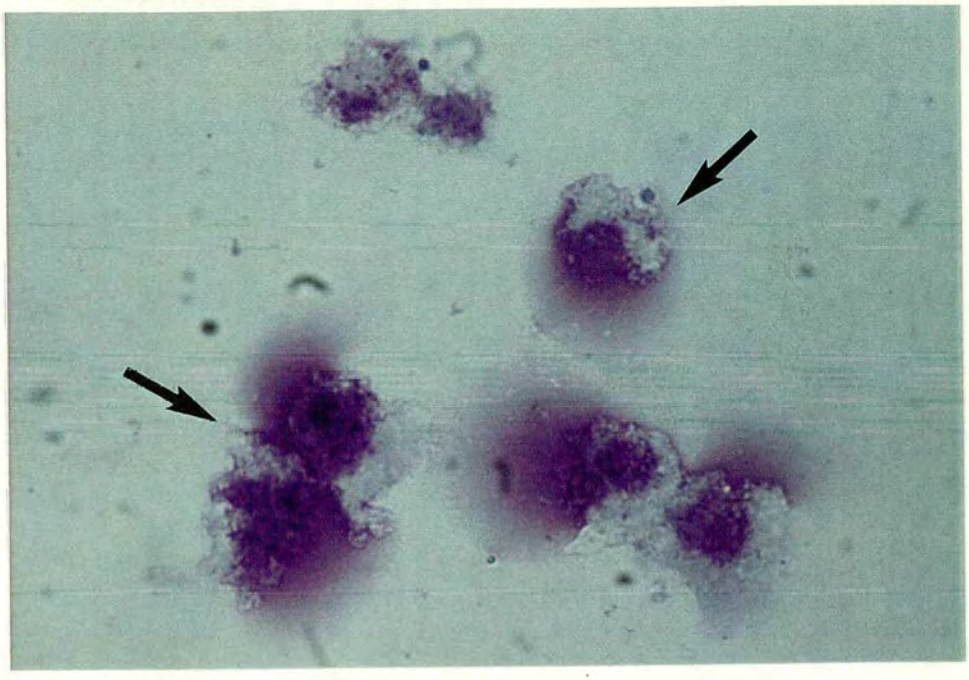

Figure 9.12 Cytospin preparation showing dead cells (arrows) in the uninfected BL20 cell line culture after 20 hours incubation with penicillamine at 1000μM, (x1000: Giemsa's stain).

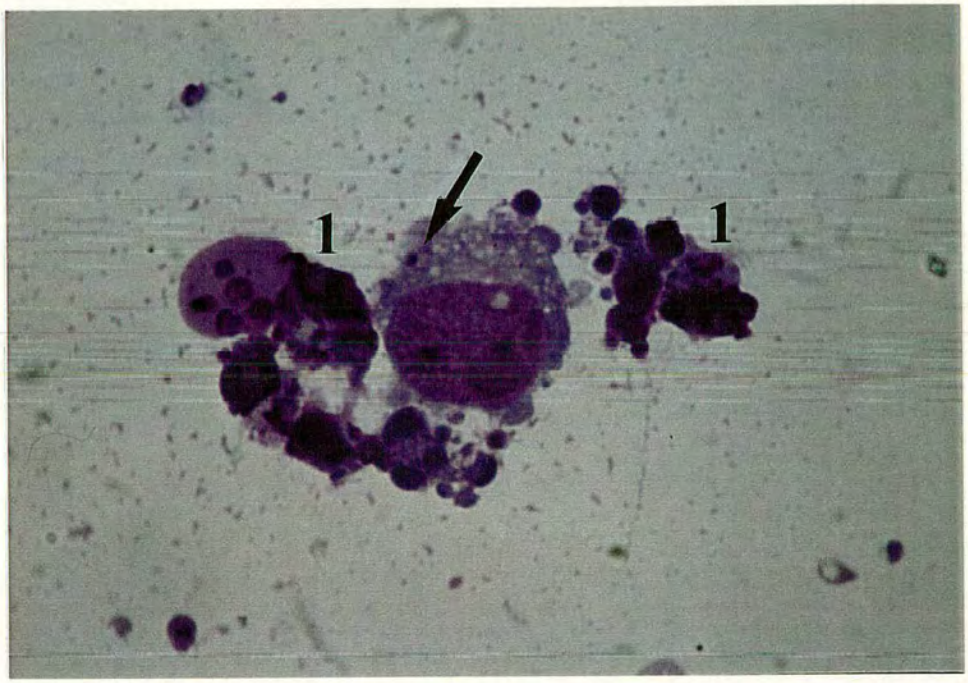

Figure 9.13 Cytospin preparation showing apoptotic cells (1) and malformed macroschizonts within the cytoplasm of the host cell (arrow) in the TaH BL20 cell line culture after 20 hours incubation with SNAP at 1000μM, (x1000: Giemsa's stain).

	Apoptosis			Cell Death			Schizont Absence		
μM	1000	200	40	1000	200	40	1000	200	40
SNAP	2	1	2	2	1	2	1	1	0
Sodium Nitrite	5	2	1	5	9	9	1	3	3
Penicillamine	3	1	3	95	30	42	16	6	8
Medium	1			10			3		

Table 9.2A Mean percentage of apoptosis, cell death and schizont absence in cultures of TaH BL20 after 3 hours incubation

	Apoptosis			Cell Death			Schizont Absence		
μM	1000	200	40	1000	200	40	1000	200	40
SNAP	29	3	0	70	78	15	15	28	3
Sodium Nitrite	0	1	0	7	7	11	1	3	2
Penicillamine	0	1	0	100	20	24	4	5	3
Medium	0			9			2		

Table 9.2B Mean percentage of apoptosis, cell death and schizont absence in cultures of TaH BL20 after 20 hours incubation

Cell death: TaH BL20 cultured with SNAP or penicillamine differed morphologically. TaH BL20 cultured with SNAP showed a marked vacuolation of the cytoplasm with malformation of schizonts which in many cases were absent (Figures 9.13 & 9.14), whereas TaH BL20 cultured with penicillamine showed complete structural breakdown so that schizonts could no longer be maintained within the cytoplasm and were therefore released (Figure 9.15).

The percentages of dead cells detected in cultures of TaH BL20 after 3 hours incubation with 1000μM, 200μM and 40μM SNAP were 2%, 1% and 2% respectively (Table 9.2A). Levels in control cultures with NO_2^- or medium alone ranged from 5-10%. The percentages of dead cells detected in cultures incubated with 1000μM, 200μM and 40μM penicillamine were 95%, 30% and 42% respectively.

After 20 hours incubation the percentages of dead cells detected in cultures of this cell line with 1000μM, 200μM and 40μM SNAP were 70%, 78% and 15% respectively (Table 9.2B). Levels in control cultures with NO_2^- or medium alone ranged from 7-11%. The percentages of dead cells detected in cultures incubated with 1000μM, 200μM and 40μM penicillamine were 100%, 20% and 24% respectively.

Alteration in schizont numbers: The percentages of cells without schizonts detected in cultures of TaH BL20 after 3 hours incubation with 1000μM, 200μM and 40μM SNAP were 1%, 1% and 0% respectively (Table 9.2A). Levels in control cultures with NO_2^- or medium alone ranged from 1-3%. The percentages of cells without schizonts detected in cultures incubated with 1000μM, 200μM and 40μM penicillamine were 16%, 6% and 8% respectively.

After 20 hours incubation the percentages of cells without schizonts detected in cultures of this cell line with 1000μM, 200μM and 40μM SNAP were 15%, 28% and 3% respectively (Table 9.2B). Levels in control cultures with NO_2^-, penicillamine or medium alone ranged from 1-3%.

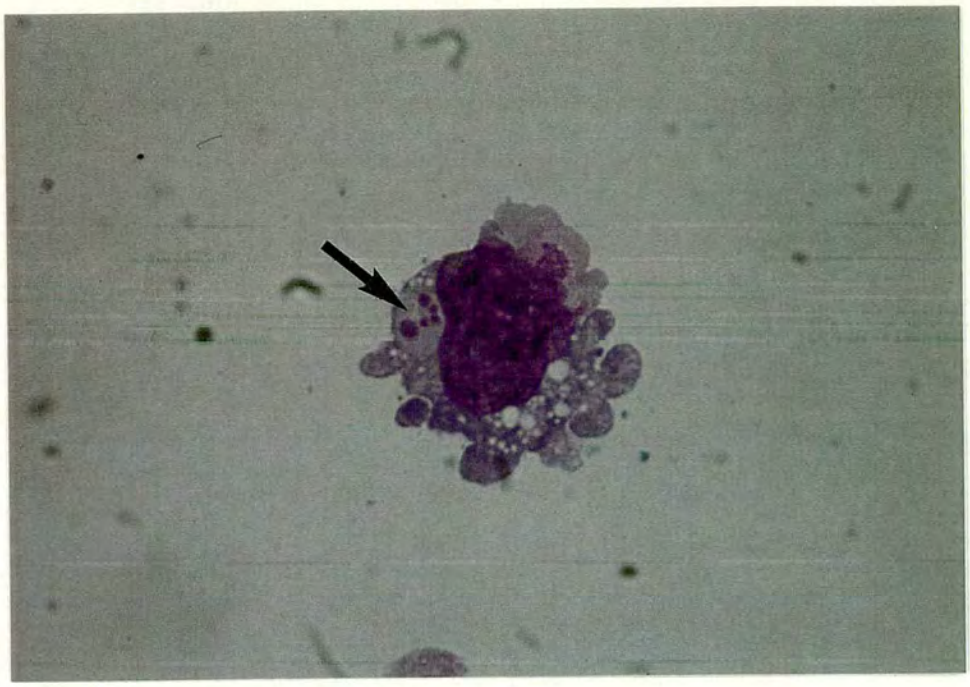

Figure 9.14 Cytospin preparation showing malformed macroschizonts within the cytoplasm of the host cell (arrow) in the TaH BL20 cell line culture after 20 hours incubation with SNAP at 1000μM. Note the vacuolation of the cytoplasm of the host cell, (x1000: Giemsa's stain).

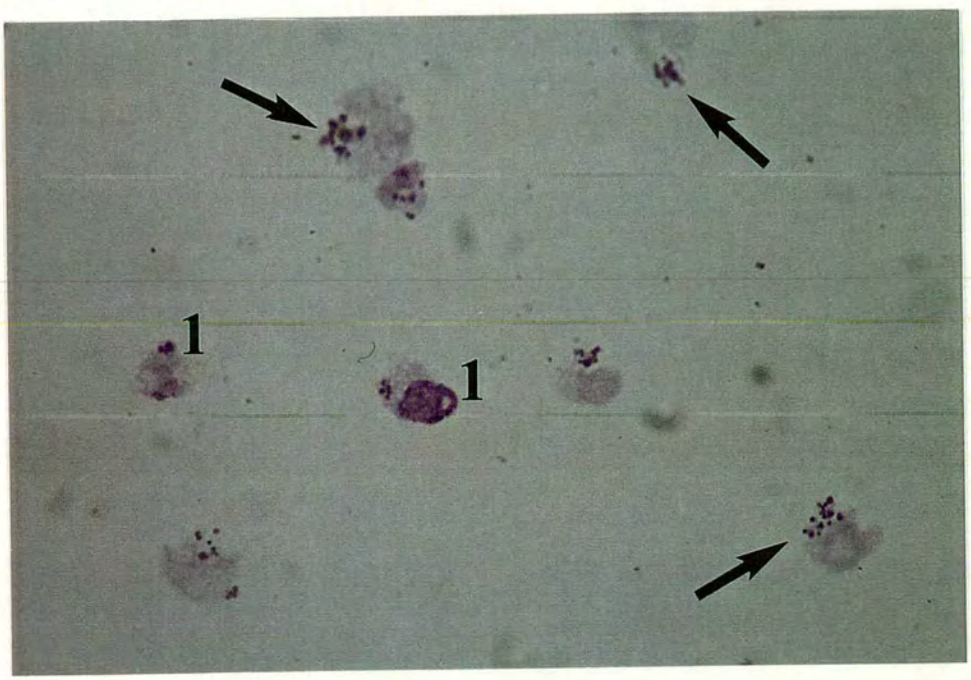

Figure 9.15 Cytospin preparation showing dead cells (1) in the TaH BL20 cell line culture after 20 hours incubation with penicillamine at 1000μM. Note the free macroschizonts (arrows), (x1000: Giemsa's stain).

9.4.3.1.3 APOPTOSIS, CELL DEATH & ALTERATION IN SCHIZONT NUMBERS IN TAANK 2

Apoptosis: The percentages of cells undergoing apoptosis in cultures of TaAnk 2 after 3 hours incubation with 1000μM, 200μM and 40μM SNAP were 6%, 4% and 3% respectively (Table 9.3A). Levels in control cultures with NO_2^-, penicillamine or medium alone ranged from 1-3%.

The percentages of cells undergoing apoptosis in cultures of this cell line after 20 hours incubation with 1000μM, 200μM and 40μM SNAP were 28%, 11% and 3% respectively (Table 9.3B). Levels in control cultures with NO_2^-, penicillamine or medium alone ranged from 1-2%.

Cell death: TaAnk 2 cultured with SNAP or penicillamine differed morphologically. TaAnk 2 cultured with SNAP showed a marked vacuolation of the cytoplasm with malformation of schizonts which in many cases were absent (Figures 9.16 & 9.17), whereas TaAnk 2 cultured with penicillamine showed complete structural breakdown so that schizonts could no longer be maintained within the cytoplasm and were therefore released (Figure 9.18).

The percentages of dead cells detected in cultures of TaAnk 2 after 3 hours incubation with 1000μM, 200μM and 40μM SNAP were 7%, 11% and 12% respectively (Table 9.3A). Levels in control cultures with NO_2^- or medium alone ranged from 20-27%. The percentages of dead cells detected in cultures incubated with 1000μM, 200μM and 40μM penicillamine were 50%, 36% and 29% respectively.

After 20 hours incubation the percentages of dead cells detected in cultures of this cell line with 1000μM, 200μM and 40μM SNAP were 65%, 16% and 11% respectively (Table 9.3B). Levels in control cultures with NO_2^- or medium alone ranged from 13-17%. The percentages of dead cells detected in cultures incubated with 1000μM, 200μM and 40μM penicillamine were 57%, 13% and 11% respectively.

	Apoptosis			Cell Death			Schizont Absence		
μM	1000	200	40	1000	200	40	1000	200	40
SNAP	6	4	3	7	11	12	4	5	8
Sodium Nitrite	2	3	3	20	27	20	11	12	9
Penicillamine	1	1	2	50	36	29	20	10	8
Medium	2			22			10		

Table 9.3A Mean percentage of apoptosis, cell death and schizont absence in cultures of TaAnk 2 after 3 hours incubation

	Apoptosis			Cell Death			Schizont Absence		
μM	1000	200	40	1000	200	40	1000	200	40
SNAP	28	11	3	65	16	11	59	23	12
Sodium Nitrite	1	1	2	17	17	13	8	10	9
Penicillamine	1	1	2	57	13	11	20	8	8
Medium	1			15			9		

Table 9.3B Mean percentage of apoptosis, cell death and schizont absence in cultures of TaAnk 2 after 20 hours incubation

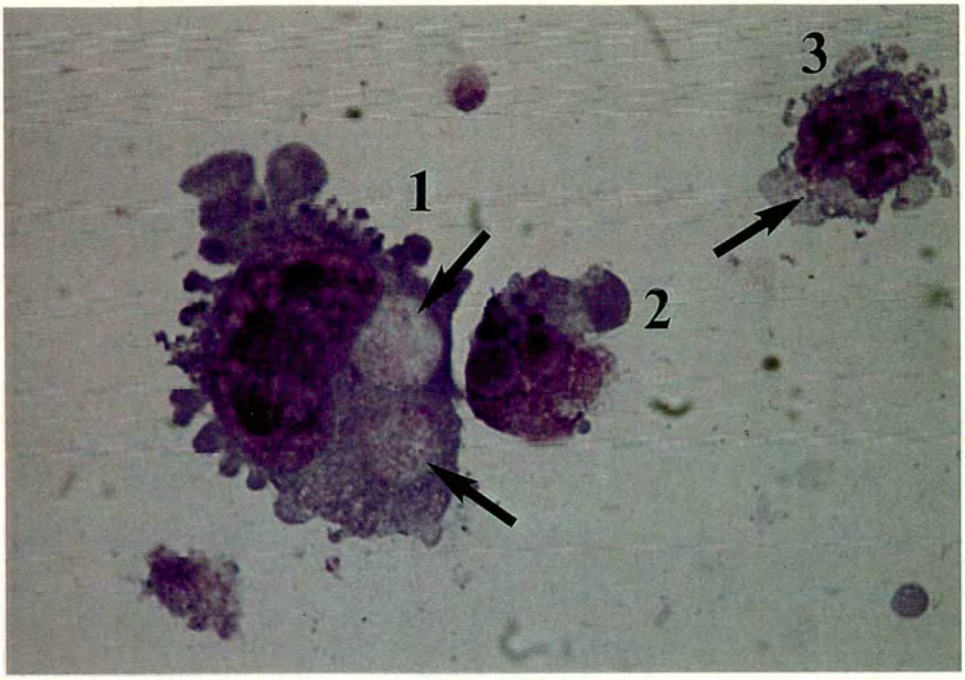

Figure 9.16 Cytospin preparation showing the following: malformed macroschizonts within the cytoplasm of the host cell (1); an apoptotic cell (2); the absence of macroschizonts within the cytoplasm of the host cell (3) in the TaAnk 2 cell line culture after 20 hours incubation with SNAP at 1000μM. Note the vacuolation of the cytoplasm of the host cell (arrows), (x1000: Giemsa's stain).

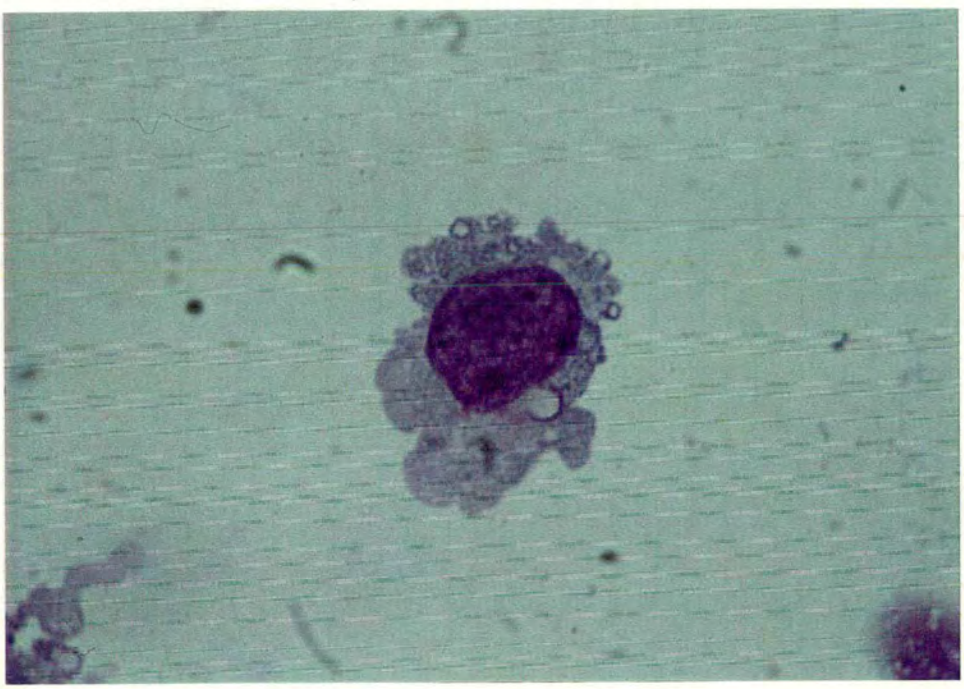

Figure 9.17 Cytospin preparation showing the absence of macroschizonts within the cytoplasm of the host cell in the TaAnk 2 cell line culture after 20 hours incubation with SNAP at 1000μM, (x1000: Giemsa's stain).

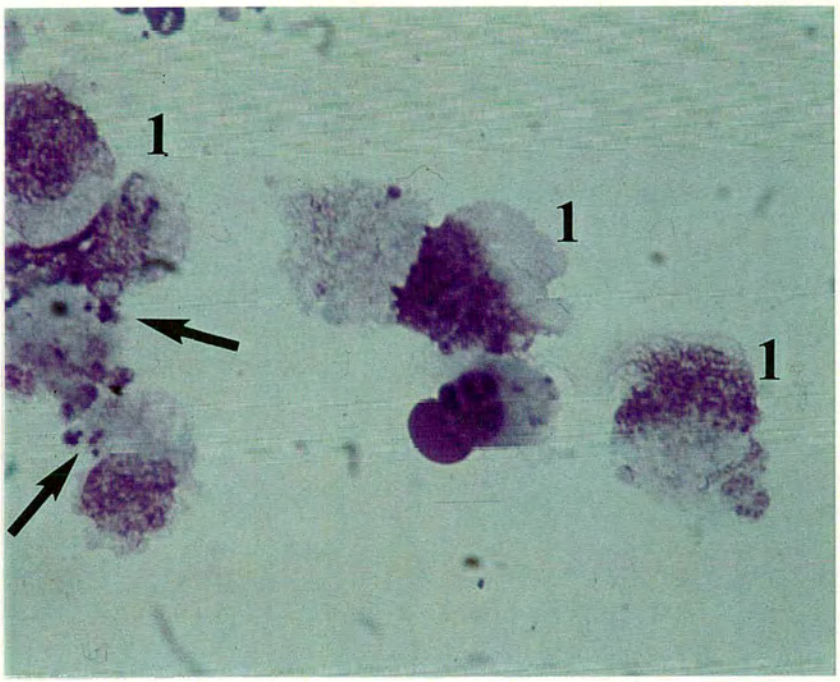

Figure 9.18 Cytospin preparation showing dead cells (1) in the TaAnk 2 cell line culture after 20 hours incubation with penicillamine at 1000μM. Note the free macroschizonts (arrows), (x1000: Giemsa's stain).

Alteration in schizont numbers: The percentages of cells without schizonts detected in cultures of TaAnk 2 after 3 hours incubation with 1000μM, 200μM and 40μM SNAP were 4%, 5% and 8% respectively (Table 9.3A). Levels in control cultures with NO_2^- or medium alone ranged from 9-12%. The percentages of cells without schizonts detected in cultures incubated with 1000μM, 200μM and 40μM penicillamine were 20%, 10% and 8% respectively.

After 20 hours incubation the percentages of cells without schizonts detected in cultures of this cell line with 1000μM, 200μM and 40μM SNAP were 59%, 23% and 12% respectively (Table 9.3B). Levels in control cultures with NO_2^- or medium alone ranged from 8-10%. The percentages of cells without schizonts detected in cultures incubated with 1000μM, 200μM and 40μM penicillamine were 20%, 8% and 8% respectively.

9.4.3.2 ASSESSMENT OF PROLIFERATION OF CELL LINES BY THE INCORPORATION OF TRITIATED THYMIDINE

Proliferation was assessed by the incorporation of tritiated thymidine by cell line (BL20, TaH BL20, TaAnk 2) cultures after 20 hours incubation.

9.4.3.2.1 PROLIFERATION IN BL20

The proliferation in cultures of BL20 incubated with 1000μM SNAP was significantly inhibited by 40% compared to proliferation in medium alone (Table 9.4A & 9.4B). The proliferation in cultures incubated with 200μM and 40μM SNAP was significantly enhanced by 33% and 97% respectively compared to proliferation in medium alone.

The proliferation in cultures of BL20 incubated with 1000μM NO_2^- was significantly enhanced by 18% compared to proliferation in medium alone (Table 9.4A & 9.4B). The proliferation in cultures incubated with 200μM and 40μM NO_2^- was not significantly different compared to proliferation in medium alone.

The proliferation in cultures of BL20 with 1000μM and 200μM penicillamine was significantly inhibited by 92% and 12% respectively compared to proliferation in

	Mean Absolute Count (dpm)			% Inhibition (-) & % Enhancement (+)		
μM	1000	200	40	1000	200	40
SNAP	79728	176134	260150	- 40	+33	+97
Sodium Nitrite	155408	148244	147055	+18	+12	+11
Penicillamine	10907	115897	130167	- 92	- 12	- 1
Medium	131842			na		

dpm Disintegrations per minute
na Not applicable

Table 9.4A Incorporation of tritiated thymidine expressed as % inhibition (-) or % enhancement (+) of growth in cultures of BL20

μM	1000			200			40		
	SNAP	Sodium Nitrite	Penicillamine	SNAP	Sodium Nitrite	Penicillamine	SNAP	Sodium Nitrite	Penicillamine
Sodium Nitrite	SD	na	SD	SD	na	SD	SD	na	SD
Penicillamine	SD	SD	na	SD	SD	na	SD	SD	na
Medium	SD	SD	SD	SD	NSD	SD	SD	NSD	NSD

na Not applicapable
SD Significantly different
NSD Not significantly different

Table 9.4B Table of significance for cultures of BL20

medium alone (Table 9.4A & 9.4B). The proliferation in cultures incubated with 40μM penicillamine was not significantly different compared to proliferation in medium alone.

9.4.3.2.2 PROLIFERATION IN TAH BL20

The proliferation in cultures of TaH BL20 incubated with 1000μM and 200μM SNAP was significantly inhibited by 76% and 41% respectively compared to proliferation in medium alone (Table 9.5A & 9.5B). The proliferation in cultures incubated with 40μM SNAP was significantly enhanced by 37% compared to proliferation in medium alone.

The proliferation in cultures of TaH BL20 incubated with 1000μM and 200μM NO_2^- was significantly enhanced by 14% and 12% respectively compared to proliferation in medium alone (Table 9.5A & 9.5B). The proliferation in cultures incubated with 40μM NO_2^- was not significantly different compared to proliferation in medium alone.

The proliferation in cultures of TaH BL20 incubated with 1000μM, 200μM and 40μM penicillamine was significantly inhibited by 98%, 14% and 43% respectively compared to proliferation in medium alone (Table 9.5A & 9.5B).

9.4.3.2.3 PROLIFERATION IN TAANK 2

The proliferation in cultures of TaAnk 2 incubated with 1000μM and 200μM SNAP was significantly inhibited by 71% and 32% respectively compared to proliferation in medium alone (Table 9.6A & 9.6B). The proliferation in cultures incubated with 40μM SNAP was significantly enhanced by 19% compared to proliferation in medium alone.

The proliferation in cultures of TaAnk 2 incubated with 1000μM NO_2^- was significantly enhanced by 14% compared to proliferation in medium alone (Table 9.6A & 9.6B). The proliferation in cultures incubated with 200μM and 40μM NO_2^- was not significantly different compared to proliferation in medium alone.

	Mean Absolute Count (dpm)			% Inhibition (-) & % Enhancement (+)		
μM	1000	200	40	1000	200	40
SNAP	20560	49366	115022	- 76	- 41	+37
Sodium Nitrite	95176	93526	93419	+14	+12	+11
Penicillamine	1777	71840	48215	- 98	- 14	- 43
Medium	83854			na		

dpm Disintegrations per minute
na Not applicable

Table 9.5A Incorporation of tritiated thymidine expressed as % inhibition (-) or % enhancement (+) of growth in cultures of TaH BL20

μM	1000			200			40		
	SNAP	Sodium Nitrite	Penicillamine	SNAP	Sodium Nitrite	Penicillamine	SNAP	Sodium Nitrite	Penicillamine
Sodium Nitrite	SD	na	SD	SD	na	SD	SD	na	SD
Penicillamine	SD	SD	na	SD	SD	na	SD	SD	na
Medium	SD	SD	SD	SD	SD	SD	SD	NSD	SD

na Not applicapable
SD Significantly different
NSD Not significantly different

Table 9.5B Table of significance for cultures of TaH BL20

	Mean Absolute Count (dpm)			% Inhibition (-) & % Enhancement (+)		
μM	1000	200	40	1000	200	40
SNAP	21150	48519	85263	- 71	- 32	+19
Sodium Nitrite	82049	74930	74379	+14	+4	+4
Penicillamine	23696	69742	68167	- 67	- 3	- 5
Medium	71770			na		

dpm Disintegrations per minute
na Not applicable

Table 9.6A Incorporation of tritiated thymidine expressed as % inhibition (-) or % enhancement (+) of growth in cultures of TaAnk 2

μM	1000			200			40		
	SNAP	Sodium Nitrite	Penicillamine	SNAP	Sodium Nitrite	Penicillamine	SNAP	Sodium Nitrite	Penicillamine
Sodium Nitrite	SD	na	SD	SD	na	NSD	SD	na	NSD
Penicillamine	SD	SD	na	SD	NSD	na	SD	NSD	na
Medium	SD	SD	SD	SD	NSD	NSD	SD	NSD	NSD

na Not applicapable
SD Significantly different
NSD Not significantly different

Table 9.6B Table of significance from cultures of TaAnk 2

The proliferation in cultures of TaAnk 2 incubated with 1000μM penicillamine was significantly inhibited by 67% compared to proliferation in medium alone (Table 9.6A & 9.6B). The proliferation in cultures incubated with 200μM and 40μM penicillamine was not significantly different compared to proliferation in medium alone.

9.4.3.3 ASSESSMENT OF NITRIC OXIDE PRODUCTION IN CULTURES BY THE GRIESS ASSAY

The Griess assay showed that 1000μM, 200μM and 40μM of SNAP had generated 876μM, 172μM and 46μM of NO_2^- respectively after 20 hours incubation. Levels of NO_2^- in wells to which 1000μM, 200μM and 40μM of $NaNO_2^-$ had been added contained 560μM, 500μM and 156μM of NO_2^- respectively after 20 hours incubation. NO_2^- was undetected in wells to which 1000μM, 200μM and 40μM of penicillamine had been added and in wells with medium alone after 20 hours incubation.

9.5 DISCUSSION

The initial work to identify apoptosis in bovine cells assessed flow cytometry and *in situ* hybridisation techniques. Apoptosis of cells was identified in suspensions of bovine B and T cell populations by flow cytometry but the levels of apoptosis in the cell populations of infected and uninfected animals after 0, 8 hours and 20 hours incubation *in vitro* were similar. Interestingly, compounds shown to induce apoptosis in cells from other species did not induce apoptosis in the bovine cells used here. It was concluded that flow cytometry would not be a useful method for assessing apoptosis in suspensions of bovine cells from infected cattle. This was unfortunate as this technique would have been useful to see if apoptosis accompanied leucopenia; a common clinical symptom of calves responding severely to infection with *T. annulata* (Laiblin 1978; Preston *et al.* 1992a) or *T. parva* (Morrison *et al.* 1981a).

In situ hybridisation based on TUNEL and immunocytochemical visualisation techniques detected apoptotic cells in paraffin tissue sections of bovine tissues. The specificity of these techniques for the identification of apoptotic cells, but not necrotic cells, was shown by the absence of immunocytochemical staining in

recognisable areas of necrosis. Initial studies on tissue sections obtained from a calf which had responded severely to infection with *T. annulata* (Hisar) showed large numbers of apoptotic cells in the extensively damaged prescapular lymph node which drained the site of inoculation. Analysis of a control prescapular lymph node of a normal calf showed fewer numbers of apoptotic cells in these areas of the lymph node which were positive in the infected calf. This suggested apoptosis accompanied the pathology associated with a lethal *T. annulata* (Hisar) infection. However, work was conducted on only a few slides due to the high financial cost of this technique.

NO production has already been demonstrated in PBM harvested from calves undergoing infection with *T. annulata* (3.4.4; Visser *et al.* 1995) and *T. parva* using the Griess assay (Visser *et al.* 1995). However, attempts to assess the presence of NO in areas of damage in tissue sections from lymphoid and non-lymphoid organs of cattle undergoing lethal infection with *T. annulata*, using antibodies to NO synthase and immunocytochemical techniques, were unsuccessful for technical reasons (personal communication Miss Kathryn Graham).

The effect of SNAP derived NO on the induction of apoptosis, cell death and alteration of schizont number in parasitised and uninfected bovine cell line cultures was assessed in cytospin preparations stained with Giemsa's stain. Apoptosis could be identified by the characteristic formation of condensed bodies of nuclear material (Kerr *et al.* 1972; Wyllie *et al.* 1980) using Giemsa's stain. This was a less expensive staining technique for identification of apoptosis in suspensions of bovine cells and so could be used to examine large numbers of cultures.

The work showed apoptosis was markedly increased in cell lines cultured with 1000μM and 200μM SNAP, a compound that generates NO when added to culture medium. This response was shown in both uninfected (BL20) and parasitised (TaH BL20, TaAnk 2) cell line cultures and was dose and time dependent. SNAP was also shown to induce cell death in all cell line cultures and alter schizont numbers in parasitised cell line cultures. The uninfected cell line culture showed an increase in cell death as did the parasitised cell line cultures associated with an increase in malformed schizonts, which in many cases were absent. Again these responses were

dose dependent. The use of TUNEL confirmed the occurrence of apoptosis in cultures exposed to SNAP (Richardson & Preston 1994).

All cell lines cultured with 1000μM penicillamine, a component of SNAP, also showed an increase in cell death. This suggested that penicillamine may have elicited the changes recorded in cell death in all the cell line cultures incubated with 1000μM SNAP instead of NO. However the cell lines which had been cultured with penicillamine appeared morphologically different from those cultured with 1000μM SNAP - the cells had been ruptured and the schizonts released.

Lower doses of penicillamine were less toxic so that a differential effect of the NO component of SNAP could be seen in cultures incubated with 200μM additives. In these cultures SNAP caused vacuolation of the cytoplasm of cells in all the cultures, altered the morphology of schizonts within the cytoplasm of cells and caused them to disappear from parasitised cell line cultures rather than altering the morphology of the infected host cells themselves. These changes were not seen in infected cultures incubated with 200μM penicillamine. No differences were seen in any of the responses when cells were incubated with 40μM additives.

Proliferation of cell lines treated with NO was assessed by the incorporation of tritiated thymidine. All cell lines cultured with the highest dose (1000μM) of SNAP and penicillamine were significantly inhibited. From the results of the cytospin preparations it was concluded that the inhibition induced by SNAP comprised apoptosis and cell death whereas, inhibition induced by penicillamine comprised cell death due to the high toxicity of penicillamine. Inhibition of cell lines cultured with SNAP and penicillamine was shown to be dose dependent. 200μM SNAP significantly inhibited the proliferation of the two infected cell lines as compared to 200μM penicillamine. It was interesting that this dose of SNAP enhanced proliferation of the BL20 cell line. These results reflected those recorded in cytospin preparations stained with Giemsa's stain. These findings therefore suggested that NO production by the cells of the host could be both beneficial to the host by controlling the parasite and detrimental to the host by inducing tissue damage.

9.6 CONCLUSION

Flow cytometry proved to be an unsuccessful technique for assessment of apoptosis in bovine cell suspensions. However, *in situ* hybridisation by TUNEL successfully detected apoptotic cells in paraffin tissue sections from bovine tissues and cultures. This initial work suggested that apoptosis had accompanied the pathology found in a calf undergoing a severe response to infection with *T. annulata*. Levels of apoptosis of uninfected and parasitised cell lines increased in the presence of NO. The schizonts within the parasitised host cells were often malformed or absent in the presence of NO. The effects of SNAP could be differentiated from those recorded in cultures incubated with control additives when 200μM additives were used.

CHAPTER TEN

GENERAL DISCUSSION

The primary objective of the study was to investigate the lesions of tropical theileriosis (*T. annulata* infection) in particular the identity of the schizont-infected cell and the contribution of macrophages to tissue damage. During the course of the study, tissues from a *T. parva* infected animal became available and were included for comparison. The work was carried out in the following stages: (i) examination of clinical responses and parasite development in cattle to ascertain that tissues were being obtained during 'acute' (lethal) infections; (ii) examination of the macroscopic pathology of the organs; (iii) histological investigation of the microscopic lesions in the tissues prepared at the initial stages of pyrexia, peak pyrexia and nadir of disease to monitor the progression of lesions over time: particular attention being given to the presence of macrophages and lymphocytes in the tissues; (iv) assessment of parasite distribution throughout the organs showing macroscopic lesions using tissue smears stained with Giemsa's stain; (v) assessment of the location of macroschizont- and microschizont-infected cells in relation to the microscopic lesions using MAbs which recognise parasite antigens and immunocytochemical techniques with Harris's haematoxylin counterstain; (vi) assessment of antibodies to identify reagents for phenotypic analyses; (vii) Use of antibodies A452 (a T (CD3) cell marker) and IL-A15 (a C3bi complement receptor marker) to identify schizont-infected cells; (viii) Use of A452 and IL-A15 to identity the uninfected cells which accompanied schizont-infected cells; (ix) Assessment of NO production by PBM and the ability of NO to induce apoptosis.

Assessment of the clinical and haematological responses of, as well as the development of parasites, in calves infected with either *T. annulata* or *T. parva* (Muguga) confirmed that the animals of this study had undergone 'acute' (lethal) infections (Neitz 1957; Anon 1989). Pyrexia was sustained for 8 or more days and leucopenia was prompt in both the *T. annulata* (Prasad 1946; Laiblin 1978; Preston *et al.* 1992a) and *T. parva* (Muguga) (Steck 1928; Wilde 1966) infected animals. The numbers of lymphocytes, monocytes and neutrophils were reduced, but the numbers of eosinophils and basophils remained unchanged. A macroschizont parasitosis

above 5% was recorded in the animals infected with both *T. annulata* and *T. parva* (Muguga) accompanied by a severe pyrexia and leucopenia. This suggested a role for the macroschizont in the clinical symptoms associated with both infections. The absence of detectable intra-erythrocytic piroplasms in the blood and liver smears of calves succumbing to *T. annulata* (Tova) infection (Pipano *et al.* 1974) provides some evidence of a role for the macroschizonts in the clinical symptoms associated with *T. annulata* infections at least. A marked anaemia was recorded in the animals infected with *T. annulata* accompanied by a high piroplasm parasitaemia. A role for the piroplasm in the pathogenesis of anaemia was suggested by the direct relation found between the numbers of RBC, PCV and piroplasm parasitaemia in these animals as described by Preston *et al.* (1992a).

Examination of selected lymphoid and non-lymphoid organs of cattle undergoing lethal infection with either *T. annulata* or *T. parva* (Muguga) showed the macroscopic lesions and the extensive tissue damage to have been elicited by both infections. Numerous petechiae or larger haemorrhages, accompanied by oedema in many cases, were seen throughout the lymph nodes, thymus, kidney, liver, abomasum, lung and adrenal gland of the *T. annulata* infected animals. Additional features included: a variable number of white "infarcts" in the kidney and liver; ulcers consisting of a central necrotic area surrounded by a haemorrhagic zone in the abomasum; cutaneous nodules in the skin. Numerous petechiae accompanied by larger haemorrhages and oedema were also seen in the lymph nodes of the *T. parva* (Muguga) infected calf, but the remaining lymphoid and non-lymphoid organs appeared normal. In all cases, the lymph node draining the site of inoculation was the most adversely affected organ. Lesions were never detected in the brain or pituitary gland. These findings resembled those described by Dschunkowsky & Luhs (1904), Sergent *et al.* (1924), Sergent *et al.* (1945), Neitz (1957), De Kock (1957), Srivastava & Sharma (1981) and Manickam *et al.* (1984). However the severe pulmonary oedema characteristic of *T. parva* infections (Gray & Robertson 1902), was not seen in one animal examined by this study. The macroscopic lesions in the *T. parva* (Muguga) infected animal resembled those of the *T. annulata* infected animals, but the greater erythrocyte destruction in the *T. annulata* infected animals

was evident by the watery blood, pale muscles and yellowish connective tissue as described by Barnett (1977).

Assessment of the microscopic lesions in tissue sections of the lymphoid and non-lymphoid organs of cattle undergoing lethal infections with either *T. annulata* or *T. parva* (Muguga) showed the extensive tissue damage, as described above, elicited by both infections. The lymph nodes of the animals infected with *T. annulata* did not show the demarcation into cortical and medullary regions seen in the lymph nodes of uninfected animals. Large numbers of macrophages and foamy macrophages were seen in the medullary sinuses and paracortical regions of the lymph nodes accompanied by sinus hyperplasia and enlargement of the medullary regions. There was a substantial depletion in the numbers of lymphocytes in the paracortical regions of the lymph nodes accompanied by the regression and disappearance of the lymphoid follicles. Interestingly, several granulomas were detected in some of the lymph nodes, in particular the lymph node which drained the site of inoculation during the peak of pyrexia, accompanied by large numbers of macrophages, eosinophils and parasitised cells. Large areas of focal/diffuse haemorrhage and necrosis were also detected. These findings differed from those described by Gill *et al.* (1977) and Baharsefat *et al.* (1977) where lymph nodes showed proliferative changes characterised by a diffuse hyperplasia of the lymphoid follicles which occasionally fused to form a sheet of lymphocytes which often extended into the medullary region. However, some similarities were recorded in these lymph nodes including inflammation of the medullary sinuses with large numbers of macrophages, depletive changes characterised by a loss of distinction between the cortex and the medulla, and exhaustion of lymphopoietic tendency as evident from the regression and degeneration of lymphoid follicles.

In contrast, the lymph nodes of the *T. parva* (Muguga) infected calf showed lymphocytic hyperplasia in the paracortical regions of the lymph node which drained the site of inoculation. Lymphoid cellular depletion was however seen in the paracortical regions of the remaining lymph nodes and lymphoid follicles were absent from most lymph nodes. Moderate numbers of macrophages and foamy macrophages were seen in the medullary sinuses of these lymph nodes, but large

numbers of these cells were not detected in the paracortical regions and sinus hyperplasia was not evident. A large area of focal haemorrhage and necrosis was seen in the medulla of the draining lymph node. Importantly, lymphocytic hyperplasia was never seen in the paracortical regions of any of the lymph nodes examined from the *T. annulata* infected animals. Previous work conducted by De Kock (1957), Barnett (1960), DeMartini & Moulton (1973) and Irvin & Morrison (1987) on animals infected with *T. parva* also described the regression and degeneration of lymphoid follicles, extensive areas of hyperplasia, paracortical lymphocytolysis and an increase in the number of macrophages in the medullary regions of lymph nodes.

Examination of the microscopic lesions in the other lymphoid and the non-lymphoid organs of the *T. annulata* or *T. parva* (Muguga) infected animals showed similarities with the lesions described by Sergent *et al.* (1924), Sergent *et al.* (1945), De Kock 1957, Gill *et al.* (1977), Baharsefat *et al.* (1977), Srivastava & Sharma (1981) and Manickam *et al.* (1984). However microscopic lesions were detected in a smaller number of non-lymphoid organs of the *T. parva* (Muguga) infected calf. In the *T. annulata* infected animals the red pulp of the spleen was congested and haemorrhagic. A marked depletion of lymphoid cells was seen in the thymus. Focal aggregations of lymphocytes and macrophages were seen in the kidneys. The liver showed diffuse infiltration of the periportal areas by large numbers of lymphocytes and macrophages and the hepatic cells showed moderate fatty changes. The intercellular spaces of the abomasum were distended and infiltrated by large numbers of foamy macrophages, macrophages and lymphocytes. The lungs showed thickened interalveolar septa with haemorrhages in the alveolar spaces. Skin lesions included haemorrhage, oedema, necrosis and cell infiltration by macrophages and lymphocytes. Large aggregates of macrophages and lymphocytes in the adrenal gland were accompanied by a certain amount of atrophy and degeneration of adjacent adrenal gland parenchyma.

Importantly, past reports described by Neitz (1957) and Barnett (1960) suggested that the microscopic findings in *T. annulata* (Neitz 1957) and *T. parva* (Barnett 1960) infected animals were essentially the same, except that the erythrocytes of *T.*

parva infected animals, unlike those of *T. annulata* infected animals, showed no degenerative or regenerative changes (Neitz 1957). However, the work reported in this thesis showed that this was not the case. Although similarities were seen in the non-lymphoid organs of the calves important differences were observed in the lymph nodes, in particular the lymph node draining the site of inoculation. In animals infected with *T. annulata* the most striking feature involved the vast infiltration of uninfected macrophages accompanied by sinus hyperplasia and the formation of granulomas whereas, in the *T. parva* (Muguga) infected calf an extensive lymphocytic hyperplasia was detected with the presence of fewer macrophages and the absence of granulomas. However, similarities were seen in the remaining lymph nodes of both infection which included the regression and disappearance of lymphoid follicles and the extensive depletion of lymphoid cells.

The detection of such large numbers of macrophages in the tissues of both the *T. annulata* and *T. parva* (Muguga) infected animals, particularly in the lymph nodes of the *T. annulata* infected animals, was of interest in respect to the damage observed in these tissues. Macrophages, activated by IFN (Mogensen & Vierelizier), have been implicated in the production of cytokines (Preston *et al.* 1993), in particular TNF-α found to induce anorexia, cachexia (Oliff *et al.* 1987), pyrexia (Beutler & Cerami 1986), leucopenia (Ulich *et al.* 1987) and disseminated haemorrhagic necrosis which closely mimics septic shock (Tracey & Cerami 1989). Interestingly, lesions found in the tissues of animals infected with *T. annulata* have been recorded as resembling those observed in haemorrhagic septicaemias (Sergent 1945). The cytokine response initiated by both *T. annulata* and *T. parva* infected animals may therefore be very dangerous to host tissues as already described in other parasitic infections (Cox 1989). Macrophages have also been reported to produce nitric oxide (Visser *et al.* 1995), a compound recorded as mediating cell lysis (Kolb & Kolb-Bachofen 1992), mucosal damage and haemorrhage (Lopez-Belmonte *et al.* 1993) and inhibition of lymphocyte proliferation (Sternberg & McGuigan 1992). Macrophages may therefore elicit detrimental effects upon the host, since cattle infected with *T. annulata* or *T. parva* (Muguga) in this study exhibited clinical signs of pyrexia and leucopenia, the tissues contained areas of haemorrhage and necrosis, and the PBM harvested from the *T. annulata* (Hisar) infected animals synthesised nitric oxide

spontaneously *in vitro*. It has been suggested that haemorrhages are caused by toxins (Neitz 1957; Barnett 1960) which had not as yet been isolated. Nitric oxide may therefore be a possible toxin candidate. Importantly, macrophages have also been implicated in immunosuppression (Preston 1981) and evidence for immunosuppression in *T. annulata* infections at least has already been documented (Preston *et al.* 1983).

Interestingly, many features of both *T. annulata* and *T. parva* infections may be due to the secretion of IFNs by the parasitised cells and to cytokines such as IFN-γ and TNF-α produced by the host cells in response to infection (Preston *et al.* 1993). *T. annulata* has been documented to secrete type 1 IFN which downregulates lymphocyte proliferation (Balkwill 1989) whereas, *T. parva* has been documented to secrete IFN-γ (DeMartini & Baldwin 1991) which upregulates lymphoproliferation (Siegel 1988). These findings may offer an explanation for the differences observed in the lymph node which drained the site of inoculation in both the *T. annulata* and *T. parva* (Muguga) infected animals, i.e. the lymphodepletion seen in the lymph node of the *T. annulata* infected animals as opposed to the lymphoproliferation detected in the *T. parva* (Muguga) infected animal.

Assessment of parasite distribution (macroschizonts, microschizonts and piroplasms) in the impression smears of lymphoid and non-lymphoid organs of *T. annulata* or *T. parva* (Muguga) infected animals showed that parasites had the ability to disseminate throughout the organs of the body, either via the lymphatic system and/or via the blood stream. Parasites occurred in more lymphoid and non-lymphoid organs as infection progressed in the calves infected with *T. annulata* (Hisar). The parasites therefore appeared to be highly mobile. Further assessment of the distribution of macroschizont- and microschizont-infected cells in the tissue sections of the lymphoid and non-lymphoid organs of *T. annulata* or *T. parva* (Muguga) infected animals showed that both stages of the parasite occurred in most of the lymphoid and non-lymphoid organs and were not restricted to any particular compartment within the organs. However, examination of lymph nodes of the calf infected with *T. annulata* (Hisar) during the initial stages of pyrexia detected macroschizont-infected cells in the medullary regions of the lymph nodes alone, although both stages of the

parasite were detected throughout the remaining areas of the lymph nodes as disease progressed. Importantly, the macroschizont- and microschizont-infected cells were present, in most cases, in areas of tissue damage and absent in the areas of undamaged tissue. Since macroschizont-infected cells appear to be highly mobile and produce cytokines (Entrican *et al.* 1991; Ahmed *et al.* 1993; Preston *et al.* 1993; Brown *et al.* 1995) this may offer a possible explanation for the widespread tissue damage which was observed. The location of schizont-infected cells resembled those described in previous studies on *T. annulata* infected animals (Dschunkowsky & Luhs 1904; Sergent *et al.* 1945; Neitz 1957; Manickam *et al.* 1984 and *T. parva* infected animals (Steck 1928; Neitz 1957; Barnett 1960).

Analysis of the phenotype of macroschizont- and microschizont-infected cells in the tissue sections of lymphoid and non-lymphoid organs of *T. annulata* infected animals showed that both stages of the parasite resided within cells which expressed CD11b, the complement receptor for C3bi present on macrophages, B cells and NK cells, although morphologically the $CD11b^+$ cells appeared to be macrophages. This finding confirmed earlier observations (Sergent *et al.* 1945) which described schizonts as living within elements of the reticulo-endothelial system, reticular cells of the lymph nodes and spleen, Kupffer cells of the liver and histiocytes. In contrast, both stages of *T. parva* (Muguga) resided within cells which expressed CD3, a T cell marker, or CD11b, although morphologically the $CD11b^+$ cells appeared to be B and/or NK cells. Importantly, since both *in vivo*-derived cell lines (Howard *et al.* 1993; Forsyth *et al.* in press) and schizont-infected cells in tissues (Forsyth *et al.* in press) express CD11b, it seems likely that the *in vivo*-derived cell lines used to prepare the attenuated cell line vaccines in current use (Pipano 1989) represent the cell types inhabited by the parasites in tissues as well as blood. The phenotypic profiles of the *in vivo*-derived cell lines recorded to date showed that the cells chosen for infection by sporozoites *in vitro* (Howard *et al.* 1993) are phenotypically similar to the cells infected *in vivo*. The production of type 1 IFN by *T. annulata* schizont-infected cells (Entrican *et al.* 1991) is consistent with the previous indications that bovine cells infected with the parasite are predominantly macrophage-like. In contrast, the production of IFN-γ by *T. parva* schizont-infected cells (Entrican *et al.* 1991; DeMartini & Baldwin 1991) is in accordance with the parasite's apparent

preference for T and B cells. The different cells resided within by both parasites may explain the differences observed in the cellular responses of the lymph nodes of both the *T. annulata* and *T. parva* (Muguga) infected animals. Importantly, in the sections of both the *T. annulata* and *T. parva* (Muguga) infected animals there were populations of schizont-infected cells which were both $CD11b^-$ and $CD3^-$. The phenotype of these unstained schizont-infected cells remained unidentified.

Finding that *T. annulata* macroschizont- and microschizont-infected cells expressed CD11b was of relevance to two unsolved problems. Firstly, the way in which *T. annulata* schizonts transferred from cell to cell, in particular during infection with cell line vaccines. It seems feasible that schizonts freed from the donor cells by a rapid host response to inoculation with allogenic cells (Preston & Brown 1988) may be opsonised by complement and/or antibody and then linked to cells bearing the C3bi receptor. Attachment of the parasite-complement complex would facilitate phagocytosis of the organism by the cell. The subsequent establishment of the parasite in the cell would depend upon whether the cell bearing the C3bi receptor could support parasite proliferation. This finding could explain why *T. annulata* schizont-infected cell lines are more successful in immunising cattle against infection than *T. parva* schizont-infected cell lines. Finding that *T. annulata*-infected cells expressed CD11b -a molecule with a well documented role in leucocyte adhesion and migration (Bevilacqua 1993)- therefore indicates ways by which *T. annulata*-schizont-infected cells could move actively from blood or lymph to host tissues. The stimulus for such movement throughout the host might lie in the constitutive expression by these cells of matrix metalloproteinase 9, an enzyme associated with metastasis in other conditions (Baylis, Megson & Hall 1995).

Immunologically mediated haemolysis involving complement has been described as a mechanism for the anaemia associated with malarial infections (Houba, Lambert, Mackey & Miescher 1980; Strickland & Hunter 1980). If this occurs in *T. annulata* infections, opsonisation of non-phagocytic erythrocytes could result in their lysis via the complement cascade and eventually contribute to anaemia. C3bi has also been reported to attach to platelets resulting in the release of detrimental vasoactive amines which cause intense inflammatory reactions and necrosis (Mims 1987). If

this also occurred in the *T. annulata* infected animals described here, this may explain the damage recorded in the tissues and the reduction in the numbers of platelets recorded during the course of the infection.

Assessment of the phenotype of the uninfected cell types which occurred alongside the infected cells in the tissues of the *T. annulata* or *T. parva* (Muguga) infected animals was conducted using the antibodies which recognised $CD11b^+$ and $CD3^+$ cells. Surprisingly the large numbers of uninfected macrophages as described above which were detected in the lymph nodes of the *T. annulata* infected animals were $CD11b^-$. Interestingly the uninfected cells in the medullary cords of these lymph nodes were stained strongly by the CD11b marker. Morphologically these cells looked like B and/or NK cells. This finding suggested that although most of the lymphoid follicles had regressed or disappeared, the activity of B cells was not completely diminished. B cells may have migrated from the germinal centres to the medullary cords. The use of the marker to identify uninfected $CD3^+$ cells gave additional evidence for the occurrence of lymphodepletion rather than for lymphoproliferation in the lymph nodes of the infected animals as described above. Surprisingly the uninfected cells of the intense lymphocytic hyperplasia detected in the draining lymph node of the *T. parva* (Muguga) infected animal were $CD3^-$ and $CD11b^-$ cells so their identity remains unknown. The cellular infiltrate observed in the non-lymphoid organs, e.g. the kidney, liver, abomasum, lung, heart, adrenal and pituitary glands of both infections was composed of both uninfected $CD3^+$ and $CD11b^+$ cells. The parasitised non-lymphoid organs of the *T. annulata* infected animals showed that the proliferation of *T. annulata* infected $CD11b^+$ cells was accompanied by an infiltration of uninfected $CD3^+$ cells. The infiltration of both uninfected $CD11b^+$ and $CD3^+$ cells was detected in the parasitised non-lymphoid organs of the *T. parva* (Muguga) infected animal.

Investigation of the *in vitro* response of nitric oxide on schizont-infected and uninfected cell lines showed an increase in apoptosis, cell death and the malformation and destruction of parasites which resided within the cytoplasm of the host cells. This finding highlighted not only the beneficial effects of nitric oxide in controlling the numbers of schizonts and schizont-infected cells, but also its

potentially detrimental effects on the destruction of uninfected, normal host cells. An increase in apoptotic cells was also seen in the tissue sections of the lymph node which drained the site of inoculation of an animal which had responded severely to infection with *T. annulata*. Interestingly, apoptosis has been reported as a natural regulatory mechanism that protects against excessive cytokine production (Golstein *et al.* 1991). It is possible that an increase in apoptosis was the result of activated host macrophages as described above. Importantly, excessive fibronectin present in sites of inflammation retards the ability of phagocytic cells to remove apoptotic cells (Savill *et al.* 1993). If this occurs, apoptotic cells release their internal contents promoting additional inflammation and increasing the risk of permanent tissue damage (Savill *et al.* 1993). These conditions may have occurred in the damaged tissues of the infected animals intensifying the tissue damage. Interestingly, apoptosis has been shown to be induced by TNF (Wyllie *et al.* 1980). In contrast, IFN-γ has been shown to rescue cells from apoptosis (Mangan & Wahl 1991).

Consideration of the lesions and cellular responses found in the tissues of *Theileria* infected animals, in particular animals infected with *T. annulata* (Hisar), e.g. oedema, haemorrhage, lymphoid depletion, granulomatous formations and anaemia suggested that the immune system of the host may have caused the damage which accompanied infection. The proliferating macroschizont-infected cells were, in most cases, associated with paracortical lymphodepletion and macrophage infiltration and accompanied by extensive areas of necrosis and haemorrhage. The detrimental effects imposed by the immune response could possibly be attributed to a macrophage and/or complement response elicited by the host to the schizont-infected cells.

Both *T. annulata* and *T. parva* have frequently been referred to as lymphoproliferative diseases of cattle (Irvin & Morrison 1987). The reasons for this are as follows: both *T. annulata* (Sergent *et al.* 1945; Neitz 1957; Gill *et al.* 1977; Srivastava & Sharma 1981; Eisler 1988) and *T. parva* (Steck 1928, Cowdry & Danks 1933; Neitz 1957; De Kock 1957; DeMartini & Moulton 1973; Barnett 1977; Morrison *et al.* 1981a) have been reported to reside within the cytoplasm of lymphocytes; lymphocytosis of both infected and uninfected cells has been recorded

in the lymph node draining the site of inoculation of both *T. annulata* (Sergent *et al.* 1945) and *T. parva* (Morrison *et al.* 1981a) infected animals leading to a dramatic three- to six-fold increase in the size of the lymph node. However, the findings of the lymph nodes of the *T. annulata* infected animals of this study examined during the course of lethal infection were as follows: parasites residing within the cytoplasm of myeloid cells and not T cells; lymphodepletion instead of lymphoproliferation; granulomatous formations; the presence of large numbers of uninfected macrophages. These results therefore suggest that lethal infection with *T. annulata*, at least, does not cause a lymphoproliferative disease. Such findings suggest that *T. annulata* infections are rather immunopathological diseases characterised by granulomatous formations, e.g. leishmania (Ridley 1979), schistosomiasis (Weinstock 1994), Johne's disease (Huchzermeyer, Bruckner & Bastianello), leprosy (Zumla 1994) and tuberculosis (James 1994). The results of this study therefore indicate that the nature of lethal infections with *T. annulata* or *T. parva* are intrinsically different.

REFERENCES

ADLER, S. & ELLENBOGEN, V. (1934). A note on the premunition of calves against *Theileria annulata*. *Veterinary Record,* **14**: 91-93.

AHMED, J. S., REHBEIN, G. & SCHEIN, E. (1984). Characterisation of *Theileria annulata*-infected lymphoblastoid cells. *Zeitschrift Parasitenkunde,* **70**: 819-821.

AHMED, J. S., WIEGERS, P., STEUBER, S., SCHEIN, E., WILLIAMS, R. O. & DOBBELAERE, D. (1993). Production of interferon by *Theileria annulata* and *Theileria parva*-infected bovine lymphoid cell lines. *Parasitological Research,* **79**: 178-182.

ALBINA, J. E., CUI, S., MATEO, R. B. & REICHNER, J. S. (1993). Nitric oxide-mediated apoptosis in murine peritoneal macrophages. *Journal of Immunology,* **150, 11**: 5080-5085.

AMEISEN, J. C. & CAPRON, A. (1991). Cell dysfunction and depletion in Aids: the programmed cell death hypothesis. *Immunology Today,* **4**: 102-105.

ANDREW, S. M. & JASANI, B. (1987). An improved method for the inhibition of endogenous peroxidase non-deleterious to lymphocyte surface markers. Application to immunoperoxidase studies on eosinophil-rich tissue preparations. *Histochemical Journal,* **19**: 426-430.

ANON (1989). Classification of *Theileria parva* reactions in cattle. In: *Theileriasis in Eastern, Central and Southern Africa.* Proceedings of a Workshop on East Coast fever Immunisation held in Lilongwe, Malawi 20-22 September 1988 (Ed. T. T. Dolan), International Laboratory for Research on Animal Diseases, Nairobi. Appendix 2.

ANON (1991). Tick-borne diseases of livestock. ILRAD Reports. Nairobi, Kenya.

BAHARSEFAT, M., AMJADI, A. R., HASHEMI-FESHARKI, R., AHOURAI, P. & ARBABI, I. (1977). Unusual cases of *Theileria annulata* infection in calves. *Archives de l'Institut Razi,* **29**: 47-58.

BALDWIN, C. L. B., GODDEERIS, B. M. & MORRISON, W. I. (1987). Bovine helper T cell clones specific for lymphocytes infected with *Theileria parva* (Muguga). *Parasite Immunology,* **9**: 499-513.

BALDWIN, C. L. B., BLACK, S. J., BROWN, W. C., CONRAD, P. A., GODDEERIS, B. M., KINUTHIA, S. W., LALOR, P. A., McHUGH, N. P., MORRISON, W. I., MORZARIA, S. P., NAESSENS, J. & NEWSON, J. (1988). Bovine T cells, B cells and Null cells are transformed by the protozoan parasite *Theileria parva. Infection and Immunity,* **56**: 426-467.

BALKWILL, F. R. (1989). *Cytokines in cancer therapy*. Oxford University Press, Oxford.

BANKS, W. J. (1993). Applied Veterinary Histology. 3rd Edition. Mosby Year Book, Inc.

BARBONI, E. (1942). Emorragie encefaliche multiple e theileriosi die bovini da *Theileria annulata*. *Nuova Veterinaria,* **21**: 11-15.

BARNETT, S. F. (1960). Connective tissue reactions in acute fatal East Coast fever (*Theileria parva*) of cattle. *Journal of Infectious Diseases,* **107, 3**: 253-282.

BARNETT, S. F. (1968). Theileriasis. In: *Infectious Blood Diseases of Man and Animals.* II. (Eds. D. Weinmann & M. Ristic) Academic Press, New York: 269-328.

BARNETT, S. F. (1977). *Theileria.* In: *Parasitic Protozoa.* IV. (Ed. J. P. Kreier). Academic Press: 77-113.

BAYLIS, H. A., MEGSON, A. & HALL, R. (1995). Infection with *T. annulata* induces expression of matrix metalloproteinase 9 and transcription factor AP-1 in bovine leucocytes. *Molecular and Biochemical Parasitology,* **19**: 211-222.

BEN MILED, L., DARGHOUTH, M., BELL SAKYI, L., MELROSE, T. R., BROWN, C. G. D. & DELLAGI, K. (1994). Parasite selection through vertebrate and invertebrate hosts in *Theileria annulata* infection. In: *The European Union Third Coordination Meeting on Tropical Theileriosis.* (Eds. R. Spooner & J. Campbell). The Roslin Institute, Edinburgh: 67-69.

BETTENCOURT, A., FRANCA, C. & BORGES, J. (1907). Un cas de piroplasmose bacilliforme chez le daim. *Institut Royal de Bacteriologie, Camara Pestana,* **1**: 341-363.

BEUTLER, B. & CERAMI, A. (1986). Cachectin and tumour necrosis factor as two sides of the same biological coin. *Nature,* **320**: 584-588.

BEVAN, D. J. & CHISHOLM, P. M. (1986). Coexpression of CD4 and CD8 molecules and *de novo* expression MHC class II antigens on activated T lymphocytes. *Immunology,* **59**: 621-625.

BEVILACQUA, M. P. (1993) Endothelial-leucocyte adhesion molecules. *Annual Review of Immunology,* **11**: 767-804.

BIELEFELDT OHMANN, H., CAMPOS, M. & SNIDER, M. (1989). Effect of chronic administration of recombinant bovine tumour necrosis factor to cattle. *Veterinary Pathology,* **26**: 462-472.

BLOOM, B. R. (1979). Games parasites play: How parasites evade immune surveillance. *Nature,* **279**: 21-26.

BLUE, M. L., DALEY, J. F., LEVINE, H. & SCHLOSSMAN, S. F. (1985). Coexpression of BoT4 and BoT8 on peripheral blood T cells demonstrated by two-colour fluorescence flow cytometry. *Journal of Immunology,* **134**: 2281-2286.

BOEHME, S. A. & LENARDO, M. J. (1993). Propriocidal apoptosis of mature T lymphocytes occurs at S phase of the cell cycle. *European Journal of Immunology,* **23**: 1552-1560.

BROCKLESBY, D. W., BARNETT, S. F. & SCOTT, J. (1961). Morbitity and mortality rates in East Coast fever (*Theileria parva* infection) and their application to drug screening procedures. *British Veterinary Journal,* **117**: 529-531.

BROWN, C. G. D., CRAWFORD, J. G., KANHAI, G. K., NJUGUNA, L. M. & STAGG, D. A. (1978). Immunisation of cattle against East Coast fever with lymphoblastoid cell lines infected and transformed by *Theileria parva.* In: *Tick-borne Diseases and their Vectors.* (Ed. J. K. H. Wilde). University of Edinburgh, Edinburgh: 331-333.

BROWN, C. G. D. (1981). Application of *in vitro* techniques to vaccination against theileriosis. In: *Advances in the Control of Theileriosis (Current Topics in Veterinary Medicine and Animal Science).* (Eds. A. D. Irvin, M. P. Cunningham & A. S. Young). The Hague, Boston, London. Martinus Nijhoff Publishers, **14:** 104-119.

BROWN, C. G. D. (1983). *Theileria.* In: *In Vitro Cultivation of Protozoan Parasites* (Ed. J. B. Jenson), CRC Press, Boca Raton, Florida: 243-284.

BROWN, C. G. D. (1990). Control of theileriosis (*Theileria annulata* infection) of cattle. *Parassitologia,* **32**: 23-31.

BROWN, D. J., CAMPBELL, J. D. M., RUSSELL, G. C., HOPKINS, J. & GLASS, E. J. (1995). T cell activation by *Theileria annulata* infected macrophages correlates with cytokine production. *Clinical Experimental Immunology,* **102**: 1-8.

BURKITT, H. G., YOUNG, B. & HEATH, J. W. (1993). Wheater's Functional Histology. A text and colour atlas. 3rd Edition. Churchill Livingstone.

BURRIDGE, M. J., BROWN, C. G. D. & KIMBER, C. D. (1974). *Theileria annulata*: Cross-reactions between a cell culture schizont antigen and antigens of East African species in the indirect fluorescent antibody test. *Experimental Parasitology,* **35**: 374-380.

CAMPBELL, J. D., BROWN, D. J., GLASS, E. J., HALL, F. R. & SPOONER, R. L. (1994). *Theileria annulata* sporozoite targets. *Parasite Immunology,* **16**: 501-505.

CARSON, D. A. & RIBEIRO, J. M. (1993). Apoptosis and disease. *Lancet,* **341**: 1251-1254.

CHAPMAN, W. E. & WARD, P. A. (1977). *Babesia rodhaini*: Requirement of complement for penetration of human erythrocytes. *Science,* **196**: 67-69.

CLARK, I. A., ROCKETT, K. A. & COWDEN, W. B. (1991). Proposed link between cytokines, nitric oxide and human cerebral malaria. *Parasitology Today,* **7, 8**: 205-207.

COHEN, J. J. & DUKE, R. C. (1984). Glucocorticoid activation of a calcium-dependent endonuclease in thymocyte nuclei leads to cell death. *Journal of Immunology,* **132**: 38-42.

CONRAD, P. A., KELLY, B. G. & BROWN, C. G. D. (1985). Intraerythrocytic schizogony of *Theileria annulata. Parasitology,* **91**: 67-82.

CONRAD, P. A., DENHAM, D. & BROWN, C. G. D. (1986). Intraerythrocytic multiplication of *Theileria parva in vitro*: An ultrastructural study. *International Journal of Parasitology,* **16**: 223-230.

CONRAD, P. A., BALDWIN, C. L. & BROWN, W. C. (1989). Infection of bovine T cell clones with genotypically distinct *Theileria parva* parasites and analysis of their cell surface phenotype. *Parasitology,* **99**: 205-213.

COOPER, N. R. (1991). Complement evasion strategies of microorganisms. *Immunology Today,* **12**: 327-331.

CORDIER, G., MENAGER, M. J. & DELORME, A. (1936). Etude de la souche Algerienne "Kouba" de *Theileria dispar.* Son importance dans la premunition antitheilerique bovine. *Bulletin Societe Pathologic et Exotique,* **29**: 313-327.

COWDRY, E. V. & HAM, A. W. (1932). Studies on East Coast fever. 1. The life cycle of the parasite in ticks. *Parasitology,* **24**: 1-49.

COWDRY, E. V. & DANKS, W. B. C. (1933). Studies on East Coast fever. II. Behaviour of the parasite and development of distinctive lesions in susceptible animals. *Parasitology,* **25**: 1-63.

COX, F. E. G. (1989). *Immunological and Molecular Basis of Pathogenesis of Parasitic Diseases.* University of Hong Kong Press: 7-13.

CREEMERS, P. (1982). Lack of reactivity of sera from *Theileria parva*-infected and recovered cattle against cell membrane antigens of *Theileria parva*-transformed cell lines. *Veterinary Immunology and Immunopathology,* **3**: 427-438.

CROEN, K. D. (1993). Evidence for an antiviral effect of nitric oxide. Inhibition of Herpes Simplex Virus Type I replication. *Journal of Clinical Investigation,* **91**: 2446-2452.

DE KOCK, G. (1957). Studies on the lesions and pathogenesis of East Coast fever (*Theileria parva* infection) in cattle with special reference to the lymphoid tissue. *Onderstepoort Journal of Veterinary Research,* **27, 3**: 431-453.

DE MAEYER, E. & DE MAEYER-GUIGNARD, J. (1988). *Interferons and other Regulatory Cytokines*. Wiley & Sons, New York: 174-193.

DECKERS, C. L. P., LYONS, A. B., SAMUEL, K., SANDERSON, A. & MADDY, A. H. (1993). Alternative pathways of apoptosis induced by methylprednisolone and valinomycin analysed by flow cytometry. *Experimental Cell Research*, **208**: 362-370.

DELPY, L. P. (1937). Les theileriosis bovines en Iran. *Archives de l'Institut Pasteur d'Algerie, Alger*, **5**: 225-264.

DEMARTINI, J. C. & MOULTON, J. E. (1973). Responses of the bovine lymphatic system to infection by *Theileria parva*. I. Histology and ultrastructure of lymph nodes in experimentally-infected calves. *Journal of Comparative Pathology*, **83**: 281- 298.

DEMARTINI, J. C. & BALDWIN, C. L. (1991). Effects of gamma interferon, tumour necrosis factor alpha and interleukin-2 on infection and proliferation of *Theileria parva*-infected bovine lymphoblasts and production of interferon by parasitised cells. *Infection and Immunity*, **59**: 4540-4546.

DICKSON, J. & SHIELS, B. R. (1993). Antigenic diversity of a major merozoite surface molecule in *Theileria annulata*. *Molecular and Biochemical Parasitology*, **57**: 55-64.

DIEJEU, J. Y., HEINBAUGH, J. A., HOLDEN, H. T. & HERBERMANN, R. B. (1978). Augmentation of mouse natural killer cell activity by interferon inducers. *Journal of Immunology*, **122**: 175-181.

DOBBELAERE, D. A. E., PROSPERO, T. D. & RODITI, I. J. (1990). Expression of Tac antigen component of bovine interleukin-2 receptor in different leucocyte populations infected with *Theileria parva* and *Theileria annulata*. *Infection and Immunity*, **58**: 3847-3855.

DOLAN, T. T. & YOUNG, A. S. (1981). An approach to the economic assessment of East Coast fever in Kenya. In: *Advances in the Control of Theileriosis*. (Eds. A. D. Irvin, M. P. Cunningham & A. S. Young). The Hague, Boston, London. Martinus Nijhoff Publishers, **14**: 412-415.

DOLAN, T. T., TEALE, A. J., STAGG, D. A., KEMP, S. J., COWAN, K. M., YOUNG, A. S., GROOCOCK, C. M., LEITCH, B. L., SPOONER, R. L. & BROWN, C. G. D. (1984a). A histocompatibility barrier to immunisation against East Coast fever using *Theileria parva* infected lymphoblastoid cell lines. *Parasite Immunology*, **6**: 243-250.

DOLAN, T. T., YOUNG, A. S., LOSOS, G. J., MCMILLAN, I., MINDER, CH. E. & SOULSBY, K. (1984b). Dose dependent responses of cattle to *Theileria parva* stabilate. *International Journal for Parasitology*, **14**: 89-95.

DONATIEN, A. & LESTOQUARD, F. (1938). Sur quelques maladies subtropicales due mediterraneen. *Report of the 13th International Veterinary Congress,* 1938, **2**: 791-799. *Archives de l'Institut Pasteur d'Algerie, Alger*, **17**: 322-330.

DSCHUNKOWSKY, E. & LUHS, I. (1904). Die Piroplasmosen der Rinder, *Zentralblatt fur Bakteriologie, Parasitenkunde, Infectionskrankheiten und Hygiene Abteilung I. Originale*, **35**: 486-492.

DUFFUS, W. P. H., WAGNER, G. G. & PRESTON, J. M. (1978). Initial studies on the properties of a bovine lymphoid cell culture line infected with *Theileria parva. Clinical and Experimental Immunology,* **34**: 347-353.

DUKE, R. C., CHERVENAK, R. & COHEN, J. J. (1983). Endogenous endonuclease-induced DNA fragmentation: An early event in cell mediated cytolysis. *Proceedings of the National Academy of Science, USA,* **80**: 6361-6365.

EISLER, M. (1988). Immunohistochemical methods in the study of tropical theileriosis. M.Sc. thesis. University of Edinburgh.

EMERY, D. L. & MORRISON, W. I. (1980). Generation of autologous mixed leucocyte responses during the course of infection with *Theileria parva* (East Coast fever) in cattle. *Immunology,* **40**: 229-237.

EMERY, D. L. (1981). Kinetics of infection with *Theileria parva* (East Coast fever) in the central lymph of cattle. *Veterinary Parasitology,* **9**: 1-16.

EMERY, D. L., EUGUI, E. M., NELSON, R. T. & TENYWA, T. (1981a). Cell-mediated immune responses to *Theileria parva* (East Coast fever) during immunisation and lethal infections in cattle. *Immunology,* **43**: 323-336.

EMERY, D. L., TENYWA, T. & JACK, R. M. (1981b). Characterisation of the effector cell that mediates cytotoxicity against *Theileria parva* (East Coast fever) in immune cattle. *Infection and Immunity,* **32**: 1301-1304.

EMERY, D. L., MACHUGH, N. D. & MORRISON, W. I. (1988). *Theileria parva* (Muguga) infects bovine T lymphocytes *in vivo* and induces coexpression of BoT4 and BoT8. *Parasite Immunology,* **10**: 379-391.

ENTRICAN, G., McINNES, C. J., LOGAN, M., PRESTON, P. M., MARTINOD, S. & BROWN, C. G. D. (1991). Production of interferons by bovine and ovine cell lines infected with *Theileria annulata* or *Theileria parva. Parasite Immunology,* **13**: 339-343.

ERDEI, A., FUST, G. & GERGELY, J. (1991). The role of C3 in the immune response. *Immunology Today,* **12**: 332-337.

EUGUI, E. N. & EMERY, D. L. (1981). Genetically restricted cell mediated cytotoxicity in cattle immune to *Theileria parva* (East Coast fever). *Nature,* **290**: 251-254.

FLANAGAN, H. O. & LE ROUX, J. M. W. (1957). Bovine cerebral theileriosis-a report on two cases occurring in the Union. *Onderstepoort Journal of Veterinary Research,* **27**: 453-461.

FORSYTH, L. M. G., JACKSON, L. A., WILKIE, G., SANDERSON, A, BROWN, C. G. D. & PRESTON, P. M. (in press) Bovine cells infected *in vivo* with *Theileria annulata* express CD11b, the C3bi complement receptor. *Veterinary Research Communications.*

GAVRIELI, Y., SHERMAN, Y. & BEN-SASSON, S. A. (1992). Investigation of programmed cell death i*n situ* via specific labeling of nuclear DNA fragmentation. *Journal of Cell Biology*, **119, 3**: 493-501.

GILES, T., DAVIES, F. G., DUFFUS, W. P. H. & HEINOSTEN, R. (1978). Bovine cerebral theileriosis. *Veterinary Record,* **102**: 313.

GILL, B. S., BHATTACHARYULU, Y., KAUR, D. & SINGH, A. (1976a). Vaccination against bovine tropical theileriosis (*Theileria annulata*). *Nature,* **264**: 355-356.

GILL, BHATTACHARYULU & KAUR (1976b). Immunisation against bovine tropical theileriosis (*Theileria annulata* infection). *Research in Veterinary Science*, **21**: 146-149.

GILL, B. S., BHATTACHARYULU, Y. & KAUR, D. (1977). Symptoms and pathology of experimental bovine tropical theileriosis (*Theileria annulata* infection). *Annales de Parasitologie,* **52, 6**: 597-608.

GILL, B. S., BONSAL, G. G., BHATTACHARYULU, Y., KAUR, D. & SINGH, A. (1980). Immunization of cattle against *Theileria annulata:* A resume of work done at Punjab Agricultural University, Ludhaina. In*: Advances in the Control of Theileriosis*: Proceedings of an International Conference held at ILRAD, Nairobi, 9-13 February, 1981. (Eds. A. D. Irvin, M. P. Cunningham & A. S. Young). The Hague, Boston, London. Martinus Nijhoff Publishers, **14**: 259-261.

GLASCODINE, J., TETLEY, L., TAIT, A., BROWN, C. G. D. & SHIELS, B. (1990). Developmental expression of a *Theileria annulata* merozoite surface antigen. *Molecular and Biochemical Parasitology*, **40**: 105-112.

GLASS, E. J., INNES, E. A., SPOONER, R. L. & BROWN, C. G. D. (1989). Infection of bovine monocyte/macrophage population with *Theileria annulata* and *Theileria parva. Veterinary Immunology and Immunopathology,* **22**: 355-368.

GOLSTEIN, P., OJCIUS, D. M. & YOUNG, D. E. (1991). Cell death mechanisms and the immune system. *Immunological Review,* **121**: 29-65.

GRAY, C. E. & ROBERTSON, W. (1902). *Report upon Texas fever or Redwater in Rhodesia.* Cape Town, South Africa: Argus Printing & Publishing Company Ltd.

HOUBA, V., LAMBERT, P. H., MACKEY, L. J. & MIESCHER, P. A. (1980). Immunopathology of malaria. *Springer Seminars in Immunopathology,* **2, 4**: 359-371.

HOOSHMAND-RAD, P. (1976). The pathogenesis of anaemia in *Theileria annulata* infection. *Research in Veterinary Science,* **20**: 324-329.

HOWARD, C. J. & NAESSENS, J. (1993). Summary of workshop findings for cattle. *Veterinary Immunology and Immunopathology*, **39**: 25-48.

HOWARD, C. J., SOPP, P., PRESTON, P. M., JACKSON, L. A. & BROWN, C. G. D. (1993). Phenotypic analysis of bovine leucocyte cell lines infected with *Theileria annulata. Veterinary Immunology and Immunopathology,* **39**: 275-282.

HSU, S., RAINE, L. & FANGER, H. (1981). Use of avidin-biotin-peroxidase complex (ABC) in immunoperoxidase techniques: A comparison between ABC and unlabeled antibody (PAP) procedures. *Journal of Histochemistry and Cytochemistry*, **29, 4**: 577-580.

HUCHZERMEYER, H. F. A. K., BRUCKNER, G. K. & BASTIANELLO, S. S. (1994). Paratuberculosis. In: *Infectious Diseases of Livestock.* (Eds. J. A. W. Coetzer, G. R. Thomson & R. C. Tustin). Oxford University Press: 1445-1457.

HULLIGER, L. (1965). Cultivation of three species of *Theileria* in lymphoid cells *in vitro. Journal of Protozoology,* **12**: 649-655.

IGNARRO, L. J., LIPTON, H., EDWARDS, J. C., BARICOS, W. H., HYMAN, A. L., KADOWITZ, P. J. & GRUETTER, C. A. (1981). Mechanism of vascular smooth muscle relaxation by organic nitrates, nitrites, nitroprusside and nitric oxide: Evidence for the involvement of S-nitrosothiols as active intermediates. *Journal of Pharmacology and Experimental Therapeutics*, **218**: 737-749.

INNES, E. A., MILLAR, P., GLASS, E. J., BROWN, C. G. D. & SPOONER, R. L. (1989a). *In vitro* infection of bovine alloreactive cytotoxic T cell lines with sporozoites of *Theileria annulata* and *Theileria parva. Research in Veterinary Science,* **46**: 367-374.

INNES, E. A., MILLAR, P., BROWN, C. G. D. & SPOONER, R. L. (1989b). The development and specificity of cytotoxic cells in cattle with autologous or allogeneic *Theileria annulata*-infected lymphoblastoid cell lines. *Parasite Immunology,* **11**: 57-68.

IRVIN, A. D. & CUNNINGHAM, M. P. (1981). *Theileria* infections other than East Coast fever In: *Diseases of Cattle in the Tropics* (Eds. M. Ristic & I. McIntyre), Martinus Nijhoff, The Hague: 393-410.

IRVIN, A. D. & MWAMACHI, D. M. (1983). Clinical and diagnostic features of East Coast fever (*Theileria parva*) infection of cattle. *Veterinary Record,* **113**: 192-198.

IRVIN, A. D. & MORRISON, W. I. (1987). Immunopathology, immunology and immunoprophylaxis of *Theileria* infections. In: *Immune Responses in Parasitic Infections: Immunology, Immunopathology and Immunoprophylaxis*, Volume III: Protozoa, (Ed. E. J. L. Soulsby). CRC Press, Boca Raton: 223-274.

JAMES, D. G. & COLLEY, S. L. (1978). Eosinophil-mediated destruction of *Schistosoma mansoni* eggs. III. Lymphokine involvement in the induction of eosinophil functional abnormalities. *Cellular Immunology,* **38**: 48-58.

JAMES, D. G. (1994). Upper Respiratory Tract. In: *Sarcoidosis and Other Granulomatous Disorders.* (Ed. D. G. James). Marcel Dekker, Inc., **73**: 417-420.

JARRETT, W. F. H. & BROCKLESBY, D. W. (1966). A preliminary electron microscopic study of East Coast fever (*Theileria parva* infection). *Journal of Protozoology,* **13**: 301-310.

JARRETT, W. F. H., CRIGHTON, G. W. & PIRIE, H. W. (1969). *Theileria parva*: Kinetics of replication. *Experimental Parasitology,* **24**: 9-25.

JURA, W. G. Z. O., BROWN, C. G. D. & KELLY, B. (1983). Fine structure and invasive behaviour of the early developmental stages of *Theileria annulata in vitro. Veterinary Parasitology,* **12**: 31-44.

KABELITZ, D. & WESSELBORG, S. (1992). Life and death of a superantigen reactive human $CD4^+$ T cell clone: staphylococcal enterotoxins induce death by apoptosis but simultaneously trigger a proliferative response in the presence of HLA-DR^+ antigen presenting cells. *International Immunology,* **4, 12**: 1381-1388.

KABELITZ, D., POHL, T. & PECHHOLD, K. (1993). Activation induced cell death (apoptosis) of mature peripheral T lymphocytes. *Immunology Today,* **14, 7**: 338-339.

KACHANI, M. (1990). Immune responses in *Theileria annulata* infection. Ph.D. thesis. University of Brunel.

KAWABE, Y. & OCHI, A. (1991). Programmed cell death and extra thymic reduction of V-beta 8^+ $CD4^+$ T cells in mice tolerant to *Staphylococcus aureus* enterotoxin B. *Nature,* **349**: 245-248.

KELLY, P. M. A., BLISS, E., MORTON, J. A., BURNS, J. & MCGEE, J. D. (1988). Monoclonal antibody EBM/11: High cellular specificity for human macrophages. *Journal of Clinical Pathology*, **41**: 510-515.

KERR, J. F. R., WYLLIE, A. H. & CURRIE, A. R. (1972). Apoptosis: A basic biological phenomenon with wide ranging implications in tissue kinetics. *British Journal of Cancer,* **26**: 239-257.

KHANNA, B. M., KHAROLE, M. U., DHAR, S. & GAUTAM, O. P. (1980). Pathogenesis of lesions in bovine cerebral theileriosis. In: *Haemoprotozoan Diseases*

of Domestic Animals. (Eds. O. P. Gautam, R. D. Sharma & S. Dhar). Department of Veterinary Medicine, Haryana Agricultural University, Hisar 125004, India.

KIMETO, B. A. (1978). Histopathological and electron microscopic studies of cutaneous lesions in calves with experimentally induced East Coast fever (Theileriosis). *American Journal of Veterinary Research,* **39**: 1117-1122.

KOCH, R. (1898). Weiterer Bericht uber das Texasfieber, *Zentralblatt fur Bakteriologie, Parasitenkunde, Infectionskrankheiten und Hygiene Abteilung I. Originale,* **24**: 202.

KOLB, H. & KOLB-BACHOFEN, V. (1992). Nitric oxide: A pathogenic factor in autoimmunity. *Immunology Today,* **13**: 157-159.

LAIBLIN, C. (1978). Klinische untersuchungen zur *Theileria annulata* infektion des rindes. *Berliner und Munchener Tierarzthiche Wochenschrift,* **91**: 48-50.

LALOR, P. A., MORRISON, W. I. & BLACK, S. J. (1986). Monoclonal antibodies to bovine leucocytes define heterogenecity of target cells for the parasitosis by *Theileria parva.* In: *The Ruminant System in Health and Disease.* (Ed. W. I. Morrison). Cambridge University Press: 72-87.

LENARDO, M. J. (1991). Interleukin-2 programs mouse alpha-beta T lymphocytes for apoptosis. *Nature,* **353**: 858-861.

LEVINE, N. D., CORLISS, J. O., COX, F. E. G., DEROUX, G., GRAIN, J., HONIGBERG, B. N., LEEDALE, G. F., LOEBLICH, A. R. II., LOM, J., LYNN, D. H., NERINFIELD, F. G., PAGE, F. C., POLJANSKY, G., SPRAGUE, V., VAURA, J. & WALLACE, F. G. (1980). A newly revised classification of the protozoa. *Journal of Protozoology,* **27**: 37-38.

LOPES, M. F., VEIGA, V. F., SANTOS, A. R., FONSECA, M. E. F. & DOSREIS, G. A. (1995). Activation-induced $CD4^+$ T cell death by apoptosis in experimental chagas' disease. *Journal of Immunology,* **154**: 744-752.

LOPEZ-BELMONTE, J., WHITTLE, B. J. R. & MONCADA, S. (1993). The actions of nitric oxide donors in the prevention or induction of injury to the rat gastric mucosa. *British Journal of Pharmacology,* **108**: 73-78.

LOUNSBURY, C. P. (1904). Transmission of African East Coast fever. *Agricultural Journal, Cape of Good Hope,* **24**: 428-432.

LYONS, A. B., SAMUEL, K., SANDERSON, A. & MADDY, A. H. (1992). Simultaneous analysis of immunophenotype and apoptosis of murine thymocytes by single laser flow cytometry. *Cytometry,* **13**: 809-821.

MANGAN, D. F. & WAHL, S. M. (1991). Differential regulation of human monocyte programmed cell death (apoptosis) by chemotactic factors and pro-inflammatory cytokine. *Journal of Immunology,* **147**: 3408-3417.

MANICKAM, R., DHAR, S., SINGH, R. P. & KHAROLE, M. U. (1984). Histopathology of cutaneous lesions in *Theileria annulata* infection of calves. *Indian Veterinary Journal,* **61**: 13-15.

MEHLHORN, H. & SCHEIN, E. (1984). The piroplasms: Life cycle and sexual stage. In: *Advances in Parasitology,* **23** (Eds. J. R. Baker & R. Muller). London Academic Press: 37-103.

MELROSE, T. R., BROWN, C. G. D. & SHARMA, R. D. (1980a). Glucose phosphate isomerase isoenzyme patterns in bovine lymphoblastoid cell lines infected with *Theileria annulata* and *Theileria parva*, with an improved enzyme visualisation method using meldola blue. *Research in Veterinary Science,* **29**: 298-304.

MELROSE, T. R., WALKER, A. R. & BROWN, C. G. D. (1980b). Identification of *Theileria* infections in the salivary glands of *Hyalomma anatolicum* and *Rhipicephalus appendiculatus* using isoenzyme electrophoresis. *Tropical Animal Health and Production,* **12**: 214-218.

MELROSE, T. R., BROWN, C. G. D., MORZARIA, S. P., OCAMA, J. G. R. & IRVIN, A. D. (1984). Glucose phosphate isomerase polymorphism in *Theileria annulata* and *Theileria parva. Tropical Animal Health and Production,* **16**: 239-45.

MIGLIORINI, P., CORRADIN, G. & BETZ CORRADIN, S. (1991). Macrophage NO_2^- production as a sensitive and rapid assay for the quantitation of murine IFN-gamma. *Journal of Immunological Methods*, **139**: 107-114.

MIMS, C. A. (1987). The immune response to infection. In: *The Pathogenesis of Infectious Disease.* 3rd Edition. Academic Press, London: 122-151.

MOGENSEN, S. C. & VIERELIZIER, J-L. (1987). The interferon-macrophage alliance. *Interferon,* **8**: 55-81.

MONCADA, S., PALMER, R. M. J. & HIGGS, E. A. (1991). Nitric oxide: Physiology. Pathophysiology and Pharmacology. *Pharmacological Reviews,* **43**: 109-142.

MORRISON, W. I., BUSCHER, G., MURRAY, M., EMERY, D. L., MASAKE, R., COOK, R. H. & WELLS, P. W. (1981a). *Theileria parva*: Kinetics of infection in the lymphoid system of cattle. *Experimental Parasitology,* **52**: 248-260.

MORRISON, W. I., BUSCHER, G., EMERY, D. L., NELSON, R. T. & MURRAY, M. (1981b). *Theileria parva* in cattle. In : *Advances in the Control of Theileriosis.* (Eds. A. D. Irvin, M. P. Cunningham & A. S. Young). The Hague, Boston, London. Martinus Nijhoff Publishers, **14**: 311-326.

MORRISON, W. I., GODDEERIS, B. M., TEALE, A. J., GROOCOCK, C. M., KEMP, S. J. & STAGG, D. A. (1987). Cytotoxic T cells elicited in cattle challenged with *Theileria parva* (Muguga): Evidence for restriction by class I MHC determinants and parasite strain specificity. *Parasite Immunology,* **9**: 563-578.

MORRISON, W. I., GODDEERRIS, B. M., BROWN, W. C., BALDWIN, C. L. & TEALE, A. J. (1989). *Theileria parva* in cattle: Characterisation of infected lymphocytes and the immune response they provoke. *Veterinary Immunology and Immunopathology,* **20**: 213-217.

MORZARIA, S. P., ROEDER, P. L., ROBERTS, D. H., CHASEY, D. & DREW, T. W. (1984). Lymphoblastoid cell line from a sporadic case of bovine lymposarcoma. *Agriculture. 5th International Symposium on Bovine Leukosis*: 519-528.

MORZARIA, S. P., IRVIN, A. D., WATHANGA, J., D'SOUZA, D., KATENDE, J., YOUNG, A. S., SCOTT, J. & GETTINBY, G. (1988). The effect of East Coast fever immunization and different acaricidal treatments on the productivity of beef cattle. *Veterinary Record,* **123**: 313-320.

MOULTON, J. E., KRAUSS, H. H. & MALMQUIST, W. A. (1971). Transformation of reticulum cells to lymphoblasts in cultures of bovine spleen infected with *Theileria parva. Laboratory Investigation,* **24**: 187-196.

MUKHEBI, A. W., PERRY, B. D. & KRUSKA, R. (in press). Estimating economic losses caused by theileriosis and the economics of its control in Africa. *Preventive Veterinary Medicine.*

MUSISI, F. L., KILGOUR, V., BROWN, C. G. D. & MORZARIA, S. P. (1981). Preliminary investigations on isoenzyme variants of lymphoblastoid cell lines infected with *Theileria* species. *Research in Veterinary Science,* **30**: 38-43.

MUSOKE, A. J., NANTUYLA, V. M., BUSCHER, G., MASAKE, R. A. & OTIM, B. (1982). Bovine immune responses to *Theileria parva*: Neutralising antibodies to sporozoites. *Immunology,* **42**: 663-668.

NAESSENS, J., NEWSON, J., BENSAID, A., TEALE, A. J., MAGONDU, J. B. & BLACK, S. J. (1985). *De novo* expression of T cell markers on *Theileria parva* transformed lymphoblasts in cattle. *Journal of Immunology,* **135**: 4183-4188.

NEITZ, W. O. & JANSEN, B. C. (1956). A discussion on the classification of the Theilerias. *Onderstepoort Journal of Veterinary Research,* **27**: 7-18.

NEITZ, W. O. (1957). Theileriosis, gonderioses and cyauxzoonoses: A review. *Onderstepoort Journal of Veterinary Research,* **27, 3**: 275-346.

NORTON, A. J. & ISAACSON, P. G. (1989). Lymphoma phenotyping in formalin-fixed and paraffin wax-embedded tissues. I. Range of antibodies and staining patterns. *Histopathology,* **14**: 437-446.

OLIFF, A., DEFEO-JONES, D. & BOYER, M. (1987). Tumours secreting human TNF/cachexia in mice. *Cell,* **50**: 555-563.

OUHELLI, H., DAKKAK, A. & OUAZZANI, B. (1987). *Theileria annulata*: Difference du potentiel transmural de l'abomasum et du duodenum et permeabilite

de leur muqueuse chez le bovin infeste experimentalement. *Experimental Parasitology,* **63**: 253-259.

OUHELLI, H., INNES, E. A., BROWN, C. G. D., WALKER, A. R., SIMPSON, S. P. & SPOONER, R. L. (1989). The effect of dose and line on immunisation of cattle with lymphoblastoid cells infected with *Theileria annulata. Veterinary Parasitology,* **31**: 217-228.

PAVLOV, P. (1942). Das vorkommen von Theileriosse in Macedonien. *Deutsche tierarztliche Wochenschrift,* **50**: 458-460.

PEARSON, T. W., LUNDIN, L. B., DOLAN, T. T. & STAGG, D. A. (1979). Cell-mediated immunity to *Theileria*-transformed cell lines. *Nature,* **281**: 678-680.

PFEFFERKORN, E. R. (1984). Interferon-g blocks the growth of *Toxoplasma gondii* in human fibroblasts by inducing the host cells to degrade tryptophan. *Proceedings of the National Academy of Science, USA,* **81**: 908-912.

PINDER, M., WITHEY, K. S. & ROELANTS, G. E. (1981). *Theileria parva* parasites transform a subpopulation of T lymphocytes. *Journal of Immunology,* **127**: 389-390.

PIPANO, E., WEISMAN, Y. & BENADO, A. (1974). The virulence of four local strains of *Theileria annulata. Refuah Veterinarith,* **31, 2**: 59-63.

PIPANO, E. (1981). Schizonts and tick stages in immunisation against *Theileria annulata* infection. In: *Advances in the Control of Theileriosis (Current Topics in Veterinary Medicine and Animal Science).* (Eds. A. D. Irvin, M. P. Cunningham & A. S. Young). The Hague, Boston, London. Martinus Nijhoff Publishers, **14**: 242-252.

PIPANO, E., SAMISH, M. & KRIGEL, Y. (1982). Relative infectivity of *Theileria annulata* stabilates derived from female and male *Hyalomma excavatum* ticks. *Veterinary Parasitology,* **10**: 21-27.

PIPANO, E. (1989). Vaccination against *Theileria annulata* theileriosis. In: *Veterinary Protozoan and Haemoparasite Vaccines.* (Ed. I. G. Wright), CRC Press. Boca Raton, Florida: 203-234.

PRASAD, B. M. (1946). Morphological studies of the blood of hill bulls in health and during acute theileriosis. *Indian Journal of Veterinary Science and Animal Husbandry,* **16**: 54-56.

PRESTON, P. M. (1981). The role of macrophages in protective immunity and immunosuppression in bovine theileriosis. In: *Advances in the Control of Theileriosis.* (Eds. A. D. Irvin, M. P. Cunningham & A. S. Young). The Hague, Boston, London. Martinus Nijhoff Publishers, **14**: 354-356.

PRESTON, P. M., BROWN, C. G. D. & SPOONER, R. L. (1983). Cell-mediated cytotoxicity in *Theileria annulata* infection of cattle with evidence for BoLA restriction. *Clinical and Experimental Immunology*, **53**: 88-100.

PRESTON, P. M. & BROWN, C. G. D. (1985). Inhibition of lymphocyte invasion by sporozoites and the transformation of trophozoite-infected lymphocytes *in vitro* by serum from *Theileria annulata* immune cattle. *Parasite Immunology,* **7**: 301-314.

PRESTON, P. M & BROWN, C. G. D. (1988). Macrophage mediated cytostasis and lymphocyte cytotoxicity in cattle immunised with *Theileria annulata* sporozoites or macroschizont-infected cell lines. *Parasite Immunology,* **10**: 631-647.

PRESTON, P. M., BROWN, C. G. D., BELL SAKYI, L., RICHARDSON, W. & SANDERSON, A. (1992a). Tropical theileriosis in *Bos taurus* and *Bos taurus* cross *Bos indicus* calves response to infection with graded doses of sporozoites of *Theileria annulata. Research in Veterinary Science*, **53**: 230-243.

PRESTON, P. M., BROWN, C. G. D. & RICHARDSON, W. (1992b). Cytokines inhibit the development of trophozoite-infected cells of *Theileria annulata* and *Theileria parva* but enhance the proliferation of macroschizont-infected cell lines. *Parasite Immunology,* **14**: 125-141.

PRESTON, P. M., BROWN, C. G. D., ENTRICAN, G., RICHARDSON, W. & BOID, R. (1993). Synthesis of tumour necrosis factor-alpha and interferons by mononuclear cells from *Theileria annulata*-infected cattle. *Parasite Immunology*, **15**: 525-534.

PURNELL, R. E. (1978). *Theileria annulata* as a hazard to cattle in countries on the Northern Mediterranean Littoral. *Veterinary Science Communications*, **2**: 3-11.

RADLEY, D. E. (1981). Infection and treatment method of immunisation against theileriosis. In: *Advances in the Control of Theileriosis.* (Eds. A. D. Irvin, M. P. Cunningham & A. S. Young). The Hague, Boston, London. Martinus Nijhoff Publishers, **14**: 227-237.

RAK, H. (1978). Tick-borne diseases and their vectors in Iran. In: *Tick-borne Diseases and their Vectors.* Proceedings of an international conference held in Edinburgh (27th September - 1st October 1976) organised by the Centre for Tropical Veterinary Medicine (Ed. J. K. H. Wilde), University of Edinburgh, Lewis Reprints Ltd: 163-165.

RAMOS-VARA, J. A., MILLER, M. A., LOPEZ, E., PRATS, N. & BREVIK, L. (1994). Reactivity of polyclonal human CD3 antiserum in lymphoid tissues of cattle, sheep, goats, rats and mice. *American Journal of Veterinary Research,* **55**: 63-66.

RAMPON, L. (1948). Remarques sur la virulence naturelle de *Theileria dispar.* Essais de traitment de la theileriose bovine par la "Lomidine". *Archives de l'Institut Pasteur d'Algerie, Alger*, **26**: 386-390.

RICHARDSON, J. O. & PRESTON, P. M. (1994). The cytostatic effects of nitric oxide on *Theileria annulata* macroschizont and microschizont cell lines. *Transactions of the Royal Society of Tropical Medicine and Hygiene,* **88, 5**: 504.

RIDLEY, D. S. & WISE, M. J. (1964). Reaction of the dermis in leprosy. *International Journal of Leprosy,* **32**: 24-36.

RIDLEY, D. S. (1979). The pathogenesis of cutaneous leishmaniasis. *Transactions of the Royal Society of Tropical Medicine and Hygiene,* **73**: 150-160.

ROBINSON, P. M. (1982). *Theileriosis annulata* and its transmission-a review. *Tropical Animal Health and Production,* **14**: 3-12.

ROITT, I. M., BROSTOFF, J. & MALE, D. K. (1989). Immunology. 2nd Edition. Churchill Livingstone.

ROMAGNANI, S. (1992). Induction of TH1 and TH2 responses: A key role for the natural immune response? *Immunology Today,* **13**: 379-381.

RUSSELL, D. G. & WRIGHT, S. G. (1988). Complement receptor type 3 (CR3) binds to an Arg-Gly-Asp-containing region of the major surface glycoprotein, gp63, of *Leishmania* promastigotes. *Journal of Experimental Medicine,* **168**: 279-292.

SARIH, M., SOUVANNAVONG, V. & ADAM, A. (1993). Nitric oxide synthase induces macrophage death by apoptosis. *Biochemical and Biophysical Research Communications,* **191, 2**: 503-508.

SAVILL, J., FADOK, V., HENSON, P. & HASLETT, C. (1993). Phagocyte recognition of cells undergoing apoptosis. *Immunology Today,* **14, 3**: 131-136.

SCHINDLER & WOKATSCH (1965). Cited in Uilenberg 1981a.

SCHOFIELD, L., FERREIRA, A., ALTSZULER, R., NUSSENZWEIG, V. & NUSSENZWEIG, R. S. (1987). Interferon-g inhibits the intrahepatocytic development of malarial parasites *in vitro. Journal of Immunology,* **139**: 2020-2025.

SCOTT, P. E., PEARCE, A. W. & CHEEVER, R. L. (1989). Role of cytokines and $CD4^+$ T cell subsets in the regulation of parasite immunity and disease. *Immunology Reviews,* **112**: 161-182.

SECOR, W. E. (1990). Eosinophils and immune mechanisms. VI. The synergistic combination of granulocyte-macrophage colony-stimulating factor and IL-5 accounts for eosinophil-stimulation promoter activity in *Schistosoma mansoni*-infected mice. *Journal of Immunology,* **144**: 1484-1489.

SEN, S. K. & SRINIVASAN, M. K. (1937). Theileriosis of cattle in India. *Indian Journal of Veterinary Science,* **7**: 15-37.

SERGENT, E., DONATIEN, A. L., PARROT, L. M., LESTOQUARD, F. PLANTUREUX, E. & ROUGEBIEF, H. (1924). Les piroplasmoses bovines d'Algerie. *Archives de l'Institut Pasteur d'Algerie, Alger*, **2**: 1-146.

SERGENT, E., DONATIEN, A. L., PARROT, L. M. & LESTOQUARD, F. (1945). Etudes sur les pirolasmoses bovines. *Archives de l'Institut Pasteur d'Algerie, Alger*: 243-582.

SHARPE, R. T. & LANGLEY, A. M. (1983). The effect of *Theileria annulata* infection on the immune responses of cattle to foot and mouth disease. *British Veterinary Journal,* **139**: 378-385.

SHI, S., KEY, M. & KALRA, K. (1991). Antigen Retrieval in formalin fixed, paraffin embedded tissues; an enhancement method for immunohistochemical staining based on microwave oven heating of tissue sections. *Journal of Histochemistry and Cytochemistry*, **39, 6**: 741-748.

SHIELS, B. R., MCDOUGALL, C., TAIT, A. & BROWN, C. G. D. (1986). Antigenic diversity of *Theileria annulata* macroschizonts. *Veterinary Parasitology*, **21**: 1-10.

SHIELS, B. R., KINNAIRD, J., MCKELLAR, S., DICKSON, J., BEN MILED, L., MELROSE, R., BROWN, C. G. D. & TAIT, A. (1992). Disruptions of synchrony between parasite growth and host cell division is a determinant of differentiation to the merozoite in *Theileria annulata. Journal of Cell Science,* **101**: 99-107.

SHITAKHA, V. M., NANTULYA, V. M., MUSOKE, A. J., RAMASAMY, R. & BUSCHER, G. (1983). Complement activation and fibrinolysis during infection with *Theileria parva* (East Coast fever) in cattle. *Veterinary Immunology and Immunopathology,* **4**: 361-373.

SIEGEL, J. P. (1988). Effects of interferon-g on the activation of human T lymphocytes. *Cellular Immunology.* **III**: 461-472.

SIEGEL, S. (1976). *Nonparametric Statistics for the Behavioral Sciences.* McGraw-Hill, New York.

SINGH, D. K., JAGDISH, S., GAUTAM, O. P. & DHAR, S. (1979). Infectivity of ground-up tick supernates prepared from *Theileria annulata*-infected *Hyalomma anatolicum anatolicum. Tropical Animal Health and Production,* **11**: 87-90.

SPLITTER, G. & MORRISON, W. I. (1991). Antigens expressed predominantly on monocytes and granulocytes: Identification of bovine CD11b and CD11c. *Veterinary Immunology and Immunopathology*, **27**: 87-90.

SPOONER, R. L., PENHALE, W. J., BURRIDGE, M. J. & BROWN, C. G. D. (1973). Some serum globulin changes in East Coast fever. *Research in Veterinary Science,* **15**: 368-374.

SPOONER, R. L. & BROWN, C. G. D. (1980). Bovine lymphocyte antigens (BoLA) of bovine lymphocytes and derived lymphoblastoid lines transformed by *Theileria parva* and *Theileria annulata*. *Parasite Immunology*, **2**: 163.

SPOONER, R. L., INNES, E. A., GLASS, E. J., MILLAR, P. & BROWN, C. G. D. (1988). Bovine mononuclear cell lines transformed by *Theileria parva* or *Theileria annulata* express different sub population markers. *Parasite Immunology*, **10**: 619-629.

SPOONER, R. L., INNES, E. A., GLASS, E. J. & BROWN, C. G. D. (1989). *Theileria annulata* and *Theileria parva* infect and transform different bovine mononuclear cells. *Immunology*, **66**: 284-288.

SRIVASTAVA, P. S. & SHARMA, N. N. (1976). Note on cerebral theileriasis in crossbred calves. *Pantnagar Journal of Research*, **1, 2**: 147-150.

SRIVASTAVA, P. S. & SHARMA, N. N. (1981). Studies on the occurrence, clinical features and clinicopathological and pathomorphological aspects of *Theileriasis* in calves. *Veterinary Research Journal*, **4, 1**: 22-29.

STAGG, D. A., CHASEY, D. D., YOUNG, A. S., MORZARIA, S. P. & DOLAN, T. T. (1980). Synchronisation of the division of *Theileria* macroschizonts and their mammalian host cells. *Annals of Tropical Medicine and Parasitology*, **74**: 263-265.

STECK, W. (1928). Histological studies on East Coast fever. *13th-14th Report of the Director of Veterinary Education & Research (South Africa)*: 243-280.

STERNBERG, J. & MCGUIGAN, F. (1992). Nitric oxide mediates suppression of T cell responses in murine *Trypanosoma brucei* infection. *European Journal of Immunology*, **22**: 2741-2744.

STRICKLAND, G. T. & HUNTER, K. W. (1980). The use of immunopotentiators in malaria. *International Journal of Nuclear Medicine and Biology*, **7, 2**: 133-140.

STURMAN, M. (1935). A note on acquired immunity to *Theileria annulata*. *Journal of Comparative Pathology and Therapy*, **48**: 298-299.

SUTHERLAND, I. A., SHIELS, B., JACKSON, L. A., BROWN, D., BROWN, C. G. D., TAIT, A. & PRESTON, P. M. (1993). Studies on the immunological and molecular basis of attenuation of *Theileria annulata* cell line vaccines. In: *Resistance or Tolerance to Disease and Veterinary Epidemiology and Diagnostic Measures.* (Eds. G. Uilenberg & R. Hamers). CIRAD-EMVT, Cedex, France: 45-47.

SZAKAL, A. K., KAPASI, Z. F., MASUDA, A. & TEW, J. G. (1992). Follicular dendritic cells in the alternative antigen transport pathway: Microenvironment, cellular events, age and retrovirus related alterations. *Seminars in Immunology*, **4**: 257-265.

SZONDY, Z. (1994). Adenosine stimulated DNA fragmentation in human thymocytes by Ca^{2+} mediated mechanisms. *Biochemical Journal,* **304, 3**: 877-885.

TAIT, A. & HALL, F. R. (1990). *Theileria annulata*: Control measures, diagnosis and the potential use of subunit vaccines. *Reviews of Scientific Techniques of International Epizootiology,* **9, 2**: 387-403.

TEALE, A. J. (1983). The major histocompatibility complex of cattle with particular reference to some aspects of East Coast fever. Ph. D thesis, University of Edinburgh.

THEILER, A. (1904). East Coast fever. *Transvaal Agricultural Journal,* **1**: 37-41.

TRACEY, K. J. & CERAMI, A. (1989). Cachectin/tumour necrosis factor and other cytokines in infectious disease. *Current Opinion in Immunology,* **1**: 454-461.

UILENBERG, G. (1976). Tick-borne livestock diseases and their vectors. 2. Epizootiology of tick-borne diseases. *World Animal Review,* **17**: 8-15.

UILENBERG, G. & ZWART, D. (1979). Skin nodules in East Coast fever. *Research in Veterinary Science,* **26**: 243-245.

UILENBERG, G. (1981a). *Theileria* species of domestic livestock. In: *Advances in the Control of Theileriosis.* (Eds. A. D. Irvin, M. P. Cunningham & A. S. Young). The Hague, Boston, London. Martinus Nijhoff Publishers, **14**: 4-37.

UILENBERG, G. (1981b). *Theileria* infections other than East Coast fever. In: *Diseases of Cattle in the Tropics* (Eds. M. Ristic & I. McIntyre). The Hague, Boston, London. Martinus Nijhoff Publishers: 411-427.

ULICH, T. R., DEL CASTILLO, J., KEYS, M., GRANGER, G. A. & NI, R. (1987). Kinetics and mechanisms of recombinant human interleukin-1 and tumour necrosis factor-a-induced changes in circulating numbers of neutrophils and lymphocytes. *Journal of Immunology,* **139**: 3406-3415.

VISSER, A. E., ABRAHAM, A., BROWN, C. G. D. & PRESTON, P. M. (1995). Nitric oxide inhibits establishment of macroschizont-infected cell lines and is produced by macrophages of calves undergoing bovine tropical theileriosis or East Coast fever. *Parasite Immunology*, **17**: 91-102.

WAGNER, G. G. & DUFFUS, W. P. H. (1974). Antilymphocyte antibody responses in cattle inoculated with *Theileria parva*-infected lymphoblastoid cell lines. In: *Parasitic Zoonoses.* (Ed. E. J. L. Soulsby). Academic Press, New York: 97-107.

WAGNER, G. G., JESSETT, D. M., BROWN, C. G. D. & RADLEY, D. E. (1975). Diminished antibody response to rinderpest vaccination in cattle undergoing experimental East Coast fever. *Research in Veterinary Science,* **19**: 209-211.

WEINSTOCK, J. V. (1994). Function and regulation of granulomatous responses (experimental granulomatosis). In: *Sarcoidosis and Other Granulomatous Disorders.* (Ed. D. G. James). Marcel Dekker, Inc., **73**: 99-133.

WILDE, J. K. H. (1963). Attempts to induce leucocytosis in normal cattle and in cattle with East Coast fever. *Bulletin of Epizootic Diseases of Africa,* **11**: 415-26.

WILDE, J. K. H. (1966). Changes in bovine bone marrow during the course of East Coast fever. *Research in Veterinary Science,* **7**: 213-224.

WILDE, J. K. H. (1967). East Coast fever. *Advances in Veterinary Science,* **11**: 207-259.

WILLIAMS, G. T., SMITH, C. A., MCCARTHY, N. J. & GRIMES, E. A. (1992). Apoptosis: final control point in cell biology. *Trends in Cell Biology*, **2**: 263-267.

WILLIAMSON, S., TAIT, A., BROWN, C. G. D., WALKER, A., BECK, P., SHIELS, B. R., FLETCHER, J. & HALL, R. (1989). *Theileria annulata* sporozoite surface antigen expressed in *Escherichia coli* elicits neutralising antibody. *Proceedings of the National Academy of Science, USA,* **86**: 4639-4643.

WYLLIE, A. H., KERR, J. F. R. & CURRIE, A. R. (1980). Cell death: The significance of apoptosis. *International Review of Cytology,* **68**: 251-306.

YAKIMOFF, W. L. & GOUSSEF, W. F. (1936). Zur Frage der Modifikation der Virulenz der *Theileria annulata. Zeitschrift fur Infektkrankheit de Haustiere,* **50**: 65-70.

ZINKERNAGEL, R. M. (1979). Cellular immune responses to intracellular parasites: Role of the major histocompatibility gene complex and thymus in determining immune responsiveness and susceptibility to disease. *Parasite Immunology,* **1**: 91-109.

ZUMLA, A. (1994). Sarcoidosis and leprosy: A comparative study. In: *Sarcoidosis and Other Granulomatous Disorders.* (Ed. D. G. James). Marcel Dekker, Inc., **73**: 681-705.

APPENDIX I

GIEMSA'S STAIN TECHNIQUE

(1) Material fixed in absolute methanol (BDH) for 2-3 minutes and air-dried.

(2) Material stained in 10% Giemsa's stain (BDH) in buffered distilled water (pH 7.2) for 30 minutes.

(3) Material rinsed in buffered distilled water (pH 7.2) and air-dried.

APPENDIX II

ISOLATION OF BOVINE PERIPHERAL BLOOD MONONUCLEAR CELLS

(1) Jugular blood taken into sterile vacutainer tubes containing lithium heparin 14i.u./ml (Becton Dickinson).

(2) Blood added to equal volume of sterile Dulbecco's A medium (PBS) (Oxoid).

(3) Mixed solution layered onto Ficoll Hypaque (Pharmacia) in a 20:8 ratio.

(4) PBM separated by centrifugation (MSE Mistral 3000) at 1000g. for 60 minutes at 15^0C.

(5) Plasma discarded and cell layer containing PBM removed by pasteur pipette.

(6) Cells added to PBS and washed by centrifugation at 800g. for 20 minutes at 5^0C.

(7) Cell pellet resuspended in fresh PBS and washed by centrifugation at 450g. for 15 minutes at 5^0C.

(8) Cell pellet resuspended in fresh PBS and washed by centrifugation at 100g. for 2 minutes at room temperature.

(9) Cell pellet resuspended in culture medium (RPMI-1640 supplemented with L-glutamine (2mM), penicillin (100µg/ml), streptomycin (100µg/ml) and 10% foetal calf serum (GIBCO BRL).

APPENDIX III

IMDM PROTOCOL

IMDM supplemented with mercaptoethanol ($5x10^5$ M), L-glutamine (4mM), penicillin (100μg/ml), streptomycin (100μg/ml) and kenomycin (100μg/ml) (GIBCO BRL) plus bovine transferrin (25μg/ml), bovine serum albumin (BSA) (Sigma A3156) (500μg/ml), aleic acid (1μg/ml), linoleic acid (1μg/ml) and palmitic acid (1μg/ml) (Sigma).

APPENDIX IV

STANDARD CURVE

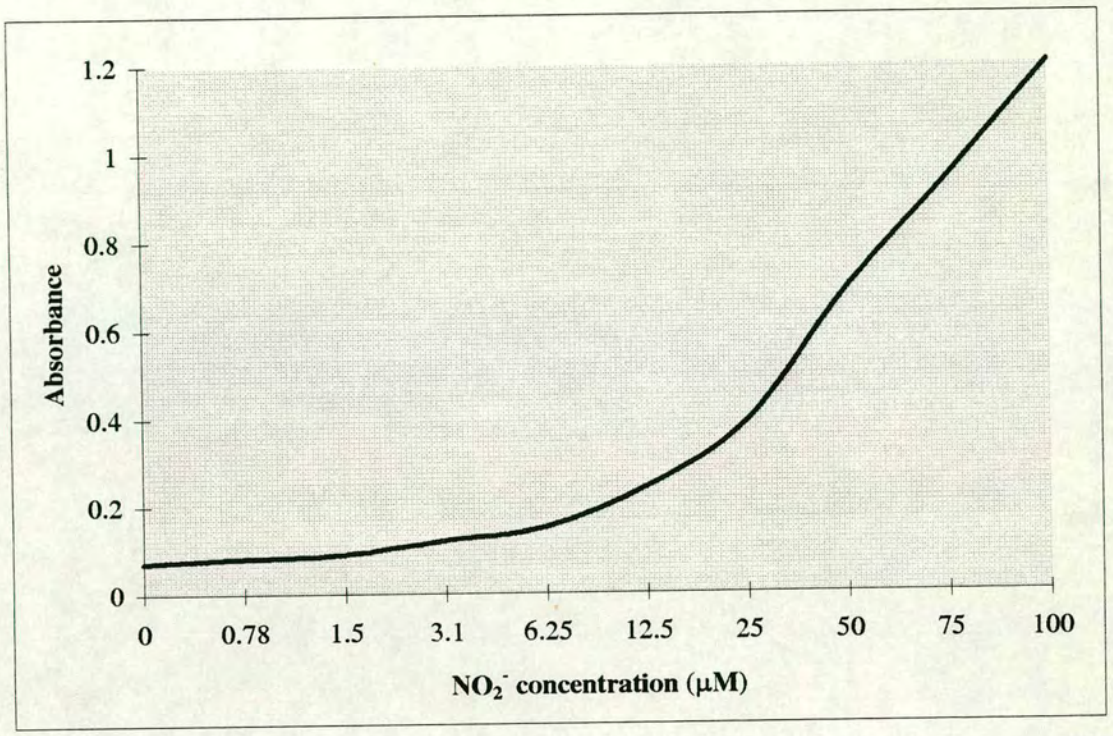

APPENDIX V

POLY-L-LYSINE ADHESIVE FOR SLIDES

(1) Poly-l-lysine solution (Raymond A. Lamb) diluted 1:10 with deionized water (Milli-Q plus: Millipore) and allowed to come to room temperature (18-26^{0}C).

(2) Slides cleaned in acid/alcohol and wiped dry.

(3) Slides placed in poly-l-lysine solution for 5 minutes, drained and dried for 1 hour at 60^{0}C.

(4) Slides stored in slide boxes.

APPENDIX VI

HARRIS'S HAEMATOXYLIN & EOSIN-Y STAINING TECHNIQUE

1. Dewax sections in histoclear - 10 min
2. Rinse in absolute alcohol - 2 min
3. Rinse in 90% alcohol - 2 min
4. Rinse in 70% alcohol - 2 min
5. Rinse in 50% alcohol - 2 min
6. Wash in water
7. Stain in Harris's haematoxylin - 5 min
8. Wash in water
9. Differentiate in acid/alcohol - 10 sec
10. Wash in water
11. Blue up in Scott's tap water - 30 sec
12. Wash in water
13. Stain in eosin-Y - 1 min
14. Wash in water
15. Rinse briefly in 50% alcohol
16. Rinse briefly in 70% alcohol
17. Rinse well in 90% alcohol
18. Rinse well in absolute alcohol (x2)
19. Clear in histoclear (x2)
20. Mount in DPX

APPENDIX VII

SOLUTIONS FOR HAEMATOXYLIN & EOSIN-Y TECHNIQUE

A. Harris's haematoxylin (Raymond A. Lamb)

Undiluted and filtered before use.

B. Eosin-Y (Raymond A. Lamb)

Solution (A) 1% aqueous eosin (distilled water) and solution (B) 0.5% alcoholic eosin (absolute alcohol) mixed in a 1:2 ratio with the addition of a spatula of calcium chloride (Sigma).

C. Scott's tap water

2g potassium bicarbonate (BDH) plus 20g magnesium sulphate (BDH) in a litre of distilled water.

D. Acid/alcohol

1% concentrated hydrochloric acid (HCl) (BDH) in 70% alcohol.

E. Absolute alcohol

Industrial strength BPC.

F. Alcohol (90%, 70% or 50%)

Industrial strength BPC diluted in distilled water.

G. Histoclear (Raymond A. Lamb) **and DPX** (BDH)

Undiluted for use.

APPENDIX VIII

AVIDIN/BIOTIN COMPLEX (ABC) HORSERADISH PEROXIDASE (HRP) IMMUNOCYTOCHEMICAL TECHNIQUES

1. Dewax sections in histoclear	- 10 min
2. Rinse in absolute alcohol	- 2 min
3. Rinse in 90% alcohol	- 2 min
4. Rinse in 70% alcohol	- 2 min
5. Rinse in 50% alcohol	- 2 min
6. Wash in tap water	
7. Incubate in 3% hydrogen peroxide (H_2O_2) * in distilled water	- 10 min
8. Wash in tap water	
9. Incubate in trypsin plus calcium chloride in distilled water @ 37^0C **	-30 min
10. Wash in tap water	
11. Wash in tris-buffered saline (TBS) (x3)	- 5 min
12. Incubate in normal serum (diluted 1:5 in TBS) ***	- 10 min
13. Incubate in monoclonal antibody	- 30 min
14. Wash in TBS (x3)	- 5 min
15. Incubate in secondary antibody	- 30 min
AT THIS STAGE PREPARE ABC/HRP	
16. Wash in TBS (x3)	- 5 min
17. Incubate in ABC/HRP	- 30 min
18. Wash in TBS (x3)	- 5 min
19. Incubate in DAB substrate	- 5 min
20. Wash in running tap water	
21. Counterstain in Harris's haematoxylin	- 10 sec
22. Wash in tap water	
23. Blue up in Scott's tap water	- 30 sec
24. Wash in tap water	
25. Rinse briefly in 50% alcohol	
26. Rinse briefly in 70% alcohol	
27. Rinse well in 90% alcohol	
28. Rinse well in absolute alcohol (x2)	
29. Clear in histoclear (x2)	

30. Mount in DPX

* Inactivation of endogenous peroxidase ** Antigen unmasking *** Blocking of non-specific background using normal serum from the same species of secondary antibody used.

APPENDIX IX

SOLUTIONS FOR ABC/HRP IMMUNOCYTOCHEMICAL TECHNIQUES

A. Protease digestion solution

0.1% trypsin (DIFCO 1:250) plus 0.1% calcium chloride (Sigma) in distilled water (pH 7.8).

B. Tris-buffered saline (TBS)

0.05M tris- (Sigma) HCl/0.15M NaCl (BDH)/0.05% tween-20 (Sigma) (pH 7.6).

C. Avidin/biotinylated horseradish peroxidase complex (ABC/HRP) (DAKO)

45µl avidin in 0.01M phosphate buffer, 0.15M NaCl, 15mM NaN_3 (pH7.2) and 45µl biotinylated horseradish peroxidase in 0.01M phosphate buffer, 0.15M NaCl, 15mM NaN_3 (pH 7.2) added to 5ml of 0.05M Tris/HCl (Sigma) (pH 7.6). Solution prepared 30 minutes before use.

D. Horseradish peroxidase substrate (3, 3' diaminobenzidine tetrahydrochloride) (DAB) (DAKO)

DAB tablet dissolved in 10ml of 0.05M Tris-HCl/0.01M imidazol (Sigma) (pH 7.6). Immediately before use 15µl of 3% H_2O_2 in distilled water added to 2ml of the DAB chromogen solution to give a final solution of 1mg/ml DAB and 0.02% H_2O_2.

APPENDIX X

ABC/AP IMMUNOCYTOCHEMICAL TECHNIQUES

1. Dewax sections in histoclear	- 10 min
2. Rinse in absolute alcohol	- 2 min
3. Rinse in 90% alcohol	- 2 min
4. Rinse in 70% alcohol	- 2 min
5. Rinse in 50% alcohol	- 2 min
6. Wash in tap water	
7. Incubate in trypsin plus calcium chloride in distilled water @ 37^0C *	-30 min
8. Wash in tap water	
9. Wash in tris-buffered saline (TBS) (x3)	- 5 min
10. Incubate in normal serum (diluted 1:5 in TBS) **	- 10 min
11. Incubate in monoclonal antibody	- 30 min
12. Wash in TBS (x3)	- 5 min
13. Incubate in secondary antibody	- 30 min
AT THIS STAGE PREPARE ABC/AP	
14. Wash in TBS (x3)	- 5 min
15. Incubate in ABC/AP	- 30 min
16. Wash in TBS (x3)	- 5 min
17. Incubate in Vector Red substrate	- 5 min
18. Wash in running tap water	
19. Counterstain in Harris's haematoxylin	- 10 sec
20. Wash in tap water	
21. Blue up in Scott's tap water	- 30 sec
22. Wash in tap water	
23. Rinse briefly in 50% alcohol	
24. Rinse briefly in 70% alcohol	
25. Rinse well in 90% alcohol	
26. Rinse well in absolute alcohol (x2)	
27. Clear in histoclear (x2)	
28. Mount in DPX	

* Antigen unmasking ** Blocking of non-specific background using normal serum from the same species of secondary antibody used.

APPENDIX XI

SOLUTIONS FOR ABC/AP IMMUNOCYTOCHEMICAL TECHNIQUES

A. Avidin/biotinylated alkaline phosphatase complex (ABC/AP) (Vector)

45µl avidin in 0.01M phosphate buffer, 0.15M NaCl, 15mM NaN_3 (pH7.2) and 45µl biotinylated alkaline phosphatase in 0.05M tris/HCl, 0.1M NaCl, 1mM $MgCl_2$, 15mM NaN_3 (pH 7.2) added to 5ml of 0.05M tris/HCl (Sigma) (pH 7.6). Solution prepared 30 minutes before use.

B. Alkaline phosphatase substrate (Vector Red) (Vector)

Immediately before use 2 drops of kit reagent 1 added to 5ml of buffer (100mM tris/HCl, (Sigma) (pH 8.2)), 2 drops of kit reagent 2 then added to the solution before the addition of 2 drops of kit reagent 3. Sections were incubated in the substrate for 20 minutes at room temperature.

C. Levamisole solution (Vector)

Endogenous phosphatase activity was blocked by the addition of 1mM levamisole to the Vector Red substrate.

APPENDIX XII

MICROWAVE ANTIGEN RETRIEVAL TECHNIQUES

(1) Sections placed in a microwaveable container and immersed in citrate buffer (1.05g citric acid (BDH) in 500ml distilled water pH to 6 using 2a NaOH (BDH)).

(2) Cling film placed over the container to prevent evaporation and punctured before microwaving.

(3) Container microwaved on high power for 3 x 5 minutes (ensuring the citrate buffer does not fall below the level of the sections).

(4) Container removed and left to cool for 20 minutes in the citrate buffer.

(5) Slides then washed in running tap water.

APPENDIX XIII

GLUCOSE OXIDASE PROTOCOL

8.5ml phosphate buffered saline (PBS) (Oxoid) plus 1ml of beta-D-glucose (0.36mg beta-D-glucose (Sigma) in 20ml PBS to give a 100mM solution) plus 100µl sodium azide (Sigma) mixed and preheated to 37^0C before the addition of 0.5ml glucose oxidase (5.6mg glucose oxidase (Sigma) in 1ml PBS). The glucose oxidase was made immediately before use to ensure the optimal inactivation of endogenous peroxidase.

APPENDIX XIV

ABC/HRP & ABC/AP DOUBLE STAINING IMMUNOCYTOCHEMICAL TECHNIQUES

1. Dewax sections in histoclear	- 10 min
2. Rinse in absolute alcohol	- 2 min
3. Rinse in 90% alcohol	- 2 min
4. Rinse in 70% alcohol	- 2 min
5. Rinse in 50% alcohol	- 2 min
6. Wash in tap water	
7. Incubate in 3% hydrogen peroxide (H_2O_2) * in distilled water	- 10 min
8. Wash in tap water	
9. Incubate in trypsin plus calcium chloride in distilled water @ 37^0C **	-30 min
10. Wash in tap water	
11. Wash in tris-buffered saline (TBS) (x3)	- 5 min
12. Incubate in normal serum (diluted 1:5 in TBS) ***	- 10 min
13. Incubate in monoclonal antibody	- 30 min
14. Wash in TBS (x3)	- 5 min
15. Incubate in secondary antibody	- 30 min
AT THIS STAGE PREPARE ABC/HRP	
16. Wash in TBS (x3)	- 5 min
17. Incubate in ABC/HRP	- 30 min
18. Wash in TBS (x3)	- 5 min
19. Incubate in DAB substrate	- 5 min
20. Wash in running tap water	
21. Wash in tris-buffered saline (TBS) (x3)	- 5 min
22. Incubate in normal serum (diluted 1:5 in TBS) ***	- 10 min
23. Incubate in monoclonal antibody	- 30 min
24. Wash in TBS (x3)	- 5 min
25. Incubate in secondary antibody	- 30 min
AT THIS STAGE PREPARE ABC/AP	
26. Wash in TBS (x3)	- 5 min
27. Incubate in ABC/AP	- 30 min
28. Wash in TBS (x3)	- 5 min

29. Incubate in Vector Red substrate - 5 min
30. Wash in running tap water
31. Counterstain in Harris's haematoxylin - 10 sec
32. Wash in tap water
33. Blue up in Scott's tap water - 30 sec
34. Wash in tap water
35. Rinse briefly in 50% alcohol
36. Rinse briefly in 70% alcohol
37. Rinse well in 90% alcohol
38. Rinse well in absolute alcohol (x2)
39. Clear in histoclear (x2)
40. Mount in DPX

* Inactivation of endogenous peroxidase ** Antigen unmasking *** Blocking of non-specific background using normal serum from the same species of secondary antibody used.

APPENDIX XV

ISOLATION OF BOVINE THYMOCYTES

(1) A piece of thymus 3 x 1 x 2 cm was removed and washed twice in RPMI-1640 (Gibco BRL).

(2) The material was sieved into a centrifuge tube, suspended in RPMI medium and allowed to stand for several minutes.

(3) The supernatant was transferred to a clean centrifuge tube and spun at 250g. for 5 minutes.

(4) The pellet was resuspended in sterile Dulbecco's A medium (PBS) (Oxoid) and spun at 250g. for 5 minutes (x3).

(5) The final cell pellet was resuspended in RPMI-1640 supplemented with L-glutamine (2mM), penicillin (100μg/ml), streptomycin (100μg/ml) and 10% foetal calf serum (GIBCO BRL).

APPENDIX XVI

TDT-MEDIATED-DUTP-BIOTIN NICK END LABELLING TECHNIQUE

1. Dewax sections in histoclear	- 10 min
2. Rinse in absolute alcohol	- 2 min
3. Rinse in 90% alcohol	- 2 min
4. Rinse in 70% alcohol	- 2 min
5. Rinse in 50% alcohol	- 2 min
6. Wash in double distilled water	- 2 min
7. Incubate in proteinase K *	- 15 min
8. Wash in double distilled water (x4)	
9. Incubate in 2% hydrogen peroxide (H_2O_2) (Sigma) in double distilled water **	- 5 min
10. Rinse in double distilled water	
11. Immerse in TdT buffer	
12. Incubate in TdT and biotinylated dUTP in TdT buffer	- 60 min
AT THIS STAGE PREPARE ABC/HRP COMPLEX	
13. Immerse in TB buffer	- 15 min
14. Rinse in double distilled water	
15. Incubate in 2% aqueous BSA (Sigma: A9418) ***	- 10 min
16. Rinse in double distilled water	
17. Immerse in phosphate buffered saline (PBS)	- 5 min
18. Incubate in ABC/HRP	- 30 min
19. Rinse in double distilled water	
20. Incubate in DAB substrate	- 5 min
21. Wash in running tap water	
22. Rinse briefly in 50% alcohol	
23. Rinse briefly in 70% alcohol	
24. Rinse well in 90% alcohol	
25. Rinse well in absolute alcohol (x2)	
26. Clear in histoclear (x2)	
27. Mount in DPX	

* Strips proteins from nuclei of paraffin tissue sections ** Inactivation of endogenous peroxidase *** Blocking of non-specific background.

APPENDIX XVII

STANDARD CURVE

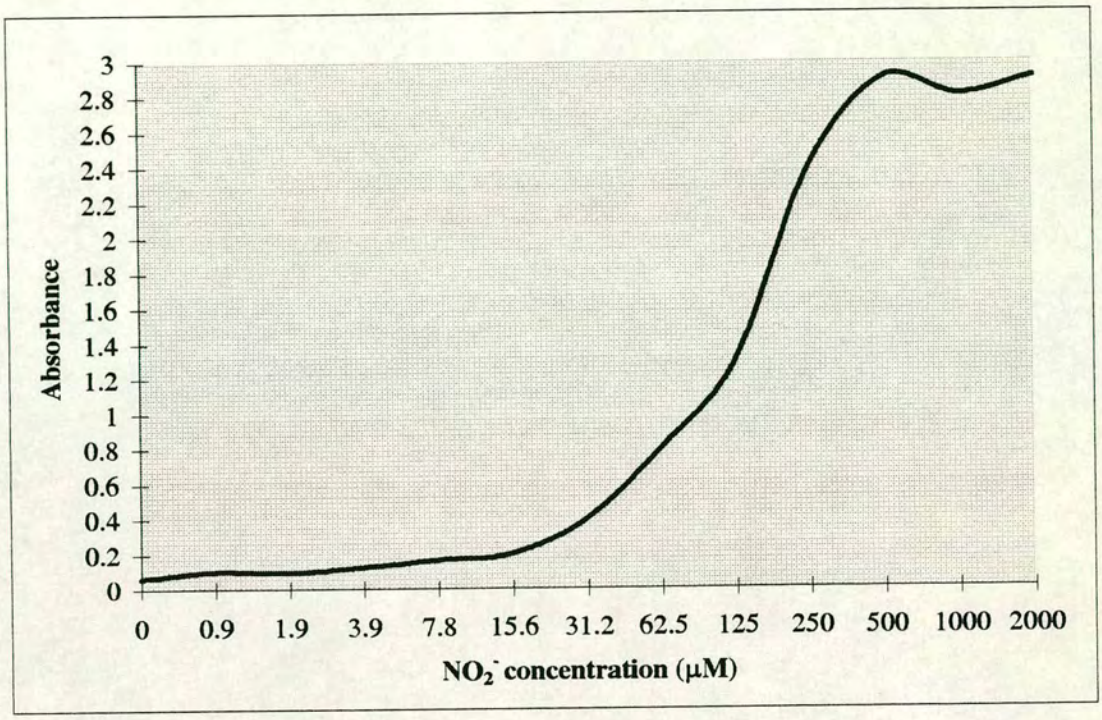

GLOSSARY

APOPTOSIS a form of cell death in which the cell activates an internal death program.

ATROPHY the wasting away or shrinking in size of an organ or tissue.

CACHEXIA profound weakness, general ill health, resulting from serious disease.

CONGESTION the abnormal accumulation of fluids.

DEGENERATIVE CHANGES the deterioration in structure or chemical composition of a tissue or organ by which its vitality is lowered or its function interfered with.

DIFFUSE PARACORTICAL HYPERPLASIA an abnormal increase in the number of cells throughout the paracortex of a lymph node.

DISRUPTIVE CELLULAR INFILTRATE deteriorative changes in the structure of a tissue or organ caused by a cellular infiltrate.

FOAMY MACROPHAGES activated macrophages.

FOLLICULAR HYPERPLASIA an abnormal increase in the number of cells in the lymphoid follicles of a lymph node.

FRIABLE easily crumbled.

GRANULOMA a site of chronic inflammation usually triggered by persistent infectious agents.

HAEMORRHAGE bleeding.

HYPERPLASIA an abnormal increase in the number of cells in a tissue.

INFARCT an area of dead tissue resulting from complete blockage of its blood supply.

LEUCOPENIA a deficiency in the number of white blood cells.

LYMPHOBLASTS activated lymphocytes.

LYMPHOCYTIC an expansion/increase in the number of white blood cells.

LYMPHOCYTOLYSIS the destruction/breakdown of white blood cells.

LYMPHOPOIESIS the formation of white blood cells.

LYMPHOPROLIFERATION active division/mitosis leading to an increase in the number of white blood cells.

NADIR terminal/end.

NECROSIS death of a localised portion of tissue surrounded by living tissue.

OEDEMA excessive accumulation of fluid in blood cavities and spaces around cells.

PETECHIAL HAEMORRHAGES pin point haemorrhages.

POLYMORPHONUCLEAR CELLS white blood cells with multi-lobed nuclei and cytoplasmic granules.

REGENERATIVE CHANGES reformation or reorganisation in the structure or chemical composition of a tissue or organ by which its vitality is increased or its function improved.

SINUS HYPERPLASIA an abnormal increase in the number of cells in the medullary sinuses of a lymph node.

TICK EQUIVALENTS a measure of the concentration of tick derived material.

ULCERS open sores with inflamed bases; local disintegration of tissues of the skin or mucous membranes.

PUBLICATIONS

The sections were counterstained with Harris's haematoxylin with acid (Raymond Lamb) for 15 s, washed briefly in tap water and blued up in Scott's tap water (0.2% potassium bicarbonate–2% magnesium sulphate in distilled water). After washing briefly in tap water, the sections were dehydrated through ascending percentages of alcohol (50%–absolute ethanol), cleared in Histoclear and mounted in DPX (BDH Laboratory Supplies, Poole, UK).

RESULTS

Flow cytometric profiles of macroschizont-infected cell lines

The phenotypic profiles of the Ta His46C and Ta His47C lines were almost identical. Both comprised an overwhelming percentage of cells expressing MHC class II antigens, CD11b and CD49d and the antigens recognized by MAbs IL-A24, IL-A96 and J5 (Figure 1). A substantial number of cells (45%) expressed CD2. Far fewer cells (<12%) were $CD3^+$, $CD4^+$, $CD8^+$, TCR^{1+} or $BoWC3^+$ or recognized by MAbs IL-A25, IL-A106, IL-A109 (putative CD64) or Du 1-29 (CD62b) (Table I).

Parasitized cells detected in tissue sections by MAb 1C7

Although schizont-infected cells were easily identified in haematoxylin-stained sections during the later stages of infection (days 12–14), they were difficult to detect in tissues prepared earlier, 7 days after infection, owing to the infrequency and small size of the parasites at this stage of their life cycle. MAb 1C7 therefore proved very useful, as it not only revealed the parasitized, macroschizont-infected cells in the early set of tissues but also differentiated macroschizont-infected cells ($1C7^+$-schizont-infected cells) from microschizont-infected cells ($1C7^-$-schizont-infected cells) in tissues prepared during the later stages of infection (Figure 2a). By 7 days after infection, macroschizonts were detectable in tissue sections of both prescapular lymph nodes, both precrural lymph nodes, the mesenteric lymph nodes, the thymus and spleen, as well as in the lung, liver, kidney, abomasum, pituitary and adrenal glands. At this time, they were not detectable in the hepatic lymph nodes or the heart. By day 12, parasites in the form of macroschizonts and microschizonts occurred in all 15 organs examined except for the heart, and by day 14 all tissues contained parasitized cells. At this time, many more microschizonts had developed.

CD11b expressed by parasitized cells in infected tissues

The patterns of staining with MAb IL-A15 in uninfected, control tissues resembled those recorded by Splitter and Morrison (1991). The MAb recognized large macrophage-like cells in the paracortex of prescapular, mesenteric and precrural lymph nodes, the white pulp of the spleen and the alveolar walls of the lungs as well as cells in

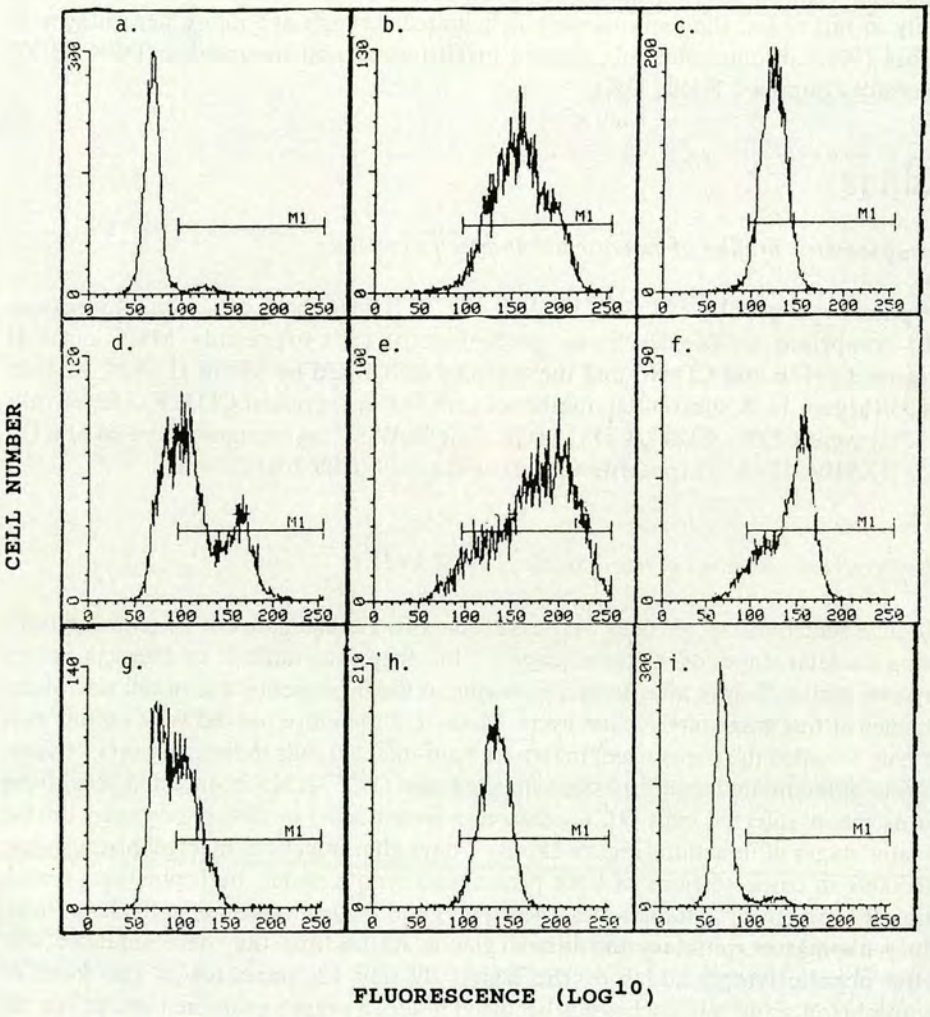

Figure 1. Representative flow cytometric results obtained by incubating the Ta His46C cell line with the following MAbs, prior to incubation with sheep anti-mouse fluorescein-labelled gammaglobulin: (a) medium; (b) MAb IL-A15; (c) MAb IL-A24; (d) MAb IL-A96; (e) MAb IL-A21; (f) clone 218; (g) CC42; (h) J5; (i) MMIA. Histograms represent cell number versus fluorescence (log_{10}). Events within the M1 marker represent positive fluorescence; events to the left of M1 represent unstained cells

TABLE I
Phenotypic analysis of two *in vivo*-derived *T. annulata* (Hisar) macroschizont-infected cell lines with a panel of monoclonal antibodies recognizing bovine leukocyte antigens[a]

MAb	Antigen	Percentage cells reactive	
		Ta His46C	Ta His47C
Medium alone	–	3:1 (–)	0:0 (–)
Medium/FITC	–	6:6 (+)	2:2 (+)
Lymphoid markers			
CC42	CD2	44:45 (+)	47:45 (+)
MM1A	CD3	11:11 (+)	3:4 (+)
CC30	CD4	9:9 (+)	7:6 (+)
CC63	CD8	19:18 (+)	10:8 (+)
CACT61A	TCR1	11:11 (+)	7:8 (+)
J5	Activated T cells[b]	97:ND (+)	97:ND (+)
CC51	BoWC3	12:12 (+)	13:14 (+)
Myeloid markers			
IL-A25	Myeloid cells[c]	10:10 (+)	4:4 (+)
IL-A106	Monocytes/ALVC	12:12 (+)	5:5 (+)
IL-A109	Monocytes[d]	14:15 (+)	7:7 (+)
IL-A24	Myeloid cells	96:87 (+)	98:98 (+)
IL-A96	Myeloid cells	65:65 (++)	67:66 (++)
MHC antigens/adhesion antigens/complement receptor			
ILA-21	MHC II Ags	94:98 (+++)	96:95 (+++)
ILA-15	CD11b	98:98 (++)	99:99 (++)
Clone 218	CD49d	81:80 (++)	93:93 (++)
Du-1-29	CD62L	10:9 (+)	2:2 (+)

ND, not done

[a]Duplicate samples of cells were stained with each MAb and results expressed as percentage of cells reactive; intensity of staining assessed by peak forward scatter: 100–150 (+); 150–200 (++); >200 (+++)

[b]J5, bovine T cell activation marker (Naessens *et al.*, 1985)

[c]Pulmonary macrophages (MacHugh, personal communication)

[d]Putative CD64 (MacHugh *et al.*, 1990). ALVC afferent lymph veiled cells

the germinal centres of lymph nodes. These observations confirmed that the preparations of MAb IL-A15 used here had a similar specificity for bovine tissues to those used to define the MAb's reactivity (Splitter and Morrison, 1991).

MAb IL-A15 also reacted with parasitized and uninfected cells in sections of tissues prepared from infected cattle at all stages of acute disease. The surfaces of cells infected

with parasites at all stages of differentiation – from macroschizont to microschizont – were stained. Such stained, parasitized cells occurred in the lymphoid organs, i.e. the thymus, spleen and lymph nodes, including the prescapular nodes draining the site of inoculation, the hepatic, mesenteric and precrural nodes, as well as in the reticuloendothelial tissues of the liver, kidney, lung, abomasum, adrenal and pituitary glands. MAb IL-A15 labelled 30%, 58% and 73% of the schizont-infected cells detected in the tissues of the three calves harvested on days 7, 12 and 14, respectively. The numbers of positive cells varied from organ to organ. In some lymph nodes, the thymus, liver and abomasum, 80–90% of schizont-infected cells were IL-A15$^+$. In contrast, the antibody which detected CD3 reacted with uninfected paracortical cells in all lymph nodes but not with schizont-infected cells.

These findings are illustrated by the results obtained when sections prepared from the prescapular lymph node draining the site of inoculation of calf 41B on day 12 after infection were double-stained with MAb IL-A15 and MAb 1C7. Both the paracortical and medullary regions of this lymph node contained macroschizont-infected cells (1C7$^+$ schizonts) and microschizont-infected cells (1C7$^-$ schizonts). Both 1C7$^+$ (macro) schizont-infected, IL-A15$^+$ cells (Figure 2b) and 1C7$^-$ (micro) schizont-infected, IL-A15$^+$ cells (Figure 2c) were found in the paracortex. Not all the parasitized cells seen in this area were stained by MAb IL-A15: 1C7$^+$ (macro) schizont-infected, IL-A15$^-$ cells (Figure 2b) and 1C7$^-$ (micro) schizont-infected, IL-A15$^-$ cells (Figure 2d) occurred as well. Some 1C7$^+$ (macro) schizont-infected, IL-A15$^+$ cells were seen to be undergoing mitosis (Figure 2e). Parasitized cells with similar staining patterns for MAbs IL-A15 and 1C7 were also found in the medulla: e.g. 1C7$^+$ (macro) schizont-infected, IL-A15$^+$ cells; 1C7$^+$ (macro) schizont-infected, IL-A15$^-$ cells; 1C7$^-$ (micro) schizont-infected, IL-A15$^-$ cells (Figure 2f). In a number of instances, MAb IL-A15 coated the outer rim of schizonts lying within the cytoplasm of the host cells as well as the walls of the parasitized host cells (Figure 2b). Uninfected macrophage-like IL-A15$^+$ cells were also noted (Figure 2f).

Figure 2. Immunocytochemical studies of tissue sections from *T. annulata*-infected calf 41B: MAb 1C7 was revealed using the ABC/HRP system (yellow stain); the IL-A15 binding was revealed using the ABC/AP system (red stain). Sections were counterstained with Harris's haematoxylin. Macroschizonts appear as bodies containing few, large nuclei within the cytoplasm of infected cells; microschizonts as intracytoplasmic bodies containing numerous relatively smaller nuclei. See Materials and Methods for details. Magnification × 750.
(a) Macroschizont-infected cells (IC7$^+$ schizonts) (1) and microschizont-infected cells (1C7$^-$ schizonts) (2) in the paracortex of the prescapular lymph node draining the site of inoculation of calf 41B. (b) Two IC7$^+$ (macro)schizont-infected, IL-A15$^+$ cells (both schizonts coated with IL-A15$^+$) (1) and one 1C7$^+$ (macro)schizont-infected, IL-A15$^-$ cell (2) in the paracortex of the prescapular lymph node draining the site of inoculation of calf 41B. (c) A 1C7$^-$ (micro)-schizont-infected, IL-A15$^+$ cell (1) plus a 1C7$^+$ (macro)schizont-infected, IL-A15$^-$ cell (2) in the paracortex of the prescapular lymph node draining the site of inoculation of calf 41B. (*cont.*)

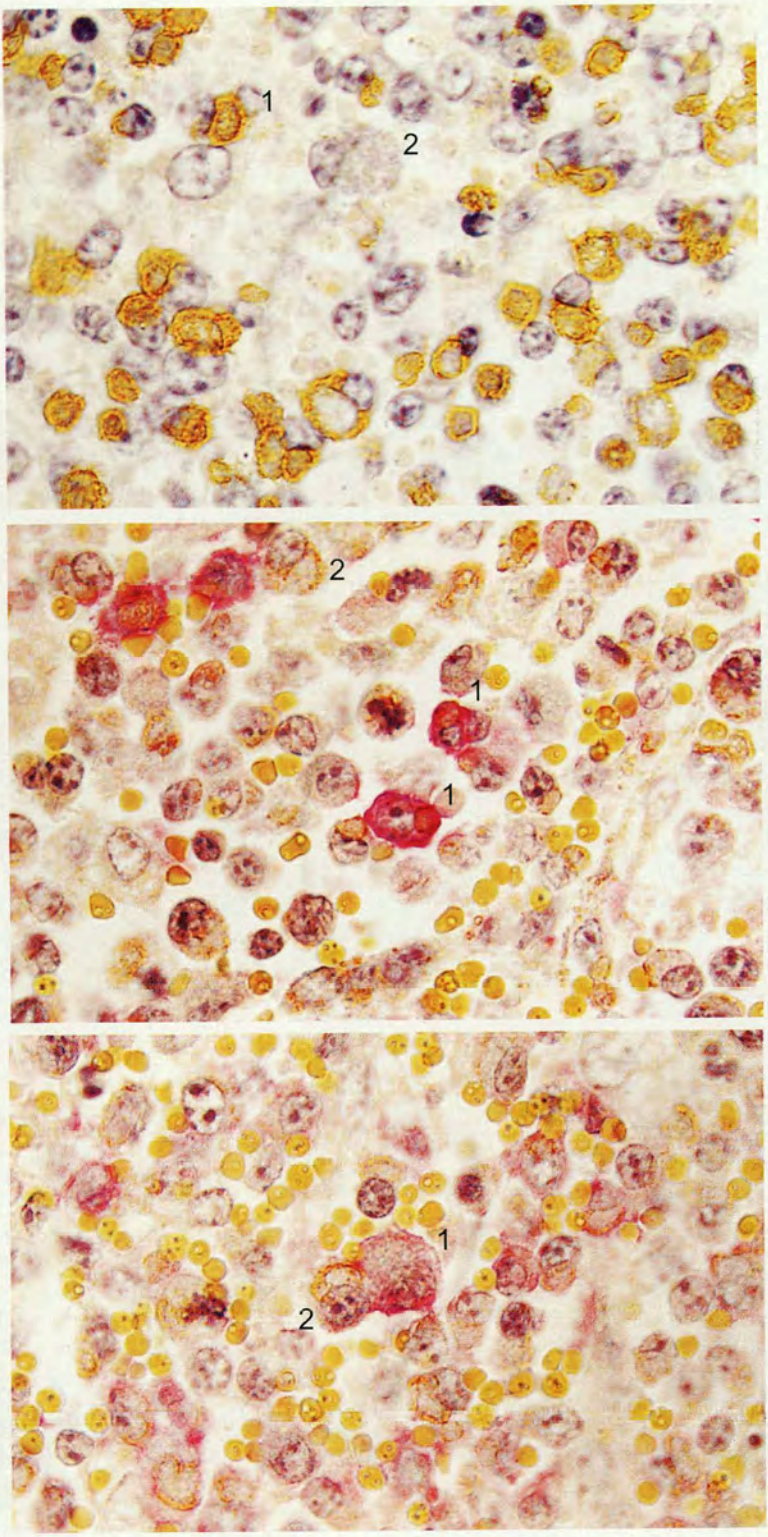

Figures 2a, b and c

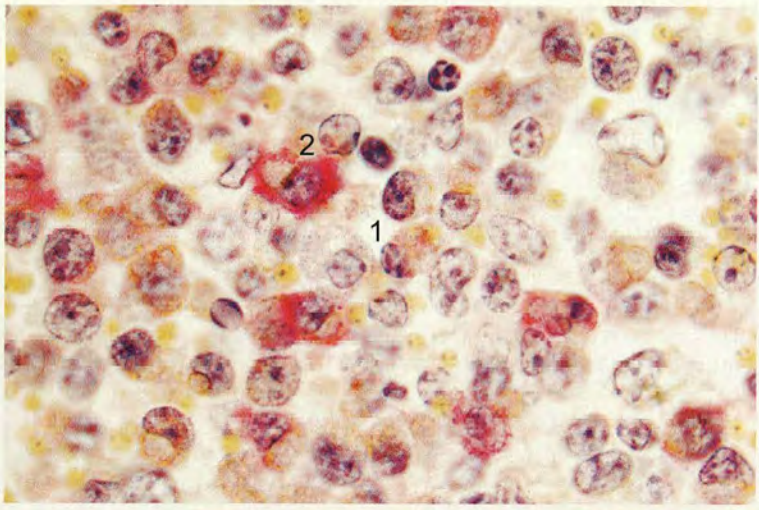

d

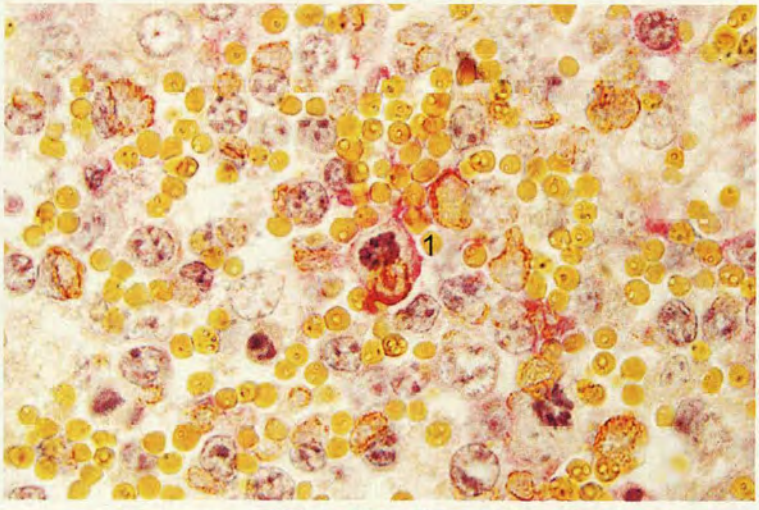

e

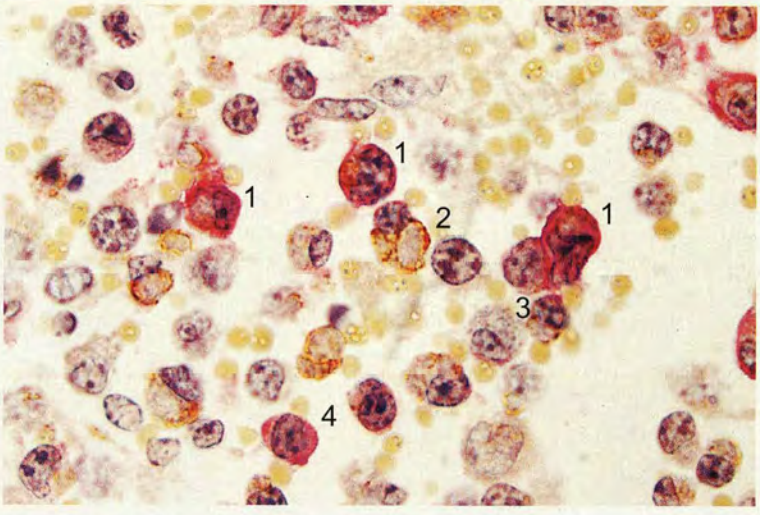

f

Figures 2d, e and f

DISCUSSION

This is the first published work, as far as is known, to use MAbs recognizing bovine leukocyte antigens to characterize schizont-infected cells in the tissues of *T. annulata*-infected cattle. It provides the first record of bovine cells infected *in vivo* by *T. annulata* being recognized by MAb IL-A15 by flow cytometry and by immunocytochemical techniques. CD11b, the molecule detected by this MAb, has a number of functions. It serves as the membrane receptor for C3bi and acts as an opsonin for many microorganisms (Cooper, 1991), is involved in the adhesion and transmigration of blood leukocytes (Belvilacqua, 1993), and promotes NK cell binding to targets (Erdei *et al.*, 1991). Finding that *T. annulata* macroschizont-infected cells in tissues expressed CD11b, but not CD3, is therefore of relevance to three unsolved problems. These are (i) the nature of the cell inhabited by *T. annulata* schizonts in cattle undergoing tropical theileriosis; (ii) the way in which *T. annulata* schizonts transfer from cell to cell, in particular during infection or immunization with cell line vaccines; and (iii) the route of dissemination of the parasite in infected animals.

Although co-expression of markers such as IL-A24 and CD2 hindered a previous attempt to identify *T. annulata* cell lines (Howard *et al.*, 1993), the new finding that 90% of cells of the Ta His46C and Ta His47C *in vivo*-derived lines expressed CD11b as well as being recognized by MAbs IL-A24 and IL-A96 strengthened the case for a myeloid rather than a lymphoid origin for *in vivo*-derived *T. annulata* cell lines. For the CD11b leukocyte integrin is found most widely on macrophages, PBM monocytes, dendritic cells, granulocytes and B cells (Howard and Naessens, 1993); Il-A24 has been observed to stain macrophages and dendritic cells, but not $CD2^+$, $BoWC1^+$, T cells or B cells (Howard and Naessens, 1993); Il-A96 is a widely distributed molecule found on monocytes, all granulocytes, platelets, but not $CD2^+$ T cells and few gamma/delta T cells or B cells (Muiya *et al.*, 1993), which also reacts with ALVC and NK-like bovine cell populations (MacHugh *et al.*, 1990).

The Ta His46C and Ta His47C lines also expressed antigens usually associated with lymphoid cells – CD2, CD3, CD4, CD8, TCR1, BoWC3 and the T-cell activation factor recognized by MAb J5 (Naessens *et al.*, 1985). Since expression of these 'lymphoid' antigens accompanied a very high level of 'myeloid' markers, their occurrence appeared to be a further example of co-expression of lineage markers rather than an indicator of T or B lymphoid cells serving as hosts to *T. annulata*. Co-expression of CD2 and the antigen recognized by MAb J5 does not necessarily militate

Figure 2 (cont.). (d) A $1C7^-$ (micro)schizont-infected, $IL\text{-}A15^-$ cell (1) plus a $1C7^+$ (macro)-schizont-infected, $IL\text{-}A15^+$ cell (2) in the paracortex of the prescapular lymph node draining the site of inoculation of calf 41B. (e) A $1C7^+$ (macro)schizont-infected, $IL\text{-}A15^+$ cell (1) undergoing mitosis in the paracortex of the prescapular lymph node draining the site of inoculation of calf 41B. (f) $1C7^+$ (macro)schizont-infected, $IL\text{-}A15^+$ cells (1), $1C7^+$ (macro)-schizont-infected $IL\text{-}A15^-$ cells (2), a $1C7^-$ (micro)schizont-infected, $IL\text{-}A15^-$ cell (3) and an uninfected $IL\text{-}A15^+$ cell (4) in the medulla of the prescapular lymph node draining the site of inoculation of calf 41B

against a myeloid origin for *T. annulata* lines as ovine monocyte–macrophage lines have been found to co-express CD2, CD11b and the antigen recognized by IL-A24 (Haig *et al.*, 1991). However, so long as no definite marker for bovine NK cells exists, co-expression of CD11b and CD2 may be a sign that *T. annulata* inhabits such cells.

While the overall phenotypic profile of the two *in vivo*-derived cell lines described here resembled those of four *in vitro*-derived lines and a cloned *in vivo*-derived line originating from this laboratory (Howard *et al.*, 1993), the Ta His46C and the Ta His47C lines differed in being recognized by MAb IL-A15. Lack of expression of CD11b by the lines described by Howard and colleagues (1993) may have reflected a loss of expression of surface antigens – a frequent, but as yet unpublished, event in cultured *T. annulata* cell lines.

The observations that bovine cells infected *in vivo* after inoculation of *T. annulata* sporozoites expressed CD11b was confirmed by MAb IL-A15 reacting with schizont-infected cells in tissues prepared from calves undergoing acute theileriosis. The presence of the parasite in the cells was observed readily by double staining with the anti-macroschizont MAb 1C7 (Shiels *et al.*, 1986) or counterstaining with Harris's haematoxylin. The morphological appearance of the infected cells was indicative of a myeloid cell. Although the patterns of staining with MAb IL-A15 indicated that other cell types were infected, the lack of detectable $CD3^+$ schizont-infected cells suggested that T cells, at least, were not acting as hosts in these infections. The specificity of our preparations of MAb IL-A15 was confirmed by the finding that they reacted with cells in similar areas of tissues to those reported by Splitter and Morrison (1991) and Hall *et al.* (1993). Cross-reactivity between the antibody which recognized human CD3 and bovine T cells was confirmed by its reacting predominantly with cells in the paracortical areas and with only a few cells in the germinal centres and medullary regions of bovine lymph nodes.

Although the expression of CD11b may not have established a definite identity for *T. annulata*-infected cells, since the C3bi receptor is expressed by a variety of cell types, its detection on schizont-infected cells, in particular in tissues, has considerable biological significance. Thus, the expression of CD11b by *in vivo*-derived cell lines and parasitized cells in tissues from infected animals suggests a mechanism by which schizonts can transfer from host cell to host cell. While such transfer may not be necessary for completion of a life cycle initiated by tick-borne sporozoites, during which the parasite undergoes clonal expansion culminating in a sequence of stages leading to the production of merozoites, without the apparent necessity of having to leave the cell (Hulliger, 1965) as described here, the way in which *T. annulata* schizonts inoculated as macroschizont-infected and transformed cell lines enter and proliferate in their recipient's cells has hitherto been unclear. It now seems feasible that schizonts freed from the donor cells by a rapid host response to inoculation with allogenic cells (Preston and Brown, 1988) may be opsonized by complement and/or antibody and then linked to cells bearing the C3bi receptor. Attachment of the parasite–complement complex would facilitate phagocytosis of the organism by the cell. The subsequent establishment of the parasite in the cell would depend upon whether the cell bearing the C3bi receptor could support parasite proliferation. Evidence for schizonts being transferred during the infections studied here was obtained by finding that some

schizonts inhabited host cells expressing CD11b and were themselves coated with CD11b. These events strongly suggested that such parasites were living within a phagocytic vacuole formed by the host cell wall which still expressed CD11b, even though internalized within the cytoplasm.

While the circulatory routes used by *T. annulata* to establish in the lymphoid tissues and other organs of the host are as yet unknown, the high levels of expression of CD2 (LFA-2), CD11b and VLA-4 (CD49d) on schizont-infected cells, as revealed by MAb Clone 218, are of particular interest. For in other animal species, CD2 (LFA-1) interacts with LFA-3, a molecule expressed by vascular endothelial cells, to mediate cellular adhesion; the β_2 integrins (CD11a, CD11b) appear to contribute to adhesion and transmigration of blood leukocytes through interaction with intracellular adhesion molecules on vascular endothelial cells (ICAM-1, ICAM-2); VLA-4 integrins may participate in homing to mucosal tissues ($\alpha_4\beta_1$ integrin) or support adhesion to mucosal high endothelial venules ($\alpha_4\beta_7$ integrin) (Bevilacqua, 1993). Finding that *T. annulata*-infected cells express CD2, CD11b and VLA-4 – all molecules with a well-documented role in leukocyte adhesion and migration – therefore indicates ways by which *T. annulata*-schizont-infected cells could move actively from blood or lymph into host tissues. The stimulus for such movement throughout the host might well lie in the constitutive expression by these cells of matrix metalloproteinase 9, an enzyme associated with metastasis in other conditions (Baylis *et al.*, 1995).

Since both *in vivo*-derived cell lines and schizont-infected cells in tissues express CD11b, it seems likely that the *in vivo*-derived cell lines used to prepare the attenuated cell line vaccines in current use represent the cell types inhabited by the parasite in tissues as well as blood. The phenotypic profiles of the *in vivo*-derived cell lines recorded to date showed that cells chosen for infection by sporozoites *in vitro* (Howard *et al.*, 1993) are phenotypically similar to the cells infected *in vivo*.

In brief, this work has shown that bovine cells infected with *T. annulata*, after inoculation of cattle with sporozoites, expressed CD11b but not CD3. This finding provides evidence that the host cells of this parasite belong to the myeloid lineage, indicates the mode of invasion of host cells by parasites administered in *T. annulata* cell line vaccines, and suggests ways by which parasitized cells can travel around the host's tissues. In addition, with respect to NK cell-mediated lysis of *T. annulata*-infected cells (Preston *et al.*, 1983), possession of the C3bi receptor by the parasitized cells may facilitate binding of NK cells to their targets via C3 fragments bound to their own C3bi receptors (Erdei *et al.*, 1991).

Co-expression of lineage markers by the *in vivo*-derived cell lines described here was reminiscent of the well-documented phenomenon of lineage infidelity reported in human leukaemias (Greaves *et al.*, 1986). Such an unusual expression of cell surface molecules by bovine cells, if proved to occur *in vivo* and shown not merely to be a consequence of establishing infected cells in culture, must have profound implications for host–parasite interactions and the pathogenesis of the disease.

ACKNOWLEDGEMENTS

We are grateful to the European Commission (L.M.G.F., P.M.P., L.A.J.) and to the Overseas Development Administration of the United Kingdom (C.G.D.B, G.W.) for their financial support of this work; to Dr C.J. Howard, Institute of Animal Health, Compton, Newbury, UK; to Drs N. MacHugh and J. Naessens, International Livestock Research Institute, Nairobi, Kenya; and to Dr B. Shiels and Professor A. Tait, University of Glasgow, Scotland, UK for their gifts of monoclonal antibodies which made this work possible. We thank Mr D. Elliot and Mr J. Lauder of the Pathology Department, University of Edinburgh Medical School for their advice and practical assistance with this work.

REFERENCES

Baylis, H.A., Megson, A. and Hall, R., 1995. Infection with *Theileria annulata* induces expression of matrix metalloproteinase 9 and transcription factor AP-1 in bovine leucocytes. *Molecular and Biochemical Parasitology*, **19**, 211–222

Bevilacqua, M.P., 1993. Endothelial-leukocyte adhesion molecules. *Annual Review of Immunology*, **11**, 767–804

Brown, C.G.D., 1987. Theileriidae. In: A.E.R. Taylor and J.R. Baker (eds), *In Vitro Methods for Parasitic Cultivation*, (Academic Press, London), 230–253

Campbell, J.D., Brown, D.J., Glass, E.J., Hall, F.R. and Spooner, R.L., 1994. *Theileria annulata* sporozoite targets. *Parasite Immunology*, **16**, 501–505

Cooper, N.R., 1991. Complement evasion strategies of microorganisms. *Immunology Today*, **12**, 327–331

Dschunkowsky, E. and Luhs, J., 1904. Die Piroplasmosen der Rinder. (Vorl. Mitt.) *Centralblatt fur Bakteriologie, Parasitenkunde, Infektionskrankheit und Hygiene. Abteilung 1*, **35**, 486–492

Erdei, A., Fust, G. and Gergely, J., 1991. The role of C3 in the immune response. *Immunology Today*, **12**, 332–337

Gill, B.S., Bhattacharyulu, Y. and Kaur, D., 1976. Immunisation against bovine tropical theileriosis (*Theileria annulata* infections). *Research in Veterinary Science*, **21**, 146–149

Glascodine, J., Tetley, L., Tait, A., Brown, D. and Shiels, B., 1990. Developmental expression of a *Theileria annulata* merozoite surface antigen. *Molecular and Biochemical Parasitology*, **40**, 105–112

Glass, E.J. and Spooner, R.L., 1990. Parasite–accessory cell interactions in Theileriosis. Antigen presentation by *Theileria annulata* infected macrophages and production of continuously growing antigen-presenting cell lines. *European Journal of Immunology*, **20**, 2491–2497

Glass, E.J., Innes, E., Spooner, R.L. and Brown, C.G.D., 1989. Infection of bovine monocyte/macrophage populations with *Theileria annulata* and *Theileria parva*. *Veterinary Immunology and Immunopathology*, **22**, 355–368

Greaves, M.F., Chan, L.C., Furley, A.J.W., Watt, S.M. and Molgaard, H.V., 1986. Lineage promiscuity in hemopoietic differentiation and leukemia. *Blood*, **67**, 1–11

Haig, D.M., Thomson, J. and Dawson, A., 1991. Reactivity of the workshop monoclonal antibodies with ovine bone marrow cells and bone marrow derived monocyte/macrophage and mast cell lines. *Veterinary Immunology and Immunopathology*, **27**, 135–145

Hall, G.A., Sopp, P. and Howard, C.J., 1993. An investigation of temporary workshop clusters reacting with cells of the mononuclear phagocytic system. *Veterinary Immunology and Immunopathology*, **39**, 225–236

Howard, C.J. and Naessens, J., 1993. Summary of workshop findings for cattle. *Veterinary Immunology and Immunopathology*, **39**, 25–48

Howard, C.J., Sopp, P., Preston, P.M., Jackson, L.A. and Brown, C.G.D., 1993. Phenotypic analysis of bovine leukocyte cell lines infected with *Theileria annulata*. *Veterinary Immunology and Immunopathology*, **39**, 275–282

Hsu, S., Raine, L. and Fanger, H., 1981. Use of avidin–biotin–peroxidase complex (ABC) in immunoperoxidase techniques: a comparison between ABC and unlabelled antibody (PAP) procedures. *Journal of Histochemistry and Cytochemistry*, **29**, 577–580

Hulliger, L., 1965. Cultivation of three species of *Theileria* in lymphoid cells *in vitro*. *Journal of Protozoology*, **12**, 649–655

MacHugh, N.D., McKeever, D.J. and Goddeeris, B.M., 1990. Monoclonal antibodies recognising differentiation antigens on bovine peripheral blood monocytes and afferent lymph veiled cells (ALVC), (*Unpublished Annual Scientific Report, International Laboratory for Research on Animal Diseases, Nairobi, Kenya*), 26

Muiya, P., Logan-Henfrey, L. and Naessens, J., 1993. Expression of antigens on haemopoietic progenitor cells in bovine bone marrow. *Veterinary Immunology and Immunopathology*, **39**, 237–248

Naessens, J. and Howard, C.J., 1993. Leukocyte antigens of cattle and sheep. *Veterinary Immunology and Immunopathology*, **39**, 1–312

Naessens, J., Newson, J., Bensaid, A., Teale, A.J., Magondu, J.G. and Black, S.J., 1985. *De novo* expression of T cell markers on *Theileria parva* infected lymphoblasts in cattle. *Journal of Immunology*, **135**, 4183–4188

Preston, P.M. and Brown, C.G.D., 1988. Macrophage mediated cytostasis and lymphocyte cytotoxicity in cattle immunised with *Theileria annulata* sporozoites or macroschizont-infected cell lines. *Parasite Immunology*, **10**, 631–647

Preston, P.M., Brown, C.G.D. and Spooner, R.L., 1983. Cell mediated cytotoxicity in *Theileria annulata* infection with evidence for BoLA restriction. *Clinical and Experimental Immunology*, **53**, 88–100

Preston, P.M., Brown, C.G.D. and Richardson, W., 1992a. Cytokines inhibit the development of trophozoite-infected cells of *Theileria annulata* and *Theileria parva* but enhance the proliferation of macroschizont-infected cell lines. *Parasite Immunology*, **14**, 125–141

Preston, P.M., Brown, C.G.D., Bell-Sakyi, L.J., Richardson, W. and Sanderson, A., 1992b. Tropical theileriosis in *Bos taurus* and *Bos taurus* × *Bos indicus* calves. Response to infection with graded doses of sporozoites. *Research in Veterinary Science*, **53**, 230-243

Purnell, R.E., 1978. *Theileria annulata* as a hazard to cattle in the countries on the Northern Mediterranean Littoral. *Veterinary Science Communications*, **2**, (Elsevier Scientific, Amsterdam), 3–10

Shiels, B., McDougall, C., Tait, A. and Brown, C.G.D., 1986. Antigenic diversity of *Theileria annulata*. *Veterinary Parasitology*, **21**, 1–10

Splitter, G. and Morrison, W.I., 1991. Antigens expressed predominantly on monocytes and granulocytes: identification of bovine CD11b and CD11c. *Veterinary Immunology and Immunopathology*, **27**, 87–90

Spooner, R.L., Innes, E.A., Glass, E.J., Millar, P. and Brown, C.G.D., 1988. Bovine mononuclear cell lines transformed by *Theileria parva* or *Theileria annulata* express different subpopulation markers. *Parasite Immunology*, **10**, 619–629

Spooner, R.L., Innes, E.A., Glass, E.J. and Brown, C.G.D., 1989. *Theileria annulata* and *Theileria parva* infect and transform different bovine mononuclear cells. *Immunology*, **66**, 284–288

(Accepted: 19 August 1996)